DIETARY DIVALENT METAL UPTAKE AND INTERACTIONS IN FRESHWATER FISH: IMPLICATIONS FOR METAL TOXICITY

A Thesis Submitted to the College of

Graduate Studies and Research

In Partial Fulfillment of the Requirements

For the Degree of Doctor of Philosophy

In the Toxicology Graduate Program

University of Saskatchewan

Saskatoon

By

Raymond W. M. Kwong

PERMISSION TO USE

In presenting this thesis in partial fulfilment of the requirements for a Postgraduate degree from the University of Saskatchewan, I agree that the Libraries of this University may make it freely available for inspection. I further agree that permission for copying of this thesis in any manner, in whole or in part, for scholarly purposes may be granted by the professor or professors who supervised my thesis work or, in their absence, by the Head of the Department or the Dean of the College in which my thesis work was done. It is understood that any copying or publication or use of this thesis or parts thereof for financial gain shall not be allowed without my written permission. It is also understood that due recognition shall be given to me and to the University of Saskatchewan in any scholarly use which may be made of any material in my thesis.

Requests for permission to copy or to make other use of material in this thesis in whole or part should be addressed to:

Dr. Barry Blakley
Toxicology Graduate Program, Program Chair
University of Saskatchewan
Saskatoon, Saskatchewan S7N 5B3

ABSTRACT

The overall goal of the present research project was to investigate the physiology of dietary iron absorption and its interactions with the uptake and metabolism of other divalent metals, especially cadmium, in freshwater fish, using rainbow trout (*Oncorhynchus mykiss*) as a model species. Using intestinal sac preparations, iron absorption was found to occur along the entire intestinal tract of fish, with anterior intestine being the major site of absorption compared to either mid or posterior intestine. Ferrous iron was more bioavailable than ferric iron, and the uptake of ferrous iron was significantly reduced at alkaline pH ($p < 0.05$). These findings suggested that a homolog of the mammalian apical ferrous iron transporter, divalent metal transporter-1 (DMT1, a Fe^{2+}/H^{+} symporter), is involved in the absorption of iron in the fish intestine. Ferric iron appeared to be absorbed through the same pathway as ferrous iron following reduction by an apical ferric reductase. Several divalent metals, both essential (nickel, copper and zinc) and non-essential (cadmium and lead), inhibited intestinal ferrous iron absorption in fish. Importantly, elevated luminal iron reciprocally reduced the accumulation of cadmium in the fish intestine, indicating the significance of the iron transport pathway in dietary cadmium absorption. Two different DMT1 isoforms, *Nramp-β* and *-γ*, were found to be expressed along the entire gastrointestinal tract of fish. My study showed that in isolated rainbow trout enterocytes, ferrous iron uptake occurred through a saturable and proton-dependent process, providing further evidence of DMT1-mediated ferrous iron transport. Both cadmium and lead inhibited ferrous iron uptake in the enterocytes in a concentration-dependent manner. Kinetic characterization revealed that the apparent affinity for ferrous iron uptake is significantly decreased (increased K_m) in the presence of either cadmium or lead ($p < 0.05$), whereas the maximum uptake rate (J_{max}) remains unchanged. These results indicated that the interaction

between ferrous iron and cadmium or lead is competitive in nature, and the uptake of these metals occurs through a common transport pathway (likely DMT1). The uptake characteristics of cadmium were further examined in isolated rainbow trout enterocytes, and my findings indicated that in addition to DMT1, cadmium uptake can be mediated by zinc transport pathway (ZIP8, a Zn^{2+}/HCO_3^- symporter). My study also showed that cysteine-conjugated cadmium was readily bioavailable to fish enterocytes, possibly *via* a cysteine-specific transport pathway. The efflux of cadmium from the enterocytes was found to occur *via* an ATPase-driven pathway. On the other hand, chronic exposure to dietary cadmium at an environmentally-relevant concentration significantly increased cadmium burden in target organs as well as in the whole-body of fish ($p < 0.05$). Exposure to dietary cadmium increased the mRNA expression level of key stress-inducible proteins such as metallothioneins (MT-A and MT-B) and heat shock proteins-70 (HSP-70a and HSP-70b). Interestingly, each MT and HSP-70 mRNA isoform responded differently in various target organs of fish following dietary cadmium exposure. Fish exposed to dietary cadmium also exhibited an increase in the hepatic transferrin mRNA level as well as the plasma transferrin protein level, indicating the role of transferrin in cadmium handling in fish. Importantly, an iron-supplemented diet reduced cadmium burden in the gut and the whole-body, and ameliorated the expression of MT and HSP-70 genes in fish. These results suggested the protective effects of elevated dietary iron against chronic dietary cadmium toxicity in fish. Overall, findings from the present research project provided novel and important physiological and molecular insights into the uptake, interactions and homeostasis of dietary divalent metals in freshwater fish. This information greatly enhances our current understanding of the toxicological implications for dietary metal exposure in metal contaminated wild fish populations, and may ultimately help the regulators to develop better strategies for ecological risk assessment of metals.

ACKNOWLEDGEMENTS

I would like to thank my graduate supervisor, Dr Som Niyogi, for his support, enthusiasm, patience, and providing insightful suggestions for my scientific research. He also provided critical support in preparing this thesis. I would also like to thank the members of my graduate committee, Dr. Barry Blakley, Dr. Andrew Van Kessel, Dr. David Janz, and Dr. Yangdou Wei, for the time they have dedicated to my graduate program and the valued advice in the completion of my thesis. My sincere thanks also go to Dr. John Giesy, Dr. Markus Hecker and Dr. Jose Andrés for their guidance and support during my study. I also thank Dr. Michael Wilkie from the Wilfrid Laurier University for serving as the external examiner of my thesis.

I thank past and present members of Niyogi's lab, especially Sougat Misra, Aditya Manek, Jacob Ouellet, Charmain Hamilton, Sayanty Roy and Keegan Hicks. Thank you to everyone in the Department of Biology and the Toxicology Centre.

I thank my family for their love, patience and encouragement throughout my study, especially my parents, aunts and uncles. They have lost a lot due to my study abroad. Without their encouragement and understanding, it would have been impossible for me to finish this work.

At last, I would like to acknowledge my funding sources, the Toxicology Devolved Scholarship, the Natural Sciences and Engineering Research Council of Canada (NSERC), the Canadian Foundation for Innovation (CFI), and the Society of Environmental Toxicology and Chemistry (SETAC)/ICA Chris Lee Award for Metals Research (sponsored by the International Copper Association).

TABLE OF CONTENTS

LIST OF TABLES

LIST OF FIGURES

LIST OF ABBREVIATIONS

^{o}C = Degree Celsius

µl = Microliter

µg/g = Micrograms

µM = micromolar concentration

ANOVA = Analysis of variance

ATPase = Adenosine triphosphatase

Ca = Calcium

Cd = Cadmium

cDNA = Complementary deoxyribonucleic acid

Ci = Curie

Co = Cobalt

cm = Centimeter

CPM = Radioactivity counts per minute

Ctr1 = Copper transporter-1

Cu = Copper

Cys = Cysteine

DFO = Desferrioxamine mesylate

DIDS = 4,4'-Diisothiocyano-2,2'-stilbenedisulfonic acid

DMT1 = Divalent metal transporter-1

DNA = Deoxyribonucleic acid

dNTA = Deoxyribonucleotides

ECaC = Epithelial calcium channels

EDTA = Ethylenediaminetetraacetic acid

Fe = Iron

FTR = Fluid transporter rate

g = gram

GFAAS = Graphic furnace atomic absorption spectrometry

h = hour

HCL = Hydrochloric acid

HCO_3^- = Bicarbonate

HEPES = 4-(2-hydroxyethyl)-1-piperazineethanesulfonic acid

HNO_3 = Nitric acid

HSI = Hepato-somatic index

HSP = Heat shock protein

HSP70a = 70 kDa heat shock protein isoform a

HSP70b = 70 kDa heat shock protein isoform b

IC_{50} = The half maximal inhibitory concentration

IREG1 = Iron regulated protein-1

ISA = Intestinal surface area

ISI = Gastro-intestinal somatic index

J_{in} = Metal uptake rate

J_{max} = Maximum uptake rate of metal

kg = Kilogram

K_m = Apparent binding affinity / the concentration of metal that leads to half-maximal velocity

LDH = Lactate dehydrogenase

LSD = A least significant difference test

mg = Milligram

mCi = Millicurie

min = Minute

mL = milliliter

mM = Millimolar

Mn = Manganese

mOsm = Milliosmole

mRNA = Messenger ribonucleic acid

MS-222 = Tricaine methanesulfonate

MT = Metallothionein

MT-A = Metallothionein isoform A

MT-B = Metallothionein isoform B

N = Normality

NaOH = Sodium hydroxide

ng = Nanogram

nmol = Nanomole

Ni = Nickel

Nramp = Natural resistance-associated macrophage protein

Nramp-β = Natural resistance-associated macrophage protein isoform β

Nramp-γ = Natural resistance-associated macrophage protein isoform γ

NTA = Nitrilotriacetic acid

Oligo = Oligonucleotide

Pb = Lead

PCR = Polymerase chain reaction

pmol/mg protein/min = picomole per milligram of protein per minute

Q_{10} = Temperature coefficient

r^2 = Regression coefficient

RNA = Ribonucleic acid

RT-qPCR = real time quantitative polymerase chain reaction

SA = Specific activity / amount of radioactivity per unit amount of metal

SEM = Standard error of the mean

slc11 = Solute carrier 11

t = Time

Tf = Transferrin

TIBC = Total iron binding capacity

UD = Under the detection limit

UIBC = Unsaturated iron binding capacity

ZIP = Zrt- and Irt-like proteins

Zn = Zinc

CHAPTER 1: General Introduction

1.1 Importance of dietary exposure in metal accumulation and toxicity in wild fish

Fish are unique among the vertebrates since they are exposed to metals *via* both water and diet. Presently, the mechanisms of uptake, regulation and toxicity of waterborne trace metals in fish are quite well characterized (Wood, 2001; Bury *et al.*, 2003). In contrast, the current understanding of uptake, homeostasis and toxicity of dietary trace metals in fish is limited. This is despite the fact that dietary exposure is often considered to be more important than the waterborne exposure in natural environments contaminated with metals (Woodward *et al.*, 1994; Farag *et al.*, 1999). It has been shown that chronic dietary treatment with invertebrates collected from a metal-contaminated environment increases metal body burden and produces oxidative stress in rainbow trout (*Oncorhynchus mykiss*) (Farag *et al.*, 1994). Cutthroat trout (*Oncorhynchus clarki*) fed with a similar diet exhibits a reduction in feeding activity and degeneration of intestinal epithelium (Farag *et al.*, 1999). In addition, an increase in plasma glucose and cortisol levels was reported in fish fed with a metal-contaminated natural diet (Hodson *et al.*, 1978; Farag *et al.*, 1999), indicating the elevated stress responses in fish. Such pathophysiological effects induced by elevated dietary metal exposure may lead to growth impairment, and ultimately death (Woodward *et al.*, 1994; Hansen *et al.*, 2004; Ng and Wood, 2008). These findings highlight the importance of dietary exposure in metal accumulation and toxicity to wild fish populations. However, the current water quality regulations for metals in Canada, and many other jurisdictions across the world, do not account for the effects of dietary exposure. Presently, there is a recognized need for further research to develop our understanding

of the link between the uptake/accumulation and chronic toxicity of dietary metal exposure in fish.

1.2. Overview of the gastrointestinal system of freshwater fish

The gastrointestinal system of teleost fishes varies considerably due to factors such as adaptation to food type and phylogeny (evolutionary history of species). Since the present research project used a freshwater salmonid species, rainbow trout, as the experimental model (see section 1.8 for details), the overview of the gastrointestinal function is focused on this species.

As opposed to herbivorous or omnivorous fish which typically have no stomach, rainbow trout is a carnivorous fish and has a defined stomach for initial physical and enzymatic breakdown of food. The gastric glands in the stomach secrete concentrated hydrochloric acid (HCl) to denature protein and to break down macromolecules into smaller units. Stomach pH in trout varies between 1 and 5, depending on the feeding state (Buddington and Kuz'mina, 2000). The partially digested food (chyme) entering into the intestine is then mixed with secretions from the intestine as well as from the pancreas and gall bladder through pancreatic and bile ducts, respectively. The secretions include digestive enzymes, electrolytes and bicarbonate. Bicarbonate neutralizes the acidic pH of the chyme coming from the stomach, and is believed to play some role in osmoregulation during acclimation to saltwater (rainbow trout is a euryhaline species which can adapt to both freshwater and saltwater environments) (Wilson *et al.*, 2002; Grosell *et al.*, 2007). The pH in the intestinal lumen of rainbow trout is around 7.3 (Vielma and Lall, 1997; Saghari Fard *et al.*, 2007), and the intestinal tract can be broadly divided into three sections morphologically: the anterior intestine which contains a number of blind-sacs known as pyloric caecae, the mid intestine which is narrower and free of caeca, and the posterior intestine which

has a larger diameter, visible external annular folds and internal mucosal folds. It is believed that the presence of pyloric caecae in the anterior intestine increases the surface area for nutrient digestion and absorption (Buddington and Diamond, 1986), while the internal mucosal folds in the posterior intestine increases absorptive surface areas as well as increasing retention time of food (Ezeasor and Stokoe, 1980).

Despite the distinct morphological difference along the intestinal tract of rainbow trout, the cell type in the mucosal epithelium along the tract is reported to be quite similar (Buddington and Diamond, 1987). Typically, four major types of epithelial cells are found in the intestine of trout, absorptive enterocytes and three secretory cells, entero-endocrine cells, goblet cells, and paneth cells, which secrete hormones, mucus and lysozymes, respectively. However, the absorptive mechanisms for most of the nutrients remain largely unknown. Simple diffusion, paracellular and carrier-mediated pathways (e.g., through specific transporters or channels) have been proposed to be the possible routes for nutrient absorption (Grosell *et al.*, 2011). In general, cellular uptake of nutrients across the intestine involves three steps: (1) absorption of nutrients through the apical membrane into the epithelial cells, (2) intracellular trafficking of nutrients to the basolateral membrane, and (3) extrusion of nutrients from the cells into the bloodstream.

1.3. Current understanding of the physiological and molecular characteristics of dietary divalent metal uptake in fish

Among different divalent trace metals, the dietary uptake mechanisms of only copper and zinc in freshwater fish have been studied in considerable depth. Several recent studies have provided important physiological and molecular insights into the uptake of copper in the piscine gastro-intestinal tract. In freshwater rainbow trout, the anterior intestine has been found to be the

major site for copper absorption (Clearwater *et al.*, 2000; Ojo and Wood, 2007). Clearwater *et al.* (2000) has suggested that the apical uptake of luminal copper in rainbow trout occurs through a passive diffusive mechanism, whereas a carrier-mediated transport process is involved in the basolateral extrusion of copper. Similar observations have also been reported in the African walking catfish (*Clarias gariepinus*) (Handy *et al.*, 2000). However, recent studies have demonstrated that the apical uptake of luminal copper in rainbow trout occurs through a proton-coupled mechanism, at least partially (Handy *et al.*, 2002; Burke and Handy, 2005; Nadella *et al.*, 2007). These studies suggested that luminal copper transport is possibly mediated by the homologs of mammalian iron (divalent metal transporter-1, DMT1) and/or copper transporters (copper transporter-1, Ctr1). Both DMT1 and Ctr1 are proton-divalent metal symporters, which have been shown to be of physiological importance in copper absorption in the mammalian intestine (Arredondo *et al.*, 2003; Sharp, 2003). In rainbow trout, the intestinal expression of DMT1 remains to be investigated, while a cDNA sequence that shows high similarity to the mammalian Ctr1 has been found to be expressed along the entire gastrointestinal tract of rainbow trout (Nadella *et al.*, 2011). This finding suggests Ctr1 may be involved in dietary copper uptake in rainbow trout. Basolateral extrusion of copper into the bloodstream in the piscine intestine is also probably similar to the mechanism in the mammalian gut, which is mediated by a Menkes copper-ATPase (Camakaris *et al.*, 1999). This transport protein has been recently cloned in zebrafish (*Danio rerio*) (Craig *et al.*, 2009). In the African catfish however, copper extrusion is suggested to occur mainly *via* a copper/chloride symporter (Handy *et al.*, 2000).

Similar to copper, zinc absorption occurs primarily in the anterior intestine of rainbow trout (Ojo and Wood, 2007). Similar observations have also been reported in marine fish such as plaice (*Pleuronectes platessa*) (Shears and Fletcher, 1983) and black sea bream (*Acanthopagrus*

schlegeli) (Zhang and Wang, 2007). In rainbow trout, a saturable uptake mechanism for luminal zinc has been demonstrated, indicating the involvement of a carrier-mediated process (Glover and Hogstrand, 2002). The precise mechanism for zinc transport across the intestinal epithelium of fish is poorly understood. However, cDNA sequences highly similar to the mammalian apical (ZIP family, Zrt- and Irt-like proteins) and basolateral (ZnT family) zinc transporters have been identified and cloned in zebrafish and rainbow trout (Feeney *et al.*, 2005; Qiu *et al.*, 2007). Feeney *et al.* (2005) also observed that aqueous exposure to zinc modulates the intestinal expression of ZIP and ZnT in zebrafish, suggesting the potential role of these transporters in the homeostatic regulation of dietary zinc absorption.

A few previous studies have investigated the mechanisms of dietary iron uptake in fish, however the focus has been exclusively on marine fish. Mammalian homologs of an apical iron transporter DMT1 (a ferrous iron/proton symporter) have been cloned in a number of marine fish, such as puffer fish (*Takifugu rubripes*) (Sibthorpe *et al.*, 2004), striped bass (*Morone saxatilis*) (Burge *et al.*, 2004), and Japanese flounder (*Paralichthys olivaceus*) (Chen *et al.*, 2006). Recent physiological studies have shown that ferrous iron (Fe^{2+}) is more bioavailable than ferric iron (Fe^{3+}) in the intestine of the marine fish European flounder (*Platichthys flesus*) (Bury *et al.*, 2001) and gulf toadfish (*Opsanus beta*) (Donovan *et al.*, *2000*), suggesting the involvement of DMT1. DMT1 in marine fish is suggested to transport iron efficiently at circum-neutral pH (Bury *et al.*, 2001; Cooper *et al.*, 2006a), which is different from the functional properties of the mammalian DMT1 (see section 1.4.1 for details).

To date, the physiological characteristics of dietary iron absorption in freshwater fish have not been investigated. The chemical environment of the gut in freshwater fish is markedly

different from that in marine fish, which may be reflected by different mechanisms of iron uptake. For instance, marine fish maintain a more alkaline pH and significantly higher bicarbonate level in the gut lumen (Wilson, 1999). Therefore, one goal of my thesis is to examine whether the strategy of dietary iron absorption in freshwater fish is different from that in marine fish.

1.4. Insights of iron uptake and its interactions with other divalent metals from mammalian studies

1.4.1. Physiological and molecular mechanisms of iron uptake and homeostasis

In mammals, it is generally believed that iron homeostasis is primarily regulated through the absorption process, and the excretion of iron plays a minor role (Andrews, 2000). Dietary iron primarily exists in two forms: inorganic forms [ferric (Fe^{3+}) and ferrous iron (Fe^{2+})] and the organic form (heme iron). The heme iron is believed to be more bioavailable than the inorganic iron (Mackenzie and Garrick, 2005), however the mechanism for heme absorption is poorly understood. It has been proposed that the heme carrier protein-1 mediates heme uptake (Shayeghi *et al.*, 2005), the absorbed heme is then disassembled by microsomal heme oxygenase, and the liberated iron enters the same storage and transport pathways as the inorganic iron (Raffin *et al.*, 1974). In the diet, most inorganic iron is present as ferric iron complex (e.g., chelated to organic ligands). After ferric iron is dissociated from the complex in the acidic stomach, an iron binding glycoprotein, gastroferrin, which is secreted from the stomach, binds to ferric iron and maintains it in solution (Powell *et al.*, 1999). The ferric iron is then reduced to the ferrous form by luminal components such as ascorbate (Teucher *et al.*, 2004), and/or by an apical

ferric reductase (McKie *et al.*, 2001). The absorption of ferrous iron into the enterocytes is mediated by DMT1 (Gunshin *et al.*, 1997). DMT1 is a member of the highly conserved Nramp (natural resistance-associated macrophage protein) family, and is expressed predominantly in the duodenum of the gastrointestinal tract of mammals (Gunshin *et al.*, 1997). The transport function of DMT1 is facilitated by a proton gradient (Fe^{2+}/H^{+} symporter) and membrane potential (Gunshin *et al.*, 1997; Tandy *et al.*, 2000). To date, four different DMT1 mRNA isoforms have been identified in mammals, two of which contain iron-responsive element (IRE) in the 3' untranslated region. The DMT1 mRNA transcripts with IRE have the ability to sense the intracellular iron level, whereas the DMT1 transcripts without IRE lack this function (Lee *et al.*, 1998). In addition, the relative expression as well as the cellular localization of each isoform differs in different cell types (Garrick *et al.*, 2003). A recent study has suggested that an independent absorptive pathway for ferric iron may also exist in mammalian systems (Conrad *et al.*, 2000). After iron enters the enterocytes, it binds to the ferritin protein for storage, or being transported to the basolateral membrane for extrusion into the blood stream.

Extrusion of iron from the enterocytes into the blood circulation occurs *via* an iron exporter protein called iron regulated protein-1 [IREG1, also termed as metal-transporter protein (MTP1), ferroportin, and slc11 a3] (McKie *et al.*, 2000). The IREG1 is coupled to a basolateral membrane-bound oxidase, hephaestin, which oxidizes ferrous iron into the ferric form before binding to the iron circulating protein, transferrin, in the plasma (Vulpe *et al.*, 1999). Iron is mainly transported throughout the body bound with transferrin. On the other hand, IREG1 also plays a critical role in recycling of heme iron from macrophages after erythrophagocytosis (ingestion of degenerated red blood cells) (Knutson and Wessling-Resnick, 2003). Therefore,

IREG1 controls how much dietary iron enters into blood circulation as well as providing immediate adjustment on circulating plasma iron (Knutson and Wessling-Resnick, 2003).

Regulation of dietary iron absorption is governed by several physiological and molecular processes in mammals. For example, increase in duodenal ferric reductase activity and DMT1 mRNA levels in response to iron deficiency have been reported in mammalian systems (Gunshin *et al.*, 1997; McKie *et al.*, 2001; Zoller *et al.*, 2001). In addition, DMT1 protein at the microvillus membrane of duodenal enterocytes was shown to migrate into the cytoplasm during high iron intake (Trinder *et al.*, 1999). In contrast, dietary iron appears to have less effect on the gene expression of IREG1 and hephaestin (Frazer *et al.*, 2003). Instead, both IREG1 and hephaestin expressions are more sensitive to body iron storage (Chen *et al.*, 2003). During iron overload, the liver secretes a peptide hormone hepcidin into the blood stream, and hepcidin binds to IREG1 and induces its internalization and degradation, thereby reducing iron export into the blood circulation (Nemeth *et al.*, 2004).

1.4.2. Iron transport pathway – linkage to the absorption of other divalent metals

The dietary interaction of iron with other divalent metals (e.g., copper, zinc, nickel, lead and cadmium) has long been recognized in mammals (Huebers *et al.*, 1987; Kozlowska *et al.*, 1993; Goddard *et al.*, 1997; Iturria and Nuñezb, 1998). However, the role of DMT1 in these interactions has been suggested in the fairly recent past (Gunshin *et al.*, 1997; Arredondo *et al.*, 2003; Garrick *et al.*, 2003). Interestingly, in addition to ferrous iron (Fe^{2+}), mammalian DMT1 has been shown to transport several other divalent metals, both essential [copper (Cu^{2+}), zinc (Zn^{2+}), cobalt (Co^{2+}), nickel (Ni^{2+}) and manganese (Mn^{2+})] and non-essential [cadmium (Cd^{2+}) and lead (Pb^{2+})] (Gunshin *et al.*, 1997; Sacher *et al.*, 2001; Arredondo *et al.*, 2003; Bannon *et al.*,

2003; Tallkvist *et al.*, 2003; Mackenzie and Hediger, 2004). Moreover, copper and zinc have been found to modulate the mRNA expression of DMT1, thereby potentially affecting the absorption of dietary iron (Yamaji *et al.*, 2001; Tennant *et al.*, 2002).

1.4.3. Interplay between iron and cadmium

In higher vertebrates including mammals, the adverse effect of cadmium on iron homeostasis is quite well documented (Kozlowska *et al.*, 1993; Bressler *et al.*, 2004; Moulis, 2010); however, the underlying mechanism is still unclear. Anemia (iron deficiency) is among the most common pathological symptoms reported after cadmium intoxication (Kozlowska *et al.*, 1993; Horiguchi *et al.*, 1996). In enterocytes, cadmium competes with iron for uptake *via* the apical iron transporter DMT1 (Bannon *et al.*, 2003; Okubo *et al.*, 2003), and an iron-deficient diet was shown to increase intestinal DMT1 expression as well as cadmium body burden in rats (Park *et al.*, 2002; Ryu *et al.*, 2004). These findings indicate that the mammalian DMT1 contributes to cadmium accumulation. In addition, an iron-supplemented diet was found to reduce the accumulation and toxicity of dietary cadmium in rodent models (Groten *et al.*, 1991; Włostowski *et al.*, 2003). The protective effects of elevated dietary iron are suggested to be due to the compensation of cadmium-induced deprivation of tissue iron, and/or inhibition of cadmium absorption from the gastrointestinal tract, thereby reducing its accumulation in target organs (Fox *et al.*, 1980; Groten *et al.*, 1991; Włostowski *et al.*, 2003). Moreover, transferrin and ferritin have been shown to bind to cadmium (Huebers *et al.*, 1987; Sugawara *et al.*, 1988; Granier *et al.*, 1998), suggesting their role in cadmium handling and metabolism.

1.5. Molecular evidence of iron uptake mechanism and its interactions with other divalent metals in freshwater fish

Despite the lack of mechanistic knowledge of intestinal iron uptake in freshwater fish, the physiology of dietary iron transport can be speculated based on recent molecular evidence. For example, cDNA sequences that show high similarity to the mammalian apical iron transporter DMT1 have been cloned in a number of freshwater fish, including carp (*Cyprinus carpio*) (Saeij *et al.*, 1999), rainbow trout (Dorschner and Phillips, 1999; Cooper *et al.*, 2007), and zebrafish (Donovan *et al.*, 2002). Donovan *et al.* (2002) showed that zebrafish that have defective DMT1 cannot absorb a sufficient amount of iron, which subsequently causes hypochromic (reduction of hemoglobin level) and microcytic (decrease in the size of red blood cell) anemia. Cooper *et al.* (2007) identified two isoforms of DMT1 transcripts (*Nramp-*β and $-\gamma$) in the gill of rainbow trout, and both DMT1 isoforms were found to import ferrous iron at pH $\leq$ 7.4 when expressed in *Xenopus* oocytes. On the other hand, the basolateral transfer of iron in the fish intestine has been proposed to occur *via* the mammalian IREG1 homolog. The putative IREG1 has been cloned in zebrafish, and a mutant of the protein has been shown to cause an increase in iron accumulation in the intestine (Donovan *et al.*, 2000). In addition to epithelial iron transport proteins, several other proteins that are involved in iron homeostasis in mammals are also expressed in teleost fish, such as the iron circulating protein transferrin (Ford, 2001; Yang *et al.*, 2004) and the intracellular iron storage protein ferritin (Andersen *et al.*, 1995). Presumably, the machinery for iron regulation is evolutionarily conserved between fish and mammals, and the functional role of those iron transport/binding proteins is similar to that of the mammalian homologs. The overall absorptive pathway of iron in piscine systems likely resembles to mammalian systems. A

hypothetical representation of the intestinal iron absorption pathway in fish is illustrated in Figure 1.1.

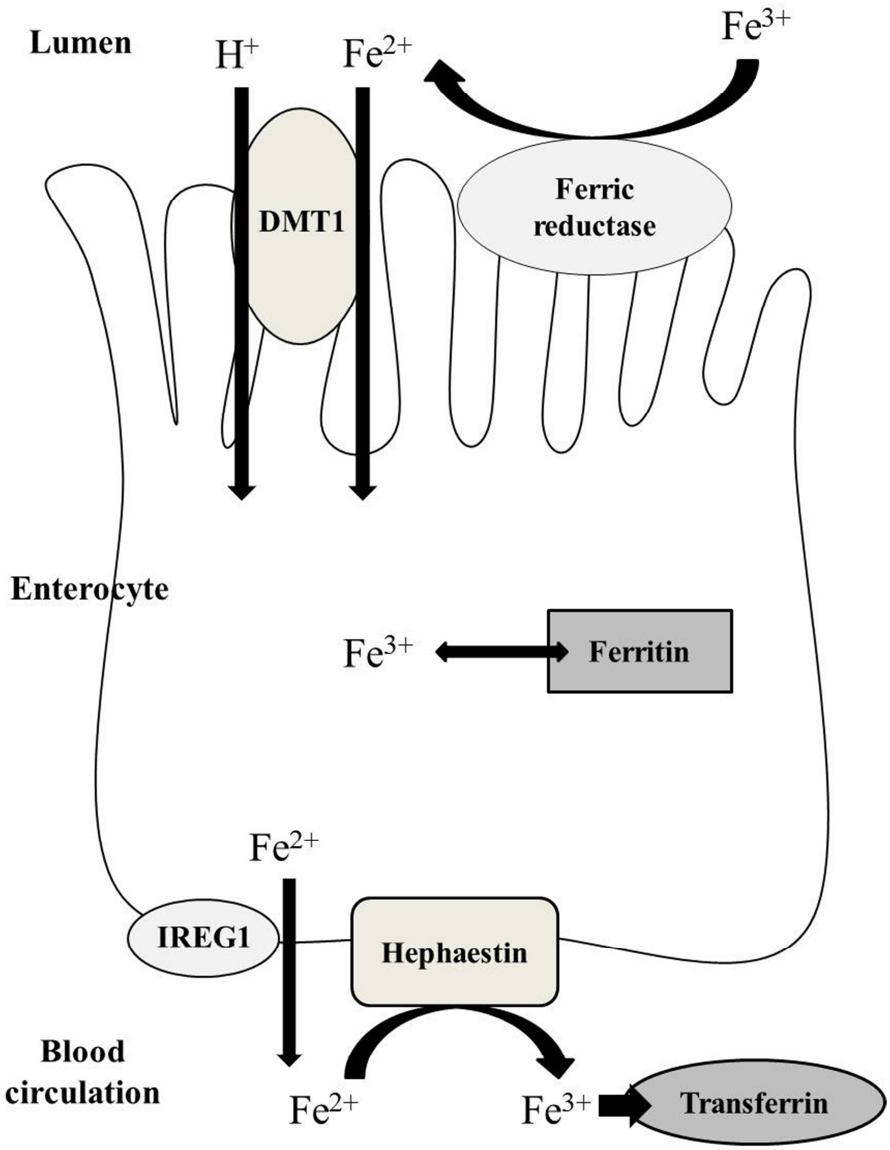

Figure 1.1: Hypothetical representation of inorganic iron uptake in the enterocytes of teleost fish. At the apical membrane, ferric iron (Fe^{3+}) is reduced to the ferrous form (Fe^{2+}) by ferric reductase. The uptake of Fe^{2+} into the enterocytes is mediated by a Fe^{2+}/H^{+} symporter, the divalent metal transporter-1 (DMT1). Intracellular Fe^{2+} is either bound to ferritin for storage following oxidation to Fe^{3+}, or moved out from the cell by iron regulated protein-1 (IREG1) at the basolateral membrane. Ferrous iron is oxidized to Fe^{3+} by hephaestin, and Fe^{3+} binds to transferrin in the blood for circulation to other internal organs.

Similar to mammalian systems, the inhibitory effects of other divalent metals [both essential (e.g., Zn^{2+} and Co^{2+}) and non-essential (Cd^{2+} and Pb^{2+})] on iron transport have been reported in *Xenopus* oocytes expressing the gill DMT1 transcripts (both *Nramp-β* and *–γ* isoforms) of rainbow trout (Cooper *et al.*, 2007). Cooper *et al.* (2007) also reported that Nramp-β can transport cadmium into the oocytes. In addition, it has been shown that exposure to waterborne cadmium inhibits branchial iron absorption in zebrafish (Bury and Grosell, 2003b), and zebrafish fed with a low iron diet exhibit an increase in the intestinal expression of DMT1 and an increase in the accumulation of cadmium in the liver (Cooper *et al.*, 2006b). These findings provide circumstantial evidence that DMT1 is probably involved in the absorption of cadmium in fish. However, the physiological role of DMT1 in the transport of iron as well as other divalent metals, including toxic metal such as cadmium, in the gut of freshwater fish remain to be investigated.

1.6. Physiological effects of cadmium exposure on freshwater fish – waterborne vs dietary

The physiological effects of waterborne cadmium exposure on freshwater fish are well documented. The primary effect of acute waterborne cadmium exposure on freshwater fish is disruption of calcium balance, leading to hypocalcaemia (low plasma calcium level) and ultimately death (Wood, 2001). At the cellular level, induction of hypocalcaemia by waterborne cadmium is associated with the impairment of active calcium transport by the competitive blockade of apical calcium channels and/or selective inhibition of basolateral calcium-ATPase transporters by cadmium in gill chloride cells (Verbost *et al.*, 1987; Verbost *et al.*, 1989). In addition, chronic exposure to sublethal waterborne cadmium level disturbs respiration (Majewski and Giles, 1981) and ion regulation (Haux and Larsson, 1984; McGeer *et al.*, 2000), and

increases the stress response in fish (Brodeur *et al.*, 1998; Lacroix and Hontela, 2004). However, fish develop an increased tolerance to acute cadmium toxicity during acclimation to chronic waterborne cadmium exposure (Hollis *et al.*, 1999; Stubblefield *et al.*, 1999), probably due to the induction of cadmium-sequestering proteins (e.g., metallothionein) which bind to cadmium and keep it in a metabolically inactive form (Hollis *et al.*, 2001; Chowdhury *et al.*, 2005).

Dietary cadmium exposure also contributes significantly to cadmium accumulation in freshwater fish (Szebedinszky *et al.*, 2001; Chowdhury *et al.*, 2004a; Ng and Wood, 2008); however its toxicological implications remain largely unknown. The current information on the effects of dietary cadmium exposure on ion homeostasis in fish is contradictory as both no effects and modest disturbances have been reported (Pratap *et al.*, 1989; Pratap and Bonga, 1993; Chowdhury *et al.*, 2004b). Nonetheless, chronic exposure to environmentally relevant dietary cadmium has been found to inhibit the growth rate (Hansen *et al.*, 2004; Ng and Wood, 2008) and to increase metallothionein level in target organs of fish (Berntssen *et al.*, 2001). In addition, dietary cadmium exposure was shown to decrease hemoglobin and haematocrit (the proportion of red blood cells to the total volume of the blood) levels in rockfish (*Sebastes schlegeli*) (Kim *et al.*, 2004), which are the symptoms of iron deficiency. Since cadmium can interact with intestinal iron transport (*via* DMT1) as well as systemic iron handling (e.g., binding to transferrin and ferritin), dietary cadmium exposure may affect iron metabolism and homeostasis in fish.

1.7. Research objectives

Rationale

Although recent molecular evidence suggests that the dietary iron absorption in fish may be similar to that in mammals, the physiological characteristics of dietary iron absorption in freshwater fish are still unknown. In mammals, it is well documented that several different divalent metals [both essential (e.g., copper and zinc) and non-essential (e.g., cadmium and lead)] interact with the iron transport pathway *via* DMT1, and DMT1 is suggested to be important in the absorption of cadmium. However, the potential linkage of iron transport with the absorption of other divalent metals in the fish intestine is virtually unknown. Importantly, iron, copper and zinc play an essential role in cellular metabolism, but can be toxic at elevated concentrations. Cadmium and lead are very toxic to freshwater fish even at low concentrations. Therefore, understanding the mechanisms of dietary divalent metal absorption and interactions in freshwater fish is important. Such interactions may influence the uptake and accumulation of divalent metals, which can have vital nutritional and toxicological importance in freshwater fish, especially in a contaminated environment.

Hypotheses

I hypothesized that (i) the physiological properties of dietary iron absorption in freshwater fish resembles that of mammals; (ii) DMT1 is expressed in the gut of freshwater fish and mediates the uptake of dietary iron; (iii) several other divalent metals (both essential and non-essential) interact with the iron transport pathway *via* DMT1, and this pathway is important in the absorption of dietary cadmium in fish; (iv) exposure to dietary cadmium increases cadmium burden in target organs, and adversely affects the physiology of fish; and (v) if dietary

iron and cadmium are absorbed through the same pathway *via* DMT1, an iron-enriched diet may reduce the absorption of dietary cadmium, thereby potentially ameliorating the effects of dietary cadmium on fish.

Experimental model

The freshwater rainbow trout was used as a model species for this research project for the following reasons: (i) Toxicological sensitivity: Among the freshwater teleost, rainbow trout is one of most sensitive species to metal exposure (US-EPA, 2001); (ii) Experimental manipulations: the larger size of rainbow trout than other freshwater species commonly used in toxicological investigations (e.g., zebrafish, minnows) allowed easier surgical manipulation for investigating intestinal transport properties (e.g., preparation of intestinal sacs, see Chapter 2 and 3) as well as providing a better yield of isolated enterocytes, used for the characterization of cellular metal uptake (Chapter 4 and 5). (iii) Availability of genetic information: The nucleotide sequence of the iron transporter DMT1 has been identified and cloned in the gill of rainbow trout. This information facilitated the examination of gastrointestinal expression of this gene, and allowed the evaluation of the functional properties of the gastrointestinal DMT1 in iron transport and its interactions with other divalent metals (Chapter 2-4). In addition, genes encoding iron-handling protein (transferrin) and key stress-response proteins (e.g., metallothioneins, heat shock proteins) have been cloned and characterized in this species, which allowed the examination of the possible alterations in their expression in response to iron and cadmium interactions (Chapter 6).

Objectives

The overall goal of my thesis was to investigate the physiology of dietary iron absorption and its importance for the uptake and metabolism of other divalent metals, with a particular emphasis on cadmium, in freshwater fish. The specific research objectives and the experimental approach employed are outlined below:

1. *Characterization of the physiological properties of intestinal iron absorption in freshwater fish (Chapter 2).* In this study, an *in vitro* gastrointestinal sac technique was employed to characterize the physiological properties of intestinal iron absorption (both ferric and ferrous) in rainbow trout. This experimental technique allowed evaluation of metal transport into different tissue compartments of the intestine (e.g., metal binding to mucus, absorption into the mucosal epithelium, and transfer into the serosal side). The spatial patterns, and the time- and concentration-dependent profile of intestinal iron absorption, as well as the effects of physio-chemical conditions (e.g., temperature, pH and chelation) on intestinal iron absorption were determined.

2. *Examination of the potential interactions of iron with other divalent metals in the fish intestine (Chapter 3).* By using isolated gastrointestinal sacs, the potential interactive effects of several divalent metals, both essential (copper, zinc, nickel and cobalt) and non-essential (cadmium and lead), on iron absorption (ferric and ferrous iron) were examined. In addition, the possible reciprocal effects of elevated luminal ferrous iron on cadmium and lead accumulation were evaluated.

3. *Characterization of the pharmacokinetic properties of iron uptake, and its interaction with cadmium and lead in isolated fish enterocytes (Chapter 4)*. To investigate the precise pharmacokinetic properties of apical iron uptake and its interactions with cadmium and lead, a more sophisticated *in vitro* experimental system, freshly isolated enterocytes, was employed in this study. This approach allowed the evaluation of apical metal uptake in the intestinal epithelium without the confounding influence of mucus secretion. The kinetic (time- and concentration-dependent profile) and functional (effects of pH, redox state of iron and membrane potential) properties of apical iron uptake were investigated. In addition, the nature of interactions (e.g., competitive or non-competitive inhibition) between iron and cadmium or lead was evaluated. The spatial expression of DMT1 along the gastrointestinal tract was also examined.

4. *Characterization of the mechanisms of cadmium transport in isolated fish enterocytes (Chapter 5).* The mechanisms of intestinal cadmium uptake (iron-dependent and iron–independent) and efflux were investigated using isolated enterocytes as the experimental system. The time- and concentration-dependent profiles of cadmium uptake, as well as the influence of extracellular iron, zinc and calcium on cadmium uptake were examined. In addition, the effects of an organic ligand cysteine and several pharmacological modulators (e.g., calcium channels blockers, ATPase and anionic transporter inhibitors) on cadmium uptake and/or efflux were evaluated.

5. *Examination of the interactive effects of dietary iron and cadmium on iron homeostasis, tissue-specific metal accumulation, and the expression of stress-inducible genes (Chapter 6).* To examine the *in vivo* chronic effects of dietary iron and cadmium interactions, fish were treated for 28 days to four different diet regimes: normal iron (control), high iron, normal iron plus cadmium, and high iron plus cadmium. The effects of dietary cadmium exposure on systemic iron handling (plasma and tissue iron status, hepatic transferrin expression), tissue-specific cadmium accumulation, and expression of stress-inducible genes (metallothioneins and heat shock proteins) in target organs, and how these variables were influenced by elevated dietary iron, were evaluated.

CHAPTER 2: An *in vitro* examination of intestinal iron absorption in a freshwater teleost, rainbow trout (*Oncorhynchus mykiss*)[1]

2.1 Introduction

Iron is an essential nutrient for most life forms, including fish. It is a component of many vital proteins and enzymes such as hemoglobin, myoglobin, cytochrome P450 and mitochondrial electron transport chain enzymes. In fish, a variety of adverse physiological consequences have been reported as a result of iron deficiency, such as anemia (Kawatsu, 1972), poor feed utilization (Gatlin and Wilson, 1986) and decrease in hatching rate (Hirao *et al.*, 1955). Iron can also be toxic if it is in excess because it can generate free radical species which may cause cellular oxidative damage (Crichton *et al.*, 2002). Therefore, the maintenance of iron homeostasis in the body is critically important. However, the precise daily dietary iron requirement for teleost fish is not known. It is believed that the concentration of iron in the diet required to prevent iron deficiency syndromes in fish is in the range of 30–170 mg iron kg^{-1} (Watanabe *et al.*, 1997). It is to be noted though that the absorption efficiency of iron in fish is relatively low (Bury and Grosell, 2003a), therefore iron level incorporated into the commercial fish diet is often higher than the potential requirement in order to ensure enough available iron.

[1] This chapter has been published in the Journal of Comparative Physiology Part B - Biochemical, Systems, and Environmental Physiology 178: 963-975 (2008) under joint authorship with Som Niyogi (University of Saskatchewan)

Much of the information about the intestinal iron absorption in vertebrates is gained from the mammalian systems. In mammals, the regulation of iron homeostasis is primarily governed by intestinal absorption (Andrews, 2000). Dietary ferric iron (Fe^{3+}) complexes are first reduced to ferrous iron (Fe^{2+}) by apical ferric chelate reductase (McKie *et al.*, 2001), and the absorption of ferrous iron into the enterocytes is facilitated by a divalent metal transporter called DMT1 (also termed as Nramp 2 and Sla 11 2a) (Gunshin *et al.*, 1997). Ferric iron can also be reduced to the ferrous form by food ingredients such as ascorbate (Raja *et al.*, 1992). Although separate absorption pathways for ferric and ferrous iron have been recently proposed (Conrad *et al.*, 2000), the mechanism of direct absorption of ferric iron into the enterocytes is not well understood. In mammals, it is suggested that DMT1 is a Fe^{2+}/H^{+} symporter and it functions most efficiently at acidic condition (Gunshin *et al.*, 1997). Interestingly, DMT1 is believed to be capable of transporting several other divalent cations (e.g., Cu^{2+}, Mn^{2+}, Cd^{2+} and Ni^{2+}) apart from ferrous (see review by Garrick *et al.*, 2003). Extrusion of iron from the enterocytes into the blood circulation occurs *via* an iron exporter protein called iron regulated protein-1 (IREG1) [also termed as ferroportin (FPN) and SLC11A3] (McKie *et al.*, 2000).

Recent molecular evidence suggests that iron absorption in the piscine intestine may have some resemblance to the mammalian systems. cDNA sequences that show high similarities to the mammalian iron transporter proteins (e.g., DMT1, IREG1) have been cloned in a number of fish species (see review by Bury and Grosell, 2003a). In rainbow trout (*Oncorhynchus mykiss*), DMT1 transcripts are located prevalently in the gill, intestine and kidney epithelia (Dorschner and Phillips, 1999). Cooper *et al.* (2007) identified two isoforms of DMT1 (*slc11β* and *slc11γ*) in rainbow trout which can transport ferrous iron. They demonstrated that *Xenopus* oocytes expressing either slc11β or slc11γ isoform can efficiently transport ferrous iron at pH 7.4,

whereas ferrous import by slc11β is more sensitive to inhibition by other divalent cations (Cooper *et al.*, 2007). In addition, Cooper *et al.* (2006b) revealed that the transcript levels of DMT1 increase in the gill and intestine of fish treated with a low iron diet. The activity of ferric chelate reductase in the piscine gut has also been recorded recently by Carriquiriborde *et al.* (2004). Taken together, the iron absorption mechanism in the piscine intestine is likely similar to that in the mammals.

Unlike mammals, fish can acquire iron by the gastrointestinal tract as well as by the gill. The ability of the gills to absorb iron has been investigated in a few recent studies (Andersen, 1997; Bury and Grosell, 2003b; Cooper and Bury, 2007). Although the gill epithelium is able to absorb iron to a certain extent, the intestinal epithelium is considered to be the major site of absorption (Watanabe *et al.*, 1997). This is primarily because ferrous iron concentration is usually quite low and ferric iron forms insoluble iron oxides in oxygenated fresh waters (Stumm and Morgan, 1996). However, information on the physiological characteristics of intestinal iron absorption in fish is very limited. Understanding the kinetics and properties of intestinal iron absorption in fish are important because the regulation of iron absorption from the diet probably plays the major role in iron homeostasis. To date, the physiological characterization of intestinal iron absorption has been conducted only in marine fish (Bury *et al.*, 2001). Bury *et al.* (2001) demonstrated that the posterior intestine is the primary site of iron absorption in European flounder (*Platichthys flesus*). They also reported that ferrous iron is preferentially absorbed over ferric iron in the intestine of marine fish, implying that a mammalian DMT1 homolog may be involved in the absorption process. These observations provided some valuable insights into the intestinal iron absorption in fish, however it is to be noted that the chemical environment of the gut in freshwater fish is markedly different from that of marine fish. For example, the intestinal

fluid in freshwater fish has lower pH and about tenfold less bicarbonate/carbonate level relative to that in marine fish (Wilson, 1999). Such differences can enhance the luminal solubility and bioavailability of iron due to reduced inorganic complexation, which can influence the physiology of intestinal iron absorption in freshwater fish.

In the present study, an *in vitro* gastrointestinal sac (gut sac) technique was employed to characterize the physiological properties of intestinal inorganic iron absorption (both ferric and ferrous iron) in freshwater fish, using rainbow trout (*O. mykiss*) as a representative species. The main objectives of this study were threefold: (1) to determine the spatial and temporal patterns of intestinal iron absorption; (2) to characterize the concentration dependent profile of intestinal iron absorption; and (3) to evaluate the effects of physico-chemical condition (e.g., temperature, pH and chelation) upon iron absorption.

2.2. Materials and methods

2.2.1. Fish and experimental solutions

Rainbow trout (*O. mykiss*; 292.6 ± 57.9 g wet weight, mean ± SD, n = 170) were obtained from Lucky Lake fish farm, SK, Canada. Fish were acclimated for at least 4 weeks in the laboratory condition and supplied with aerated, dechlorinated water in a flow-through system. The water temperature (15°C) and photoperiod mimicked natural conditions. Fish were fed Martin's commercial dried pellet feed (5-pt.; Martin Mills Inc., Elmira, ON, Canada; containing 41.0% crude protein, 11.0% crude fat, 3.5% crude fiber, 1% calcium, 0.85% total phosphate, 0.45% sodium) at a ratio of 2% wet body mass daily. To measure the iron concentration in the

feed, 1 g feed was digested in five volumes of 1 N HNO_3 for 48 h at 60°C. The digest was then analyzed for total iron by a flame atomic absorption spectrometer (AAnalyst 800, PerkinElmer, USA) following appropriate dilution. The measured iron level in the feed was 320.3 ± 36.3 mg kg^{-1} (mean ± SD, $n = 5$). Fish were starved for 48 h prior to their use in the experiments.

Iron uptake was measured using a radiotracer method. Radiolabeled iron (as $^{59}FeCl_3$) was obtained from PerkinElmer, USA (specific activity = 72.55 mCi mg^{-1}, in 0.5 M HCl). A stock solution of 1 mM ^{59}Fe was prepared by adding appropriate amount of cold $FeCl_3$ and complexed with 4 mM nitrilotriacetic acid (NTA) in MilliQ water. Since ferric iron is not soluble at physiological pH, optimal solubilization and bioavailability of ferric iron were achieved by complexing with a chelator NTA at a molar ratio of 1:4 (Fe^{3+}:NTA) (Teichmann and Stremmel, 1990). Aliquots of the stock ^{59}Fe solution were then added to the mucosal saline [modified Cortland saline: NaCl 133, KCl 5, $CaCl_2 \cdot 2H_2O$ 1, $MgSO_4 \cdot 7H_20$ 1.9, $NaHCO_3$ 1.9, $NaH_2PO_4 \cdot H_2O$ 2.9 and glucose 5.5 (all in mM)] (Wolf, 1963) to achieve the desired iron concentrations (see below for details) and buffered with 20 mM HEPES, pH 7.4. The specific activity of the mucosal saline was maintained at approximately 1.2×10^6 cpm μM^{-1} total iron. Preparation of ferrous iron was achieved by mixing the ^{59}Fe stock solution, prepared as described above, with the reducing agent sodium ascorbate at a molar ratio of 1:20 (Fe:ascorbate) for 30 min before adding into the mucosal saline. Henceforth, the term ferrous iron will refer to that prepared from ferric iron by this method. All experimental solutions were prepared freshly on the day of experiments. The total iron concentration in the mucosal salines was confirmed by a flame atomic absorption spectrometer (AAnalyst 800, PerkinElmer, USA) using a certified standard for iron (Fisher Scientific, USA).

2.2.2. Intestinal sac preparation

To characterize iron uptake in the intestine of rainbow trout, an *in vitro* gut sac technique was adopted as described by Ojo and Wood (2007). This experimental system has been successfully used recently to characterize the intestinal copper and zinc uptake in freshwater fish (Nadella *et al.*, 2006; Nadella *et al.*, 2007; Niyogi *et al.*, 2007). Briefly, rainbow trout were first euthanized with an over dose of MS-222 (0.25 g l^{-1}). The ventral side was cut open and the entire gastro-intestinal tract was dissected out. Stomach and other internal organs were removed, and the intestinal tract was transferred in the iced-cold modified Cortland saline immediately after dissection. The intestine was squeezed gently and flushed with saline to remove food and feces. Visceral fats and connective tissues were removed with forceps. Then the cleaned intestinal tract was sectioned into anterior, mid and posterior intestine based on the morphological differences (Ojo and Wood, 2007). One end of each segment was sealed with a surgical thread and a 5-cm piece of PE-50 polyethylene tubing was inserted into the other end and secured with a surgical thread to allow the manipulation of mucosal saline.

2.2.3. Concentration and time dependent iron influx and spatial distribution of iron absorption

Approximately 1–2.5 ml (depending on the size and the section of the intestine) of radiolabeled mucosal saline (containing 0.5–20 μM of $^{59}Fe^{2+}$ or $^{59}Fe^{3+}$) was injected into the gut sacs *via* a syringe. The PE-50 tubing was flare sealed and the sac preparations were blotted dry and weighed. Then the gut sacs were incubated for 2 h (except for the time-course study where incubation were conducted for 1–4 h) in either 12 ml (for mid and posterior intestine) or 30 ml

(for anterior intestine) of the modified Cortland saline serving as the serosal bath. Osmolalities of the mucosal and serosal saline were measured using a 5100C vapor pressure osmometer (Wescor Inc., Utah, USA). Osmolalities of the experimental salines were comparable across the range of iron concentrations tested (e.g., serosal saline with 0 μM iron: 270 mOsm; mucosal saline with 20 μM iron: 283 mOsm). Temperature was maintained at 15°C in a water bath (except for the experiment where the effect of increased temperature was assessed, see below). The serosal saline was constantly aerated with 99.5% O_2 and 0.5% CO_2 during the entire exposure period (i.e., *in vivo* P_{CO2} levels in the blood are approximately 3.75 Torr). A sub-sample of the mucosal saline was taken for counting of radioactivity at the beginning of the flux. Following the end of the flux period, the sac preparations were removed from the flux chamber, blotted dry and reweighed for calculation of the fluid transport rates. Subsequently, the gut sacs were drained out completely, cut open by a longitudinal incision and washed in either 5 ml (for mid and posterior intestine) or 10 ml (for anterior intestine) of modified Cortland saline and then in EDTA (1 mM) for 1 min each. The ceca of the anterior sac were carefully squeezed prior to washing to remove radioactive fluid that might have been left inside. The gut sac and the surface mucus were blotted dry using a tissue paper. The mucosal epithelium was gently scraped using a glass slide and collected in a scintillation *via*l. Surface area of the intestinal tissue was determined by tracing its outline on a graph paper (Grosell and Jensen, 1999). The washing solutions plus blotting paper, the mucosal epithelial scrapings, the tissue layer and the serosal saline were analyzed separately for radioactivity on a Wallac 1480 Wizard 3″ gamma counter (PerkinElmer, USA) following the manufacturer's guidelines.

The influx of either ferric or ferrous iron was examined in all of the experiments using the same experimental approach described above. A sample size of five fish per individual

treatment was used for all of the experiments (n = 5 per treatment). To investigate the spatial pattern of iron absorption and its interaction with temperature, all three intestinal segments (anterior, mid and posterior) were used. For other subsequent experiments, only the mid and posterior intestines were used due to the apparent lack of a carrier-mediated transport capacity in the anterior intestine (discussed below).

An influx period of 2 h was selected for all experiments except for the examination of the time course of iron uptake. This is based on our observation that the iron uptake (see Figure 2.3 and Results section) and fluid transport rates (data not shown) became steady at ≥2 h of incubation. Similarly, a concentration of 2 μM of iron was chosen except for the examination of concentration dependent iron uptake. This selection was based on the pilot studies and previous observation in the marine fish (Bury *et al.*, 2001). Fluid transport rates were measured in all experimental treatments in order to examine whether the integrity of the gut tissue was damaged or deteriorated during gut sac preparations and/or experimentations.

2.2.4. Effects of temperature and mucosal pH on ferric and ferrous iron absorption

The temperature-dependant ferric and ferrous iron uptake rate in the anterior, mid and posterior intestine were examined at 15°C (acclimation temperature) and 25°C. The desired temperatures were achieved by using a temperature-controlled water bath. This range of temperature allowed evaluation for Q_{10} analysis in trout intestine to understand the kinetic properties of iron absorption (e.g., simple diffusive or carrier-mediated).

To determine whether iron uptake rates in the mid and posterior intestine were influenced by mucosal proton concentration, the mucosal saline was prepared as described previously and then adjusted to pH 6.6, 7.4 and 8.2 using HCl or NaOH, buffered with 20 mM HEPES. These pH ranges were chosen based on a previous molecular study on iron absorption (Cooper *et al.*, 2007). The pH of the serosal saline was maintained at 7.4.

2.2.5. Effects of solvent drag on ferric and ferrous iron absorption

To examine whether solvent drag contributed to ferric or ferrous iron uptake, 350 mM mannitol was added into the mucosal saline which increased the osmolality of the saline by approximately 300 mOsm. Gut sac preparations from the mid and posterior intestine were infused with the radiolabeled mucosal saline with normal (270 mOsm) and high (570 mOsm) osmolality, then incubated and sampled as detailed above.

2.2.6. Effects of iron chelators, nitrilotriacetic acid and desferrioxamine mesylate, on ferric and ferrous iron absorption

To evaluate whether NTA, a common metal chelator, affects the rate of ferrous iron uptake in isolated mid and posterior intestine, 2 μM radiolabeled ferrous iron was prepared as described previously (i.e., complexed with NTA and ascorbate) or complexed with 40 μM ascorbate alone for 30 min before mixing with the mucosal saline. Due to the insolubility of ferric iron without complexation at physiological pH (pH 7.4), only the ferrous iron was tested in this set of experiments.

In order to examine the influence of desferrioxamine mesylate (DFO), a specific ferric iron chelator, on ferric and ferrous iron uptake in isolated intestine, a method similar to that described by Bury *et al.* (2001) was adopted. Briefly, after solubilizing the ferric iron with the aid of NTA (in case of preparing ferrous iron, ascorbate was added as well, see above for details), 10 mM DFO was added to the saline and mixed for 30 min prior to experimentation. This condition ensured all of the iron were bound to DFO (Bury *et al.*, 2001). The gut sacs were incubated with radiolabeled saline containing either ferric or ferrous iron (2 μM) in the presence or absence of DFO and incubated and sampled as detailed above.

2.2.7. Calculations and statistical analysis

The rate of fluid transport (FTR, in $\mu l\ cm^{-2}$ tissue h^{-1}) from mucosal to serosal compartments was determined as follows:

$$FTR = (IW - TW) / (ISA \times t) \qquad (2.1)$$

where IW and TW are the initial and final weight of the gut sac preparations in mg, respectively, ISA is the intestinal surface area in cm^2, and *t* is time in hour.

For each gut sac preparation, three intestinal compartments were analyzed for the measurement of iron absorption. The washing solutions plus the blotting paper represented the mucus-bound iron, the epithelial scrapings represented absorption into the epithelial cells (e.g., enterocytes), while the tissue layer plus the serosal saline represented iron transported into the

blood compartment (Nadella *et al.*, 2006). The iron uptake rates (J_{in} as nmol cm^{-2} h^{-1}) into each compartment were calculated using the following equation:

$$J_{in} = \text{Compartment cpm} / (\text{SA x ISA x } t) \quad (2.2)$$

where compartment cpm represents the total ^{59}Fe activity in each compartment as previously described. SA is the initial measured specific activity of ^{59}Fe in the mucosal saline [^{59}Fe counts in cpm divided by total iron (μmol)], ISA is the intestinal surface area in cm^2, and *t* is the time in hour. In the experiment examining the time course of iron absorption, data are presented as total iron accumulation and normalized by the intestinal surface area (nmol Fe cm^{-2}). Hereafter, ferric and ferrous iron transported into the blood compartment (tissue layer plus serosal saline) will represent the true iron uptake unless mentioned otherwise. Q_{10} analysis was performed using the following equation:

$$Q_{10} = (R_2/R_1)^{[10/T_2 - T_1]} \quad (2.3)$$

where R_2 and R_1 are the iron uptake rates at temperatures T_2 and T_1, respectively.

Regression analyses were performed using SigmaPlot (version 10; Point Richmond, CA, USA) to examine any possible relationships among the rates of fluid transport, iron binding to the mucus, iron absorption into mucosal epithelium and iron transport into the blood compartment. Either student's *t*-test or one-way analysis of variance (ANOVA) followed by a least significant difference (LSD) tests was used to identify the differences between groups. All

statistical tests were performed using SPSS for Windows (Ver 15; Chicago, IL, USA). Data are reported as mean ± SEM and differences were considered significant at $p \leq 0.05$.

2.3. Results

2.3.1. Spatial pattern of ferric and ferrous iron uptake

The anterior intestine showed significantly higher rates of iron uptake per unit surface area than the mid and posterior intestine (Figure 2.1a), while no differences were observed between mid and posterior intestine. The rates of ferric iron uptake were comparable to that of ferrous with no statistical differences within any intestinal segments.

The rates of fluid transport in different intestinal segments exhibited similar patterns as of the iron uptake rates. The anterior intestine was characterized by significantly higher fluid transport rates (Figure 2.1b), while the fluid transport rates between mid and posterior intestine were comparable. The fluid transport rates associated with either ferric or ferrous iron had no statistical differences in any intestinal segments.

An analysis of the relative distribution of iron in different compartments (mucus, epithelial cells, and tissue plus serosal saline) revealed that the partitioning of ferric and ferrous iron was similar among different intestinal compartments. Typically 55–70% was in the mucus bound fraction, 5–15% was in the mucosal epithelium and 20–40% was in the tissue layer plus serosal saline (Appendix Figure A1).

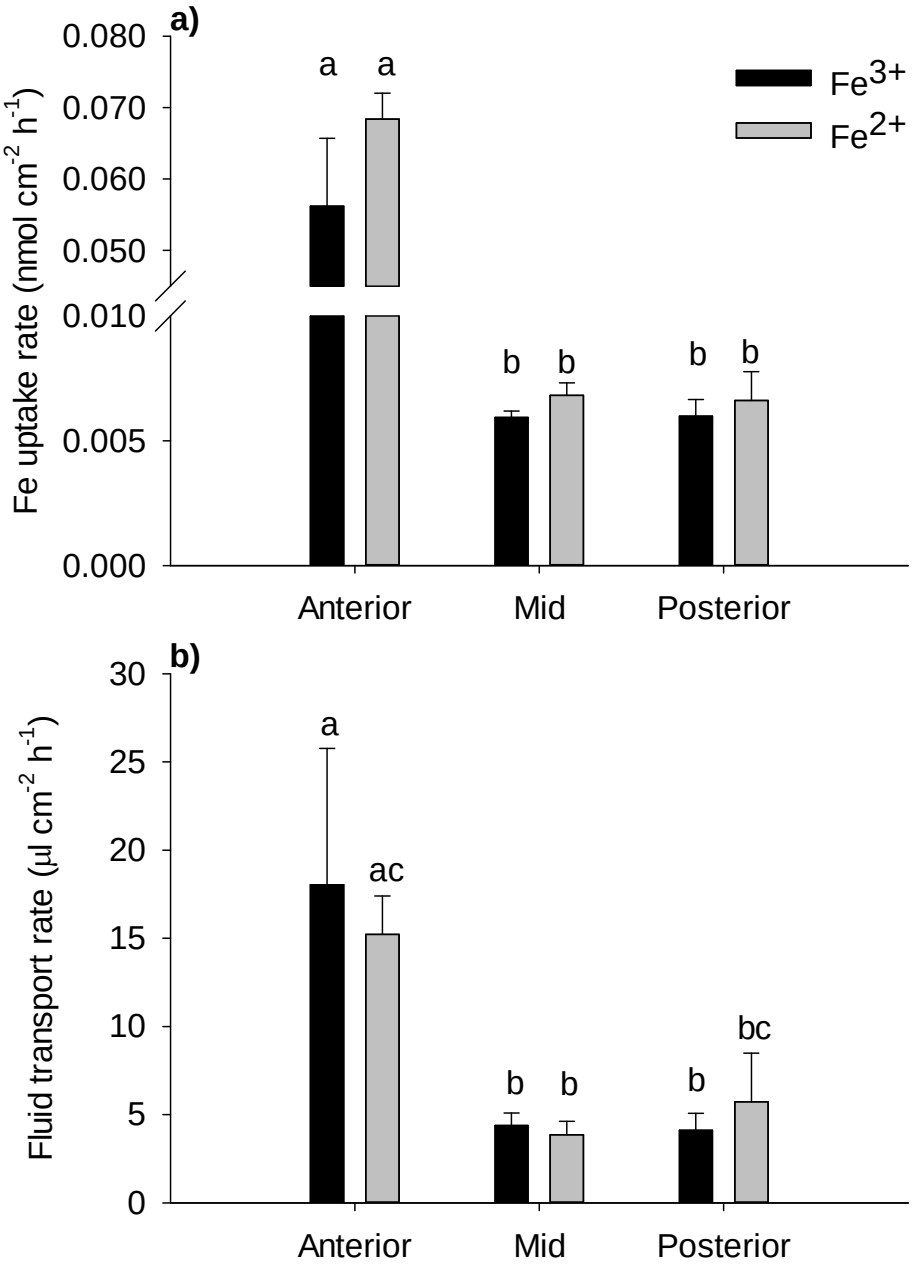

Figure 2.1: **(a)** The iron uptake rates and (**b)** fluid transport rates in the isolated anterior, mid and posterior intestine of rainbow trout, exposed to either 2 µM of ferric (Fe^{3+}) or ferrous (Fe^{2+}) iron for 2 h at 15°C. Bars labeled with different letters are significantly different (One-way ANOVA followed by a post-hoc LSD test; $p \leq 0.05$). Values are mean ± SEM ($n = 5$).

2.3.2. Effects of temperature on ferric and ferrous iron uptake

The increase in temperature from 15 to 25°C increased the rates of ferric and ferrous iron uptake in both mid and posterior intestine, although statistical significance was recorded only for ferric iron in the mid intestine (Figure. 2.2a and b). However, the increase in temperature did not affect the uptake rates of either ferric or ferrous iron in the anterior intestine (Figure 2.2a and b). The calculated Q_{10} values for ferric iron uptake in the anterior, mid and posterior intestine were 1.00, 1.53 and 1.52, respectively (Figure 2.2a). The Q_{10} values for ferrous iron uptake in the anterior, mid and posterior intestine were 0.81, 1.53 and 2.20, respectively (Figure 2.2b). No significant change in fluid transport rates was recorded between 15 and 25°C in the anterior, mid and posterior intestine (data not shown).

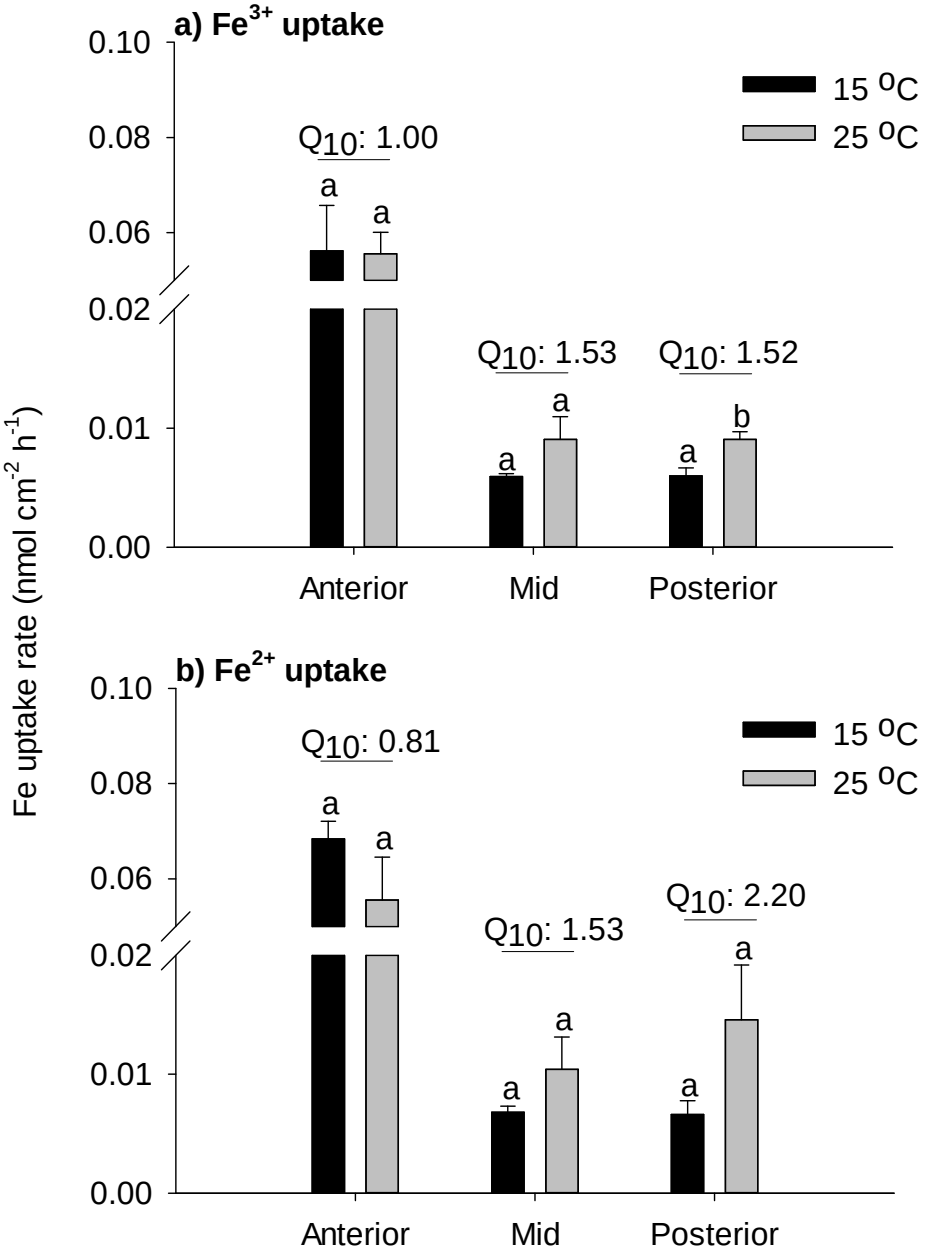

Figure 2.2: Influence of temperature on the rates of **(a)** ferric (Fe^{3+}) and **(b)** ferrous (Fe^{2+}) iron uptake in the isolated anterior, mid and posterior intestine of rainbow trout, exposed to 2 μM iron for 2 h. Bars labeled with different letters are significantly different within the same intestinal segment (Student's *t*-test; $p \leq 0.05$). The temperature coefficient (Q_{10}) are reported. Values are mean ± SEM (n = 5).

2.3.3. Time course of ferric and ferrous iron accumulation

Figure 2.3 shows the time course of ferric and ferrous iron accumulations over the range of 1–4 h. The accumulation of ferric iron in mid and posterior intestine did not change significantly over the range of 1–4 h (Figure 2.3a). The accumulation of ferrous iron became steady at 2 h (Figure 2.3b), although there was an increase at 4 h in the posterior intestine. No statistical differences were observed among the fluid transport rates over the range of experimental period tested in the mid and posterior intestine exposed to either ferric or ferrous iron (data not shown).

An analysis of partitioning of iron over time revealed that the accumulation of ferric iron was constant in the mucosal epithelium and in the tissue layer in both mid and posterior intestine, whereas increasing in the serosal saline over time (Figure 2.4a and b). Similarly, the accumulation of ferrous iron was steady in the mucosal epithelium and in the tissue layer except an increase at 4 h (Figure 2.4c and d). The accumulation of ferrous iron in the serosal saline increased with increasing incubation time.

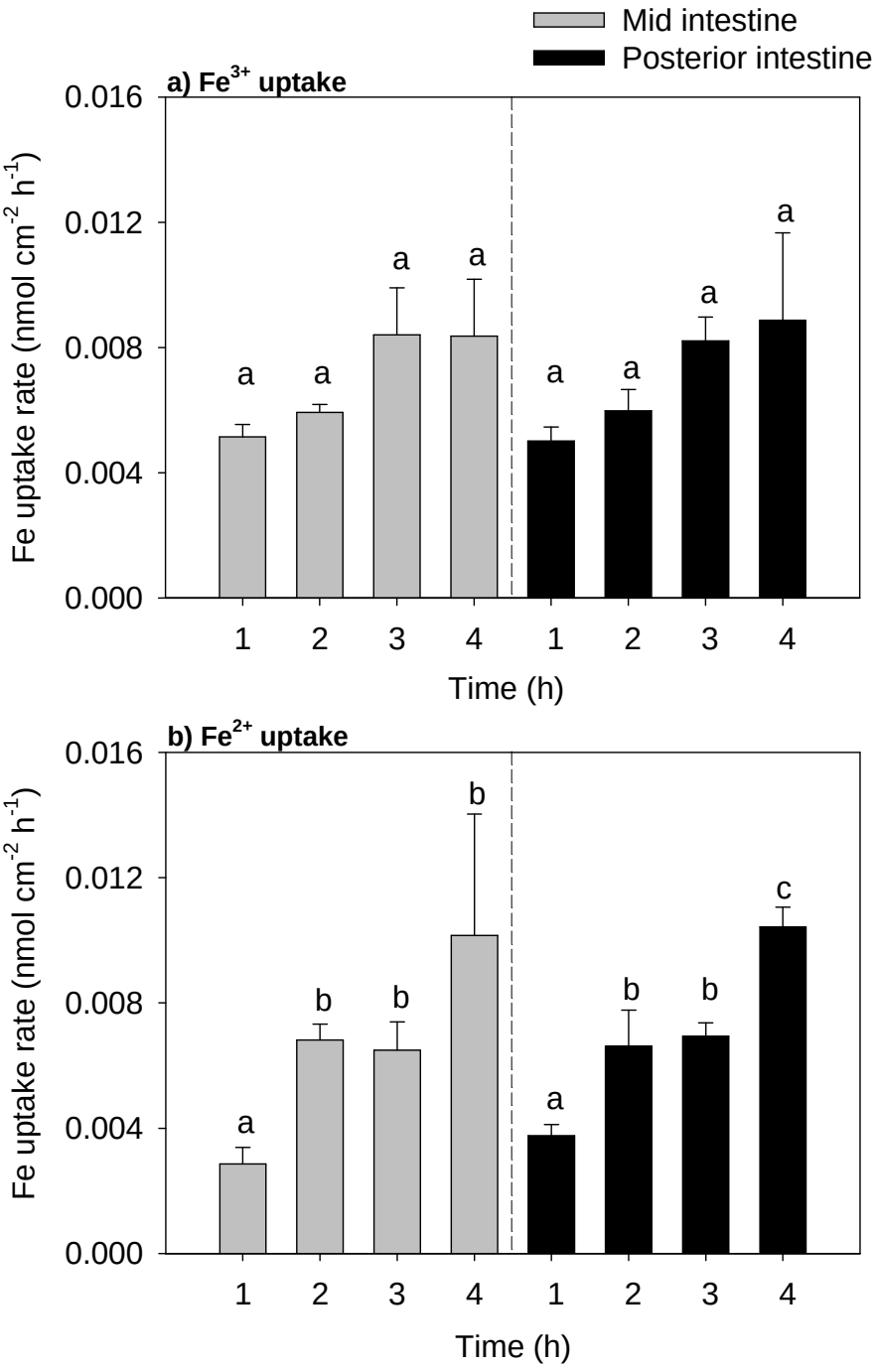

Figure 2.3: The time course of iron accumulation in the isolated mid and posterior intestine of rainbow trout exposed to 2 μM of either (**a)** ferric (Fe^{3+}) or (**b)** ferrous (Fe^{2+}) iron for 1, 2, 3 and 4 h at 15°C. Bars labeled with different letters are significantly different within the same intestinal segment (One-way ANOVA followed by a post-hoc LSD test; $p \leq 0.05$). Values are mean ± SEM (n = 5).

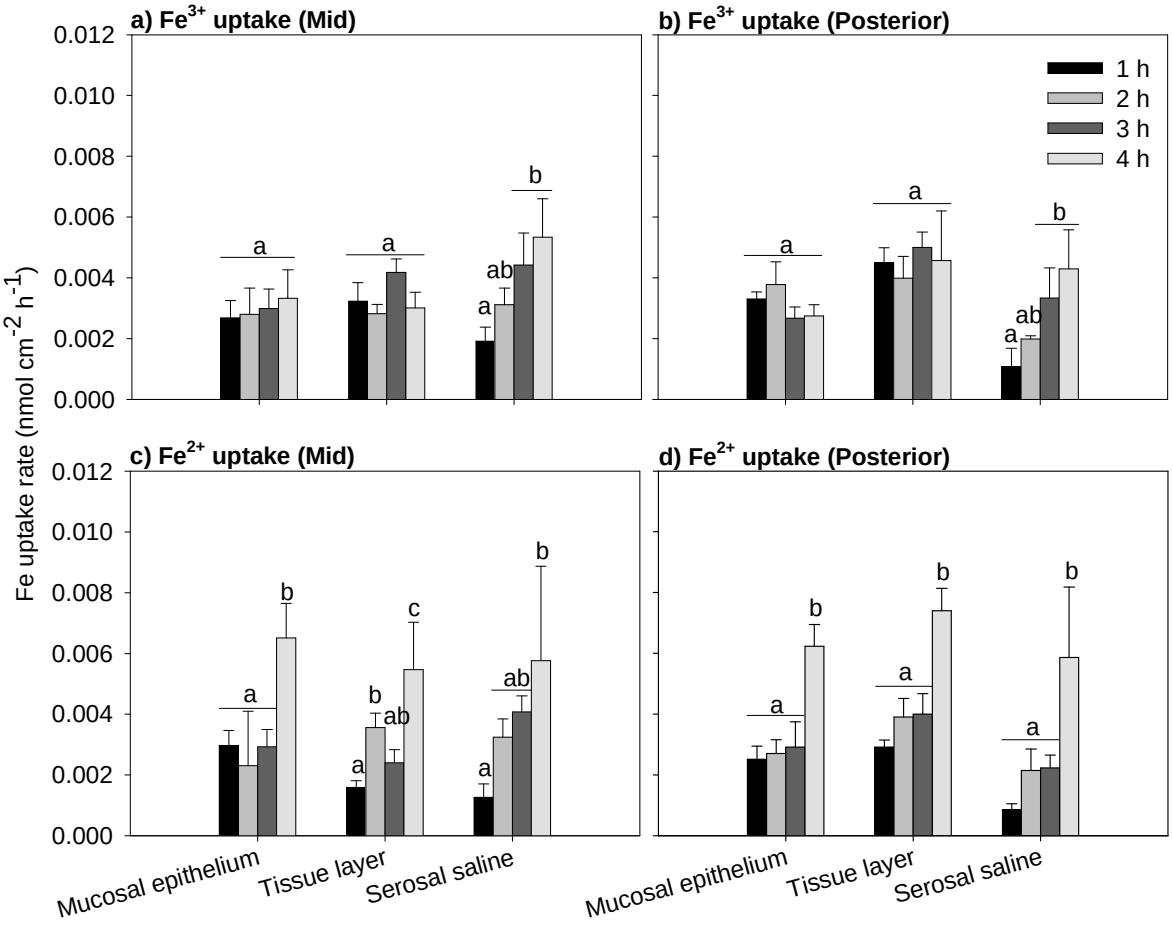

Figure 2.4: Partitioning of ferric (Fe^{3+}) and ferrous (Fe^{2+}) iron into the mucosal epithelium, tissue layer and serosal saline in the **(a, c)** mid and **(b, d)** posterior intestine of rainbow trout, after 1, 2, 3 and 4 h of exposure to 2 μM either Fe^{3+} or Fe^{2+} at 15°C. Bars labeled with different letters are significantly different within the same partition (One-way ANOVA followed by a post-hoc LSD test; $p \leq 0.05$). Values are mean ± SEM ($n = 5$).

2.3.4. Concentration dependent ferric and ferrous iron uptake

The uptake of ferric and ferrous iron in both mid and posterior intestine appeared to increase in a linear fashion with respect to the luminal iron concentrations tested (Figure 2.5a and b). It is important to note here that although both ferric and ferrous uptake seemed to have a saturable profile at low luminal iron concentration range (0–5 μM), the high variability of data precluded the characterization of uptake kinetics. The mid and posterior intestine exhibited similar iron uptake rate (both ferric and ferrous) at each luminal iron concentration with no statistical difference. In both mid and posterior intestine, no statistical differences were recorded between the uptake rates of ferric and ferrous iron at ≤15 μM of luminal iron concentrations. However, the uptake rate of ferrous iron was significantly greater than that of the ferric iron at 20 μM.

2.3.5. Effects of solvent drag on ferric and ferrous iron uptake

The addition of 350 mM mannitol in the mucosal saline reversed the direction of net fluid transport (i.e., from serosal to mucosal compartment as opposed to mucosal to serosal compartment) in both mid and posterior intestine exposed to either ferric or ferrous iron (Appendix Figure A2). However, mannitol treatments had no significant effect on ferric and ferrous iron uptake rates in these intestinal segments ($p > 0.05$) (Appendix Figure A2).

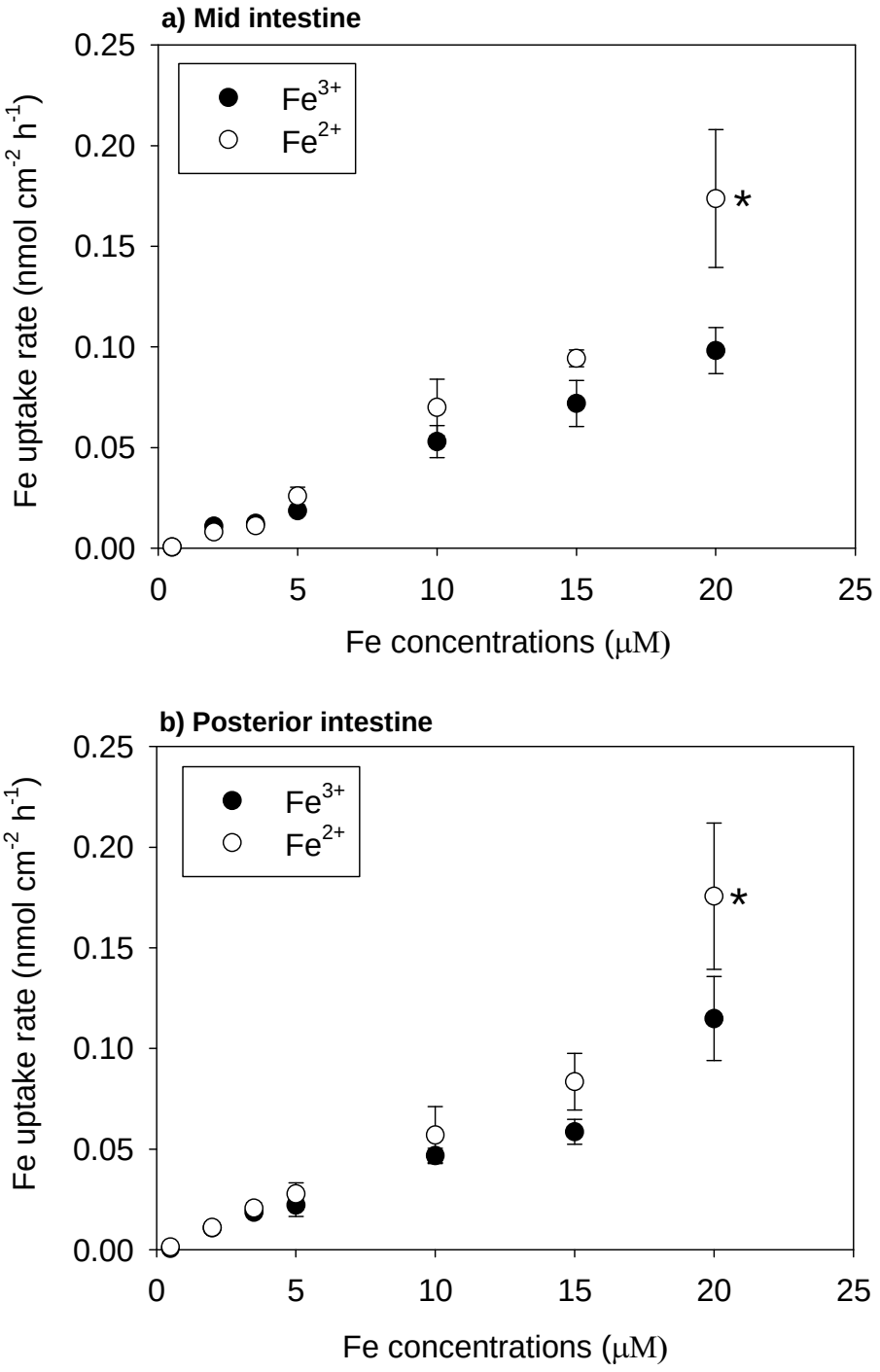

Figure 2.5: The concentration-dependent ferric (Fe^{3+}) and ferrous (Fe^{2+}) iron uptake in the isolated **(a)** mid and **(b)** posterior intestine of rainbow trout. An asterisk indicates the uptake rate of Fe^{2+} in either the mid or posterior intestine was significantly greater than that of Fe^{3+} at 20 μM (Student's *t*-test; $p \leq 0.05$) Values are mean ± SEM ($n = 5$).

2.3.6. Effects of mucosal pH and iron-chelators on iron uptake

The mucosal saline adjusted to pH 8.2 significantly reduced the rates of ferric and ferrous iron uptake in both mid and posterior intestine (Figure 2.6a and b). About 65% reduction of the ferric and ferrous iron uptake rates was observed in both segments. In contrast, a decrease in mucosal pH from 7.4 to 6.6 had no influence on the ferric and ferrous iron uptake rates in either intestinal segment.

The uptake rates of ferrous iron in the presence or absence of NTA were not statistically different in either mid or posterior intestine (Figure 2.7a). Similarly, the addition of DFO had no effect on the rates of ferric and ferrous iron uptake in any intestinal segment (Figure 2.7b).

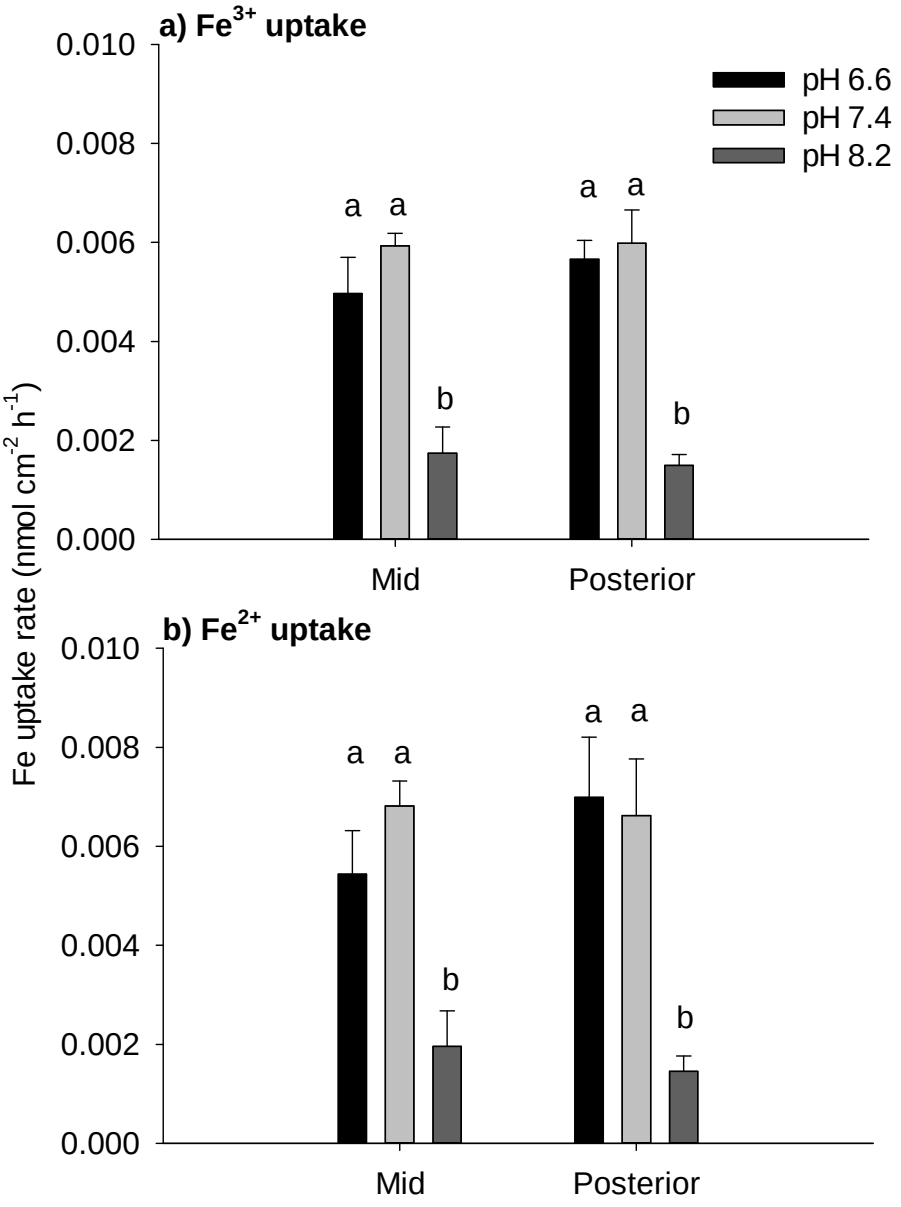

Figure 2.6: Influence of mucosal pH on the rates of **(a)** ferric (Fe^{3+}) and **(b)** ferrous (Fe^{2+}) iron uptake in the isolated mid and posterior intestine of rainbow trout exposed to 2 μM iron for 2 h at 15°C. Values are mean ± SEM ($n = 5$). Bars labeled with different letters are significantly different within the same intestinal segment (One-way ANOVA followed by a post-hoc LSD test; $p \leq 0.05$)

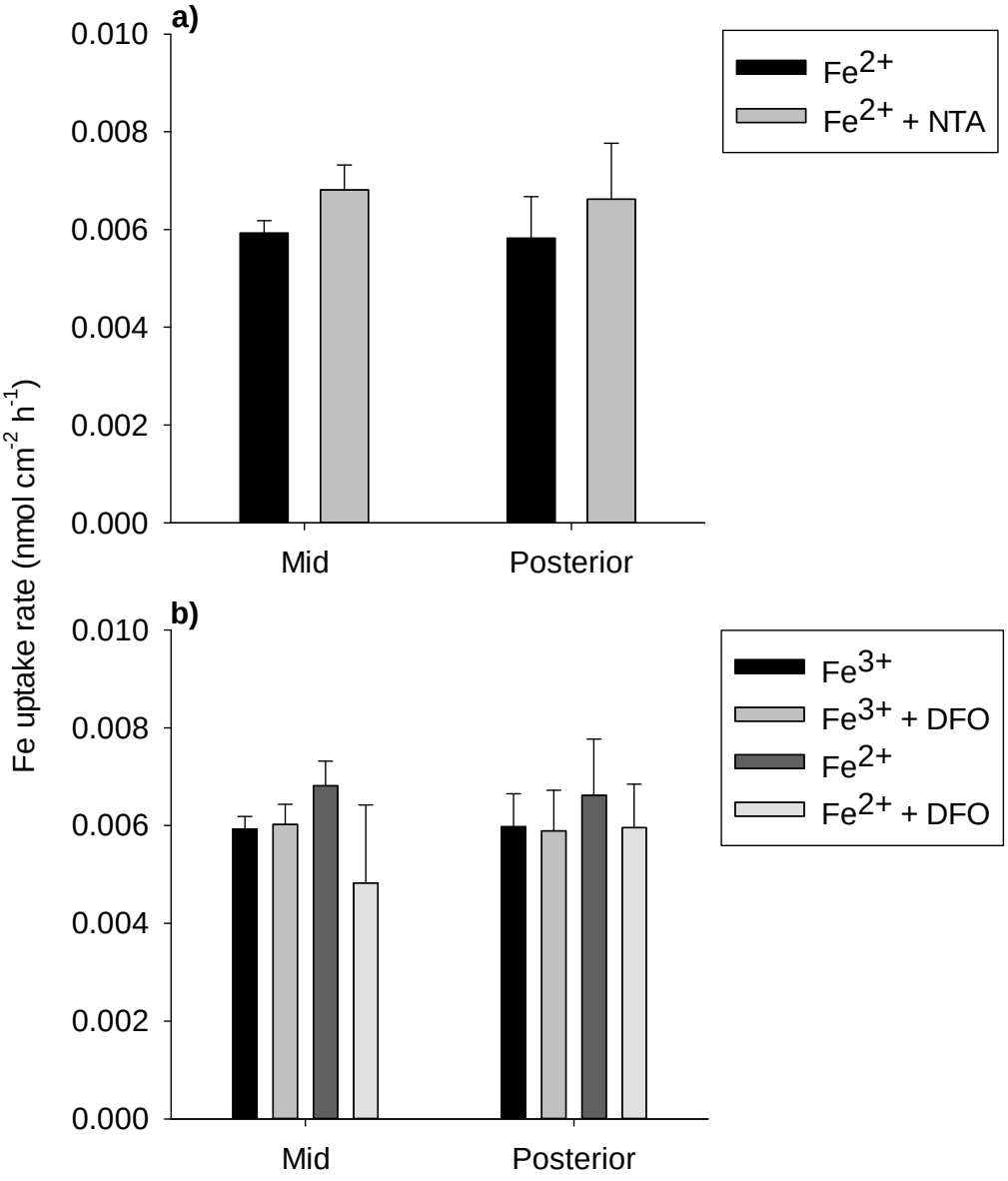

Figure 2.7: Influence of iron-chelators, **(a)** nitrilotriacetic acid (NTA) on the ferric (Fe^{3+}) iron uptake, and **(b)** desferrioxamine mesylate (DFO) on both the Fe^{3+} and ferrous (Fe^{2+}) iron uptake in the isolated mid and posterior intestine of rainbow trout exposed to 2 μM iron for 2 h at 15°C. Values are mean ± SEM (n = 5). No statistical difference was recorded among the treatments

2.3.7. Relationships among the rates of fluid transport, iron binding to mucus, mucosal epithelium iron absorption and iron transport into the blood compartment

Regression analyses were employed in order to examine whether or not the iron transport (both ferric and ferrous) into the blood compartment (tissue layer plus serosal saline) of the anterior, mid and posterior intestine is dependent on fluid transport. In the anterior intestine, no significant relationship was observed ($p = 0.30$). For the regression analysis in the mid and posterior intestine, the data were pooled because these intestinal segments exhibited similar iron uptake rates (see Figure 5a and b). Similarly, the rates of fluid transport and iron transport into the blood compartment had no significant relationship in these segments ($p = 0.88–0.94$). In addition, the relationships between either the rates of iron binding to mucus or the rates of iron absorption into the mucosal epithelium and the rate of iron transport into the blood compartment have also been examined. In the anterior intestine, no significant relationships were observed ($p = 0.40–0.49$). However, significant positive relationships with either the rates of iron binding to the mucus (Figure 8a and b) or the rates of iron absorption into the mucosal epithelium (Figure 8c and d) to the rates of iron transport into the blood compartment were observed ($p < 0.001$).

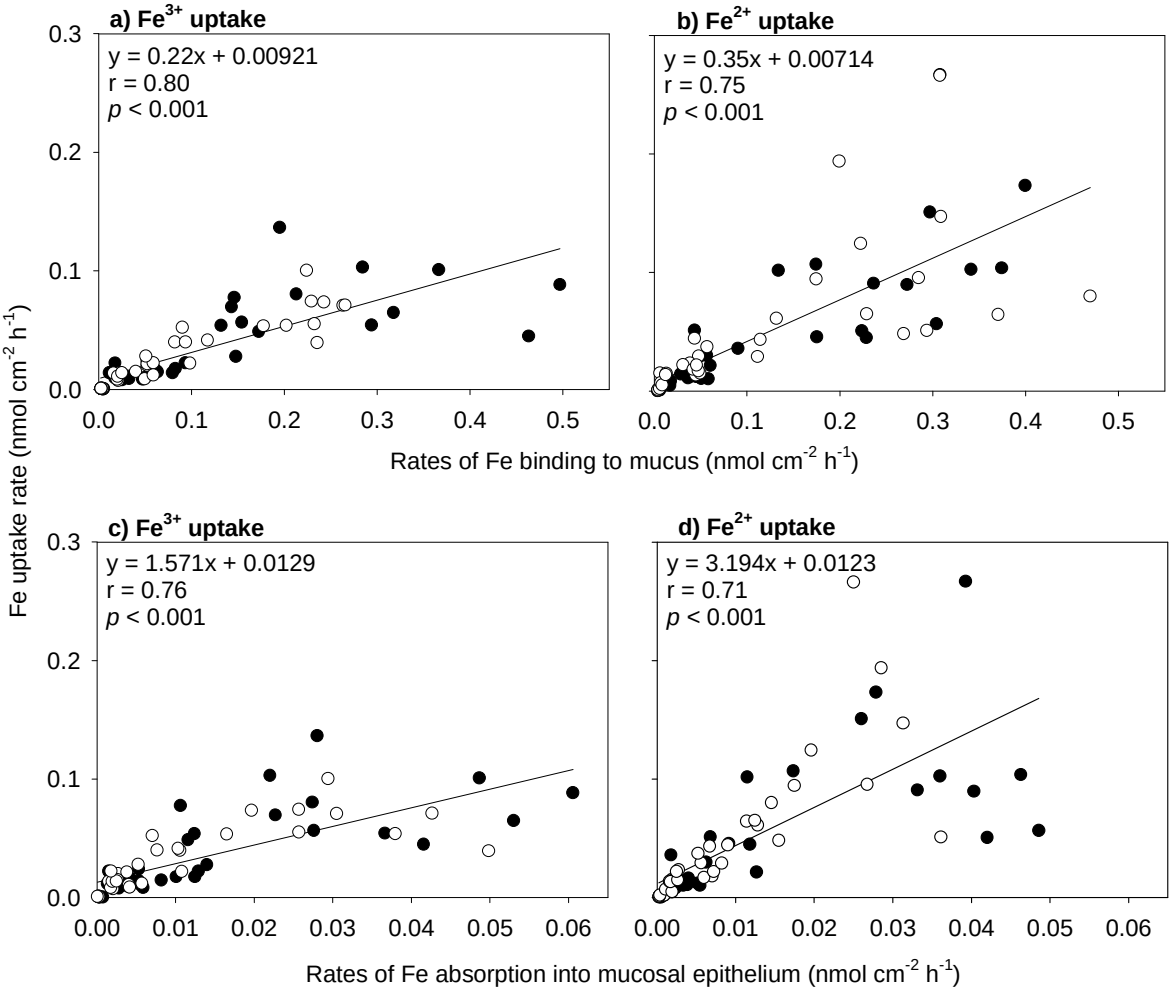

Figure 2.8: Relationships between the rates of iron binding to mucus or the rates of iron absorption into the mucosal epithelium of rainbow trout with the rates of ferric (Fe^{3+}) **(a, c)** or ferrous (Fe^{2+}) **(b, d)** iron uptake, respectively (pooled data from the isolated mid and posterior intestine, $n = 70$ for all analyses)

2.4. Discussion

To the best of our knowledge, this is the first study to examine the physiological characteristics of intestinal iron absorption in a freshwater teleost fish. Our results suggested that the rate of iron absorption (both ferric and ferrous) in the anterior intestine is significantly higher than that in the mid and posterior intestine. However, iron uptake in the anterior intestine occurs probably *via* a simple diffusive pathway, whereas a carrier-mediated process is likely involved in the mid and posterior intestine. In addition, the accumulation of iron in the mucosal epithelium and the tissue layer was fairly constant in both mid and posterior intestine over the range of exposure time, further suggesting the presence of a physiologically regulated process. We also found that ferrous iron is more bioavailable than ferric iron in piscine intestine, but only at higher luminal iron level. In addition, we revealed that the decrease in luminal proton gradient significantly reduced the absorption of both ferric and ferrous iron, and the chelation of iron did not influence the intestinal iron absorption.

Several studies in freshwater fish have demonstrated that the anterior intestine plays an important role in metal absorption due to its greater size and surface area (Clearwater *et al.*, 2000; Nadella *et al.*, 2006; Ojo and Wood, 2007). Ojo and Wood (2007) reported that the absorption of essential metals such as copper and zinc is highest in the anterior intestine, and about equal in the mid and posterior intestine. Interestingly, we observed similar spatial distribution of iron absorption in rainbow trout, with higher iron uptake in the anterior intestine compared to that in the mid and posterior intestine. This scenario is similar to the mammals where iron uptake occurs primarily in the anterior region (Trinder *et al.*, 1999). In contrast, Bury *et al.* (2001) observed that the intestinal iron absorption in a marine fish European flounder occurs predominantly in the

posterior intestine under *in vivo* conditions. Their finding is somewhat surprising because high pH and high bicarbonate/carbonate content in the posterior intestine of the marine fish are expected to hinder iron bioavailability and absorption (Bury *et al.*, 2001). Apart from the difference in species, the discrepancy between the results of Bury *et al.* (2001) and our study can be attributed to the difference in the experimental approaches. It is worth noting that Bury *et al.* (2001) did not observe any regional differences in intestinal iron absorption using *in vitro* gut sac technique. It is possible that their *in vivo* iron uptake study may have been influenced by luminal content and gut chemistry. Although the anterior intestine appears to have the highest rate of iron uptake in our study, the situation may differ under *in vivo* condition. For example, iron may be more bioavailable at the acidic environment of stomach, and the iron concentrations in the chyme may vary in different parts of the gut *in vivo*. The spatial distribution for iron absorption in freshwater fish under *in vivo* conditions awaits further investigations.

The precise mechanism of fluid absorption in the piscine gut is not very well understood. It has been proposed that fluid absorption in piscine gastrointestinal tract is driven by the active transport of ions which creates high local osmolality and draws water from the lumen *via* transcellular and/or paracellular pathway (Loretz, 1995). Our results suggested that fluid transport rate in the anterior intestine was significantly higher than that in the mid and posterior intestine. Previous studies have also shown that anterior intestine is the primary site for fluid absorption in fish (Bergman *et al.*, 2003; Ojo and Wood, 2007). Ojo and Wood (2007) reported that the fluid transport rate in the anterior intestine of rainbow trout is approximately 9.9 μl cm^{-2} h^{-1}, while that in the mid and posterior varies between 2–3 μl cm^{-2} h^{-1}. The fluid transport rates associated with either ferric or ferrous iron in the anterior, mid and posterior intestine in our study are also consistent with their findings.

In the present study, we observed that the rates of fluid transport in the anterior, mid and posterior intestine exhibited somewhat similar pattern to that of the iron uptake (see Figure 2.1), raising the possibility that iron uptake in these segments may be positively influenced by fluid transport (e.g., solvent drag). However, our regression analyses suggested that the fluid transport and iron transport (both ferric and ferrous) had no significant relationship in any intestinal segments, indicating that iron uptake was independent of fluid transport. The influence of solvent drag was further examined in the mid and posterior intestine by reversing the direction of net fluid transport. Similarly, no significant effect of reversed fluid transport on either ferric or ferrous iron uptake was recorded. These observations corroborated the notion that iron uptake in the isolated intestine was not likely linked to the intestinal fluid transport. Our results are consistent with the findings of Ojo and Wood (2007) that the fluid transport rates are not influenced by the presence of different metals in the intestinal fluid in trout.

In order to characterize the iron absorption process in the anterior, mid and posterior intestine of the trout, the influence of increased temperature upon the intestinal iron absorption was examined, and Q_{10} values were derived. Q_{10} values greater than 1.5 are generally considered to represent a biologically mediated process, while a Q_{10} below 1.5 usually indicates a process dependent on the physicochemical properties of the reaction constituents (Hoar, 1983). Our results suggest that iron absorption in the anterior intestine occurs likely through a non-specific pathway, such as simple diffusion ($Q_{10} \approx 1$), whereas a carrier-mediated pathway is probably involved in the mid and posterior intestine ($Q_{10} \geq 1.5$). Our observations were quite similar to marine fish where a carrier-mediated uptake of iron in the posterior intestine was demonstrated (Bury *et al.*, 2001). It is to be noted that the Q_{10} values derived in our study might have been somewhat underestimated because of possible tissue deterioration at the upper temperature.

Partitioning of iron accumulation among different compartments (mucosal epithelium, tissue layer and serosal saline) in both mid and posterior intestine provided further evidence that iron absorption is physiologically regulated. Accumulation of ferric and ferrous iron in the mucosal epithelium and in the tissue layer was consistent over the range of experimental period tested except an increase with ferrous iron at 4 h. The consistency of iron accumulation in these intestinal compartments suggests that entry of iron into the mucosal epithelium and extrusion of iron into the tissue layer were a physiologically regulated process. The apical and basolateral iron transporters in the enterocyte, DMT1 and IREG1, are possible candidates responsible for these processes (Donovan *et al.*, 2000; Cooper *et al.*, 2007). Since the tissue layer apparently has no ability to regulate iron movement into the serosal saline, it is not surprising to see that accumulation of both ferric and ferrous iron in the serosal saline increased with increasing incubation time. Taken together, these observations implied that mucosal epithelium (e.g., enterocytes) probably plays an important role in regulating dietary iron absorption in freshwater fish.

The uptake of ferric and ferrous iron in the mid and posterior intestine appeared to be linear over the entire range of iron concentration tested (0–20 μM), while the uptake rate of ferrous iron was significantly greater than that of ferric iron at high luminal iron concentration (20 μM). A previous study on intestinal iron absorption in a marine fish also demonstrated that ferrous iron is more bioavailable than ferric iron (Bury *et al.*, 2001). The linear uptake of iron in trout intestine also conformed to the findings in the marine fish (Bury *et al.*, 2001). In mammals, the non-saturable ferrous iron uptake has also been reported (Worthington *et al.*, 2000). It has been suggested that the iron transporter has a predominant facilitated diffusional component which is similar to other transporters for riboflavin and biotin uptake (Said and Ma, 1994;

Worthington *et al.*, 2000). This physiological property may allow fish to respond to great increases in luminal iron concentrations, increasing the effective concentration range of uptake, and thereby the dynamic range of transport.

In mammals, the apical absorption of ferrous iron is mediated by a Fe^{2+}/H^{+} symporter called DMT1 (Gunshin *et al.*, 1997). A few recent molecular studies have confirmed the presence of a mammalian DMT1 homolog in fish and its functional role in iron absorption (Dorschner and Phillips, 1999; Donovan *et al.*, 2002; Cooper *et al.*, 2007). Gunshin *et al.* (1997) suggested that pH 5.5 is the most favorable condition for DMT1 function, while a suboptimal pH of 7.4–7.5 has also been recently reported (Picard *et al.*, 2000; Thomas and Oates, 2004). In the present study, when luminal pH was increased from 7.4 to 8.2, both ferric and ferrous iron uptake rates reduced significantly. This indicates that the iron uptake was coupled with a proton gradient which resembles the characteristics of DMT1. Since an increase in pH inhibited both ferric and ferrous absorption, the absorption of ferric iron likely occurred through the same pathway as ferrous iron after apical reduction (discussed below). On the other hand, the iron uptake rates were similar when pH was decreased from 7.4 to 6.6. Our results corroborated the findings of Cooper *et al.* (2007) that DMT1 in freshwater fish can operate efficiently with a mild proton gradient. It is important to note here that the pH of the intestinal lumen in freshwater rainbow trout is about 7.3 (Vielma and Lall, 1997). Therefore, the maintenance of iron transporting efficiency at circumneutral pH is physiologically beneficial to fish.

In mammals, the apical ferric chelate reductase plays an important role in iron absorption because the majority of dietary iron exists in the form of ferric iron complexes, which must be reduced to yield ferrous iron before iron can be successfully transported by DMT1 (McKie *et al.*,

2001). The activity of ferric chelate reductase has been recorded in the intestine of rainbow trout (Carriquiriborde *et al.*, 2004), while the role of this reductase in facilitating branchial ferric iron uptake in zebrafish has also been implied (Bury and Grosell, 2003b). However, Cooper and Bury (2007) demonstrated that the branchial ferric iron uptake in rainbow trout was significantly inhibited by complexing waterborne iron with fairly high affinity iron-chelators such as NTA and DFO [the affinity constants (log K) of DFO or NTA to ferric iron are 32.5 and 15.87, respectively (Martell and Motekaitis, 1992)]. They argued that trout gill may not possess the ferric chelate reductase in aiding branchial iron absorption, or its functional capacity may be low. In the present study, we examined whether rainbow trout is able to acquire iron complexed with either NTA or DFO *via* intestine. Interestingly, our results showed that the uptake rate of iron was not affected by iron either complexed with NTA or DFO. These findings suggest that trout is able to acquire chelated iron *via* intestine, which further support the presence and functional capacity of an apical ferric chelate reductase in piscine intestine similar to the mammal systems (McKie *et al.*, 2001). It is worth noting here that Cooper and Bury (2007) used an exceptionally high molar ratio of ferric:NTA (i.e., 1:6250) which might have contributed to the decrease of branchial iron bioavailability. In contrast, a molar ratio of 1:4 (ferric:NTA) was used in the present study which has been shown to be the optimum ratio for examining ferric iron uptake in mammals (Teichmann and Stremmel, 1990). Since iron incorporated in the feed exists predominantly in a chelated form, the ability to acquire chelated iron is apparently essential to fish. Nevertheless, the effect of natural ligands present in the piscine lumen (e.g., amino acids) upon iron bioavailability remains to be explored.

Relationships between the relative distribution of a metal in the luminal environment (e.g., binding to the mucus) and its rate of transport into the blood may have important implications for

gastrointestinal metal uptake and toxicity (Ojo and Wood, 2007). Ojo and Wood (2007) observed that many essential metals such as copper, zinc and nickel as well as the non-essential metal lead exhibited a positive relationship between their binding to the mucus and the transport into the blood compartment. They also found a significant positive relationship between the absorption rate into the mucosal epithelium and the transport rate into the blood compartment for nickel, silver and lead. In the present study, we observed that both the rates of iron (ferric and ferrous) binding to the mucus and absorption into the mucosal epithelium had significant positive relationships with the rate of iron transport into the blood compartment in the mid and posterior intestine. These results suggest that binding to mucus and/or absorption into the mucosal epithelium may serve as a predictor for dietary iron transport in fish. In the mammalian systems, it is generally believed that the affinity of metal species to mucus follows the pattern of $M^{3+} > M^{2+} > M^{1+}$. This strategy is beneficial to mammals because it retards the absorption of highly toxic trivalent metal such as aluminum (Al^{3+}) and other trivalent metal ions that do not have redox potential, thereby protecting against its uptake and toxicity (see review by Powell *et al.*, 1999). However, Cooper *et al.* (2006a) have recently reported that the mucus covering the intestinal epithelia of gulf toadfish bind both ferric and ferrous iron in equal proportion, and the binding is not influenced by pH or anoxic environments. Similarly, we observed that the binding of ferric and ferrous iron to the mucus was comparable across the entire range of luminal iron concentrations tested (e.g., amount of iron binding to the mucus in posterior intestine at 20 μM iron; ferric: 0.48 ± 0.02 nmol cm^{-2}; ferrous: 0.52 ± 0.06 nmol cm^{-2}; $P > 0.5$), suggesting that the valency of iron (Fe^{3+} or Fe^{2+}) does not influence its binding to the mucus. Thus, the lower bioavailability of ferric iron at high concentrations observed in our study could not be attributed

to the immobilization by the mucus, but possibly due to the rate limiting step in absorption and/or in apical reduction.

2.5. Conclusions

In conclusion, the iron uptake rate in the anterior intestine is significantly higher than that in the mid and posterior intestine of rainbow trout. The uptake of iron in the anterior intestine occurs likely *via* a non-specific diffusive pathway whereas the uptake in the mid and posterior intestine occurs probably *via* a carrier-mediated pathway, particularly at low luminal iron concentration range. The similarity in the pattern of time-dependent ferric and ferrous iron accumulation in the mucosal epithelium and tissue layer of mid and posterior intestine further suggests that iron absorption is a physiologically regulated process. The uptake of ferric and ferrous iron appeared to be linear over the entire range of iron concentration tested (0–20 μM). The rates of ferric and ferrous iron uptake are comparable at low luminal iron concentrations but ferrous iron is more bioavailable at high concentration. Both ferric and ferrous iron uptake rates were significantly inhibited when luminal pH was increased to >8, suggesting a proton gradient is essential for the absorption of iron which resembles the characteristics of a mammalian Fe^{2+}/H^{+} symporter (DMT1). Complexation of iron with a general (NTA) or a specific ferric iron chelator (DFO) did not affect the intestinal iron absorption, suggesting that chelation of iron may not influence the intestinal bioavailability of iron. Mucus binding and mucosal epithelial absorption of iron are reliable indicators of dietary iron transport in fish.

CHAPTER 3: The interactions of iron with other divalent metals in the intestinal tract of a freshwater teleost, rainbow trout (*Oncorhynchus mykiss*)[2]

3.1. Introduction

Iron is an essential micronutrient for vertebrates including fish, but can be toxic above the threshold concentration in the body. That is why iron homeostasis needs to be efficiently regulated to prevent deficiency or oversupply. Diet is considered to be the primary source of iron in fish (Carriquiriborde *et al.*, 2004), however the mechanisms of intestinal iron absorption and its homeostatic regulation are not well understood. Much of the information about iron absorption and homeostasis in vertebrates is gained from the mammalian systems.

The pathway of dietary non-heme iron absorption is quite well characterized in mammals. Ferric iron (Fe^{3+}) is first reduced to the ferrous (Fe^{2+}) form by the apical ferric reductase (McKie *et al.*, 2001), and the absorption of Fe^{2+} into the enterocytes occurs *via* the divalent metal transporter-1 (DMT1; also known as DCT1, Nramp2 and Slc11a2) (Gunshin *et al.*, 1997). DMT1 is a proton-coupled (H^+/Fe^{2+} symporter) apical membrane transporter. Interestingly, recent molecular evidence suggests that the mammalian DMT1 is capable of transporting several other divalent metals, both essential [copper (Cu^{2+}), zinc (Zn^{2+}), cobalt (Co^{2+}), nickel (Ni^{2+}) and manganese (Mn^{2+})] and non-essential [cadmium (Cd^{2+}) and lead (Pb^{2+})], in addition to Fe^{2+} (Gunshin *et al.*, 1997; Sacher *et al.*, 2001; Arredondo *et al.*, 2003; Bannon *et al.*, 2003;

---

[2] This chapter has been published in Comparative Biochemistry and Physiology Part C-Toxicology & Pharmacology 150:442-449 (2009) under joint authorship with Som Niyogi (University of Saskatchewan)

Mackenzie and Hediger, 2004). Moreover, it has been demonstrated that iron-deficient diet can increase intestinal DMT1 expression as well as cadmium body burden in rats, thereby implying that the intestinal cadmium uptake may be linked to the uptake of iron (Park *et al.*, 2002; Ryu *et al.*, 2004). It is also important to note that DMT1 may not be the sole transporter for the absorption of dietary divalent metals. There is now molecular evidence suggesting the existence of specific transporters for Zn^{2+} [Zrt/IRT-like protein (ZIP)] and Cu^{2+} [copper transporter-1 (Ctr1)] in mammals (reviewed by Rolfs and Hediger, 1999). Similarly, it has been suggested that Cd^{2+} and Pb^{2+} may enter mammalian cells *via* Ca^{2+} channels (Hinkle *et al.*, 1987; Simons and Pocock, 1987). Cd^{2+} and Pb^{2+} are also known to enter fish gill *via* epithelial Ca^{2+} channels (Verbost *et al.*, 1987; Niyogi and Wood, 2004; Rogers and Wood, 2004), and similar mechanisms may exist in the fish intestine. However, the relative significance of different transporters/channels in the intestinal absorption of various divalent metals is yet to be fully characterized.

Recent physiological and molecular studies have also suggested that DMT1 is likely involved in waterborne and dietary iron absorption in fish. It has been demonstrated that the absorption of iron both by the gills and the intestine is dependent on the proton gradient, and the Fe^{2+} is more bioavailable than Fe^{3+} (Bury and Grosell, 2003b; Kwong and Niyogi, 2008). These properties resemble the functional characteristics of mammalian DMT1. Furthermore, a DMT1 homolog has been identified and cloned in teleosts, which exhibited a high sequence conservation to its mammalian form (Dorschner and Phillips, 1999). In fact, two isoforms of DMT1 (*slc11ß* and *slc11γ*) have been found in the gills of rainbow trout (*Oncorhynchus mykiss*), and it has been demonstrated that both isoforms have the capacity to transport Fe^{2+} when expressed in *Xenopus* oocytes (Cooper *et al.*, 2007). Cooper *et al.* (2007) also revealed that Fe^{2+}

uptake by both DMT1 isoforms can be significantly inhibited by other divalent cations such as Cd^{2+}, Mn^{2+}, Zn^{2+}, Pb^{2+} and Co^{2+}. However, when examined *in vivo* in zebrafish (*Danio rerio*), waterborne iron absorption has been found to be inhibited by cadmium (at a ten-fold higher concentration relative to iron) and not by any other divalent metals (cobalt, nickel, lead, copper, manganese and zinc) (Bury and Grosell, 2003b). This finding suggests that the branchial interactions of divalent metals may be modulated by other physiological processes (e.g., alternative uptake pathways, mucus binding of metals). To the best of our knowledge, the interactions of iron with other divalent metals in piscine intestine have not been investigated. The potential occurrence of a common absorptive mechanism for a range of divalent metals (both essential and non-essential) can have important nutritional and toxicological implications for fish.

In the present study, an *in vitro* gastrointestinal sac (gut sac) preparation was employed to characterize the intestinal interactions of iron with other divalent metals, both essential and non-essential, in rainbow trout. We have previously used this approach to characterize short-term (2–4 h) iron uptake in trout intestine (Kwong and Niyogi, 2008). This approach allows metal uptake to be measured when transport rates remain stable, and to be partitioned into different intestinal compartments (mucus, mucosal epithelium, and blood space) (Ojo and Wood, 2007; Kwong and Niyogi, 2008). Recently, this approach has been used to examine the interactive effects of copper and zinc uptake as well as cadmium and zinc uptake in trout intestine (Ojo and Wood, 2008; Ojo *et al.*, 2009). The primary objectives of this study were: (i) to examine the concentration-dependent inhibitory effect of various divalent metals (copper, zinc, nickel, cobalt, lead and cadmium) on short-term (2 h) iron absorption (both Fe^{2+} and Fe^{3+}) in the anterior, mid and posterior intestines, and (ii) to evaluate the reciprocal effects of elevated iron on the short-term (2 h) accumulation of non-essential divalent metals (cadmium and lead) in different intestinal

segments. Our overall goal was to enhance the understanding of the mechanisms of dietary absorption of various divalent metals in freshwater fish.

3.2. Material and methods

3.2.1. Fish

Rainbow trout (*O. mykiss*, Salmonidae; approximately 300 g wet wt; N = 130) were obtained from Lucky Lake fish farm, SK, Canada. Fish were acclimated for 4 weeks in the laboratory condition at 15°C, and supplied with aerated, dechlorinated water [hardness 157 mg/L, alkalinity 109 mg/L (both as CaCO3), pH 8.1–8.2, and dissolved organic carbon (DOC) 2.2 mg/L] in a flow-through system. Photoperiod mimicked natural conditions. Fish were fed Martin's commercial dried pellet feed (5-pt.; Martin Mills Inc., Elmira, ON, Canada) at a ration of 2% wet body mass daily. The measured metal concentrations in the feed were: Fe 220, Zn 167, Cu 32, Ni 4, Pb 0.1 and Cd 0.07 (all in mg/kg).

3.2.2. Intestinal sac preparations

The intestinal sac preparations and the sampling methods were identical to that described by Kwong and Niyogi (2008). Briefly, fish were euthanized with an over dose of MS-222, and the entire gastrointestinal tract was dissected out immediately. The intestinal tract was then cleaned and sectioned into anterior, mid and posterior intestines based on the morphological differences. One end of each segment was sealed with a surgical thread, and a 5-cm piece of PE-50 polyethylene tubing was inserted into the other end and secured with a surgical thread. The

entire surgical procedure was carried out while keeping the intestine in ice-cold modified Cortland saline [NaCl 133, KCl 5, CaCl2 1, MgSO4 1.9, NaHCO3 1.9, NaH_2PO_4 2.9 and glucose 5.5 (all in mM); pH 7.4 (Wolf, 1963)]. The same saline was also used as the luminal (spiked with metals of interest) and serosal salines during gut sac exposures (see below for details). The luminal saline was injected into the gut sacs by a syringe *via* the PE-50 tubing, then flared sealed. The gut sacs were blotted dry, weighed and then bathed into either 12 ml (for mid and posterior intestines) or 30 ml (for anterior intestine) of the serosal saline. Temperature was maintained at 15°C in a water bath, and the serosal saline was constantly aerated with 99.5% O2 and 0.5% CO2 during the exposure period. The gut sacs were incubated for 2 h, and following the incubation they were blotted dry and reweighed for the determination of fluid transport rates. The fluid transport rates allowed the examination of tissue integrity over the exposure period. An aliquot of the luminal and serosal salines was collected for the measurements of ^{59}Fe activity or total metal concentration. The sacs were cut open, and washed in either 5 ml (for mid and posterior intestines) or 10 ml (for anterior intestine) of modified Cortland saline, followed by a rinse in 1 mM EDTA. The tissues were blotted dry using a small piece of blotting paper, and the mucosal epithelium was gently scrapped off from the muscle layer using a glass slide, and collected separately. Subsequently, the surface area of each intestinal segment was measured by stretching it out on a graph paper. For the anterior intestine, the surface area of the cecae could not be measured, and only the exposed luminal surface area was measured. Therefore, the total surface area of the anterior intestine was somewhat underestimated in our experimental method. The radioactivity or the total metal concentration (for “cold” experiments, see below for details) in each sample was measured separately. The metal absorption in three different intestinal compartments was examined as follows: (i) the wash solutions plus the blotting paper

represented metal binding to mucus, (ii) the mucosal scrapings represented metal absorption into the mucosal epithelium (i.e., enterocytes), and (iii) the muscle layer plus the serosal saline represented metal absorption into the blood compartment. A sample size of five fish per individual treatment was used for all the experiments (n = 5 per treatment).

3.2.3. Experimental treatments

3.2.3.1. The influence of various divalent metals on intestinal iron absorption

The effects of various divalent metals on intestinal iron absorption were evaluated using a radiotracer method. Preparation of the experimental solutions was similar to that described by Kwong and Niyogi (2008). Briefly, a stock solution of $FeCl_3$ was radiolabeled with ^{59}Fe (as $FeCl_3$, specific activity = 56.92 mCi/mg; PerkinElmer, USA) and complexed with nitrilotriacetic acid (Fe:NTA = 1:4) to optimize iron solubility. To prepare Fe^{2+} solution, an aliquot of the Fe^{3+}-NTA stock solution was mixed with sodium ascorbate at a molar ratio of 1:20 for 30 min (prepared freshly on the day of experiment). Subsequently, an appropriate amount of the radioactive ^{59}Fe solution (either Fe^{2+} or Fe^{3+}) was added to the luminal saline (modified Cortland saline, see above for composition), and buffered with 20 mM HEPES at pH 7.4. The specific activity of the luminal saline was maintained at approximately 3.2×10^6 cpm/µmol iron. The potential inhibitory effect of various divalent metals on the absorption of Fe^{2+} was assessed by the addition of each metal separately in the luminal saline (copper, nickel, cobalt, lead and cadmium as nitrate salts, and zinc as a chloride salt; at 2 µM and 20 µM), and compared to the control (Fe^{2+} alone; at 2 µM). The concentration of Fe^{2+} in the luminal saline (2 µM) was selected on the basis of our previous observation that the intestinal Fe^{2+} absorption at this

luminal concentration is predominantly transporter-mediated (DMT-1 -sensitive to proton gradient) (Kwong and Niyogi, 2008). Since there was no apparent effect of cobalt on intestinal Fe^{2+} absorption, it was not included in the subsequent experiments. To evaluate whether the absorption of Fe^{3+} is similarly affected by different divalent metals, the absorption of 2 µM Fe^{3+} was assessed in the absence (control) or the presence of 20 µM nickel, lead and cadmium, using the same radiotracer approach employed for the Fe^{2+} absorption experiment as described previously. Nickel, lead and cadmium were chosen for this experiment because they were most effective in inhibiting intestinal Fe^{2+} absorption.

3.2.3.2. The influence of excess iron (Fe^{2+}) on the intestinal accumulation of cadmium and lead

A "cold" method was employed to evaluate the influence of elevated iron on the intestinal accumulation of lead and cadmium. The gut sacs were exposed to 2 µM lead or cadmium in the absence or the presence of 20 µM Fe^{2+}. The preparation of the experimental solutions was similar as described previously, except that radiolabeled $^{59}FeCl_3$ was replaced with "cold" $FeCl_3$. In addition, five fish were sacrificed prior to the exposure, and processed identically to quantify the background concentrations of lead and cadmium in different intestinal compartments. It is important to note that we did not evaluate the effect of excess iron on the intestinal absorption of copper, zinc and nickel. This was based on our assumption that the background concentrations of these essential metals in the gut tissue are considerably high, and therefore the "cold" method does not provide the sensitivity required to detect new metal accumulation under the current experimental conditions.

3.2.4. Measurement of radioactivity and cold metal concentrations

For the radioactive experiments, the radioactivity of ^{59}Fe in the sample was counted on a Wallac 1480 Wizard 3" gamma counter (PerkinElmer, USA). The actual exposure concentrations of each metal in the luminal saline were verified using a graphic furnace atomic absorption spectrometer (GFAAS; Analyst 800, PerkinElmer), and the difference between the measured and the nominal concentrations of any metals never exceeded ± 5%. For the "cold" experiments, the epithelial scrapings, the tissue layer and the blotting paper were first digested in 5 volume of 1 N HNO_3 at 60 °C for 48 h, and then centrifuged at 15,000 × g for 4 min. The supernatant was collected and diluted appropriately with 0.2% HNO_3. The luminal and serosal saline samples were also acidified with 1 N HNO_3. Subsequently, the concentrations of lead and cadmium in the samples were measured by a graphic furnace atomic absorption spectrometer as described above. The detection limits for lead and cadmium analysis were 0.06 and 0.07 µg/L, respectively. The quality control and assurance in all the analysis were maintained using appropriate method blanks and certified standards for respective metals (Fisher Scientific, Canada). In addition, the efficiency of lead and cadmium analysis in tissue samples was evaluated by analyzing a certified reference material (DOLT-3; National Research Council, Canada). The recovery of lead and cadmium in the reference material was 94% and 103%, respectively.

3.2.5. Calculations and statistics

The rate of iron (Fe^{2+} or Fe^{3+}) binding to mucus, and the rates of iron uptake in the mucosal epithelium and the blood compartment, was calculated as:

$$\text{Iron binding or uptake rate (nmol cm}^{-2}\text{ h}^{-1}\text{)} = \text{compartment cpm} / (\text{SA x ISA x } t) \quad (3.1)$$

where compartment cpm represents total ^{59}Fe activity in each compartment, SA is the specific activity of ^{59}Fe in the luminal saline, ISA is the intestinal surface area in cm^2, and *t* is the time of incubation (2 h). The fluid transport rate was calculated by dividing the net difference in gut sac weight (pre and post incubation) with ISA and *t*, defined as above.

Similarly, the lead and cadmium accumulations in each of the three intestinal compartments for the "cold" experiments were calculated as:

$$\text{Lead or cadmium accumulation (nmol cm}^{-2}\text{)} = \text{compartment metal concentration / ISA} \quad (3.2)$$

All of the statistical analyses were performed using SigmaStat (version 3.1; Systat Software, Inc., Point Richmond, CA, USA). One-way analysis of variance (ANOVA) followed by a post-hoc least significance difference (LSD) test was used to evaluate the significant effect of various competitive metals on either Fe^{2+} or Fe^{3+} binding/uptake rates within the same compartment of each intestinal segment. Similarly, one-way ANOVA followed by a post-hoc LSD test was used to compare among the background concentrations of lead or cadmium, and the accumulation of lead or cadmium following the exposure to luminal lead or cadmium with or without excess iron. Data are reported as means ± SEM, $n = 5$ for each treatment. Differences were considered significant at $p \leqslant 0.05$.

3.3. Results

3.3.1. Fluid transport rates in different intestinal segments

The fluid transport rates in all of the treatments were very similar to the rates reported previously in rainbow trout (Ojo and Wood, 2007; Kwong and Niyogi, 2008), and none of the experimental treatments in our study significantly affected the fluid transport rate (data not shown). Typically, the fluid transport rate in the anterior intestine was approximately 10 µL cm^{-2} h^{-1}, while that in the mid and posterior intestines was between 2–3 µL cm^{-2} h^{-1}.

3.3.2. The influence of luminal zinc, copper, nickel and cobalt on intestinal ferrous iron absorption

The presence of zinc, copper, nickel and cobalt did not significantly affect Fe^{2+} binding to mucus in any intestinal segments (Figure 3.1a). In the mucosal epithelium of anterior and mid intestines, the inhibition of Fe^{2+} absorption by zinc and copper was statistically significant at 20 µM exposure (Figure 3.1b). Zinc and copper, at both 2 and 20 µM exposure concentrations, significantly inhibited Fe^{2+} absorption in the mucosal epithelium of posterior intestine. In contrast, nickel caused a significant inhibition of Fe^{2+} absorption in the mucosal epithelium of all the intestinal segments at both 2 and 20 µM exposures. In the blood compartment, nickel had a significant effect on Fe^{2+} absorption at both the anterior and posterior intestines, whereas zinc had a significant effect at the anterior intestine only (Figure 3.1c). Copper did not affect Fe^{2+} absorption in the blood compartment of any intestinal segments. Cobalt did not exhibit any effect on Fe^{2+} absorption in any compartments of the anterior, mid or posterior intestine.

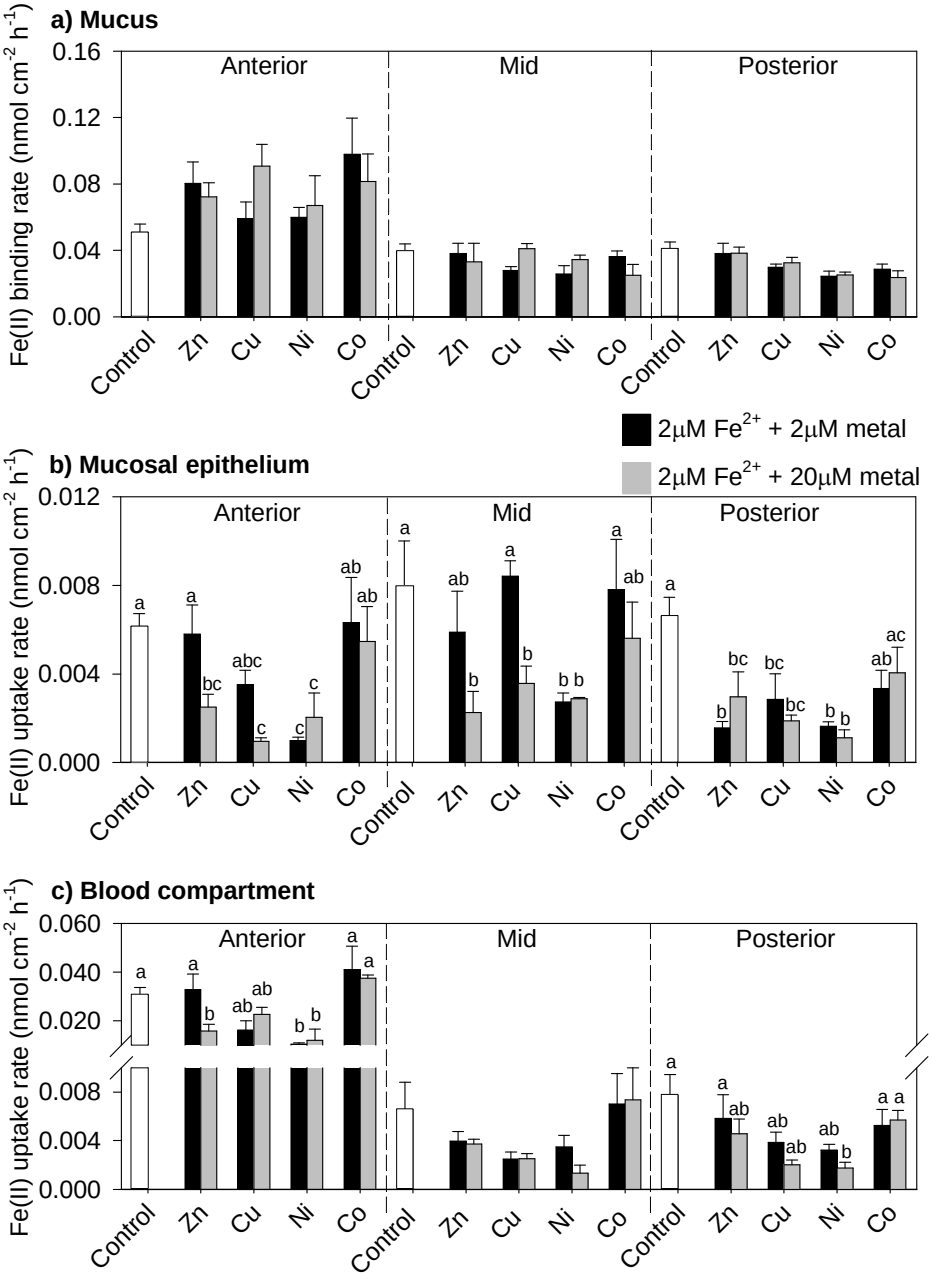

Figure 3.1: The effect of 2 µM (black bars) or 20 µM (gray bars) zinc, copper, nickel and cobalt on the rates of 2 µM Fe^{2+} (control; white bars) binding to **(a)** the mucus, or absorption into **(b)** the mucosal epithelium and **(c)** the blood compartment of different intestinal segments (anterior, mid and posterior intestine) in fish. Different letters represent a statistical difference within the same intestinal segment (One-way ANOVA followed by a post-hoc LSD test; $p \leq 0.05$). Values are mean ± SEM (n = 5).

3.3.3. The influence of luminal lead and cadmium on intestinal ferrous iron absorption

The presence of 20 μM lead in the luminal saline increased Fe^{2+} binding to the mucus, although a significant effect was recorded only in the anterior intestine (Figure 3.2a). Cadmium did not affect Fe^{2+} binding to the mucus in any intestinal segments. Both lead and cadmium inhibited Fe^{2+} absorption considerably in the mucosal epithelium of all the intestinal segments. However, lead appeared to have a stronger effect than cadmium since the significant inhibition of Fe^{2+} absorption occurred at both 2 and 20 μM luminal lead concentrations, whereas it was observed only at 20 μM luminal cadmium concentration (Figure 3.2b). The inhibition of Fe^{2+} absorption by lead was also recorded in the blood compartment of all the intestinal segments, although the magnitude of inhibition was less prominent compared to that in the mucosal epithelium (Figure 3.2c). Similarly, cadmium (20 μM) also inhibited Fe^{2+} absorption in the blood compartment, but the effect was statistically significant only in the anterior intestine (Figure 3.2c).

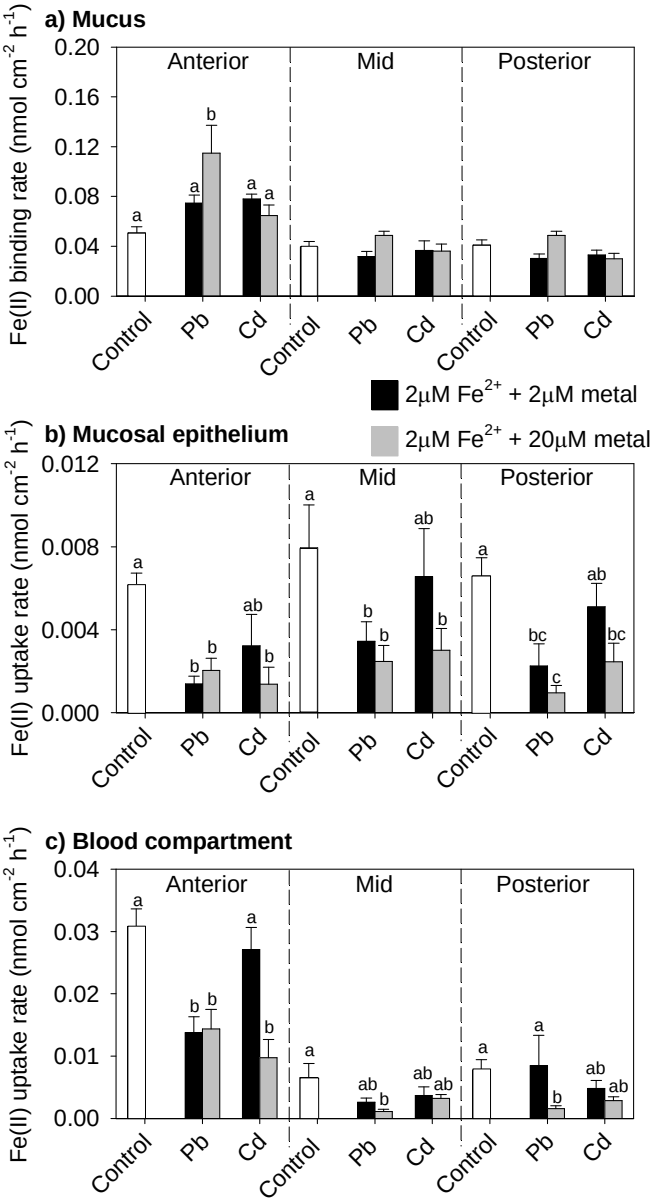

Figure 3.2: The effect of 2 µM (black bars) or 20 µM (gray bars) lead and cadmium on the rates of 2 µM Fe^{2+} (control; white bars) binding to **(a)** the mucus, or absorption into **(b)** the mucosal epithelium and **(c)** the blood compartment of different intestinal segments (anterior, mid and posterior) in fish. Different letters represent a statistical difference within the same intestinal segment (One-way ANOVA followed by a post-hoc LSD test; $p \leq 0.05$). Values are mean ± SEM (n = 5).

3.3.4. Relative magnitude of inhibition of ferrous iron absorption in the mucosal epithelium by various divalent metals

Table 3.1 summarizes the influence of zinc, copper, nickel, lead and cadmium on the relative rate of Fe^{2+} absorption in the mucosal epithelium of the anterior, mid and posterior intestines. The inhibitory effects varied spatially and different metals produced different degrees of inhibition (i.e., lower Fe^{2+} absorption rate = greater magnitude of inhibition). The effect of copper, nickel and lead on the rate of Fe^{2+} absorption in the anterior and posterior intestines appeared to be more prominent than that in the mid intestine. However, the effect of zinc and cadmium on the rate of Fe^{2+} absorption did not show any distinct spatial pattern. Nickel and lead did not exhibit a clear dose-dependent inhibitory effect on Fe^{2+} absorption rate along the whole intestine. However, the dose-dependent inhibitory effect by zinc, copper and cadmium was evident, particularly in the anterior and mid intestines. Overall, the magnitude of inhibition of Fe^{2+} absorption by other divalent metals along the entire intestine appeared to follow the order of: $Ni^{2+} \sim Pb^{2+} > Cd^{2+} \sim Cu^{2+} > Zn^{2+}$.

Table 3.1: The relative rate of ferrous iron (Fe^{2+}) absorption in the presence of zinc, copper, nickel, lead and cadmium in the mucosal epithelium of the anterior, mid and posterior intestines of rainbow trout.

	Anterior		Mid		Posterior	
	2µM	20µM	2µM	20µM	2µM	20µM
Control	100.0 ± 9.3^{Aa}		100.0 ± 15.9^{Aa}		100.0 ± 13.2^{Aa}	
Zinc	94.4 ± 15.8^{Aab}	40.7 ± 9.5^{Bb}	74.0 ± 23.4^{Aa}	28.4 ± 12.1^{Bb}	23.8 ± 4.3^{Bb}	45.1 ± 17.0^{Bb}
Copper	57.1 ± 10.8^{Bb}	15.6 ± 2.7^{Cb}	105.8 ± 8.9^{Aa}	45.0 ± 9.9^{Bb}	43.3 ± 17.5^{Bbc}	28.5 ± 4.1^{Bb}
Nickel	16.2 ± 2.4^{Bc}	33.3 ± 17.7^{Bb}	34.4 ± 5.2^{Bb}	36.3 ± 0.7^{Bb}	24.9 ± 3.2^{Bb}	17.0 ± 5.4^{Bb}
Lead	22.7 ± 6.0^{Bc}	33.2 ± 9.6^{Bb}	43.4 ± 11.8^{Bb}	31.2 ± 9.6^{Bb}	34.2 ± 16.2^{Bb}	14.5 ± 5.5^{Bb}
Cadmium	52.6 ± 14.4^{Bb}	22.5 ± 13.2^{Bb}	82.5 ± 29.2^{Aa}	37.9 ± 11.9^{Bb}	77.6 ± 17.6^{Aac}	37.3 ± 13.5^{Bb}

The absorption rate at 2 µM luminal Fe^{2+} was examined in the presence of other divalent metals at 0 (control: iron alone), 2 or 20 µM in the luminal saline. Data are presented as percent Fe^{2+} absorption rate relative to the control (considered as 100%), and as mean±SEM, n=5. One-way ANOVA analysis with post-hoc LSD test was used to compare differences across the concentrations and among the metals. The different capital letters represent significant differences across the three different concentrations for the same metal tested (0, 2 and 20 µM). The different small letters represent significant differences among the metals at each concentration tested (2 or 20 µM; including control in each comparison). All statistical comparisons were made within the same intestinal segment, and $p \leq 0.05$ was considered as statistically significant.

3.3.5. The influence of luminal nickel, lead and cadmium on intestinal ferric iron absorption

The presence of 20 µM nickel, lead and cadmium in the luminal saline did not affect Fe^{3+} (2 µM) binding to the mucus (Figure 3.3a). Fe^{3+} absorption in the mucosal epithelium was strongly inhibited by nickel, lead and cadmium in the mid and posterior intestines, whereas it was inhibited only by lead in the anterior intestine (Figure 3.3b). Similarly, lead significantly inhibited Fe^{3+} absorption in the blood compartment of the anterior intestine (Figure 3.3c). Cadmium and nickel did not have any effect on Fe^{3+} absorption in the blood compartment of any intestinal segments.

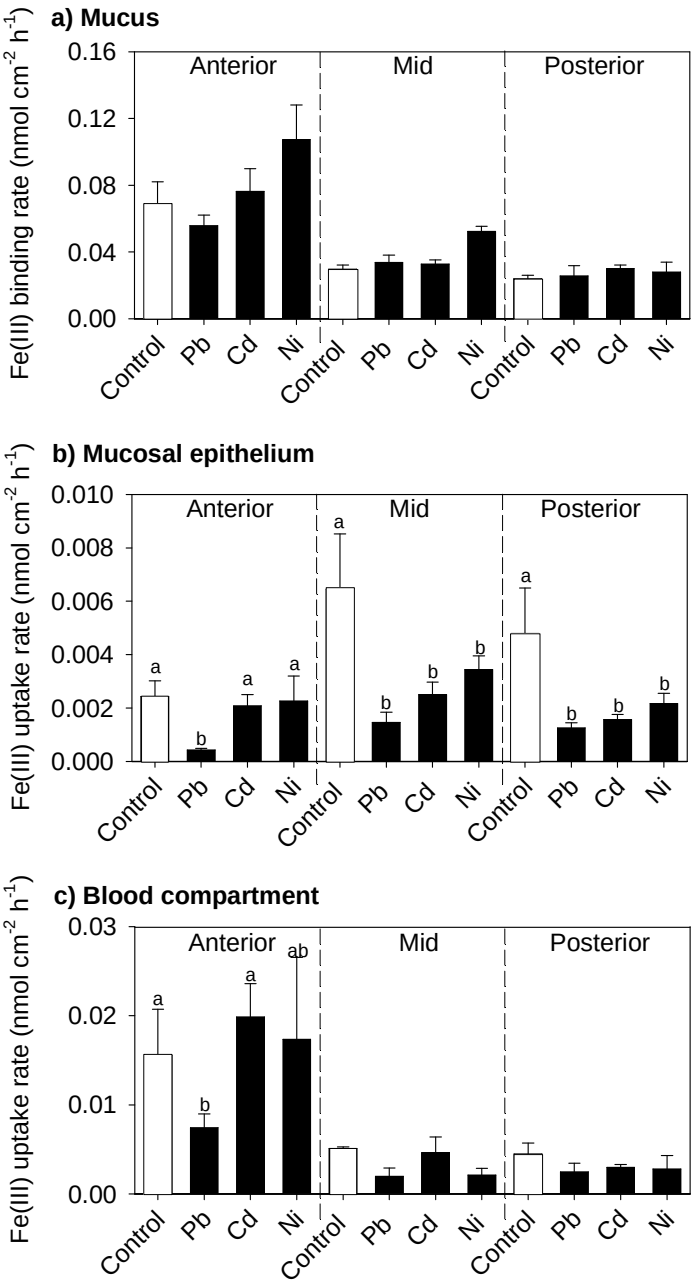

Figure 3.3: The effect of 20 µM lead, cadmium and nickel on the rates of 2 µM Fe^{3+} binding to **(a)** the mucus, or absorption into **(b)** the mucosal epithelium and **(c)** the blood compartment of different intestinal segments (anterior, mid and posterior) in fish. Different letters represent a statistical difference within the same intestinal segment (One-way ANOVA followed by a post-hoc LSD test; $p \leq 0.05$). Values are as mean ± SEM ($n = 5$).

3.3.6. The influence of excess luminal ferrous iron on intestinal lead and cadmium accumulation

The background concentrations of lead and cadmium in different compartments of the intestines were in the range of 0 (non-detectable) – 0.0013 nmol/cm^2 and 0 – 0.0139 nmol/cm^2, respectively. The exposure to lead and cadmium significantly increased their concentrations in all the compartments of the intestines (Figure 3.4). The presence of excess Fe^{2+} (20 µM) in the luminal saline did not affect lead binding to the mucus in any intestinal segments (Figure 3.4a). However, less cadmium was bound to the mucus in the presence of excess Fe^{2+}, although the effect was statistically significant only in the posterior intestine. The exposure to 2 µM lead in the presence of excess Fe^{2+} did not affect lead accumulations in the mucosal epithelium and blood compartment of any intestinal segments (Figure 3.4b and 3.4c). In contrast, cadmium accumulation in the mucosal epithelium and blood compartment of both mid and posterior intestines showed a notable decrease in the presence of excess Fe^{2+}, and a statistical difference was recorded in the blood compartment of the posterior intestine (Figure 3.4b and 3.4c). Overall, 49–52% reduction in cadmium accumulation (combining the mucosal epithelium and blood compartment) in the mid and posterior intestines was recorded in the presence of excess luminal Fe^{2+}.

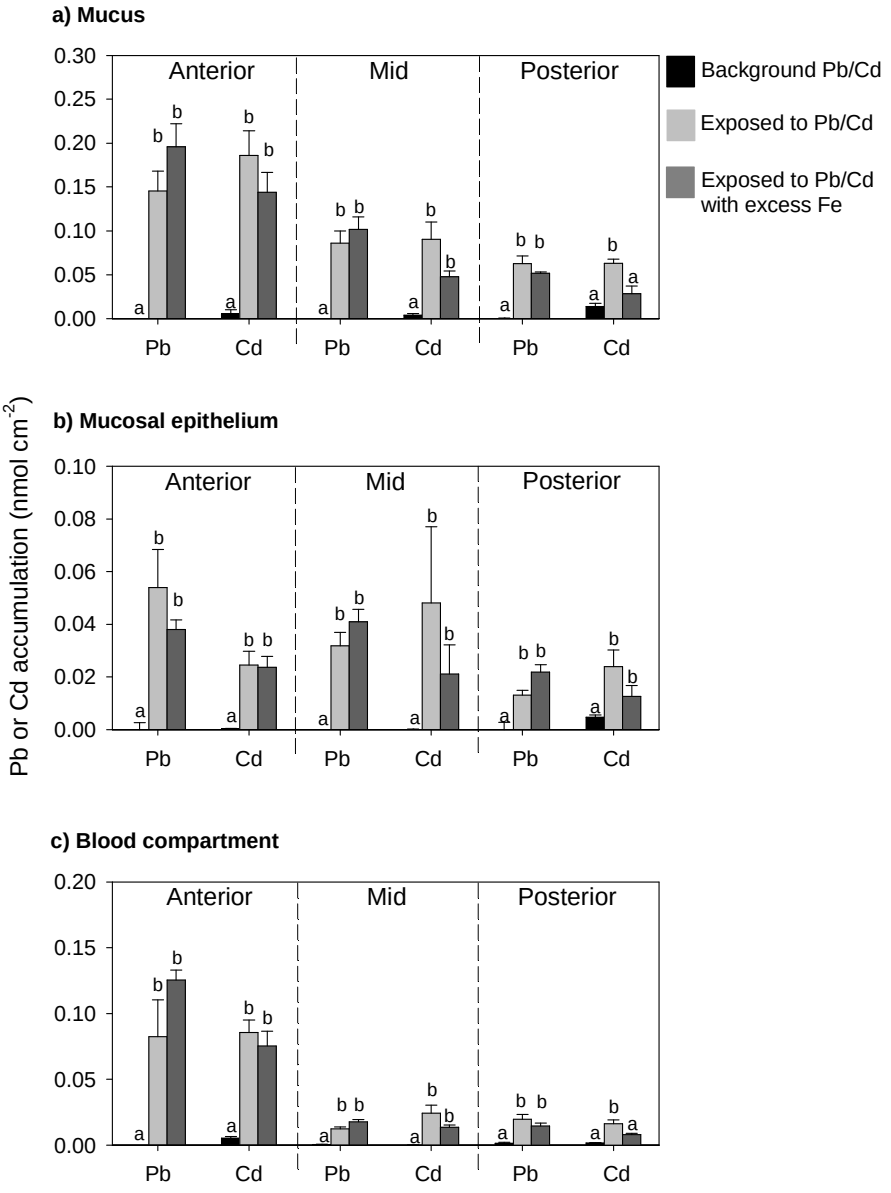

Figure 3.4: The effect of excess ferrous iron (Fe^{2+}) on the accumulation of lead and cadmium in **(a)** the mucus, **(b)** the mucosal epithelium and **(c)** the blood compartment of different intestinal segments (anterior, mid and posterior) in fish. The background concentrations of lead and cadmium are presented as black bars, and the accumulation of lead and cadmium following exposure to 2 µM lead or cadmium in the absence and presence of 20 µM Fe^{2+} are presented as light gray and dark gray bars, respectively. Bars labelled with different letters represent a statistical significance for the same metal within the same intestinal segment (One-way ANOVA followed by a post-hoc LSD test; $p \leq 0.05$). Values are mean ± SEM ($n = 5$).

3.4. Discussion

It has been suggested that iron absorption in fish gut occurs *via* DMT1, and the piscine DMT1 resembles the functional characteristics of the mammalian homologue (Dorschner and Phillips, 1999; Kwong and Niyogi, 2008). However, the interactions of iron with other divalent metals in fish gut remained virtually unknown. The present study provides evidence that several divalent metals (both essential and non-essential) can interact with the iron absorption pathway along the entire intestinal tract of fish. Moreover, the magnitude of these interactions varies spatially along the intestinal tract and depends on the metals as well.

In the present study, we observed that the absorption of Fe^{2+} into the mucosal epithelium was inhibited by copper in all three intestinal segments of the fish. Nadella *et al.* (2007) reported that intestinal copper absorption in rainbow trout is dependent on the luminal proton gradient, thereby suggesting the involvement of DMT1 in copper absorption. They also observed that copper absorption in the blood compartment is significantly inhibited by ten-fold excess luminal iron concentration (50 μM copper and 500 μM iron) in the mid intestine. Thus, our observation complements their finding indicating that the interaction between iron and copper in the fish intestine is reciprocal in nature, and thereby suggesting that the uptake of dietary Fe^{2+} and Cu^{2+} likely occurs through the same pathway (probably DMT1), at least partially. We also observed a similar inhibition of Fe^{2+} absorption by zinc both in the mucosal epithelium and the blood compartment, which could be due to the shared transport of Fe^{2+} and Zn^{2+} *via* DMT1 as well. Interestingly, Glover and Hogstrand (2003) reported that copper inhibits intestinal zinc uptake in rainbow trout at equimolar luminal concentrations (50 μM copper and zinc). Recently, Ojo *et al.* (2009) demonstrated the reciprocal inhibitory effect of copper and zinc in the mid and posterior intestines of rainbow trout. They suggested that the intestinal absorption of copper and zinc is

probably mediated by DMT1, at least in part, which is consistent with our findings. It is important to note though that the absorption of copper and zinc in the fish intestine may also occur through Cu^{2+}- and Zn^{2+}-specific transporters. For example, recent molecular evidence suggests that apical Cu^{2+} and Zn^{2+} transport in the fish intestine can occur *via* Ctr1 and ZIP, respectively (Mackenzie *et al.*, 2004; Feeney *et al.*, 2005). The spatial difference in the magnitude of inhibition of intestinal Fe^{2+} absorption by copper and zinc observed in our study might have occurred due to the differential localization of these transporters (DMT1, Ctr1 and ZIP) along the fish intestine.

Davidson *et al.* (2005) reported that Ni^{2+} can compete with Fe^{2+} for transport *via* DMT1 in human lung (A549) and embryonic kidney (HEK) cell lines. In the present study, nickel was found to be the strongest inhibitor of intestinal Fe^{2+} absorption among all of the divalent essential metals examined. Unlike copper and zinc, nickel significantly inhibited Fe^{2+} absorption in the mucosal epithelium of all three intestinal segments independent of its exposure concentration (2 or 20 μM). Nickel also had a significant effect on Fe^{2+} absorption in the blood compartment of anterior and posterior intestines. These results indicate that Ni^{2+} probably has a greater affinity to the intestinal Fe^{2+} absorption pathway in fish than Cu^{2+} and Zn^{2+}. Interestingly however, we did not observe any inhibitory effects of cobalt on the intestinal Fe^{2+} absorption in trout. This finding is different from the mammalian systems, where cobalt has been reported to inhibit Fe^{2+} absorption in human intestinal (Caco-2) (Yeung *et al.*, 2005) and embryonic kidney (HEK293) cell lines (Garrick *et al.*, 2006). It may be possible that cobalt interacts with the intestinal Fe^{2+} absorption pathway with a relatively low affinity and/or the intestinal cobalt absorption primarily occurs through alternative pathways in fish.

It is becoming increasingly evident that dietary exposure can be an important factor for the accumulation and toxicity of lead and cadmium in fish (Farag *et al.*, 1994; Mount *et al.*, 1994; Farag *et al.*, 1999; Ng and Wood, 2008). Waterborne lead and cadmium may enter into the fish body *via* the branchial Ca^{2+} uptake pathway (Verbost *et al.*, 1987; Niyogi and Wood, 2004; Rogers and Wood, 2004). However, the mechanisms of dietary lead and cadmium absorption in fish are poorly understood. Our study indicates that both lead and cadmium interact with the intestinal Fe^{2+} absorption in fish, and the Fe^{2+} absorption pathway probably plays an important role in dietary cadmium accumulation.

As observed with nickel, lead also inhibited Fe^{2+} absorption in the mucosal epithelium of all intestinal segments independent of the exposure concentration (2 or 20 μM), thereby suggesting its strong affinity to the Fe^{2+} absorption pathway. Similarly, Fe^{2+} absorption in the blood compartment was also inhibited by lead in all three intestinal segments, although the effect was more prominent at higher exposure concentration (20 μM) in the mid and posterior intestines. Notably, Fe^{2+} binding to the mucus increased in the anterior intestine when exposed to lead. The underlying reason of this phenomenon is unclear, however the increased mucus binding of Fe^{2+} may have played some role in reducing Fe^{2+} absorption in the anterior intestine by decreasing its availability to the site of absorption. On the other hand, ten-fold excess Fe^{2+} in the luminal saline did not cause any reciprocal inhibitory effect on lead accumulation in any intestinal compartments. The lack of reciprocal effect might be due to the higher affinity of Pb^{2+}, relative to Fe^{2+}, to the Fe^{2+} uptake pathway (probably DMT1). Alternatively, it is possible that the absorption of dietary lead occurs *via* additional routes such as calcium transport pathways. Alves and Wood (2006) suggested the interaction of lead and calcium in the fish intestine based on the observation that elevated dietary calcium protects against the dietary lead accumulation in trout.

Further investigations are needed to understand the significance of intestinal Fe^{2+} absorption pathway in dietary lead accumulation in fish.

The link between dietary iron and cadmium absorption *via* DMT1 is quite well characterized in mammalian systems (Park *et al.*, 2002; Bannon *et al.*, 2003; Ryu *et al.*, 2004). Bury and Grosell (2003b) reported that the *in vivo* branchial absorption of Fe^{2+} is inhibited by ten-fold excess waterborne cadmium in fish. Cooper *et al.* (2006b) also provided indirect evidence that iron and cadmium may share a common transport pathway in piscine intestine. They demonstrated that treatment with low iron diet increased the expression of DMT1 in the gut as well as cadmium uptake in rainbow trout. Other recent studies with trout have suggested that cadmium uptake in the stomach occurs *via* a calcium-sensitive pathway, whereas cadmium absorption in the intestine is mediated predominantly by a calcium-insensitive pathway (probably DMT1) (Wood *et al.*, 2006; Ojo and Wood, 2008). Our study demonstrated that Fe^{2+} absorption into the mucosal epithelium was markedly inhibited by cadmium in all three intestinal segments. In addition, cadmium accumulation both in the mucosal epithelium and the blood compartment was reduced considerably (approximately 50%) by excess Fe^{2+}, notably in the mid and posterior intestines. These findings clearly suggest that Fe^{2+} and Cd^{2+} are transported by a common pathway in the fish intestine, possibly *via* DMT1.

In mammals, the apical ferric reductase plays an important role in dietary iron absorption (McKie *et al.*, 2001). This is because non-heme iron in the diet primarily exists as ferric iron (Fe^{3+}) which must be reduced to ferrous iron (Fe^{2+}) prior to absorption by DMT1. Recently, the activity of ferric reductase has been recorded (Carriquiriborde *et al.*, 2004), and its functional capacity has also been implicated in piscine gut (Kwong and Niyogi, 2008). Therefore, if Fe^{3+} is absorbed essentially *via* the same pathway as Fe^{2+}, its absorption should also be inhibited by

other divalent metals. Yeung *et al.* (2005) reported that cobalt and manganese inhibit both Fe^{3+} and Fe^{2+} uptake in a similar manner in human Caco-2 cells. In the present study, we demonstrated that the absorption of both Fe^{2+} and Fe^{3+} in the mucosal epithelium of mid and posterior intestines was strongly inhibited by nickel, lead and cadmium at a ten-fold higher concentration relative to iron. This finding further corroborates our previous observation that Fe^{3+} is likely absorbed by the same pathway as Fe^{2+} in the mid and posterior intestines of fish. On the other hand, the interactions of Fe^{3+} with the divalent metals in the anterior intestine were somewhat different from that of the mid or posterior intestine, as only lead caused a significant reduction of Fe^{3+} absorption in the anterior intestine. The reason for this phenomenon is unclear since nickel, lead and cadmium caused strong inhibition of Fe^{2+} absorption in the mucosal epithelium of the anterior intestine. Perhaps there are alternative pathways for Fe^{3+} absorption in the anterior intestine and/or the mechanism of interaction between Pb^{2+} and Fe^{3+} is different. It is possible that the reduced Fe^{3+} absorption, at least partially, was due to the inhibition of ferric reductase activity by lead, as observed in plants (Chang *et al.*, 2003).

The magnitude of inhibition of intestinal Fe^{2+} absorption by other divalent metals provides insights into the relative affinity of these metals to the Fe^{2+} transport pathway. However, the current information on the affinity of various divalent metals to the Fe^{2+} transport pathway (e.g., DMT1) is highly variable. For example, Garrick *et al.* (2006) reported that the affinity of different divalent metals to DMT1 in human embryonic kidney cell lines (HEK293 cells) was in the order of: $Mn^{2+} > Cd^{2+} > Fe^{2+} > Pb^{2+} \sim Co^{2+} \sim Ni^{2+} > Zn^{2+}$. Goddard *et al.* (1997) reported that the inhibition of Fe^{2+} uptake by other metals in human enterocytes followed the order of: $Zn^{2+} > Pb^{2+} > Co^{2+} > Mn^{2+}$. On the other hand, Cooper *et al.* (2007) expressed the transcripts of two different DMT1 isoforms (*slc11γ* and *slc11β*) of trout gill in *Xenopus* oocytes, and observed that

the magnitude of inhibition of Fe^{2+} transport by other metals was dependent on the isoform. They found the inhibition of Fe^{2+} transport *via* slc11γ followed the order of: $Cd^{2+} > Mn^{2+} > Co^{2+} > Zn^{2+} > Pb^{2+}$, whereas all the metals caused similar magnitude of inhibition with slc11β. In the present study, the magnitude of inhibition of intestinal Fe^{2+} absorption by other divalent metals followed the order of: $Ni^{2+} \sim Pb^{2+} > Cd^{2+} \sim Cu^{2+} > Zn^{2+}$. The different patterns of inhibition in different cells and species indicate that the divalent metal interactions may depend on various physiological factors such as differential expression of various transporters/channels (e.g., DMT1, CTR1, ZIP, Ca^{2+} channels) and their functional characteristics.

We previously demonstrated that iron (both Fe^{2+} and Fe^{3+}) absorption in the mucosal epithelium (enterocytes) of piscine intestine is physiologically regulated, and likely occurs *via* DMT1 (Kwong and Niyogi, 2008). In the present study, we found that the inhibitory effects of various divalent metals on iron absorption occur primarily in the mucosal epithelium, which clearly indicates that these interactions occur through DMT1. Moreover, the magnitude of inhibition of Fe^{2+} absorption by other divalent metals in the anterior and posterior intestines was quite similar, and was relatively higher than that in the mid intestine. The surface area of the anterior intestine in rainbow trout has been reported to be about two-fold greater than that of the mid or posterior intestine (Nadella *et al.*, 2006). Therefore, the anterior intestine is likely to be the most important site physiologically for the interaction of iron with other divalent metals relative to either mid or posterior intestine.

3.5. Conclusions

Overall, our findings suggest that several divalent metals, both essential and non-essential, inhibit intestinal Fe^{2+} absorption in fish, likely *via* DMT1, and the magnitude of inhibitory effect by various metals follows the order of: $Ni^{2+} \sim Pb^{2+} > Cd^{2+} \sim Cu^{2+} > Zn^{2+}$. Cobalt does not seem to have any effect on intestinal Fe^{2+} absorption in fish. Nickel, cadmium and lead caused similar inhibitory effects on Fe^{3+} absorption in the mid and posterior intestines, indicating Fe^{2+} and Fe^{3+} are absorbed by the same pathway in these intestinal segments. Interestingly, the intestinal accumulation of lead was not reciprocally inhibited by excess Fe^{2+}, possibly because of its greater affinity to the Fe^{2+} transport pathway and/or the existence of alternative pathways for its absorption. In contrast, the accumulation of cadmium in the intestinal tissue was substantially reduced in the presence of excess Fe^{2+}, indicating the importance of Fe^{2+} transport pathway in dietary cadmium uptake in fish. Thus, we suggest that an iron-rich diet may potentially protect fish against cadmium accumulation and toxicity. There is a growing awareness that dietary exposure is often the primary source of metal accumulation and toxicity in fish in metal contaminated environments (Meyer *et al.*, 2005). Our findings have important implications for understanding the mechanisms of dietary metal uptake in fish.

CHAPTER 4: Molecular evidence and physiological characterization of iron absorption in isolated enterocytes of rainbow trout (*Oncorhynchus mykiss*): Implications for dietary cadmium and lead absorption[3]

4.1. Introduction

Fish are exposed to metals *via* both water and diet. The waterborne metal uptake is generally considered to be the major route for acute metal toxicity in fish, although some recent studies have suggested that the diet can also play a significant role in metal accumulation and toxicity in fish (Farag *et al.*, 1994; Farag *et al.*, 1999; Ng and Wood, 2008). The mechanisms of dietary metal uptake and toxicity in fish are not very well understood. Interestingly, some recent studies have indicated that the uptake of several divalent metals, both essential [e.g., copper (Cu) and nickel (Ni)] and non-essential [e.g., cadmium (Cd) and lead (Pb)], may occur *via* the iron (Fe) absorption pathway in the intestine as well as in the gills (Bury and Grosell, 2003b; Bury and Grosell, 2003a; Cooper *et al.*, 2006b; Cooper *et al.*, 2007; Kwong and Niyogi, 2009).

Cadmium and Pb are common contaminants in many polluted aquatic environments and pose a serious threat to the health of aquatic animals, including fish. The absorption of waterborne Cd and Pb is believed to occur primarily through apical calcium (Ca) channels in the branchial chloride cells of fish (Verbost *et al.*, 1987; Rogers and Wood, 2004). However in mammals, it has been reported that the absorption of Cd and Pb from the diet is mediated mainly

[3] This chapter has been published in Aquatic Toxicology 99:343–350 (2010), under joint authorship with Jose A. Andrés (University of Saskatchewan) and Som Niyogi (University of Saskatchewan)

by an apical Fe^{2+} transporter called divalent metal transporter-1 (DMT1, also known as *slc11a2* and *Nramp2*) (Tallkvist *et al.*, 2001; Bressler *et al.*, 2004). It has been shown that DMT1 is expressed ubiquitously along the gastrointestinal tract of mammals, with the maximum expression in the duodenum (Gunshin *et al.*, 1997). The transport of Fe^{2+} *via* DMT1 has been reported to be an active process, and is facilitated by a proton gradient (Fe^{2+}/H^{+} symporter) and membrane potential (Gunshin *et al.*, 1997; Tandy *et al.*, 2000). To date, three different isoforms of *Nramp* have been identified in rainbow trout (*Oncorhynchus mykiss*): -*α*, -*β* and -*γ* (Dorschner and Phillips, 1999; Cooper *et al.*, 2007), and it has been suggested that *Nramp-β* and -*γ* can function as DMT1 (Cooper *et al.*, 2007). For example, Cooper *et al.* (2007) demonstrated that gill *Nramp-β* and -*γ* isoforms of rainbow trout could import Fe^{2+} when expressed in *Xenopus* oocytes. Moreover, they also reported that several different divalent metals, including Cd and Pb, inhibit Fe^{2+} import through *Nramp-β* and -*γ* (Cooper *et al.*, 2007). Although *Nramp* (-*α* and -*β*) have been shown to be expressed in most tissues (e.g., brain, liver, spleen, heart, ovary) of rainbow trout (Dorschner and Phillips, 1999), the expression of *Nramp* in the gastrointestinal tract of fish has not been investigated. Previous studies have suggested that the intestinal Fe^{2+} absorption in fish is likely mediated by a DMT1 homologue (Bury *et al.*, 2001; Kwong and Niyogi, 2008). We have also demonstrated that Cd and Pb can inhibit Fe^{2+} transport in the fish intestine (Kwong and Niyogi, 2009). However, further investigations are required for elucidating the kinetic characteristics of Fe^{2+} transport in piscine intestinal epithelium (i.e., enterocytes) and the functional properties of DMT1. Similarly, we need to examine the mechanisms of the intestinal interaction between Fe^{2+} and Cd or Pb in order to enhance our understanding of the shared dietary uptake of Fe and Cd or Pb in fish.

In the present study, we used freshly isolated enterocytes of rainbow trout in suspension to characterize Fe^{2+} absorption and its interaction with Cd and Pb. The isolated enterocytes in suspension represent a good experimental system to study the precise characteristics of epithelial metal transport in the fish intestine without the confounding influence of mucus. This approach has been used previously to characterize the mechanisms of intestinal Ca and Cu uptake in fish (Larsson *et al.*, 1998; Burke and Handy, 2005). The objectives of the present study were 4-fold: (i) to examine the mRNA expression of DMT1 (*Nramp-β* and -*γ*) in the gastrointestinal tissues including enterocytes of rainbow trout; (ii) to characterize the kinetic properties of Fe^{2+} uptake in isolated enterocytes; (iii) to examine the potential concentration-dependent inhibitory effect of Cd and Pb on Fe^{2+} uptake in isolated enterocytes, and (iv) to characterize the kinetics of such inhibitory interactions.

4.2. Materials and methods

4.2.1. Fish

The freshwater rainbow trout (*O. mykiss*; 600–800 g wet weight) were obtained from Lucky Lake fish farm, SK, Canada. Fish were acclimated for at least 4 weeks in the laboratory condition and supplied with aerated, dechlorinated water [hardness 157 mg/L, alkalinity 109 mg/L (both as $CaCO_3$), pH 8.1–8.2, dissolved organic carbon (DOC) 2.2 mg/L, Fe 5.5 μg/L, Cd <0.1 μg/L, and Pb 0.2 μg/L] in a flow-through system. The water temperature was maintained at 15 °C and photoperiod mimicked natural conditions. Fish were fed Martin's commercial dried pellet feed (5-pt.; Martin Mills Inc., Elmira, ON, Canada) at a daily ration of 2% wet body mass.

The measured metal concentrations in the feed were: Fe 220, Zn 167, Cu 32, Ni 4, Cd 0.07 and Pb 0.1 (all in mg/kg).

4.2.2. mRNA expression of divalent metal transporter-1 isoform genes

A previous study has shown that two different DMT1 isoforms (*Nramp-β* and *-γ*) are involved in the transport of Fe^{2+} in the gills of rainbow trout (Cooper *et al.*, 2007). We hypothesized that these isoforms are also expressed and involved in Fe transport in the intestine of trout. A qualitative PCR approach was employed to examine the mRNA expressions of *Nramp-β* and *-γ* in the gastrointestinal tract of fish. Fish were first euthanized using MS-222, and the gastrointestinal tract was dissected and carefully cleaned. The tract was then sectioned into stomach, anterior intestine (included pyloric ceacae), mid intestine and posterior intestine based on the morphological differences. Each tissue was processed separately for total RNA extraction and later PCR reaction, and three individual fish were used. The mRNA expressions of *Nramp-β* and *-γ* were also examined in enterocytes isolated from three different fish (see below for method of isolating enterocytes). Total RNA was extracted using Trizol® (Invitrogen, USA). To avoid genomic DNA contamination the extracted RNA was treated with DNase I (Invitrogen, USA). This RNA was then used to synthesize single-stranded cDNA using SuperScript III reverse transcriptase (Invitrogen, USA) and an oligo (dT) primer. Tissue-specific RNA/DNA heteroduplexes were diluted in water (molecular grade) and used as PCR templates. Specific primers were designed for *Nramp-β* (Accession number AF048761; Forward: 5′-CCT CCC CTC CGG CTT CAG AC-3′, Reverse: 5′-GGT CCC GTA AAG GCC CAG AGT T-3′) and *-γ* (Accession number EF495162; Forward: 5′-ACC CGC TCC ATC GCC ATC TT-3′, Reverse: 5′-

ACC CCT CCG CCT ATC TTC CAC A-3′). As positive controls of our diagnostic PCR assays, small portions of two different housekeeping genes, *α-Tubulin* and *β-Actin*, were also amplified using the primers and conditions described in Aegerter *et al.* (2005). All amplifications were conducted in 10 µl reaction volumes containing 1× reaction buffer, 2 mM $MgCl_2$, 0.2 mM of each dNTP, 0.25 µM of each primer and 1 U of Platinum® *Taq* DNA polymerase (Invitrogen, USA). The amplification was performed in a thermal cycler (C1000; Bio-Rad, USA) with the following conditions for *Nramp-β*: 38 cycles of 94 °C (50 s), 62 °C (25 s), and 72 °C (25 s); and for *Nramp-γ*: 38 cycles of 94 °C (50 s), 65 °C (30 s), and 72 °C (30 s). These PCR conditions were selected because the resolution and the specificity of the amplification were optimal under these conditions. The specificity of *Nramp-β* and *-γ* primers was confirmed by DNA sequencing and BLAST analyses. All amplicons were sequenced on a 3130XL DNA Analyzer using the BigDye Terminator Kit (Applied Biosystems, Canada).

4.2.3. Isolation of enterocytes

A technique of isolating enterocytes from rainbow trout intestine was developed based on the methods described by Weiser (1973) and Larsson *et al.* (2003). Fish were euthanized using MS-222 and bled to remove as much blood as possible. The whole intestinal tract (anterior to posterior intestine) was dissected out and immediately transferred to an ice-cold physiological saline [modified Cortland saline: NaCl 133, KCl 5, $CaCl_2$ 1, $MgSO_4$ 1.9, $NaHCO_3$ 1.9, NaH_2PO_4 2.9, glucose 5.5 (all in mM) (Wolf, 1963), buffered with 10 mM Hepes, pH 7.4]. The intestine was carefully cleaned and rinsed several times with the saline until the saline became almost clear. The intestine was then transferred to 100 ml citrate buffer [NaCl 96, KCl 1.5, KH_2PO_4 8,

Na_2HPO_4 5.6, Na-Citrate 27 (all in mM), pH 7.4] and shaken for 5 min. The intestine was subsequently removed from the buffer, blotted lightly with Kimwipes, and then transferred to 50 ml isolation buffer [NaCl 154, Na_2HPO_4 10, EDTA 2, dithiothreitol 1 (all in mM), pH 7.4]. The buffer was gently pipetted for 20 min with a Pasteur pipette. The intestine was removed from the isolation buffer and spread on a piece of aluminum foil. The loose mucosal epithelial cells were gently detached from the tissue layer using a cell scraper and transferred to the same isolation buffer. The clumped cells were dispersed by pipetting gently, and the suspension was filtered *via* a 230 μm mesh [cell dissociation sieve (CD-1), with 60 mesh screen (S1020); Sigma, USA]. The filtered cell suspension was centrifuged at 600 × *g* for 4 min at 4 °C. The cells were washed 3 times with 50 ml modified Cortland saline by centrifugation at 600 × *g* for 4 min at 4 °C. Subsequently, the cell pellet was resuspended with 5–10 ml of the modified Cortland saline and filtered *via* a 70 μm mesh (Product no. 352350; BD Falcon, Canada). The entire isolation procedure was performed on ice, and the salines were stirred vigorously for at least 30 min and stored at 4 °C before use. The purity of enterocyte suspension was checked under a light microscope, and the cell number and viability were checked using a trypan blue exclusion method and an automated cell counter (Countess® Automated Cell Counter; Invitrogen, USA). Only cell suspensions enriched with >80% enterocytes with *via*bility >85% were used for experiments. The cells were appropriately diluted to 1×10^6 cells/ml with the modified Cortland saline, and five 20 μl aliquots were stored at −20 °C for subsequent protein determination. The cells were allowed to incubate in a refrigerated water bath (Linberg Blue M; Thermo Scientific, USA) with gentle oscillation at 15 °C for 30 min prior to their use in any experiments. Each experiment was performed at least five times with cell preparations from an individual fish at each time. To avoid any potential variations due to the use of different batches of fish,

simultaneous controls were conducted for each set of experiment. For some experiments dealing with Cd and Pb exposures, the membrane integrity of the enterocytes (leakage of lactate dehydrogenase) was also evaluated (CytoTox-ONE Homogeneous Membrane Integrity Assay, G7890; Promega, USA). The protein content of the cells was determined using a protein assay kit (Total protein kit, TP0300; Sigma, USA).

4.2.4. Measurement of iron uptake in isolated enterocytes

The uptake of Fe^{2+} by enterocytes was determined using a radiotracer method ($^{59}FeCl_3$; PerkinElmer Life Science, USA). The preparation of the Fe^{2+} solution for the uptake experiments was similar as described by Kwong and Niyogi (2008). In brief, a stock solution of $FeCl_3$ was prepared by mixing cold $FeCl_3$ with nitrilotriacetic acid (NTA) at a molar ratio of 1:4 (Fe^{3+}:NTA), then an aliquot of the stock solution was radiolabeled with $^{59}Fe^{3+}$ (0.08 mCi/ml). Na-ascorbate was freshly mixed with the ^{59}Fe-NTA solution at a molar ratio of 1:20 (Fe:ascorbate) for 15 min before experiments. Nitrilotriacetic acid maintains the solubility of Fe while ascorbate maintains Fe in a reduced state (Fe^{2+}). To prepare Fe^{3+}, the solution was prepared similarly as described above except the addition of ascorbate.

To examine the concentration-dependent Fe^{2+} uptake (0.5–20 μM) at pH 6.0, 7.4 or 8.2, the cells were first pelleted and resuspended in modified Cortland saline at the desired pH, and 400 μl cell suspensions (1×10^6 cells/ml) were transferred into 1.5 ml microfuge tubes. The uptake was initiated by adding an appropriate amount of $^{59}Fe^{2+}$ solution into the cell suspensions. The microfuge tubes were gently inverted several times to ensure proper mixing. During exposure, the tubes were incubated in a refrigerated water bath at 15 °C with gentle oscillation.

To terminate the Fe^{2+} uptake, the tubes were removed from the water bath and 600 µl of ice-cold washing saline (modified Cortland saline, freshly supplemented with 2 mM NTA, pH 7.4) was added into the cell suspensions. The tubes were gently inverted several times and then centrifuged at 1000 × *g* for 1 min. The supernatant was removed and the cell pellet was washed 2 more times with 1 ml ice-cold washing saline. Subsequently, the radioactivity of ^{59}Fe in the cell pellet was measured by a Wallac 1480 Wizard 3″ gamma counter (PerkinElmer Life Science, USA). The non-specific binding (e.g., adsorption) of ^{59}Fe was evaluated in the presence of a 100-fold excess of cold iron, and was found to be around the background level (undetectable). To examine the time-dependent Fe^{2+} accumulation, the enterocytes were exposed to 2.5 µM Fe^{2+} at 15 °C and pH 7.4, and were sampled at 1, 2, 5, 10, 20 and 30 min. A Fe^{2+} concentration of 2.5 µM was chosen for this experiment because our calculated binding affinity (K_m) for Fe^{2+} uptake in isolated enterocytes was quite similar to this value (see Section 4.3).

4.2.5. Effect of ferrozine and high extracellular potassium on ferrous or ferric iron uptake

The effect of 100 µM ferrozine on the uptake rates of 2.5 µM Fe^{2+} and Fe^{3+} in isolated enterocytes was examined for 10 min at 15 °C and pH 7.4. Ferrozine is a membrane impermeable specific Fe^{2+} chelator. The use of ferrozine allowed us to confirm the Fe in the exposure saline was in Fe^{2+} state after ascorbate was added, and to evaluate the potential conversion of Fe^{3+} to Fe^{2+} by an apical ferric reductase of enterocytes (Raja *et al.*, 1992). To examine the effects of membrane depolarization on Fe^{2+} uptake in isolated enterocytes, the cells were exposed to 2.5 µM Fe^{2+} in a K^+-based saline at 15 °C for 10 min, pH 7.4. The K^+-based saline was prepared by replacing 110 mM NaCl with KCl in the modified Cortland saline. The

high K^+ saline has been reported to cause disruption of the membrane potential in human intestinal Caco-2 cells and significantly reduce Fe^{2+} uptake (Tandy *et al.*, 2000).

4.2.6. Inhibitory effect of cadmium and lead on ferrous iron uptake

The inhibitory effects of Cd and Pb on Fe^{2+} uptake in isolated enterocytes were examined in a CO_3^{2-} and PO_4^{2-}-free saline (modified Cortland saline without $NaHCO_3$ and NaH_2PO_4). Na-citrate in a molar ratio of 1:5 (Pb:citrate) was also used in the Pb experiment which maintained the solubility of Pb in the saline (Bannon *et al.*, 2003). Following exposure, the cells were washed with saline containing no CO_3^{2-} and PO_4^{2-}. The effects of varying Cd (as $CdCl_2$; 0–2 mM) and Pb (as Pb-acetate; 0–100 μM) concentrations on the absorption of 1 μM Fe^{2+} were conducted following the same experimental procedures and conditions as described above (10 min exposure at 15 °C and pH 7.4). In addition, the effect of 10 μM Cd on the uptake of 1 μM Fe^{2+} in isolated enterocytes was examined over 10, 20, 30 and 60 min.

To characterize the inhibitory properties of Cd or Pb on Fe^{2+} uptake, the concentration-dependent Fe^{2+} uptake (0.5–20 μM) was measured in the presence of either 1 mM Cd or 10 μM Pb for 10 min at 15 °C, pH 7.4. These concentrations were chosen based on our findings that the Fe^{2+} absorption could be significantly inhibited by 1 mM Cd or 10 μM Pb following 10 min of exposure (see Section 4.3). Since we found that the kinetic parameters of Fe^{2+} uptake, such as the apparent binding affinity (K_m) and the maximum transport rate (J_{max}), were very consistent in any control experiments, the data were pooled to generate a single curve from all the control replicates.

4.2.7. Calculations and statistics

All the statistical analyses and curve-fitting were performed using Sigmaplot® version 11.0. The data were presented as the mean ± SEM, and were expressed as either the Fe uptake rate (both Fe^{2+} and Fe^{3+}) [pmol Fe/(mg protein × min)] or Fe accumulation (pmol Fe/mg protein). The Fe^{2+} uptake data were analyzed using the Michaelis–Menten equation:

$$J_{in} = (J_{max} \text{ x } [X]) / ([X] + K_m) \quad (4.1)$$

where J_{in} is the Fe^{2+} uptake rate, $[X]$ is the concentration of Fe^{2+} in the exposure saline, J_{max} is the maximum uptake rate, and K_m is the concentration of Fe^{2+} that led to half-maximal uptake rate.

The concentrations of Cd and Pb, which resulted in 50% inhibition on Fe^{2+} uptake rate (IC_{50}) in isolated enterocytes, were estimated by fitting the log(dose)–response curves with the Hill equation:

$$J_{in} = [\text{min} + (\text{max} - \text{min})] / [1 + 10^{(\log(IC_{50}) - [X] \times (\text{Hill coefficient}))}] \quad (4.2)$$

where min and max represented the lowest and the highest Fe^{2+} uptake rates, respectively. The min was allowed to be predicted by the model, while the max was user-defined to the observed value of the 1 μM Fe^{2+} uptake rate in the absence of Cd and Pb (control).

The statistical difference between the control and treatment groups were analyzed either by an unpaired Student's *t*-tests (two-tailed) or by a one-way analysis of variance (ANOVA) followed by a least significant difference (LSD) test. Differences were considered significant at $p < 0.05$.

4.3. Results

4.3.1. mRNA expression of divalent metal transporter-1 and the viability of isolated enterocytes

The PCR analysis revealed the expressions of mRNA transcripts of both *Nramp-β* and *-γ* along the entire intestinal tract (anterior, mid and posterior intestine), as well as in the isolated enterocytes of rainbow trout (Figure 4.1). *Nramp-β* and *-γ* expressions were also recorded in the stomach, gill and liver (data not shown).

The viability of isolated enterocytes was typically 89–96% immediately after isolation, and remained >85% after 3 h of isolation at 15 ◦C, and for about 4 h when the cells were kept on ice (verified by trypan blue exclusion and LDH leakage assays). Figure 4.2a shows an overview of the enterocytes in suspension after 30 min of isolation. Some of the enterocytes maintained their usual cylindrical shape immediately following isolation (Figure 4.2b), however virtually all of the enterocytes changed to a spherical shape after 30 min (Figure 4.2a and c). Nevertheless, the microvillus structure was still distinguishable at the apical membrane of the enterocytes (Figure 4.2c). On the other hand, the exposure to Cd or Pb under our experimental conditions did not significantly affect the cell viability and membrane integrity (i.e., LDH leakage) (Appendix Figure A3).

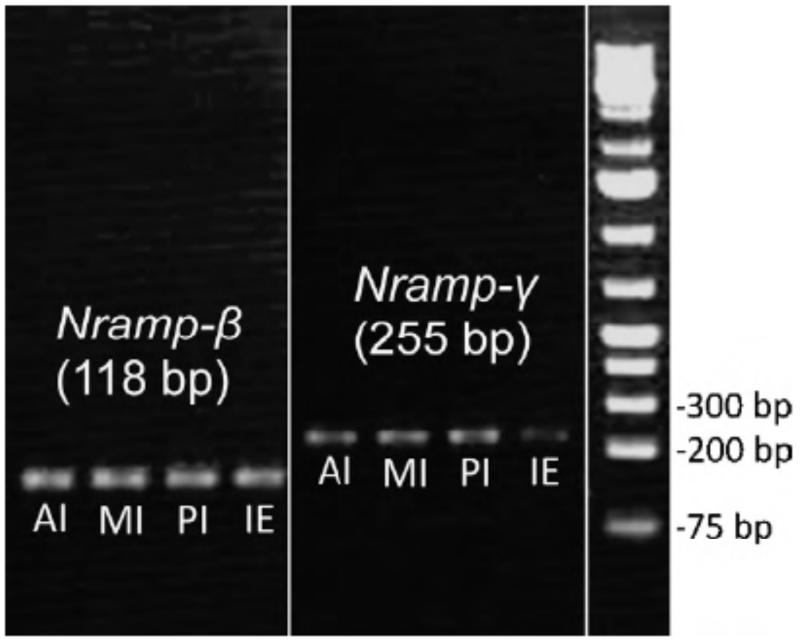

Figure 4.1: A representative picture showing the mRNA (messenger ribonucleic acid) expression of *Nramp-β* and *-γ* extracted from the tissue of intestines as well as from the isolated enterocytes of rainbow trout. The four bands for each gene are in the order of (from left to right): anterior intestine (AI), mid intestine (MI), posterior intestine (PI) and isolated enterocytes (IE).

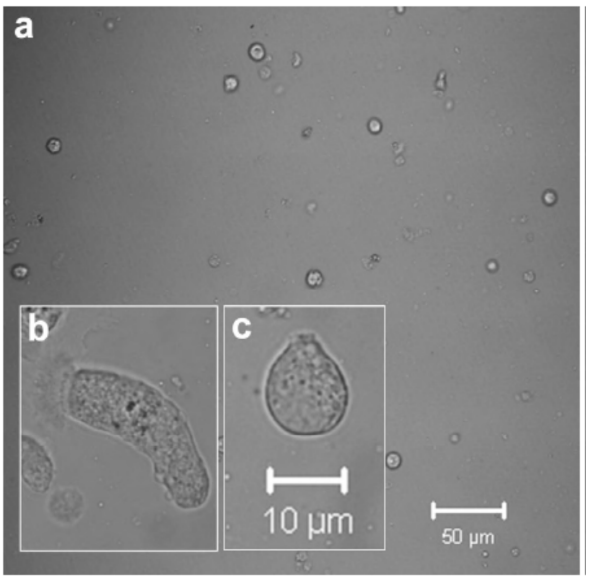

Figure 4.2: Representative photographs of isolated rainbow trout enterocytes in suspension: **(a)** the overview of the enterocytes in suspension after 30 min of isolation (objective magnification: 10×). **(b)** Immediately following isolation, the enterocytes remained in their cylindrical shape. **(c)** After 30 min, most of the enterocytes adopted a spherical shape. The microvillus structure is distinguishable indicating the apical membrane of the cells **(b and c)**. Photographs were captured using a Zeiss® Axioplan microscope equipped with a digital charge-coupled device (CCD) camera.

4.3.2. Concentration and time-dependent ferrous iron uptake in isolated enterocytes

Figure 4.3a shows the concentration-dependent Fe^{2+} uptake in isolated enterocytes at pH 6.0, 7.4 and 8.2, and the data were characterized by Michaelis–Menten relationship (r^2 = 0.92–0.98). The apparent K_m for Fe^{2+} uptake at pH 6.0, 7.4 and 8.2 were 1.7 ± 0.4, 2.3 ± 0.4 and 3.4 ± 1.3 μM, respectively, while the J_{max} at these pH levels were 0.61 ± 0.04, 0.62 ± 0.03 and 0.33 ± 0.04 pmol/mg protein/min, respectively. No statistical differences were observed among the K_m values at different pH (p = 0.36), whereas the J_{max} at pH 8.2 was significantly lower than that at pH 6.0 and 7.4 ($p < 0.001$). Figure 4.3b shows the accumulation of Fe^{2+} in the enterocytes over time following the exposure to 2.5 μM Fe^{2+}. Fe^{2+} accumulation in the enterocytes increased with the exposure time, and appeared to reach a steady state beyond 10 min with respect to the rate of accumulation.

4.3.3. Effect of ferrozine and membrane depolarization on ferrous or ferric iron uptake

The uptake rate of 2.5 μM Fe^{2+} in isolated enterocytes was significantly higher than that of 2.5 μM Fe^{3+} ($p < 0.001$) (Figure 4.4a). The uptake rates of both Fe^{2+} ($p < 0.001$) and Fe^{3+} ($p < 0.05$) were significantly reduced in the presence of 100 μM ferrozine. On the other hand, depolarization of the enterocytes induced by the K^+-based saline significantly reduced the uptake rate of Fe^{2+} ($p < 0.05$) (Figure 4.4b).

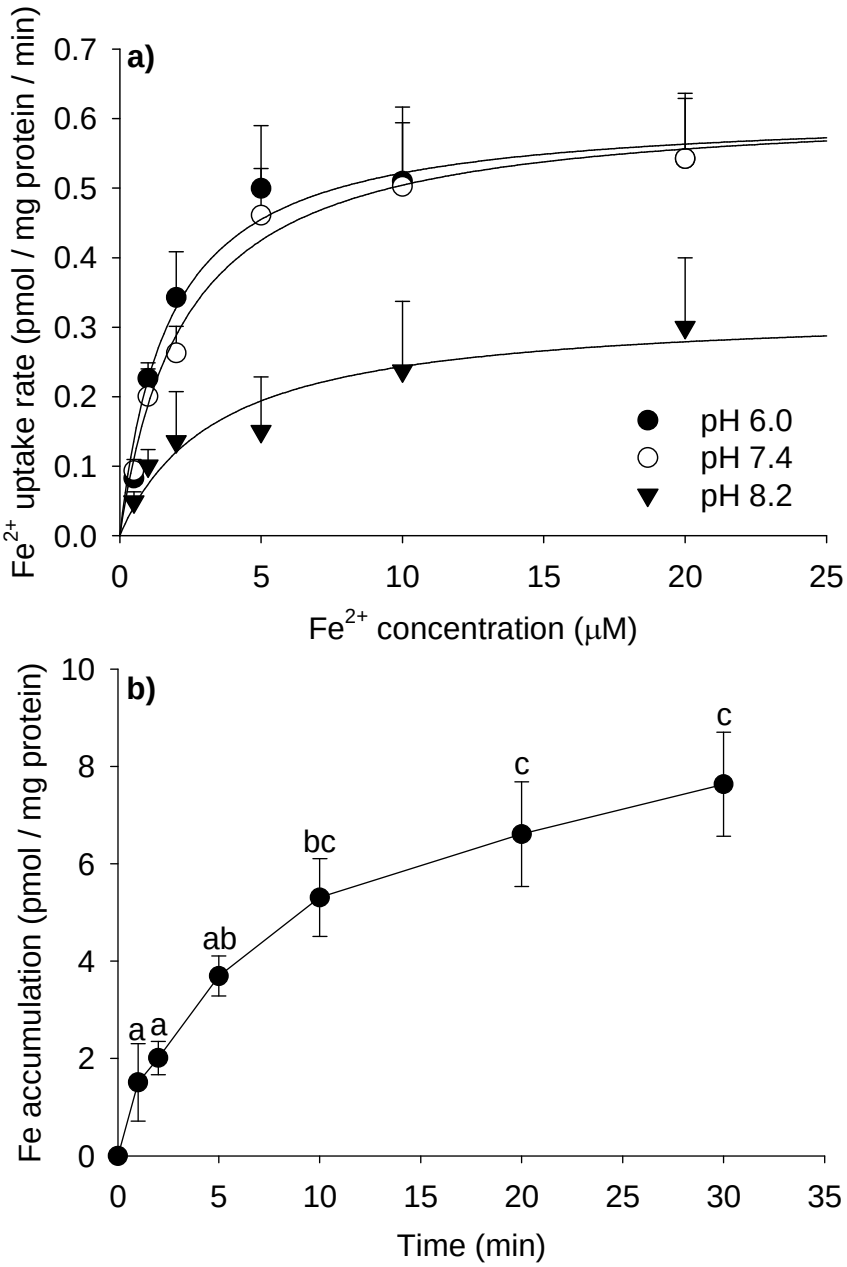

Figure 4.3: **(a)** The concentration-dependent ferrous (Fe^{2+}) iron uptake in isolated enterocytes of rainbow trout exposed to 0.5–20 μM Fe^{2+} at pH 6.0, 7.4 and 8.2 for 10 min. The curves were characterized by Michaelis–Menten relationship. **(b)** The time-dependent iron accumulation in isolated trout enterocytes following the exposure to 2.5 μM Fe^{2+} at pH 7.4 for 1–30 min. Different letters represent a significant difference among the data points (One-way ANOVA followed by a post-hoc LSD test; $p < 0.05$). Values are means±SEM (n = 5–10).

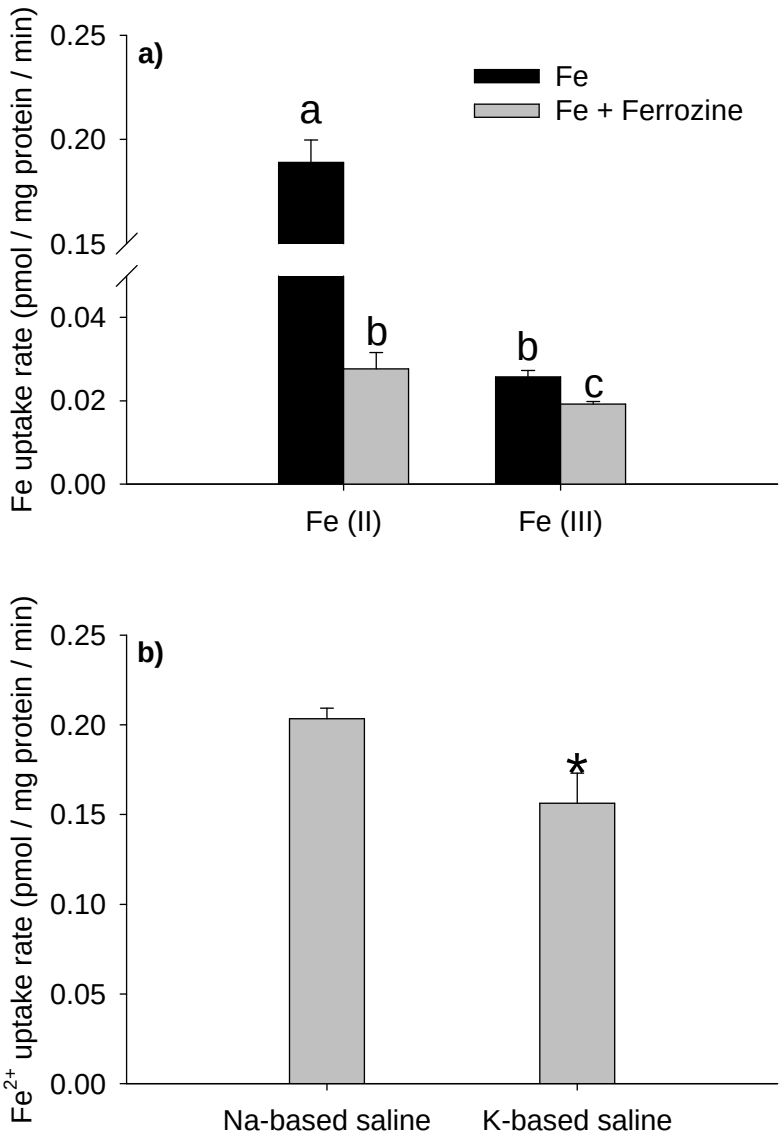

Figure 4.4: **(a)** The effect of a specific ferrous (Fe^{2+}) iron chelator ferrozine (100 µM) on the uptake rates of either 2.5 µM Fe^{2+} or ferric (Fe^{3+}) iron in isolated enterocytes of rainbow trout. Bars labeled with different letters are significantly different from each other (One-way ANOVA followed by a post-hoc LSD test; $p < 0.05$). **(b)** The Fe^{2+} uptake rates in isolated trout enterocytes exposed to 2.5 µM Fe^{2+} in a control saline (sodium-based saline; 133mM NaCl and 5mM KCl) and in a potassium-based saline (23mM NaCl and 115mM KCl). An asterisk indicates a significant difference compared to the control (Student's *t*-test; $p < 0.05$). Values are means±SEM ($n = 5$).

4.3.4. Effect of cadmium or lead on ferrous iron uptake in isolated enterocytes

Both Cd and Pb inhibited the uptake rate of 1 μM Fe^{2+} in a concentration-dependent manner in isolated enterocytes (Figure 4.5a). Concentrations of Cd at ≥1 mM or Pb at ≥10 μM significantly reduced Fe^{2+} uptake ($p < 0.05$). The log dose–response relationship of the inhibitory effects of both Cd and Pb was characterized by the Hill equation ($r^2 = 0.99$) (data not shown). The concentrations of Cd and Pb that caused 50% reduction (IC_{50}) of the uptake rate of 1 μM Fe^{2+} were 690.4 ± 1.2 and 7.1 ± 0.5 μM, respectively. The inhibitory effect of Cd on Fe^{2+} accumulation was also dependent on the exposure time (Figure 4.5b). 10 μM Cd significantly reduced the accumulation of Fe^{2+} in the enterocytes at 30 min ($p = 0.001$), whereas no statistical differences were observed at 10–20 min and at 60 min.

4.3.5. Kinetic analysis of ferrous iron and cadmium/lead interactions

The effects of 1 mM Cd and 10 μM Pb on the uptake kinetics of Fe^{2+} in isolated enterocytes exposed to 0.5–20 μM Fe^{2+} were shown in Figure 4.6a and b, respectively. In the presence of 1 mM Cd, the apparent K_m of Fe^{2+} uptake (11.91 ± 4.27 μM) increased significantly ($p < 0.05$) when compared to the control (Fe^{2+} alone; 2.30 ± 0.36 μM), whereas no statistically significant difference ($p = 0.09$) was recorded between the J_{max} values [control: 0.62 ± 0.03 pmol/(mg protein × min), and Cd treatment: 0.96 ± 0.17 pmol/(mg protein × min)]. Similarly, 10 μM Pb significantly ($p = 0.008$) increased the apparent K_m of Fe^{2+} uptake (6.24 ± 0.83 μM) without changing the J_{max} (0.60 ± 0.07 pmol/(mg protein × min)) when compared to the control ($p = 0.8$). The observed increase in the apparent K_m without any change in J_{max} indicated that both Cd and Pb inhibited Fe^{2+} uptake by competitive interaction in isolated enterocytes.

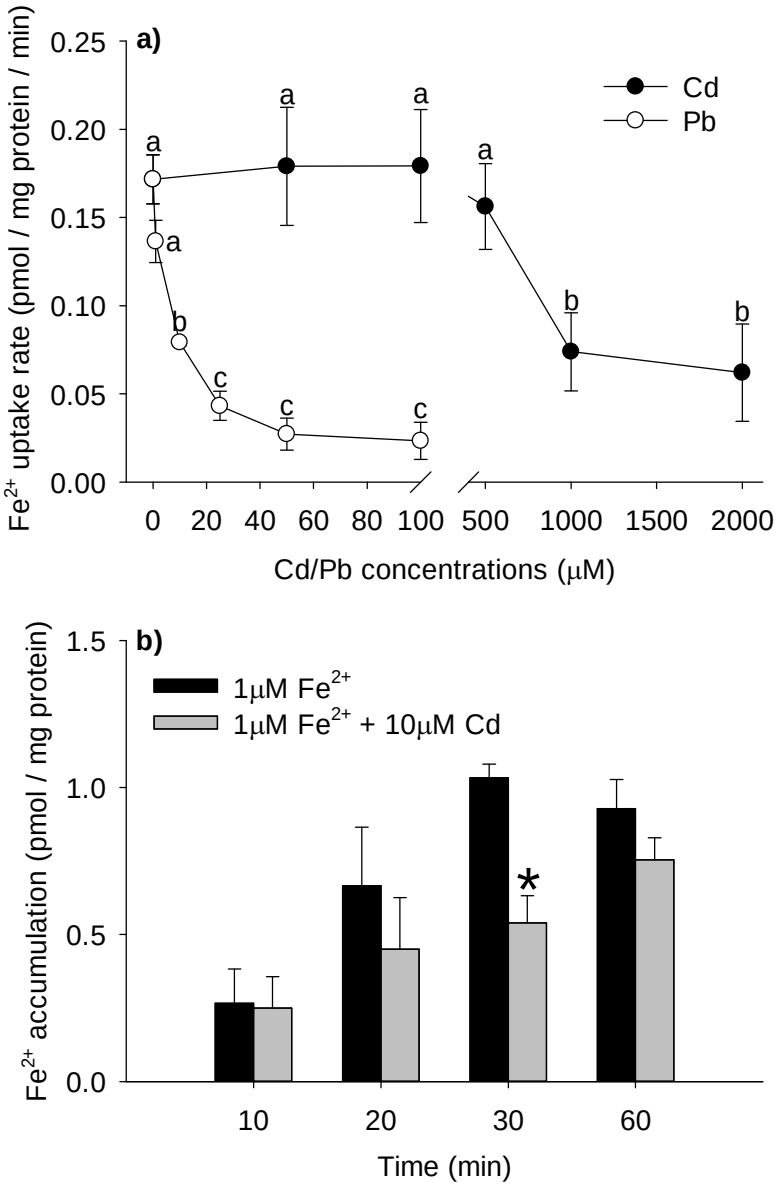

Figure 4.5: **(a)** The effect of increasing cadmium (Cd) or lead (Pb) concentrations on the uptake rate of 1 μM ferrous (Fe^{2+}) iron in isolated enterocytes of rainbow trout following 10 min of exposure. Statistical comparison among the Cd or Pb concentrations was performed separately, and different letters represent a significant difference (One-way ANOVA followed by a post-hoc LSD test; $p < 0.05$). **(b)** The effect of 10 μM Cd on the accumulation of 1 μM Fe^{2+} in isolated trout enterocytes following 10–60 min of exposure. An asterisk indicates a significant difference compared to the control (1 μM Fe^{2+} alone) at 30 min (Student's *t*-test; $p < 0.05$). Values are means±SEM ($n = 5$).

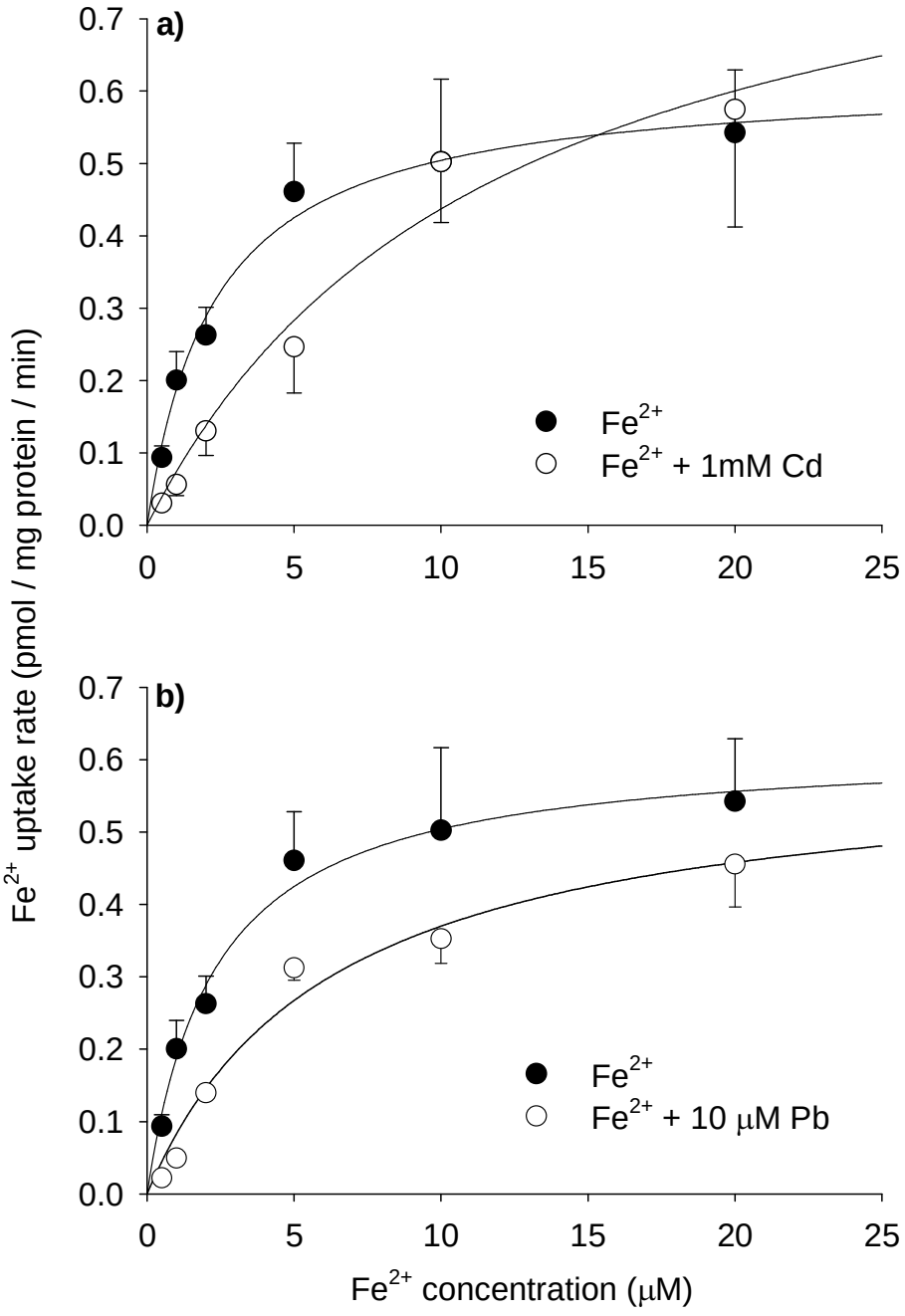

Figure 4.6: The concentration-dependent ferrous (Fe^{2+}) iron uptake in isolated enterocytes of rainbow trout exposed to 0.5–20 μM Fe^{2+} for 10 min in the presence of: **(a)** 1 mM cadmium (Cd) or **(b)** 10 μM lead (Pb). The curves were characterized by Michaelis–Menten relationship. Values are means±SEM (n = 5–10).

4.4. Discussion

To date, three different isoforms of *Nramp* gene products have been identified and cloned in rainbow trout (*O. mykiss*), *Nramp-α, -β* and *-γ* (Dorschner and Phillips, 1999; Cooper *et al.*, 2007). It has been suggested that *Nramp-α* is involved in antimicrobial activity, while *Nramp-β* and *-γ* function as divalent metal transporters (DMT1) and are involved in Fe^{2+} absorption in fish (Dorschner and Phillips, 1999; Cooper *et al.*, 2007). Cooper *et al.* (Cooper *et al.*, 2007) isolated *Nramp-β* and *-γ* transcripts from the rainbow trout gills and demonstrated that both isoforms can import Fe^{2+} when expressed in *Xenopus* oocytes. They also showed that Fe^{2+} transport by both DMT1 isoforms (*Nramp-β* and *-γ*), like their mammalian homologues, is dependent on a proton gradient (i.e., a Fe^{2+}/H^{+} symporter). Dorschner and Phillips (1999) reported *Nramp* (*-α* and *-β*) are expressed in brain, liver, heart, kidney, muscle, spleen and ovary of rainbow trout, however its expression has not been examined previously in the gastrointestinal tract of fish. This study is the first to report the gastrointestinal expression of DMT1 (*Nramp-β* and *-γ* isoforms), and provides evidence of its probable involvement in dietary Fe^{2+} uptake in fish enterocytes.

In the present study, we observed that the mRNA transcripts of DMT1 (*Nramp-β* and *-γ*) were expressed along the entire intestinal tract (anterior, mid and posterior intestines) as well as in the stomach (data not shown) of rainbow trout. Similarly, enterocytes isolated from the whole intestinal tract of trout showed the mRNA expression of *Nramp-β* and *-γ*, suggesting a role for the proteins in apical Fe^{2+} absorption in trout intestine. Using *in vitro* gut sac preparations, we have previously demonstrated that the absorption of Fe^{2+} occurs across the entire intestine of trout (Kwong and Niyogi, 2008). Several previous studies have suggested that Fe^{2+} transport by mammalian DMT1 is driven by a proton gradient and membrane potential (Gunshin *et al.*, 1997;

Tandy *et al.*, 2000; Mackenzie *et al.*, 2007). Cooper *et al.* (2007) reported that the rate of Fe^{2+} transport by gill Nramp-β and -γ proteins of trout is significantly higher at pH range of 5–7.5 than at pH 8–9. In the present study, we found that the uptake of Fe^{2+} in trout enterocytes was saturable over 0–20 μM of Fe^{2+} exposure, and the maximum rate of uptake (J_{max}) was about 2-fold greater at pH 6 and 7.4 relative to that at pH 8.2. In addition, disruption of the membrane potential of isolated enterocytes by substituting Na^+ with K^+ in the exposure saline significantly reduced the uptake of Fe^{2+}. Taken together, these results suggest that Fe^{2+} absorption in trout enterocytes occurs *via* DMT1 (Nramp-β and -γ). The affinity of Fe^{2+} transport (K_m: 2.3 μM) observed in the present study is comparable to that reported in mammalian Caco-2 cells (K_m: 2.9–7 μM) (Bannon *et al.*, 2003; Linder *et al.*, 2006), but considerably higher than that observed in isolated human enterocytes (K_m: 52.5 μM) (Goddard *et al.*, 1997). These discrepancies could be possibly due to the differences in acclimation to different dietary Fe regime, and Fe status and requirement of different species. Cooper and Bury (2007) reported a K_m value of 21.3 nM for *in vivo* branchial Fe transport in rainbow trout following the exposure of $FeCl_3$ for 3 h. This result indicates that the trout gill has a much higher affinity for Fe transport than the intestine. This is not surprising since the fish intestine operates in a Fe-rich environment relative to the gill, and dissolved Fe (especially in Fe^{2+} form) concentration is usually quite low in circum-neutral natural waters (Bury and Grosell, 2003a; Bury and Grosell, 2003b).

The present study showed that the maximum rate of Fe^{2+} uptake (J_{max}) in isolated enterocytes of rainbow trout was markedly lower at high pH (pH 8.2). However, it did not increase when the pH was decreased from 7.4 to 6.0. Cooper *et al.* (2006a) also reported that the rate of intestinal Fe^{2+} absorption in marine gulf toadfish (*Opsanus beta*) was not affected when pH was decreased from 7.0 to 5.5. Bury *et al.* (2001) observed that the intestinal Fe^{2+} uptake rate

did not change over a pH range of 7.1–7.8 in European flounder (*Platichthys flesus*). Therefore, it appears that both freshwater and marine fish can effectively acquire Fe from the diet at circum-neutral luminal pH. Nevertheless, it is possible that marine fish are more efficient in absorbing dietary Fe in alkaline pH (>8.0), unlike our observation in rainbow trout, since marine fish maintain a much stronger alkaline luminal environment than freshwater fish.

The present study demonstrated that the rate of Fe^{2+} uptake is approximately 10-fold higher than that of Fe^{3+} in isolated trout enterocytes. The higher bioavailability of Fe^{2+} over Fe^{3+} *via* both gill and intestine has been reported in fish by several previous studies (Bury *et al.*, 2001; Bury and Grosell, 2003b; Kwong and Niyogi, 2008). Non-heme iron in the food exists predominantly in Fe^{3+} form, and in mammals Fe^{3+} is first reduced to Fe^{2+} in the lumen by an apical ferric reductase (also known as duodenal cytochrome b; *Dcytb*) prior to its absorption *via* DMT1 (McKie *et al.*, 2001). Ferric reductase activity has been recorded in rainbow trout intestine (Carriquiriborde *et al.*, 2004), and its functional role in the intestinal absorption of Fe^{3+} has also been suggested (Kwong and Niyogi, 2008). The present study demonstrated that the membrane impermeable specific Fe^{2+} chelator (ferrozine) significantly reduced both Fe^{2+} and Fe^{3+} uptake in trout enterocytes, although the effect was more pronounced for Fe^{2+} than Fe^{3+}. This finding suggests that the extracellular conversion of Fe^{3+} to Fe^{2+} may have occurred, which was possibly mediated by the apical ferric reductase.

Previously, using *in vitro* gut sac preparations we demonstrated that several other divalent metals such as Cu, Cd, Ni, Pb and Zn inhibit intestinal Fe^{2+} absorption in trout, and suggested that these interactions occur likely *via* DMT1 (Kwong and Niyogi, 2009). Cooper *et al.* (2007) also reported that Fe^{2+} transport by trout gill Nramp-β and -γ proteins is sensitive to

inhibition by several divalent metals (e.g., Cd, Co, Mn, Pb and Zn), with the former being more sensitive to inhibition. Similar inhibition of Fe^{2+} transport by other divalent metals has also been reported in mammalian cells as well including enterocytes (Goddard *et al.*, 1997; Garrick *et al.*, 2006). Based on these observations, it can be suggested that DMT1 is likely involved in the dietary absorption of several divalent metals in addition to Fe^{2+} in fish. We also observed the mRNA expression of DMT1 (*Nramp-β* and *-γ*) in the trout stomach, suggesting stomach is a potential site of Fe^{2+} absorption in fish. Although the role of stomach in Fe^{2+} absorption has yet to be confirmed, other recent studies have demonstrated that the absorption of several divalent metals (e.g., Cd, Cu, Ni, Pb) occurs in the stomach of fish (Wood *et al.*, 2006; Ojo and Wood, 2007; Ojo and Wood, 2008). Overall, these results further indicate the possible role of DMT1 in the divalent metal absorption in the gastrointestinal tract of fish.

It is well recognized that DMT1 is involved in the absorption of dietary Cd in mammals (Park *et al.*, 2002; Bressler *et al.*, 2004; Ryu *et al.*, 2004). Recent evidence suggests that the absorption of both waterborne and dietary Cd in fish occurs *via* DMT1 as well, at least in part (Cooper *et al.*, 2006b; Cooper *et al.*, 2007; Kwong and Niyogi, 2009). In the present study, we found that Cd can competitively inhibit Fe^{2+} uptake in trout enterocytes. This finding is in agreement with several mammalian studies. For example, competitive inhibition of Fe^{2+} uptake by Cd has been observed in mammalian erythroid cells (Savigni and Morgan, 1998). Reciprocal interaction between Fe^{2+} and Cd uptake has also been demonstrated in mammalian kidney cell lines over-expressing DMT1 (Olivi *et al.*, 2001). However, the concentration of Cd required (1 mM) to significantly inhibit the uptake of 1 μM Fe^{2+} in trout enterocytes (exposed for 10 min) was considerably higher compared to that recorded in our previous study. We previously demonstrated that 20 μM Cd can inhibit the absorption of 2 μM Fe^{2+} in gut sac preparations of

rainbow trout following 2 h of exposure (Kwong and Niyogi, 2009). Therefore, we further examined the inhibitory effect of Cd with a longer exposure period, and observed that 10 μM Cd can significantly reduce the accumulation of 1 μM Fe^{2+} in trout enterocytes over an exposure period of 30 min, thereby corroborating our previous observation. Tandy *et al.* (Tandy *et al.*, 2000) also reported that the uptake of 1 μM Fe^{2+} can be significantly inhibited by 100 μM Cd in Caco-2 cells expressing rat duodenal DMT1 over an exposure period of 1 h. Nonetheless, the requirement of a relatively high concentration of Cd (at least 10-fold excess) in the exposure media in order to inhibit Fe^{2+} uptake in trout enterocytes suggests that Cd has a weaker affinity to the Fe^{2+} transport pathway (DMT1) than Fe^{2+}. Although the reciprocal effect of Fe^{2+} on Cd uptake by trout enterocytes was not examined in the present study, we previously reported that a 10-fold excess of Fe^{2+} exposure concentration could significantly reduce intestinal Cd accumulation in fish using *in vitro* gut sac approach. Interestingly, Cooper *et al.* (2007) demonstrated that although Fe^{2+} absorption *via* both DMT1 isoforms (*Nramp-β* and *-γ*) of rainbow trout can be inhibited by Cd when expressed in *Xenopus* oocytes, only *Nramp-β* mediates Cd absorption. The present study demonstrated that trout enterocytes do express the mRNA transcripts of DMT1 (both *Nramp-β* and *-γ*), and the interaction between Fe^{2+} and Cd in the enterocytes is competitive in nature. Collectively, these results suggest that Fe^{2+} and Cd have a shared uptake pathway in fish enterocytes *via* DMT1.

We previously observed that Pb was a stronger inhibitor than Cd on intestinal Fe^{2+} absorption in fish using *in vitro* gut sac preparations (Kwong and Niyogi, 2009). Consistent with that observation, the present study also demonstrated that the inhibition constant for Pb was approximately 100-fold lower than that for Cd. Moreover, our study also revealed that Pb can competitively inhibit Fe^{2+} uptake in trout enterocytes, as observed with Cd, but at a 100-fold

lower exposure concentration than Cd. These results indicate that Pb probably has a higher affinity for DMT1 than Cd, and intestinal Pb uptake in fish likely occurs *via* DMT1 as well. The inhibitory effect of Pb on Fe^{2+} uptake has been reported in isolated human enterocytes (Goddard *et al.*, 1997), and the role of mammalian DMT1 in Pb uptake has also been demonstrated (Bannon *et al.*, 2002). Interestingly, our previous study has shown that a 10-fold excess of Fe^{2+} in the exposure media could not reciprocally reduce Pb accumulation in trout intestine, suggesting additional pathways may be involved in Pb absorption (Kwong and Niyogi, 2009). In mammals, the physiological role of DMT1 in dietary Pb absorption is also inconclusive. For example, Bannon *et al.* (Bannon *et al.*, 2002) expressed rat DMT1 in a yeast cell line and observed that DMT1 can mediate both Fe^{2+} and Pb absorption with a similar affinity (K_m for Fe^{2+} and Pb uptake: 1.3 and 1.8 μM, respectively). However, it has also been demonstrated that Pb uptake was not impacted in DMT1-knockdown Caco-2 cells (Bannon *et al.*, 2003). These results suggest that DMT1 is not the only transporter for Pb uptake in mammalian intestinal cells. In fish, the role of apical Ca^{2+} channel has been implicated in the absorption of dietary Pb (Alves and Wood, 2006). The physiological importance of DMT1 in intestinal Pb absorption in fish requires further investigation.

4.5. Conclusions

This is the first study to report the expression of an apical Fe^{2+} transporter, DMT1 (*Nramp-β* and *-γ*), in the gastrointestinal tract of fish. We also characterized the kinetic properties of Fe^{2+} uptake in isolated fish enterocytes and its interaction with Cd and Pb. Our results suggest that Fe^{2+} uptake in fish enterocytes is carrier-mediated and sensitive to a proton gradient and

membrane potential, thereby indicating the involvement of DMT1. We also demonstrated that both Cd and Pb can competitively inhibit Fe^{2+} uptake in fish enterocytes, and Pb appears to be a stronger inhibitor than Cd. Overall, our study provides strong evidence that both Cd and Pb uptake may occur in the fish intestine *via* a Fe^{2+} transporting pathway (likely through DMT1). The present study also demonstrates that isolated enterocytes can serve as a useful experimental system to study the mechanisms of dietary divalent metal uptake in fish.

CHAPTER 5: Cadmium transport in isolated enterocytes of freshwater rainbow trout: interactions with iron and zinc, effects of complexation with cysteine, and an ATPase-coupled efflux[4]

5.1. Introduction

Cadmium (Cd) in its free ionic form (Cd^{2+}) is highly toxic to vertebrates including fish. The uptake of Cd in fish occurs primarily *via* the gills and gut. Cadmium is known to act like a calcium (Ca) analogue, and the antagonistic interaction between the branchial uptake of Ca^{2+} and Cd^{2+} is well documented (Hollis *et al.*, 2000; Niyogi and Wood, 2004; Niyogi *et al.*, 2008). The acute toxicity of waterborne Cd exposure in freshwater fish is generally associated with the impairment of active Ca^{2+} transport by the competitive blockade of apical lanthanum sensitive voltage-independent Ca^{2+} channels and/or selective inhibition of basolateral Ca^{2+}-ATPase transporters by Cd in gill mitochondria-rich chloride cells (Verbost *et al.*, 1987; Verbost *et al.*, 1989). The competitive interaction between Cd^{2+} and Ca^{2+} *via* apical Ca^{2+} channels have also been reported in mammalian hepatic and kidney cells (Friedman and Gesek, 1994; Souza *et al.*, 1997).

Recent studies have shown that exposure to elevated dietary Ca reduces Cd accumulation in the gastrointestine and the whole-body of fish (Franklin *et al.*, 2005; Klinck *et al.*, 2009; Ng *et*

[4] This chapter is conditionally accepted (pending minor revisions) for publication in Biometals, under joint authorship with Som Niyogi (University of Saskatchewan). The revised manuscript has been submitted and is currently under review.

al., 2009). However, the mechanism of interaction between luminal Ca and Cd remains unclear. The stomach is found to be an important site of Cd absorption in fish (Wood *et al.*, 2006; Ojo and Wood, 2007; Klinck and Wood, 2011), and the gastric Cd absorption appears to occur *via* a mechano-sensitive L-type (voltage-gated) Ca^{2+} channel, at least in part (Klinck and Wood, 2011). Unlike in the gills Cd uptake in the fish intestine is found to be largely Ca insensitive (Wood *et al.*, 2006; Ojo and Wood, 2008), which is similar to that observed in the mammalian enterocytes cell model (Caco-2 cells) (Jumarie *et al.*, 1997; Pigman *et al.*, 1997). Although Klinck and Wood (2011) have recently suggested the possible role of both L-type and lanthanum-sensitive Ca^{2+} channels in the intestinal Cd uptake of fish, the existence of such channels in the enterocyte are not clearly established. Presently, the mechanism(s) of Cd extrusion from enterocytes into the bloodstream is not well understood, although Schoenmakers *el al.* (1992) have linked the basolateral transport of Cd^{2+} to the Na^{+}/Ca^{2+} exchanger, and to the Ca^{2+}-ATPase and Na^{+}/K^{+}-ATPase – indicating that the basolateral Cd transport may be a Ca sensitive and/or ATP-dependent process.

There is a growing body of evidence suggesting that the intestinal Cd absorption in vertebrates occurs through the apical ferrous iron (Fe^{2+}) transporter, the divalent metal transporter-1 (DMT1) (Park *et al.*, 2002; Bannon *et al.*, 2003; Cooper *et al.*, 2006b; Kwong *et al.*, 2010). DMT1 is a proton-coupled Fe^{2+} transporter (i.e. Fe^{2+}/H^{+} symporter), and is ubiquitously expressed in various transport epithelia including intestine (Gunshin *et al.*, 1997; Kwong *et al.*, 2010). It has been reported that clonal knockdown of the DMT1 gene reduces the uptake of both Fe^{2+} and Cd^{2+} in Caco-2 cells (Bannon *et al.*, 2003). Recently, the expression of DMT1 has been recorded both in the stomach and intestine of fish (Kwong *et al.*, 2010). Kwong *et al.* (2010) have also demonstrated that Cd^{2+} inhibits the apical uptake of Fe^{2+} in the enterocytes in a

competitive manner – indicating their shared uptake *via* DMT1 in the fish intestine (Kwong *et al.*, 2010). In addition, treatment with a Fe-deficient diet has been found to increase the intestinal DMT1 expression as well as Cd accumulation, both in fish and mammals (Park *et al.*, 2002; Cooper *et al.*, 2006b). Similarly, exposure to a Fe-enriched diet has been shown to reduce Cd-burden in target organs including the gastrointestine (Włostowski *et al.*, 2003; Kwong *et al.*, 2011).

Recent molecular evidence from mammalian systems have suggested that luminal Cd^{2+} uptake can also occur *via* the Zn^{2+} transporters, the ZIP family of transporters (e.g., ZIP8) (Girijashanker *et al.*, 2008). These transporters are expressed predominantly on the apical membrane of enterocytes, and are believed to be functionally dependent on the extracellular bicarbonate (HCO_3^-) concentration (a Zn^{2+}/HCO_3^- symporter) (He *et al.*, 2006; Liu *et al.*, 2008). The mammalian homologues of the ZIP family of transporters are known to be expressed in the teleost gut (Feeney *et al.*, 2005; Qiu *et al.*, 2005). However, the current knowledge on their possible role in Cd absorption remains inconclusive. For example, Ojo and Wood (2008) and Klinck and Wood (2011) demonstrated that Cd^{2+} absorption can be inhibited by Zn^{2+} in rainbow trout (*Oncorhynchus mykiss*) intestine, providing circumstantial evidence of a potential shared uptake mechanism for Cd^{2+} and Zn^{2+}. In contrast, Glover *et al.* (2004) reported that Cd^{2+} does not compete with Zn^{2+} for uptake at the brush border membrane vesicles prepared from trout intestine. Clearly, further study is required to gain more precise insights into the mechanism of Cd and Zn interactions in the fish intestine.

Moreover, in the gut lumen Cd may form sulphur-conjugates with low molecular weight thiols such as cysteine, and it has been proposed that these conjugates act as molecular homologues which can be transported by specific transport proteins for amino acids or

oligopeptides (Zalups and Ahmad, 2003). Jumarie *et al.* (2001) has suggested that Cd bound to thiol-containing peptides (e.g., glutathione) is absorbed *via* transport pathways that differ from those involved in the absorption of inorganic Cd species (e.g., Cd^{2+}). To date, the effects of thiols on intestinal Cd absorption have rarely been investigated in fish (Zhang and Wang, 2007), and the evidence of bioavailability of any thiol-conjugated Cd species has not been reported.

In general, it appears that intestinal Cd transport may occur *via* multiple pathways in fish; however the physiological characteristics of these different pathways are poorly understood. The present study used freshly isolated enterocytes from a freshwater teleost, rainbow trout, to investigate the mechanisms of apical uptake and basolateral extrusion of Cd in the intestinal epithelium. The isolated enterocytes provide a more physiologically relevant experimental system than cultured cell lines, and allow us to characterize intestinal metal transport free of luminal and systemic interferences. We have recently used this system to characterize the kinetic and pharmacological properties of Fe transport in the teleost intestine (Kwong *et al.*, 2010). The objectives of the present study were five-fold: (i) to determine the time and concentration dependent profile of Cd uptake; (ii) to evaluate the interactive effects of extracellular Ca^{2+}, Zn^{2+} and Fe^{2+} on the kinetics of Cd uptake; (iii) to examine the effects of Ca^{2+} channel blockers, HCO_3^-, pH and ATPase activity on Cd uptake; (iv) to investigate the effects of Cd-cysteine complexation on Cd uptake and the potential existence of a specific transport mechanism for Cd-cysteine conjugate; and (v) to examine the role of ATPase activity in the basolateral extrusion of Cd.

5.2. Materials and methods

5.2.1. Experimental Fish

The freshwater rainbow trout (*Oncorhynchus mykiss*; ~1.0 kg wet weight) were obtained from Lucky Lake fish farm, SK, Canada. Fish were acclimated for at least 4 weeks in the laboratory condition and supplied with aerated, dechlorinated water [hardness 157 mg/L, alkalinity 109 mg/L (both as CaCO3), pH 8.1 – 8.2, dissolved organic carbon (DOC) 2.2 mg/L, Fe 5.5 µg/L, Zn 3.2 µg/L and Cd <0.1 µg/L] in a flow-through system. The water temperature was maintained at 15^{o}C and photoperiod mimicked natural conditions. Fish were fed Martin's commercial dried pellet feed (5-pt.; Martin Mills Inc., Elmira, ON, Canada) at a daily ration of 2% wet body mass. The measured metal concentrations in the feed were: Fe 220, Zn 167, Cu 32, Ni 4, Cd 0.07 and Pb 0.1 (all in mg/kg).

5.2.2. Isolation of enterocytes

Enterocytes from rainbow trout intestine were isolated as described by Kwong *et al.* (2010), with slight modifications. Briefly, fish were euthanized using MS-222 and bled to remove blood. The whole intestinal tract was dissected out and transferred to an ice-cold physiological saline [Modified Cortland Saline: NaCl 133, KCl 5, $CaCl_2$ 1, $MgSO_4$ 1.9, glucose 5.5 (all in mM) (Wolf, 1963), buffered with 10 mM Hepes, pH 7.4]. The intestinal tract was cut open longitudinally, rinsed several times with the saline until the saline became almost clear. Subsequently, the intestine was transferred to 100 ml citrate buffer [NaCl 96, KCl 1.5, KH_2PO_4 8, Na_2HPO_4 5.6, Na-Citrate 27 (all in mM), pH 7.4] and shaked for 5 min. The intestine was then removed from the buffer, blotted lightly with Kimwipes, and transferred to 100 ml isolation buffer [NaCl 154, Na_2HPO_4 10, EDTA 2, dithiothreitol 2, glucose 5.5 (all in mM), pH 7.4]. The buffer was gently pipetted for 20 min. The intestine was removed from the isolation buffer and

the loose mucosal epithelial cells were gently collected from the tissue layer using a cell scraper and transferred to the same isolation buffer. The clumped cells were dispersed by pipetting gently, and the suspension was filtered *via* a 230 µm mesh [Cell dissociation sieve (CD-1), with 60 mesh screen (S1020); Sigma, USA]. The filtered cell suspension was centrifuged at 600 g for 4 min at 4^{o}C. The cell pellet was resuspended and washed 3 to 5 times with 50 ml modified Cortland saline by centrifugation at 600 x *g* for 4 min at 4^{o}C. Subsequently, the cell pellet was resuspended with the modified Cortland saline and filtered *via* a 70 µm mesh (BD Falcon, Canada). The entire isolation procedure was performed on ice, and all the salines used were stirred vigorously for at least 30 min and stored at 4^{o}C before use. The purity of enterocytes suspension was checked under a light microscope, and the cell *via*bility and density were checked using a trypan blue exclusion method and an automated cell counter (Countess® Automated Cell Counter; Invitrogen, USA), respectively. The cell suspensions enriched with >80% enterocytes with *via*bility >85% were used for experiments. Our preliminary experiments showed that the *via*bility of enterocytes remained >85% for about 3 hours after isolation (data not shown), and all the experiments described in this study were completed within 2-2.5 hours. The cells were appropriately diluted to 1 x 10^6 cells / ml with the modified Cortland saline, and subsamples were saved and stored at -20^{o}C for protein measurement. The cells were incubated at 15^{o}C for 30 min prior to their use in any experiments. All the experiments described below were performed using the modified Cortland saline.

5.2.3. Experimental approach

The uptake of Cd in isolated enterocytes was determined using a radiotracer approach (as $^{109}CdCl_2$; PerkinElmer Life Science, USA) similar to the method described by Kwong *et al.*

(2010). In brief, 400 µl of cells (1 x 10^6 cell / ml) was transferred to a microfuge tube, and the uptake of Cd was initiated by adding an appropriate amount of Cd from the stock solution ($CdCl_2$ radiolabeled with ^{109}Cd, 0.03 mCi/ml). The total Cd concentration of the stock solution was verified by graphite furnace atomic absorption spectrometry (Analyst 800, PerkinElmer, USA). The exposure tube was gently inverted several times to ensure thorough mixing. To terminate the uptake of Cd, 600 µl of ice-cold washing saline (Modified Cortland saline plus 2 mM EDTA, pH 7.4) was added and mixed gently. The cells were then centrifuged at 1000 x *g* for 1 min and supernatant was removed. The cells were washed 2 more times with 1 ml of the washing saline. Subsequently, the radioactivity of ^{109}Cd in the cell pellet was counted on a gamma counter (Wallac 1480 Wizard 3"; PerkinElmer Life Science, USA). Each experiment was performed at least five times with cell preparations from an individual fish at each time, and 3 – 5 replicates and simultaneous controls were included for each experiment. The cell viability was not affected by any of the experimental treatments used in this study (data not shown).

5.2.4. Time and concentration-dependent cadmium uptake

We first evaluated the cellular Cd^{2+} uptake rate in a series of experiments with varying free Cd^{2+} concentrations (0.08 – 3.04 µM Cd^{2+}) and exposure time (1 – 30 min). The free Cd^{2+} concentrations in the saline were calculated using Visual MINTEQ (version 3.0) (Gustafsson, 2010). The saline Cd concentrations in subsequent treatments are also expressed as the free Cd^{2+} concentrations, unless stated otherwise. We observed that the cellular Cd^{2+} accumulation reaches a steady state at 10 min (see results), and the K_m [(the substrate concentration at which the rate of uptake is half of the J_{max} (maximum rate of uptake)] for Cd^{2+} uptake at 10 min was approximately 0.84 µM. Therefore, the subsequent experiments examining the effects of various

treatments on cellular Cd^{2+} uptake were performed at this condition (0.84 µM Cd^{2+} in saline, for 10 min), except where mentioned otherwise.

5.2.5. Effects of calcium, zinc and ferrous iron on cellular cadmium uptake

The possible inhibitory effects of Ca^{2+} (as $CaCl_2$; 0 – 50 mM), Zn^{2+} (as $ZnCl_2$; 1 – 100 µM) and Fe^{2+} (as Fe-ascorbate; 0 – 5 mM) on the uptake rate of 0.15 µM Cd^{2+} were examined for 10 min. Since the modified Cortland saline contained 1mM of $CaCl_2$, it was removed from the saline to achieve Ca^{2+} free exposure condition (0 mM Ca^{2+}). The Fe^{2+} exposure saline was prepared freshly by mixing $FeCl_3$ with ascorbate at a molar ratio of 1:2 for 30 min prior to experiment. Since we did not observe any inhibitory effects of Ca^{2+} on Cd^{2+} uptake after 10 min of exposure, we also examined the effect of 10 mM Ca^{2+} on Cd^{2+} uptake over 20 and 30 min of exposure periods. In addition, to evaluate the nature of interaction (competitive or non-competitive) between Cd^{2+} and Zn^{2+}, and Cd^{2+} and Fe^{2+}, the kinetics of Cd^{2+} uptake (0.08 – 3.04 µM Cd^{2+}, for 10 min) was examined in the presence of 10 µM Zn^{2+} or 2.5 mM Fe^{2+}. These concentrations of Zn^{2+} and Fe^{2+} were found to inhibit the uptake of 0.15 µM Cd^{2+} by 50% (see results).

5.2.6. Effects of calcium channel blockers, pH and ATPase inhibitor on cellular cadmium uptake

To examine the potential involvement of Ca^{2+} channels in Cd^{2+} uptake, the effects of two different Ca^{2+} channel blockers, verapamil (a voltage-gated or L-type Ca^{2+} channel blocker) and lanthanum (a non-voltage-gated Ca^{2+} channel blocker) (Sigma-Aldrich, USA), on Cd^{2+} uptake were examined. The cells were exposed to 10 µM or 100 µM of verapamil or lanthanum for 20 min prior to the examination of Cd^{2+} uptake rate. To examine the effect of pH on Cd^{2+} uptake,

the cells were resuspended in saline with pH 6.0, 7.4 (control) and 8.2 prior to the addition of radiolabeled Cd. The pH of the saline was modified by the addition of either 5N HNO_3 or NaOH. The effect of ATPase activity on Cd^{2+} uptake was evaluated by pre-exposing the cells to 10 or 100 µM sodium orthovanadate (a competitive inhibitor of ATPase) (Sigma-Aldrich, USA) for 20 min.

5.2.7. Effects of bicarbonate on cellular cadmium uptake

To evaluate the effects of bicarbonate (HCO_3^-) on Cd^{2+} uptake, the rate of uptake was measured in the presence of varying HCO_3^- concentrations (0 – 10 mM sodium bicarbonate). Freshly prepared HCO_3^- solution was added to the exposure saline, and pH was adjusted to 7.4 prior to the experiments. Since we found a significant increase in Cd^{2+} uptake rate at 10 mM HCO_3^- (see results), we further evaluated the role of HCO_3^- in Cd^{2+} uptake by pre-exposing the cells to a HCO_3^--transporter blocker, disodium 4,4′-diisothiocyanatostilbene-2,2′-disulfonate (DIDS; Sigma-Aldrich, USA) at 100 µM for 20 min.

5.2.8. Effects of cadmium-cysteine complexation on cellular cadmium uptake

The influence of complexation of L-cysteine (Sigma-Aldrich, USA) and Cd on cellular Cd uptake was investigated. To achieve different Cd-cysteine complexes, a total Cd concentration of 5.5 µM (radiolabeled, equivalent to 0.84 µM free Cd^{2+} in the saline) was mixed with different concentrations of L-cysteine (0 – 550 µM cysteine) for 30 min prior to any uptake experiments. The cysteine solution was prepared freshly before the experiment. The effect of L-cysteine on Cd speciation in the saline was evaluated by incorporating the conditional formation constants (log

K) for 6 possible Cd-cysteine complexes (Cole *et al.*, 1985) into the Visual MINTEQ. These 6 Cd-cysteine complexes and their respective formation constants are: $Cd(Cys)^+$ 10.3, $Cd(Cys)_2$ 16.92, $Cd(Cys)_3^-$ 19.78, $CdH(Cys)_2^+$ 24.97, $CdH(Cys)_3$ 29.21, and $CdH_2(Cys)_2^{2+}$ 30.93. The percentage of different Cd-cysteine species in the exposure media at different total Cd to cysteine ratios are summarized in Table 1. Since $Cd(Cys)^+$ complex appeared to be bioavailable to enterocytes (see results), experiments were designed to examine the concentration-dependent uptake of $Cd(Cys)^+$. Exposure media with different concentrations of $Cd(Cys)^+$ were prepared by mixing radiolabeled Cd and L-cysteine at a molar ratio of 1:1 (total Cd to cysteine) [74.3% existed as $Cd(Cys)^+$ at this condition; see Table 1], and the rate of cellular Cd uptake was measured as described previously.

5.2.9. Temporal profile of cellular cadmium efflux and the effects of ATPase inhibitor

To examine the kinetic and pharmacological characteristics of Cd efflux, the enterocytes were first incubated with radiolabeled Cd^{2+} (0.84 µM) in a 50 ml centrifuge tube for 30 min. The cells were then washed (with modified Cortland saline plus 2 mM EDTA, pH 7.4) by centrifugation (600 g for 4 min at 4°C). The supernatant was removed and the cells were resuspended in a Cd-free modified Cortland saline. 400 µl of cell suspensions (1 x 10^6 cells / ml) were transferred to each microfuge tube, and subsamples were collected to evaluate the initial Cd accumulation in the cells (time zero). The cells were maintained at 15°C during the efflux, and cell pellets were collected by centrifugation (1000 g for 1 min) at 5, 10, 20, 30 and 60 min for the estimation of the amount of accumulated Cd retained by the cells, relative to time zero. To evaluate the possible involvement of ATPase activity in Cd extrusion, the efflux experiment was performed in the presence of 10 µM sodium orthovanadate in the saline.

5.2.10. Calculations and statistical analysis

The amount of Cd in the enterocytes was calculated by dividing the ^{109}Cd radioactivity (in cpm; counts per minute) in the cells by the measured specific activity of Cd in the exposure media [^{109}Cd counts divided by total Cd (pmol)]. All the curve-fitting and statistical analyses were performed using GraphPad Prism® (version 5.0; GraphPad Software, San Diego California, USA). The data were presented as the mean ± SEM, and were expressed as either the Cd^{2+} uptake rate [pmol Cd^{2+}/(mg protein × min)] or Cd accumulation (pmol Cd/mg protein). The protein content of the cells was determined using a protein assay kit (Total Protein Kit, TP0300; Sigma, USA). The uptake kinetics of Cd^{2+} and $Cd(Cys)^{+}$ [at 0 – 7.4 µM $Cd(Cys)^{+}$] were analyzed using the Michaelis-Menten equation:

$$J_{in} = J_{max} \times [X] / ([X] + K_m) \quad (5.1)$$

where J_{in} is the Cd^{2+} or $Cd(Cys)^{+}$ uptake rate, [X] is the free Cd^{2+} or $Cd(Cys)^{+}$ concentration in the exposure saline, J_{max} is the maximum uptake rate, and K_m is the concentration of free Cd^{2+} or $Cd(Cys)^{+}$ that resulted in half-maximal uptake rate. The uptake kinetics of $Cd(Cys)^{+}$ at 7.4 – 22.2 µM was analyzed by the linear regression.

The 50% inhibition (IC_{50}) of 0.15 µM Cd^{2+} uptake by Zn^{2+} and Fe^{2+} were calculated using the log(dose) – response curves with the Hill equation:

$$J_{in} = \min + (\max - \min) / [1 + 10^{(\log(IC_{50}) - [X] \times (\text{Hill coefficient}))}] \quad (5.2)$$

where min and max represented the lowest and the highest Cd^{2+} uptake rates, respectively.

The statistical differences between any treatment groups were analyzed either by an unpaired Student's *t*-tests (two tailed) or by a one-way analysis of variance (ANOVA) followed by a post-hoc least significant difference (LSD) test. Except for the experiments with HCO_3^- and DIDS (HCO_3^- and DIDS treatments as two independent variables) and the Cd efflux study (efflux time and orthovanadate treatments as two independent variables), where a two-way ANOVA was employed, followed by the LSD test.. Differences were considered significant at $p < 0.05$.

5.3. Results

5.3.1. Cadmium speciation in different experimental conditions using Visual MINTEQ

The Cd speciation in the exposure media is summarized in Table 5.1. In the absence of cysteine, approximately 15.2% of the total Cd existed as free ion (Cd^{2+}), while 64.6% and 19.6% existed as $CdCl^+$ and $CdCl_{2(aq)}$, respectively. The presence of cysteine markedly changed the Cd speciation profile in the exposure saline. At the total Cd to cysteine ratio of 1:1, the major fraction of the total Cd (74%) existed as $Cd(Cys)^+$, however $CdH(Cys)_3$ became the predominant species when the total Cd to cysteine ratio increased to 1:10 or 1:100. The addition of $CaCl_2$, $ZnCl_2$ or Fe-ascorbate as well as the alteration of pH (6.0-8.2) did not affect the Cd speciation profile in the exposure saline, except a marginal reduction (2%) of free Cd^{2+} level in the presence of 50 mM $CaCl_2$ (data not shown). However, at 10 mM HCO_3^-, almost all the Cd was complexed with HCO_3^- (100%).

Table 5.1: The influence of cadmium (Cd) and L-cysteine complexation at different concentration ratios on Cd speciation profile in the modified Cortland saline.

Major Cd species	**Ratio of total Cd to L-cysteine**				
	1:0	**1:0.5**	**1:1**	**1:10**	**1:100**
Cd^{2+}	15.2%	7.8%	2.0%	-	-
$CdCl^{+}$	64.6%	33.2%	8.4%	-	-
$CdCl_{2(aq)}$	19.7%	10.1%	2.6%	-	-
$Cd(Cys)^{+}$	-	47.3%	74.3%	-	-
$Cd(Cys)_2$	-	-	1.8%	4.9%	-
$CdH(Cys)_2^{+}$	-	1.1%	10.7%	29.6%	3.3%
$CdH(Cys)_3$	-	-	-	60.9%	90.5%
$Cd(Cys)_3^{-}$	-	-	-	3.7%	5.6%

The Cd speciation was derived by Visual MINTEQ (version 3.0) (Gustafsson, 2010). Species listed are those existed more than 1% of the total dissolved metal in the saline.

5.3.2. Time and concentration-dependent of cadmium uptake

The accumulation of Cd^{2+} in isolated enterocytes increased with increasing exposure time, and appeared to reach a steady state at 10 min with each Cd^{2+} exposure concentration tested (Figure 5.1a). The concentration-dependent cellular uptake of Cd^{2+} uptake exhibited saturable Michaelis–Menten kinetics (r^2 = 0.95) (Figure 5.1b). The K_m and J_{max} values for Cd^{2+} uptake were found to be 0.86±0.13 µM and 3.7±0.5 pmol/min/mg protein, respectively.

5.3.3. Effects of calcium, zinc and ferrous iron on cadmium uptake

The uptake of 0.15 µM Cd^{2+} was not significantly affected by extracellular Ca^{2+} (0 – 50 mM) (Figure 5.2a), even after a longer exposure time (30 min) at 10 mM Ca^{2+} (data not shown). In contrast, the uptake of Cd^{2+} was inhibited by extracellular Zn^{2+} and Fe^{2+} (Figure 5.2b and 5.2c), and the IC_{50} for Zn^{2+} and Fe^{2+} was 9.8±1.1 µM and 2.6±1.3 mM, respectively.

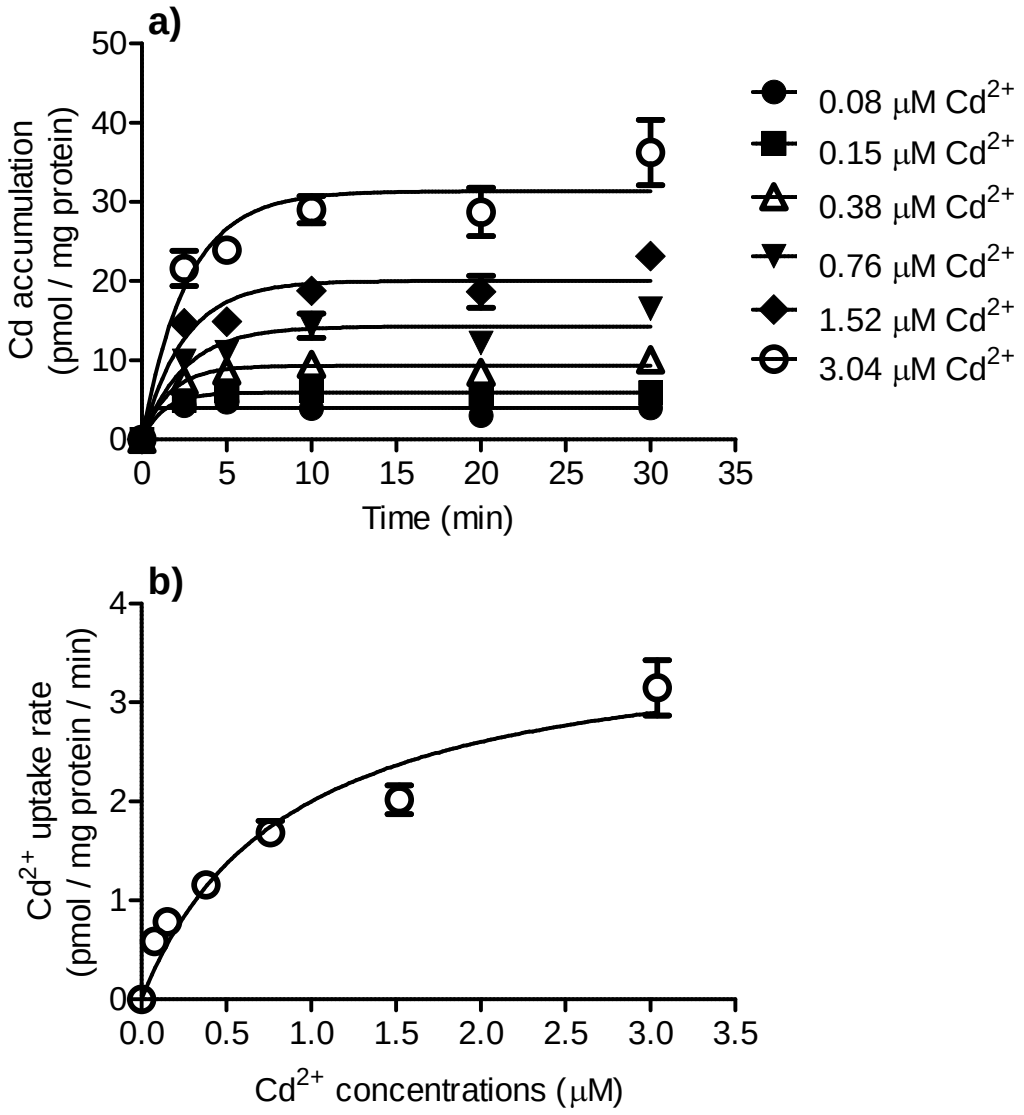

Figure 5.1: **(a)** The time-dependent accumulation of cadmium (Cd) in isolated rainbow trout enterocytes exposed to different free Cd^{2+} concentrations. **(b)** The concentration-dependent Cd^{2+} uptake rate in isolated enterocytes exposed to 0.08 – 3.04 μM free Cd^{2+}. The data were plotted using the Michaelis–Menten equation. Values are means ± SEM (*n* = 6-10).

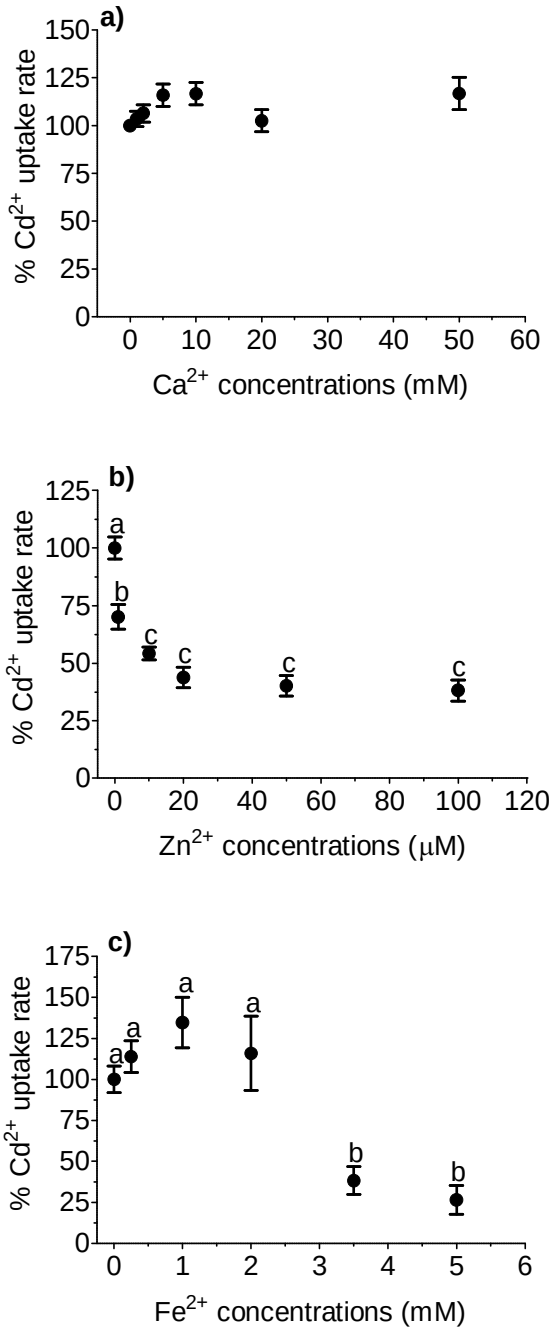

Figure 5.2: The effects of increasing extracellular **(a)** calcium (Ca^{2+}), **(b)** zinc (Zn^{2+}), and **(c)** ferrous iron (Fe^{2+}) on the uptake rate of 0.15 μM free cadmium (Cd^{2+}) in isolated rainbow trout enterocytes. The rate of Cd^{2+} uptake in different treatments is expressed as percentage (%) relative to the control (Cd^{2+} alone). Different letters represent a significant difference (One-way ANOVA followed by a post-hoc LSD test; $p \leq 0.05$). Values are means ± SEM ($n = 6$).

5.3.4. Kinetic analysis of zinc/cadmium and ferrous iron/cadmium interactions

The presence of 10 µM Zn^{2+} or 2.5 mM Fe^{2+} significantly reduced the rate of cellular Cd^{2+} uptake up to 0.38 µM Cd^{2+} in the exposure media (Figure 5.3). The concentration-dependent uptake of Cd^{2+} (0 – 3.04 µM) followed Michaelis–Menten kinetics in the presence of 10 µM Zn^{2+} and 2.5 mM Fe^{2+} (r^2 = 0.97-0.98). The apparent K_m of Cd^{2+} uptake (0.86±0.13 µM) increased significantly in the presence of Zn^{2+} (K_m: 1.93±0.56 µM) and Fe^{2+} (K_m: 1.69±0.26 µM) (p = 0.01 – 0.03). However, the apparent J_{max} of Cd^{2+} uptake (3.7±0.5 pmol/mg protein/min) was not significantly affected by the presence of Zn^{2+} (J_{max}: 4.1±0.6 pmol/mg protein/min) and Fe^{2+} (J_{max}: 4.0±0.7 pmol/mg protein/min).

5.3.5. Effects of calcium channel blockers, pH and ATPase inhibitor on cellular cadmium uptake

Pre-exposure to verapamil or lanthanum did not exhibit any effects on the cellular Cd^{2+} uptake rate (Figure 5.4a). The rate of Cd^{2+} uptake at pH 6.0 and 7.4 was not statistically different (p = 0.09). However, the uptake rate at pH 8.2 was significantly higher than that at pH 6.0 and 7.4 (p < 0.005) (Figure 5.4b). Pre-exposure to either 10 or 100 µM orthovanadate did not affect the cellular Cd^{2+} uptake rate (Figure 5.4c).

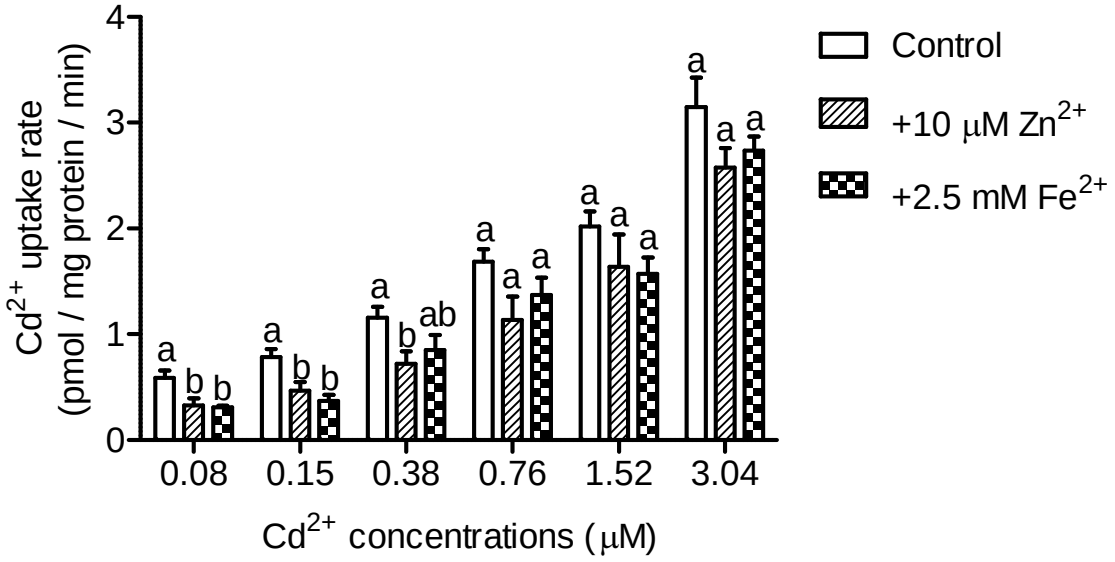

Figure 5.3: The effects of 10 μM zinc (Zn^{2+}) or 2.5 mM ferrous iron (Fe^{2+}) on the free cadmium (Cd^{2+}) uptake rate at different Cd^{2+} concentrations in isolated rainbow trout enterocytes. Control represents the uptake rate of Cd^{2+} alone. Different letters represent a significant difference within the same Cd^{2+} exposure concentration (One-way ANOVA followed by a post-hoc LSD test; $p \leq 0.05$). Values are means ± SEM (n = 6-10).

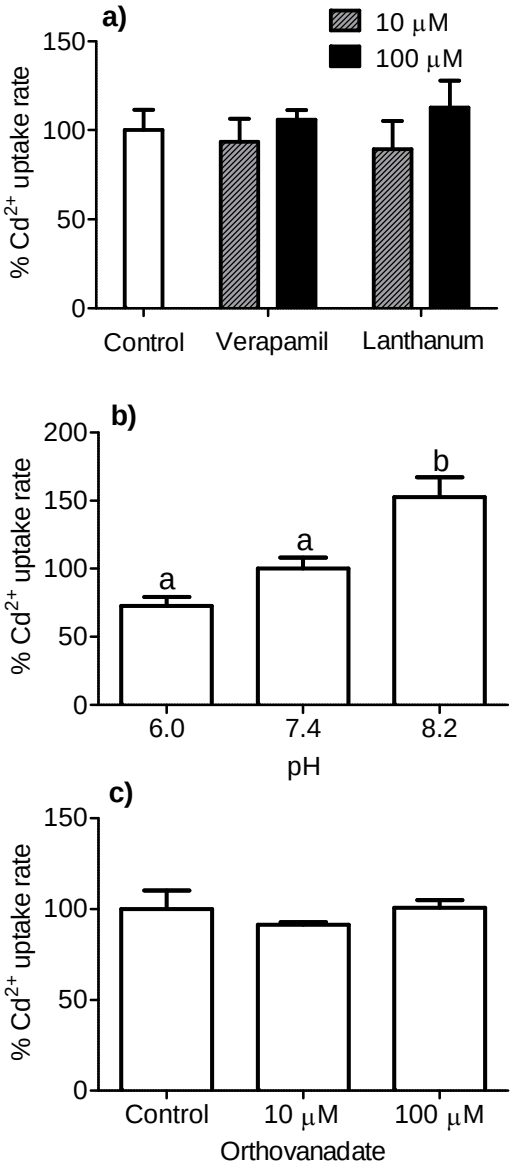

Figure 5.4: The effects of **(a)** calcium (Ca^{2+}) channels blockers, verapamil and lanthanum (10 µM and 100 µM), **(b)** varying pH [6.0, 7.4 (control), and 8.2], and **(c)** an ATPase inhibitor orthovanadate (10 µM and 100 µM), on the uptake rate of 0.84 µM free cadmium (Cd^{2+}) in isolated rainbow trout enterocytes. The rate of Cd^{2+} uptake in different treatments is expressed as percentage (%) relative to the control. Bars labelled with different letters represent a significant difference (One-way ANOVA followed by a post-hoc LSD test; $p \leq 0.05$). No statistical difference was recorded for the treatments of Ca^{2+} channels blockers and orthovanadate. Values are means ± SEM ($n = 5$).

5.3.6. Effects of bicarbonate and DIDS on cellular cadmium uptake

A significant increase (~25%) in the rate of cellular Cd^{2+} uptake was recorded at 10 mM HCO_3^- relative to the control (0 mM HCO_3^-) (Figure 5.5). Pre-exposure to DIDS significantly reduced the rate of Cd^{2+} uptake both in the presence and absence of HCO_3^- ($p < 0.005$), although the uptake rate remained significantly elevated in the presence of HCO_3^-. Two-way ANOVA revealed no significant interaction between HCO_3^- and DIDS ($p = 0.5$).

5.3.7. Effects of L-cysteine on cellular cadmium uptake and the uptake kinetics of admium-cysteine complex

A significant reduction in the rate of cellular Cd uptake was observed when the ratio of total Cd to cysteine was at 1:10 or higher ($p = 0.001$-0.03). However, the uptake rate was not affected when the ratio of total Cd to cysteine was 1:1 or below (Figure 5.6a). The rate of cellular Cd uptake as a function of $Cd(Cys)^+$ concentration in the exposure saline showed a concentration dependent increase (Figure 5.6b). The kinetic analysis revealed a biphasic uptake of $Cd(Cys)^+$. At $\leq$ 7.4 µM $Cd(Cys)^+$, the uptake was characterized by a saturable Michaelis–Menten kinetics ($r^2 = 0.99$), with the K_m and J_{max} values of 1.54±0.19 µM and 2.11±0.09 pmol/mg protein/min, respectively. The K_m value of $Cd(Cys)^+$ uptake was significantly higher than that of free Cd^{2+} uptake (0.86±0.13 µM) ($p < 0.01$), whereas no statistical difference was recorded between the J_{max} values. The uptake of $Cd(Cys)^+$ at the exposure concentration range of 7.4 – 22.2 µM was characterized by the linear kinetics ($r^2 = 0.99$).

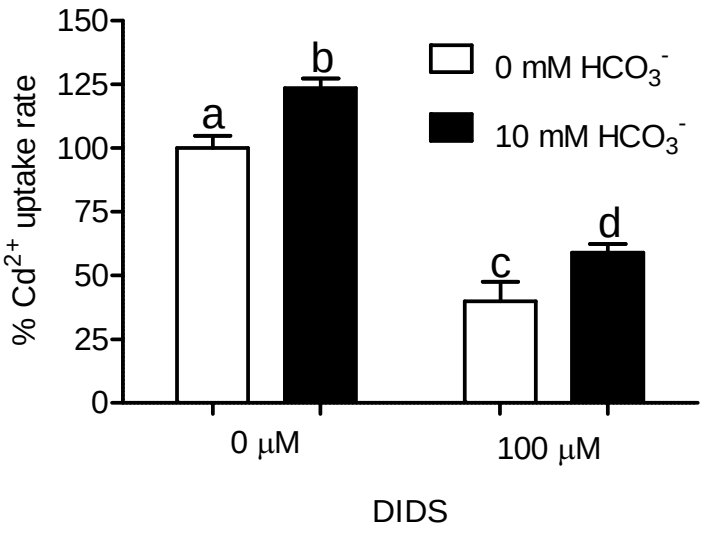

Figure 5.5: The effects of 10 mM bicarbonate (HCO_3^-) on the uptake rate of 0.84 μM free cadmium (Cd^{2+}) in isolated rainbow trout enterocytes, both in the presence and absence of an anion transport blocker, 4,4'-diisothiocyano-2,2'-stilbenedisulfonic acid (DIDS; 100 μM). The rate of Cd^{2+} uptake is expressed as percentage (%) relative to the control (No HCO_3^- and DIDS added). Bars labelled with different letters represent a significant difference (Two-way ANOVA with HCO_3^- and DIDS treatments as two independent variables, followed by a post-hoc LSD test; $p \leq 0.05$). Values are means ± SEM ($n = 5$).

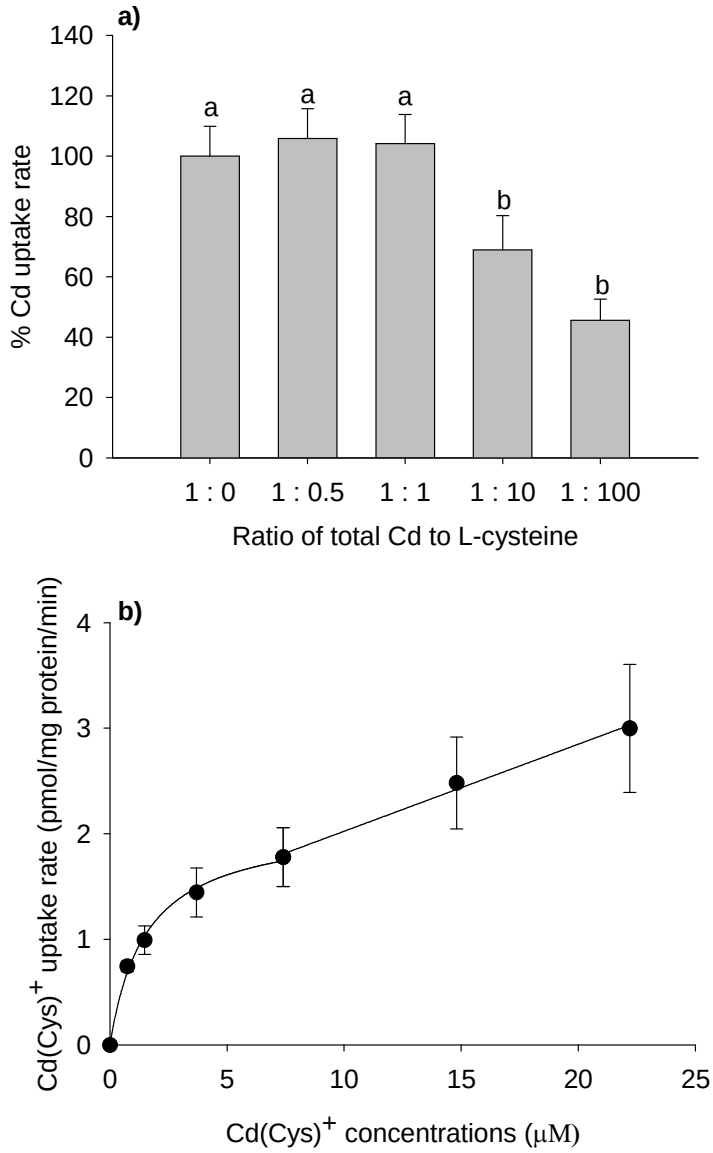

Figure 5.6: **(a)** The relative uptake rate (% relative to control) of 0.84 μM Cd^{2+} in isolated enterocytes, at different molar ratio of total Cd to L-cysteine in the exposure medium. The concentrations (% of total Cd) of different cysteine-conjugated Cd species are summarized in Table 1. Bars labelled with different letters represent a significant difference among the treatment groups (One-way ANOVA followed by a LSD test, $p < 0.05$). **(b)** The concentration-dependent uptake of $Cd(Cys)^+$ in isolated fish enterocytes. At 0 - 7.4 μM $Cd(Cys)^+$, the data were plotted using the Michaelis–Menten equation; at 7.4 – 22.2 μM $Cd(Cys)^+$, the data were plotted using the linear regression. Values are means ± SEM ($n = 5$).

5.3.8. Temporal profile of cellular cadmium efflux and the effects of orthovanadate

Two-way ANOVA revealed a significant interaction between efflux time and orthovanadate treatment ($p < 0.001$). After 60 min efflux, approximately 40% and 20% of accumulated Cd in the enterocytes was lost in the absence (control) and presence of orthovanadate, respectively, when compared to 0 min ($p < 0.001$) (Figure 5.7). However, the amount of Cd retained in the cells exposed to orthovanadate was significantly higher than that of the control after 60 min efflux ($p < 0.001$). No significant effect of orthovanadate on Cd efflux was recorded after 5, 10, 20 and 30 min of efflux (data not shown).

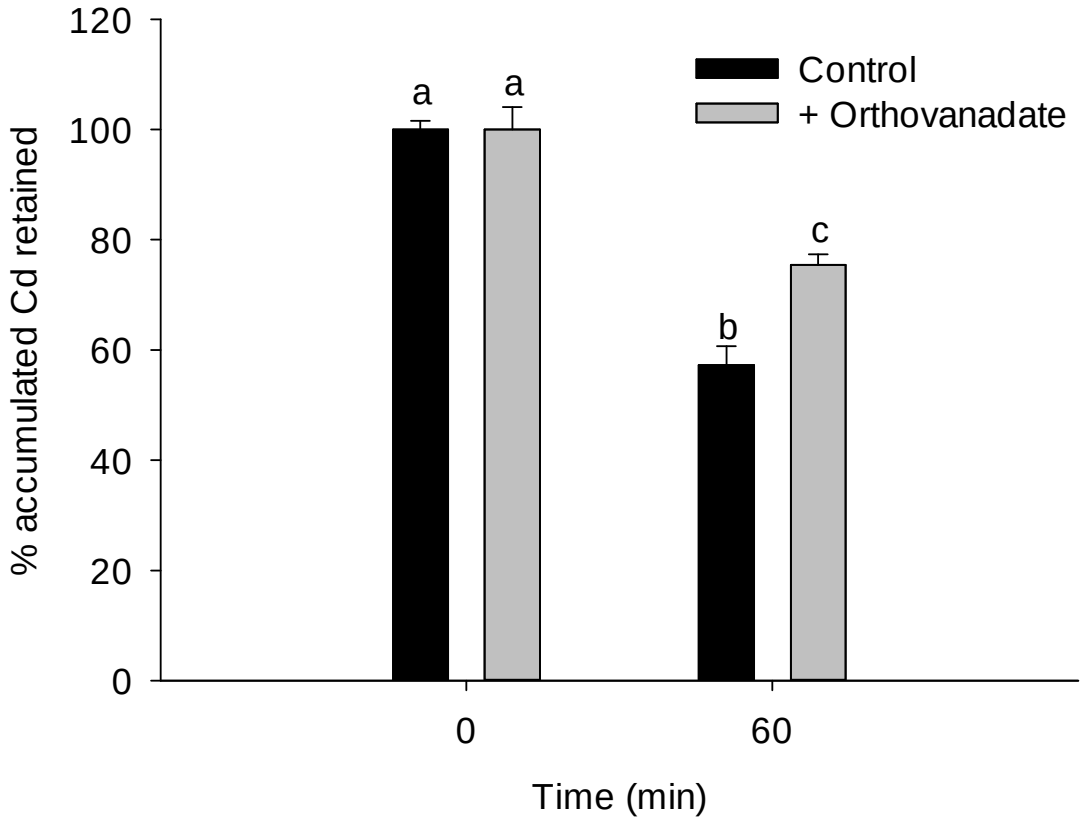

Figure 5.7: The percentage of accumulated cadmium (Cd) retained by the isolated fish enterocytes in the absence (control) and presence of an ATPase inhibitor, orthovanadate (10 µM), in the saline at 0 and 60 min of efflux. Bars labelled with different letters represent a significant difference among the treatment groups and across the efflux time (Two-way ANOVA followed by a LSD test, $p < 0.05$). Values are means ± SEM ($n = 6$).

5.4. Discussion

In the present study, we have provided evidence that Cd uptake in fish enterocytes can occur through multiple pathways. We have demonstrated that both Fe^{2+} and Zn^{2+} inhibit cellular Cd^{2+} uptake by competitive inhibition - indicating a shared apical uptake pathway for Cd^{2+} with Fe^{2+} and Zn^{2+}, likely *via* DMT1. The increase in Cd^{2+} uptake in the presence of HCO_3^- suggests that the ZIP transporters (e.g., ZIP8, a Zn^{2+}/HCO_3^- symporter) may also be involved in Cd^{2+} uptake. In addition, we have demonstrated for the first time that a specific transport pathway probably exists for the absorption of Cd-cysteine complex(es), and Cd extrusion from enterocytes likely occur *via* ATP-coupled transport mechanisms.

In our study, we observed that Cd^{2+} uptake in isolated fish enterocytes is a saturable, high-affinity transport process (K_m = 0.86 µM). The high affinity transport system for Cd^{2+} uptake has also been described in the mammalian enterocytes cell model, Caco-2 cells (K_m = 1.1 µM) (Elisma and Jumarie, 2001). Interestingly, we found that up to five orders of magnitude higher extracellular Ca^{2+} relative to Cd^{2+} did not have any effect on the cellular Cd^{2+} uptake. In addition, both verapamil (a voltage-gated Ca^{2+} channel blocker) and lanthanum (a voltage-insensitive Ca^{2+} channel blocker) did not produce any significant reduction in Cd^{2+} uptake. Calcium transport pathways have been suggested to play an insignificant role in intestinal Cd absorption in mammals (Thévenod, 2010). In freshwater fish, it has been suggested that Ca^{2+} transport pathways are important in the gastric uptake of Cd^{2+}, whereas the intestinal uptake of Cd^{2+} is primarily mediated by Ca^{2+}-insensitive pathways (Franklin *el al.* 2005; Ojo and Wood, 2008; Klinck *et al.* 2009). Using *in vitro* intestinal sac preparations, Klinck and Wood (2011) have recently shown that the Cd^{2+} absorption into the blood space (Cd that had been extruded from enterocytes into the muscle layer and the serosal fluid) was reduced by luminal Ca^{2+}. They have

also reported that Cd^{2+} absorption in the mucosal epithelium (enterocytes) and blood space of the mid and posterior intestines was inhibited by lanthanum but not by varapamil, although no comparable effect of lanthanum on Ca^{2+} absorption was observed in any intestinal compartments. Moreover, the expression of voltage-insensitive Ca^{2+} channels in the fish intestine is much lower relative to that in the gills (Shahsavarani *et al.*, 2006), where these channels are suggested to be the primary route of apical Cd^{2+} uptake (Verbost *et al.*, 1987; Verbost *et al.*, 1989). Klinck and Wood (2011) reported that the Cd^{2+} absorption in the mucosal epithelium of the mid intestine was also sensitive to nifedepine (an inhibitor of the dihydropyridine subclass of L-type Ca^{2+} channel), but the permeability of Cd^{2+} through L-type Ca^{2+} channels is known to be extremely low relative to that of Ca^{2+} (Tsien *et al.*, 1987). Nevertheless, it has been shown that intracellular Cd inhibits the basolateral Ca^{2+}-ATPase activity in the fish intestine (Schoenmakers *et al.*, 1992), and in the present study we found that Cd efflux from enterocytes was significantly reduced by an ATPase inhibitor (discussed below) – indicating the basolateral membrane of enterocytes might be the main site of Cd^{2+} and Ca^{2+} interaction. Based on the information discussed here, it is reasonable to suggest that the interaction of luminal Cd^{2+} and Ca^{2+} has a marginal significance, if any, on apical Cd^{2+} absoprtion in the intestinal epithelium of fish.

Recent molecular evidence has suggested that Cd^{2+} may be absorbed in the mammalian intestine through the ZIP family of Zn^{2+} transporters (e.g., ZIP8) (Girijashanker *et al.*, 2008). Although the interactive effects between luminal Cd^{2+} and Zn^{2+} have been documented in fish, the precise mechanism(s) of such interactions remains inconclusive. Glover *et al.* (2004) reported that Cd^{2+} does not affect apical Zn^{2+} uptake in brush-border membrane vesicles of trout enterocytes. In contrast, Ojo and Wood (2008) showed that Cd^{2+} uptake can be inhibited by Zn^{2+} in the mucosal epithelium of trout intestine and *vice versa*. The present study demonstrated a

somewhat dose-dependent inhibitory effect of Zn^{2+} on Cd^{2+} uptake in enterocytes, and the kinetic analysis revealed a competitive interaction between the two metal ions since the presence of Zn^{2+} increased the K_m of Cd^{2+} uptake without any change in the J_{max}. These results strongly suggest that the apical uptake of Cd^{2+} and Zn^{2+} occurs through the same transport pathway. Similar type of Cd^{2+} and Zn^{2+} competition was also reported in the brush border membrane vesicles prepared from the pig intestine (Tacnet *et al.*, 1990). The interactions of Cd^{2+} and Zn^{2+} in the fish gill is known to occur *via* the shared Ca^{2+} transport pathway (Hogstrand *et al.*, 1994; Wicklund Glynn, 2001), which is evidently not the case in the present study since Ca^{2+} did not have any effect on Cd^{2+} uptake in the enterocytes. The competitive interaction of Cd^{2+} and Zn^{2+} observed in our study is possibly a result of their shared uptake *via* the ZIP family of Zn^{2+} transporters. The expression of ZIP homologues has been reported in the teleost gut (Feeney *et al.*, 2005; Qiu *et al.*, 2005), although their functional properties have not been investigated. Mammalian ZIP transporters are known to function as Zn^{2+}/HCO_3^- symporter, and can be effectively blocked by DIDS (He *et al.*, 2006; Girijashanker *et al.*, 2008). Similarly, we observed that increased HCO_3^- concentration in the exposure media significantly stimulated Cd^{2+} uptake, and pre-exposure to DIDS reduced Cd^{2+} uptake by ~ 60% in the enterocytes, with or without elevated HCO_3^-. We therefore postulate that a major fraction of intestinal Cd^{2+} absorption in freshwater fish occur *via* the Zn^{2+} transport systems, likely the ZIP family of transporters (e.g., ZIP8). It is important to note here that although our Cd speciation estimation at 10 mM HCO_3^- revealed no free Cd^{2+} in the exposure media, it was probably not a true reflection of the actual experimental condition. This is because Visual MINTEQ operates on the basis of a chemical equilibrium, whereas our experimental condition was not in equilibrium since the Cd^{2+} was freshly added to the exposure media to initiate the uptake studies.

Several previous studies have suggested that the intestinal uptake of Cd^{2+}, both in mammals and fish, can occur *via* the apical Fe^{2+} transporter, DMT1 (Elisma and Jumarie, 2001; Park *et al.*, 2002; Bannon *et al.*, 2003; Kwong *et al.*, 2010). We have recently shown that elevated dietary iron reduces chronic dietary cadmium accumulation in the gastro-intestinal tissue of fish - indicating the physiological importance of the intestinal Fe absorption pathways in dietary Cd accumulation (Kwong *et al.*, 2011). The present study also demonstrated that Fe^{2+}, like Zn^{2+}, inhibited Cd^{2+} uptake in the enterocytes through competitive interaction. This complements our previous observation that Cd^{2+} competitively inhibits Fe^{2+} uptake in trout enterocytes (Kwong *et al.*, 2010), further corroborating the notion that Cd^{2+} and Fe^{2+} share a common apical uptake mechanism in the intestinal epithelium of fish. The inhibitory effect of Fe^{2+} on Cd^{2+} uptake has also been observed in Caco-2 cells, and the inhibition constant (K_i) was reported to be in the micromolar range (Elisma and Jumarie, 2001). However, the present study suggested that millimolar concentrations of Fe^{2+} are required to significantly reduce Cd^{2+} uptake in trout enterocytes, which is in accordance with our previous finding that Cd^{2+} has a relatively weak affinity to the Fe^{2+} transport pathway in trout enterocytes (Kwong *et al.*, 2010). The apparent contradiction between the observation of Elisma and Jumarie (2001) and our finding is likely due to the difference in the expression level of DMT1 and/or its Cd^{2+} transport function between the two cell types. Similar differences were also observed between freshly isolated human enterocytes and other mammalian cell models with regards to the inhibitory effect of Mn^{2+} on Fe^{2+} transport (Goddard *et al.*, 1997; Garrick *et al.*, 2003). On the other hand, our previous investigations have indicated that the transport efficiency of Fe^{2+} *via* DMT1 in the fish intestine is reduced at alkaline pH (>8.0) (Kwong and Niyogi, 2008; Kwong *et al.*, 2010). In the present study however, we found that the uptake of Cd^{2+} in the enterocytes increased at alkaline

pH (8.2) relative to that at the acidic to circum-neutral range (6.0 – 7.4). Considering DMT1 is not the only transporter that mediates Cd^{2+} uptake, it is possible that when the function of DMT1 is not optimal, Cd^{2+} is transported into the enterocytes by other transporters which operate efficiently at the alkaline pH. For example, the efficiency of Zn^{2+} transport *via* ZIP transporters was shown to increase with increasing pH (He *et al.*, 2006). In the rat intestinal brush border membrane vesicles, Cd absorption was found to increase at alkaline pH (Endo *et al.*, 2000). Endo et al. (2000) proposed that at high extracellular pH, Cd^{2+} might be transported across the brush border membrane *via* a Cd^{2+}/H^{+} antiport. On the other hand, we observed that Zn^{2+} has a higher affinity than Fe^{2+} for the Cd^{2+} transport systems in fish enterocytes (the IC_{50} for Fe^{2+} was about 260 fold higher than Zn^{2+}). It is also important to note that in addition to Fe^{2+} and Cd^{2+}, DMT1 is also known to mediate the transport of several other divalent metals including Zn^{2+} (Gunshin *et al.*, 1997; Garrick *et al.*, 2006; Mackenzie *et al.*, 2006). However, Cd^{2+} was shown to have a greater affinity for DMT1 than Zn^{2+} in the fish intestine (Kwong and Niyogi, 2009). Therefore, DMT1 was probably not the major site of interaction between Cd^{2+} and Zn^{2+} in the present study. Overall, it is apparent that both Zn^{2+} and Fe^{2+} transport pathways play a significant role in the absorption of Cd^{2+} in the intestinal epithelium of fish.

It has been proposed that Cd^{2+} may form stable S-conjugates with cysteine in the gut lumen, and Cd-cysteine conjugates serve as molecular homologues of some amino acids or peptides for amino acid or peptide transporters (Zalups and Ahmad, 2003). However, the effects of cysteine on intestinal Cd^{2+} uptake and the presence of a specific transport mechanism for Cd-cysteine conjugate(s) have not been fully elucidated. Zhang and Wang (2007) reported that 50 μM cysteine reduces the accumulation of 0.1 μM Cd^{2+} in the mucosal epithelium of the marine fish *Acanthopagrus schlegeli*. In the present study, we observed that the effect of cysteine on

Cd^{2+} uptake in trout enterocytes was largely dependent on Cd-cysteine speciation. For example, the uptake of Cd was not affected, relative to that in the control (uptake of only inorganic free Cd^{2+}), when Cd existed predominantly as $Cd(Cys)^{+}$ – indicating that $Cd(Cys)^{+}$ is readily bioavailable to enterocytes. In contrast, a significant reduction of Cd uptake was observed when Cd existed primarily as $CdH(Cys)_2^{+}$ and $CdH(Cys)_3$. Interestingly, even when there was no free Cd^{2+} or $Cd(Cys)^{+}$ in the exposure media, Cd uptake only decreased by 40-60% relative to that in the control, suggesting that Cd-cysteine conjugate(s) other than $Cd(Cys)^{+}$ may also be bioavailable to the enterocytes. Under exposure conditions where the concentration of free Cd^{2+} was kept constant (2%), Cd uptake in the enterocytes increased with increasing concentrations of $Cd(Cys)^{+}$. Kinetic analysis clearly revealed that the apical uptake of $Cd(Cys)^{+}$ occurred through a biphasic transport mechanism. At low $Cd(Cys)^{+}$ concentrations, $Cd(Cys)^{+}$ uptake was characterized by a saturable Michaelis-Menten kinetics, suggesting the involvement of a specific transport mechanism. The specific uptake of $Cd(Cys)^{+}$ was possibly mediated by the amino acid (cysteine) transporter (Zalups and Ahmad, 2003). Interestingly, the affinity of $Cd(Cys)^{+}$ uptake was about two fold lower than that of free Cd^{2+} uptake. Similar observation was also reported in Caco-2 cells, where the affinity for the uptake of another thiol conjugate, Cd- glutathione (GSH), was about three fold lower than that of free Cd^{2+} (Elisma and Jumarie, 2001; Jumarie *et al.*, 2001). However, the linear uptake of $Cd(Cys)^{+}$ at high $Cd(Cys)^{+}$ concentrations observed in the present study suggested that the uptake of $Cd(Cys)^{+}$ may also occur through a non-specific diffusive process.

In the present study, we observed that Cd efflux is a remarkably slow process relative to the Cd influx, as almost 60% of the accumulated Cd still remained in the enterocytes after 60 min of efflux. The ability of enterocytes to retain Cd would minimize the amount of Cd entering

into the systemic circulation, thereby reducing the load of Cd transported to the target organs. Previous studies have also shown that the majority of Cd (~80%) accumulated by the fish was confined in the intestinal tissues relative to other internal organs after chronic exposure to dietary Cd (Ng and Wood, 2008; Kwong *et al.*, 2011). Schoenmakers et al. (1992) reported that intracellular Cd inhibits the basolateral Na^+/K^+-ATPase and Ca^{2+}-ATPase in the fish intestine; however whether these transporters are actually involved in Cd extrusion remain unknown. In the mammalian systems, it has been reported that the activities of Na^+/K^+-ATPase and Ca^{2+}-ATPase can be inhibited by a P-type ATPase inhibitor, orthovanadate (Robinson and Mercer, 1981; Pick, 1982). In the present study, we demonstrated that Cd efflux from enterocytes was significantly inhibited by orthovanadate, indicating Cd extrusion occurred through an ATPase-driven process, at least partially. The extrusion of Cd is likely associated with the basolateral Na^+/K^+-ATPase and/or Ca^{2+}-ATPase (Schoenmakers *et al.*, 1992).

5.5. Conclusions

In conclusion, our results suggest that Cd^{2+} is taken up *via* the Zn^{2+} (ZIP transporters) and Fe^{2+} (DMT1) transport pathways in fish enterocytes. Evidence from the present study as well as from other studies suggest that Cd^{2+} does not directly interact with Ca^{2+} at the apical membrane of enterocytes, but possibly interacts with Ca^{2+} intracellularly and/or at the basolateral Ca^{2+} transporters. In addition, we found that the effect of Cd-cysteine complexation on Cd uptake in the enterocytes is largely dependent on Cd-cysteine speciation. $Cd(Cys)^+$ appears to be rapidly bioavailable and its uptake seems to occur through a low affinity transport mechanism, which is different from the high affinity transport mechanism for free inorganic Cd^{2+}. Our study also provides direct evidence that Cd extrusion from the enterocytes is mediated by an ATP-driven

process. Overall, our study provides new mechanistic insights into the intestinal Cd transport in freshwater fish.

CHAPTER 6: Effects of dietary cadmium exposure on tissue-specific cadmium accumulation, iron status and expression of iron-handling and stress-inducible genes in rainbow trout: Influence of elevated dietary iron[5]

6.1. Introduction

Cadmium (Cd) is a non-essential element and highly toxic to vertebrates including fish. Fish can be exposed to Cd *via* both water and diet. In freshwater fish, the waterborne Cd^{2+} is taken up primarily by the branchial Ca^{2+} transport pathway (Hollis *et al.*, 2000; Niyogi and Wood, 2004; Niyogi *et al.*, 2008), and the acute toxicity of waterborne Cd is generally associated with the impairment of active Ca^{2+} transport by the competitive blockade of apical Ca^{2+} channels and/or selective inhibition of basolateral Ca^{2+}-ATPase transporters by Cd^{2+} in gill chloride cells (Verbost *et al.*, 1987; Verbost *et al.*, 1989). In contrast, the mechanisms of dietary Cd uptake and toxicity are not quite well characterized, although several studies have demonstrated the importance of diet in Cd accumulation and toxicity in freshwater fish (Farag *et al.*, 1994; Szebedinszky *et al.*, 2001; Baldisserotto *et al.*, 2005; Chowdhury *et al.*, 2005; Ng and Wood, 2008; Ng *et al.*, 2009). Previous studies have suggested that dietary Cd absorption may occur through the Ca (Schoenmakers *et al.*, 1992; Franklin *et al.*, 2005; Ng *et al.*, 2009) and Fe transport pathways (Cooper *et al.*, 2006b; Kwong and Niyogi, 2009; Kwong *et al.*, 2010) in fish gut.

---

[5] This chapter has been published in Aquatic Toxicology 102:1–9 (2011), under joint authorship with Jose A. Andrés (University of Saskatchewan) and Som Niyogi (University of Saskatchewan)

In mammals, the adverse effects of dietary Cd on Fe metabolism and homeostasis have long been recognized (Schafer and Forth, 1985), and a Fe-supplemented diet was found to reduce Cd accumulation and toxicity (Włostowski *et al.*, 2003). Free cadmium ion is absorbed in the mammalian intestine through an apical iron (Fe^{2+}) transporter, the divalent metal transporter-1 (DMT1, also known as *Nramp2*, *slc11a2*) (Park *et al.*, 2002; Ryu *et al.*, 2004; Kim *et al.*, 2007). The expression of a DMT1 homologue and its physiological characteristics have been reported in teleost gut (Cooper *et al.*, 2006b; Kwong and Niyogi, 2009; Kwong *et al.*, 2010). It has also been demonstrated that Cd inhibits intestinal Fe uptake and vice versa through competitive interaction (Kwong and Niyogi, 2009; Kwong *et al.*, 2010), and treatment with a Fe-deficient diet increases intestinal DMT1 expression and uptake of Cd in fish (Cooper *et al.*, 2006b). These observations strongly indicate that the dietary Cd uptake mechanism in fish is similar to that in mammals, at least in part. In addition, Cd is known to bind to transferrin (Tf), the major circulating Fe-binding protein, in fish (De Smet *et al.*, 2001a). Tf is synthesized in the liver and secreted into the blood, and plasma Tf level is an indicator of Fe status in the body. Chen *et al.* (2008) reported that short-term acute waterborne cadmium exposure increases the expression of Tf gene in fish liver as well as plasma Tf level. All of these findings indicate that the interaction of dietary Fe and Cd can have important implications for Fe homeostasis as well as Cd accumulation and toxicity in fish.

Metallothioneins (MTs) are the primary Cd binding and storage proteins in vertebrates. Several studies have demonstrated that chronic Cd exposure, *via* both water and diet, induces tissue-specific MT expression in fish (De Smet *et al.*, 2001b; Hollis *et al.*, 2001; Lange *et al.*, 2002; Chowdhury *et al.*, 2005). Genetic determinants of MTs have been isolated from a number of teleost fish belonging to a wide array of taxa, and many fish species have been reported to

possess at least two MT genes (MT-A and MT-B) in their genomes (Scudiero *et al.*, 2005). Recent studies have suggested that MT-A may have a more important role in Cd detoxification than MT-B in fish (Vergani *et al.*, 2007; Wu *et al.*, 2008). However, this aspect needs further investigation, particularly focusing on the expression profile of two MT genes in tissues (e.g., gut, kidney, liver and gill) where cadmium is primarily accumulated in fish.

Heat shock proteins (HSPs) are representative stress-defense proteins that aid in the proper folding and repair of proteins as well as targeting of proteins for degradation. The 70 kDa subfamily of HSPs (HSP70) is highly conserved across phyla and induced in response to a wide variety of environmental pollutants (Bierkens, 2000). Recent studies have reported induction of HSP70 expression in fish embryo following brief exposure to acute waterborne Cd (Hallare *et al.*, 2005; Blechinger *et al.*, 2007; Matz and Krone, 2007) – indicating its protective role against Cd toxicity. However, further investigations are required to characterize the protective role of HSP70 against Cd toxicity in fish, particularly during an environmentally relevant Cd exposure regime. Similar to MTs, the existence of at least two HSP70 genes has been reported in fish (HSP70a and HSP70b) (Ojima *et al.*, 2005). Hence, a goal of this work was to examine whether their tissue-specific expression profile differs in response to chronic Cd exposure.

The objectives of the present study were to investigate: (I) the effects of dietary Cd exposure on Fe homeostasis, Cd accumulation and detoxification responses in fish, and (II) to examine how these variables were influenced by elevated dietary Fe. Juvenile rainbow trout (*Oncorhynchus mykiss*) were exposed chronically to four different environmentally relevant dietary regimes of Fe and/or Cd, and the following endpoints were analyzed: (i) physiological parameters (condition factor, and gastro-intestinal and liver somatic index), (ii) tissue-specific Fe

and Cd level, (iii) plasma Fe status and hepatic mRNA expression of Tf, and (iv) tissue-specific mRNA expression of MTs (MT-A and MT-B) and HSP70s (HSP70a and HSP70b).

6.2. Materials and methods

6.2.1. Experimental fish

Juvenile rainbow trout (*O. mykiss*, ~10 g) were obtained from Lucky Lake fish farm, SK, Canada. Fish were acclimated for 8 weeks in the laboratory with aerated, dechlorinated water [hardness 157 mg/L, alkalinity 109 mg/L (both as $CaCO_3$), pH 8.1–8.2, dissolved organic carbon (DOC) 2.2 mg/L, Fe 5.5 μg/L, Cd <0.1 μg/L] in a flow-through system (1 L/min) and fed Martin's commercial dried pellet (a daily ration of 1.5% wet body mass) (2-pt; Martin Mills Inc., ON, Canada). The water temperature was maintained at 12 °C and photoperiod was set at 16:8 light to dark cycle. Ten days prior to the beginning of the experiment, the fish were transferred to a control freeze-dried brine shrimp diet (see below for details) at 1.5% daily ration (dry feed/wet body weight).

6.2.2. Diet preparation

Diets were prepared using the brine shrimp, *Artemia franciscana* (Sally's Frozen Brine Shrimp; San Francisco Bay Brand, USA), containing 5.8% crude protein, 0.6% crude fat, 0.25% crude fiber (all on a wet wt basis). The shrimp was first rinsed several times with deionized water and then ground in a commercial blender. A known amount of Fe^{2+} (as $FeSO_4$) and/or Cd^{2+} (as $CdCl_2$) (J.T. Baker, USA; dissolved in deionized water) was added into the mix and blended for

about 10 min to ensure homogenous mixing. The mix was kept at −20 °C until frozen and was subsequently dried in a freeze-drier (Labconco Freezone, USA). The diets were then cut into small pieces (~0.3 cm) and stored at 4 °C until use. The control diet (normal Fe diet) was prepared in the same fashion without the addition of $FeSO_4$ or $CdCl_2$. The Fe and Cd concentrations in the diets were analyzed by atomic absorption spectroscopy (see below for details), and their concentrations and daily doses in different diets are presented in Table 6.1. The four different diets used in the present study were identified as: normal Fe, high Fe, normal Fe plus Cd, and high Fe plus Cd diets. The Fe level (260–280 μg/g dry wt) in the normal Fe diets of the present study was comparable to the dietary Fe level (100–250 μg/g dry wt) suggested for normal physiological functioning in salmonids (Andersen *et al.*, 1996). It should also be noted here that no adverse physiological consequences were reported in rainbow trout following 4 weeks of treatment with a Fe-rich diet containing approximately 2-fold higher Fe level (1975 μg/g dry wt) relative to the Fe-supplemented diets of the present study (800–1100 μg/g dry wt) (Carriquiriborde *et al.*, 2004).

Table 6.1: The measured iron (Fe) and cadmium (Cd) concentrations (μg Fe or Cd/g feed dry weight) in four different experimental diets, and the associated daily Fe and Cd doses (μg Fe or Cd/g fish wet weight/day) to fish.

Treatment	Fe level	Daily Fe dose	Cd level	Daily Cd dose
Normal Fe	279.1 ± 5.2	4.2	1.6 ± 0.2	0.02
High Fe	1108.5 ± 8.4	16.6	1.9 ± 0.2	0.03
Normal Fe + Cd	260.8 ± 4.4	3.9	35.9 ± 1.8	0.54
High Fe + Cd	823.1 ± 22.0	12.3	38.5 ± 0.5	0.58

Values are mean ± SEM, n = 10 for the Fe and Cd concentrations in the diets.

6.2.3. Experimental treatments and sampling

A total of 160 fish were divided equally into eight 180 L tanks (20 fish in each tank, 2 replicates per treatment). Each tank received continuous aeration and water flow, and the water flow-through rate was maintained at 8 L/min to ensure rapid flushing of Fe or Cd potentially leached from the diet. Nevertheless, water samples were collected from each treatment tank three times a week 1 h post feeding for the measurement of Fe and Cd (see below for details), and no elevation of either metal in the exposure water was recorded at any time. Fecal matter was removed daily from each tank. The fish were fed with four different diets (see Table 6.1) at a daily ration of 1.5% (dry feed/wet body weight), divided equally into two rations per day. The fish were weighed weekly and the food ration was adjusted accordingly. No fish mortality occurred in any treatments during the exposure.

Initially, eight fish were randomly sampled on the day the experiment was started (day 0), then 8 fish from each treatment (4 from each replicate) were sampled on days 14 and 28 for Fe and Cd tissue concentration analysis (see below for details). The fish were sampled prior to feeding and killed by an overdose of MS-222 (Syndel Laboratories Ltd., Canada). The weight and length of individual fish were recorded. Blood samples were taken immediately by caudal puncture (on days 0 and 28) with a 1-mL syringe pre-rinsed with heparin (Sigma–Aldrich, USA), and centrifuged for 4 min at 10,000 x *g* to collect plasma. The gill, stomach, intestine, liver, kidney and carcass were dissected out. The stomach and intestine were cut open, and rinsed with deionized water to remove the undigested food from the lumen. Each tissue was weighed individually and stored at −20 °C. Similarly, an additional random sample of 8 fish on day 0 as

well as 8 fish from each treatment (4 from each replicate) on day 28 were sacrificed, and the gill, liver, intestine and kidney collected for gene expression analysis (see below for details).

6.2.4. Measurement of iron and cadmium in water, diet and tissue

The water samples were acidified (1% HNO_3) and analyzed for Fe and Cd concentrations using flame and graphite-furnace atomic absorption spectroscopy, respectively (Analyst 800, PerkinElmer, USA). The experimental diets and tissue samples were digested in 5 volumes of 1 N HNO_3 at 60 °C for 48 h, and then centrifuged at 15,000 x *g* for 4 min (Kwong and Niyogi, 2009). The supernatant was collected and diluted appropriately with 0.2% HNO_3, and analyzed for Fe and Cd concentrations as described above. The quality control and assurance of Fe and Cd analysis were maintained using appropriate method blanks and certified standards for each metal (Fisher Scientific, Canada), and were validated with certified reference materials (DOLT-3; National Research Council, Canada).

6.2.5. Plasma iron-binding assay

Plasma Fe status was evaluated by measuring the level of total Fe, unsaturated Fe binding capacity (UIBC), total Fe binding capacity (TIBC), and Tf saturation (%) in the plasma. The Tf saturation (%) reflected the percentage of Tf in the plasma bound with Fe. Total Fe and UIBC were measured colorimetrically at 560 nm in a microplate reader (Varioskan Flash, Thermo Scientific, USA) using a commercial kit (Pointe Scientific, USA). Subsequently, the total Fe and

UIBC values were used to determine TIBC and Tf saturation (%) according to manufacturer's instructions.

6.2.6. mRNA expression analysis of genes

For each experimental fish (n = 8 per treatment), the dissected gill, liver, intestine and kidney tissues were preserved in RNA*later*® (Applied Biosystem, USA) and stored at −80 °C until further processing. For each stored sample, total RNA extraction, DNase treatment and cDNA synthesis were carried out as described in Kwong *et al.* (2010). First-strand cDNA was then used as a template to estimate the transcript expression of two metallo-thionein (MT) isoforms (MT-A and MT-B), two different heat-shock proteins (HSP70a and HSP70b), transferrin (Tf), and the reference gene β-actin, using the real time quantitative polymerase chain reaction (RT-qPCR). The mRNA expression levels of MT and HSP70 genes were quantified in all the extracted samples, however Tf was quantified only in the liver which is the primary site of Tf synthesis in vertebrates. Prior to retro-transcription experiments, RNA concentration was estimated using a NanoDrop ND-1000 (Thermo Scientific, USA), and nuclease-free water was added to obtain a concentration of ~1000 ng/µL. All RT-qPCR assays were performed on a real-time thermocycler (IQ5, Bio-Rad, USA), using SYBR Master Mix (Fermentas, Canada), and the primer sequences used for respective genes are presented in Table 6.2. RT-qPCR was performed in triplicates using the following conditions: 94 °C for 10 min, 45 cycles of 95 °C for 10 s, 60 °C for 30 s and 72 °C for 25 s. The specificity of primers for PCR was checked at the end of each amplification using a DNA melt curve analysis with a ramping rate of 1 °C/min over a temperature range of 60–95 °C. All mRNA expression data were normalized to the mRNA

expression of β-actin gene. The mRNA expression of β-actin in different fish tissues was found to be stable since no significant change occurred among the four different dietary treatment regimes during the experimental period (data not shown). Relative mRNA expression was calculated based on the method described by Pfaffl (2001), where the mRNA expression levels of each gene at day 28 were calculated relative to day 0.

Table 6.2: The accession numbers and primer sequences of metallothionein-A and -B (MT-A, MT-B), heat shock protein-70a and -70b (HSP-70a, HSP-70b), transferrin, and the reference gene β-actin.

Gene (GenBank)	**Sequence (5′–3′)**	**Reference**
MT-A (M18103)	Forward: CATGCACCAGTTGTAAGAAAGCA Reverse: GCAGCCTGAGGCACACTTG	(Bury *et al.*, 2008)
MT-B (M18104)	Forward: TCAACAGTGAAATTAAGCTGAAATACTTC Reverse: AAGAGCCAGTTTTAGAGCATTCACA	(Bury *et al.*, 2008)
HSP-70a (AB176854)	Forward: CGGGAGTTGTAGCGATGAGA Reverse: CTTCCTAAATAGCACTGAGCCATAA	(Ojima *et al.*, 2005)
HSP-70b (AB176855)	Forward: AGGCCCAACCATTGAAGAGA Reverse: GCAATGTCCAGCAATGCAATA	(Ojima *et al.*, 2005)
Transferrin (D89083)	Forward: CCACCTCCAGGGCCATTAAATG Reverse: ATCCACCGCTATGGCATCTGCC	(Talbot *et al.*, 2009)
β-Actin (AJ438158)	Forward: TCCTTCCTCGGTATGGAGTCTT Reverse: ACAGCACCGTGTTGGCGTACAG	(Aegerter *et al.*, 2005)

6.2.7. Calculations and statistics

Condition factor [K = 100 × weight (g)/length (cm)^3], gastro-intestinal somatic index (ISI) and hepato-somatic index (HSI) [ISI or HSI (%) = weight of gastro-intestinal tissue or liver × 100/total body weight] were calculated from individual fish sampled on days 0, 14 and 28 (n = 8 per treatment). The whole-body Fe or Cd concentrations of individual fish were calculated by dividing the sum of Fe or Cd levels of individual tissues by the sum of individual tissue weights.

All the statistical analyses were performed using Sigmaplot® (version 11.2; Systat Software, Inc., Point Richmond, CA, USA). The HSI, ISI, condition factor, and Fe and Cd tissue concentrations were analyzed by three-way analysis of variance (ANOVA) followed by a post-hoc least significance test (LSD), with time, dietary Fe, and dietary Cd as independent variables. The relative changes in mRNA levels were analyzed by two-way ANOVA followed by a post hoc least significant test, with dietary Fe and Cd as independent variables. Data were log or square-root transformed when the assumptions of equal variance and normal distribution did not meet the requirement. Data are reported as the mean ± SEM, and $p < 0.05$ was taken as the level of significance.

6.3. Results

6.3.1. Physiological conditions

The HSI values in fish treated with the normal and high Fe diets increased significantly during the exposure, however no such increase was observed in fish fed with the normal Fe plus Cd or high Fe plus Cd diet (Table 6.3). The ISI remained unaffected among the treatments except a marked decrease in fish treated with the normal Fe plus Cd diet at day 14 ($p < 0.05$). No statistical difference in the condition factors was recorded among the different treatments.

Table 6.3: Physiological indicators of juvenile rainbow trout after exposure to the normal iron, high iron, normal iron + cadmium, and high iron + cadmium diets for 28 days.

	Day	**Normal iron**	**High iron**	**Normal iron + cadmium**	**High iron + cadmium**
HSI (%)	0	0.94 ± 0.07^{A}			
	14	1.57 ± 0.14^{Ba}	1.38 ± 0.10^{Bab}	1.06 ± 0.07^{Ac}	1.11 ± 0.06^{Abc}
	28	1.34 ± 0.03^{Ba}	1.26 ± 0.16^{Bab}	1.01 ± 0.07^{Ac}	1.06 ± 0.09^{Abc}
ISI (%)	0	6.05 ± 0.29^{A}			
	14	5.30 ± 0.66^{Aa}	5.31 ± 0.21^{Aa}	5.03 ± 0.22^{Ba}	5.46 ± 0.19^{Aa}
	28	5.55 ± 0.82^{Aa}	5.78 ± 0.61^{Aa}	5.75 ± 0.29^{Aa}	5.92 ± 0.37^{Aa}
Condition	0	0.95 ± 0.02^{A}			
factor	14	1.02 ± 0.02^{Aa}	1.05 ± 0.03^{Aa}	0.96 ± 0.02^{Aa}	1.01 ± 0.03^{Aa}
	28	1.00 ± 0.02^{Aa}	1.04 ± 0.02^{Aa}	0.92 ± 0.03^{Aa}	0.93 ± 0.02^{Aa}

HSI, hepatosomatic index; ISI, gastro-intestinal index. Values labelled with different letters indicate statistically different (Three-way ANOVA with time, dietary iron, and dietary cadmium as independent variables, followed by a post-hoc LSD test; $p < 0.05$). Upper case: among days in the same diet treatment (including comparison with day 0 with normal iron); Lower case: among treatments in the same day. Values are mean ± SEM, $n = 8$.

6.3.2. Tissue-specific iron and cadmium levels

The Fe concentration did not change in any fish tissues among the four different dietary treatments except for a transient increase in the stomach ($p < 0.01$) at day 14 in fish treated with the high Fe diet (Appendix Figure A4). In contrast, exposure to the Cd-supplemented diet, both in the presence of normal and high Fe, significantly increased Cd concentrations in all fish tissues, including plasma and red blood cells (Table 6.4), as well as in the whole-body (Figure 6.1). A high proportion of Cd (~80%) accumulated from the diet was distributed in the intestine of fish (Figure 6.1d). At days 14 and 28, the tissue Cd accumulation pattern in fish exposed to dietary Cd were in the order of: intestine > kidney > stomach > liver > gill > carcass. Interestingly, fish fed with the high Fe plus Cd diet exhibited a significant reduction in Cd accumulation in the stomach, intestine and the whole-body compared to fish fed with the normal Fe plus Cd diet (Figure 6.1c, 6.1d and 6.1g). The three-way ANOVA revealed a significant interactive effect among time, dietary Fe and dietary Cd treatments in the stomach ($p = 0.009$). Similarly, there was also a significant interaction between time and dietary Cd treatment in all fish tissues as well as between dietary Fe and Cd treatments in the gastrointestinal tissue ($p < 0.001$). However, no interactive effect was observed between time and dietary Fe treatment in any tissue compartments.

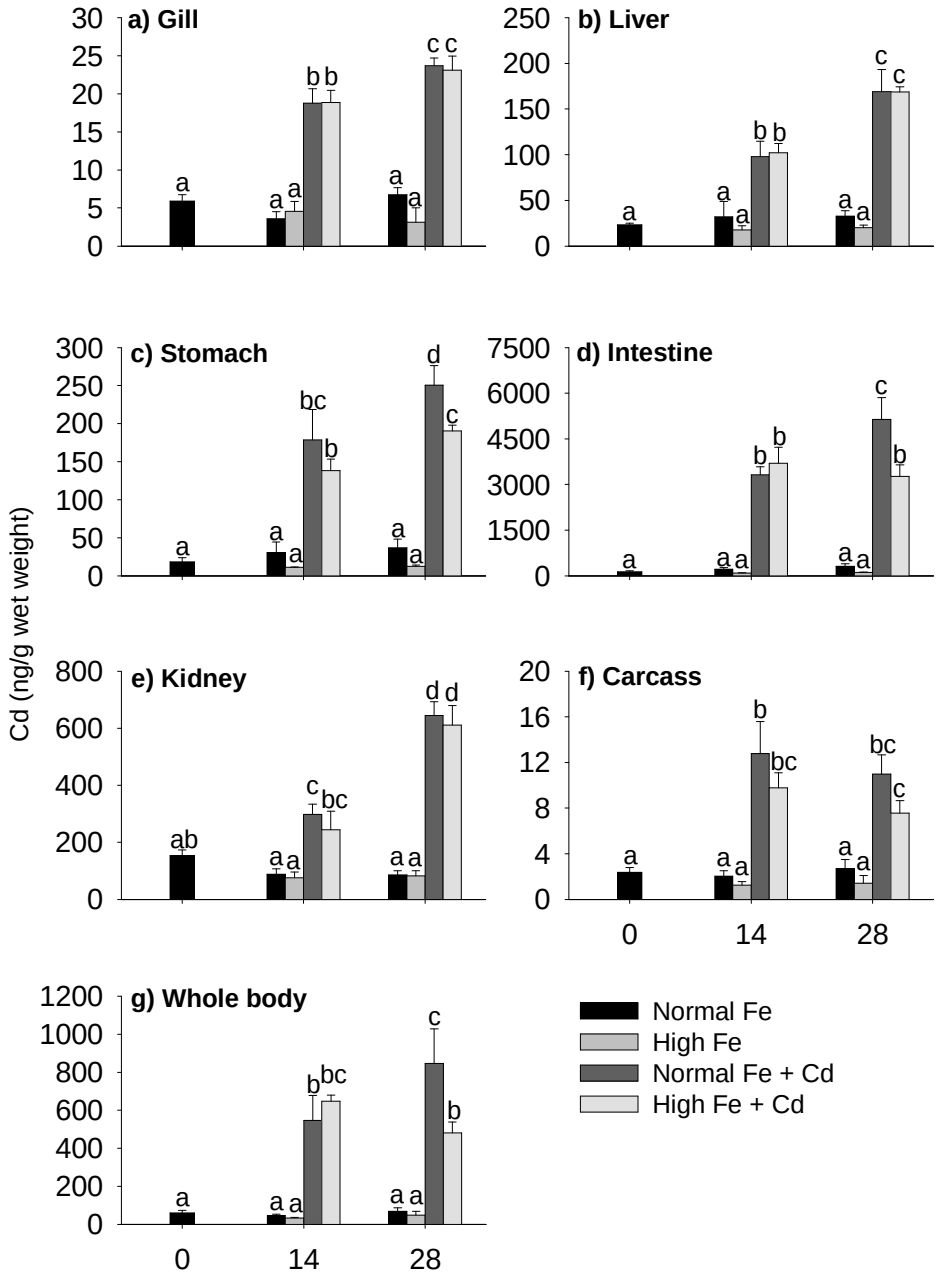

Figure 6.1: Concentrations of cadmium (Cd) (ng/g wet weight) in the **(a)** gill, **(b)** liver, **(c)** stomach, **(d)** intestine, **(e)** kidney, **(f)** carcass and **(g)** whole-body of rainbow trout exposed to the normal iron (Fe), high Fe, normal Fe + Cd, and high Fe + Cd diets. Bars labelled with different letters represent statistical difference within the same tissue (Three-way ANOVA with time, dietary Fe, and dietary Cd as independent variables, followed by a post-hoc LSD test; $p < 0.05$). Values are mean ± SEM ($n = 8$).

6.3.3. Plasma iron status and mRNA expression of transferrin in the liver

Plasma Fe, TIBC and Tf saturation (%) values in four different dietary treatments are summarized in Table 6.4. No significant change in plasma Fe level was recorded in any of the four different treatments. Fish fed with the normal Fe plus Cd diet exhibited a significant increase in TIBC compared to control fish (normal Fe diet) at day 0 and day 28. However, no increase in TIBC occurred in fish treated with the high Fe plus Cd diet. No significant change in Tf saturation (%) was recorded in any of the four different dietary treatments. A significant increase (~4-fold) in the hepatic Tf mRNA expression was observed in fish treated with the normal Fe plus Cd diet compared to the control, however no such change occurred in fish fed with the high Fe diet, with or without Cd-supplementation (Figure 6.2). A two-way ANOVA revealed a significant interaction between dietary Fe and Cd treatments for the hepatic Tf mRNA expression ($p < 0.05$).

Table 6.4: Haematological parameters of juvenile rainbow trout after exposure to the normal iron, high iron, normal iron + cadmium, and high iron + cadmium diets for 28 days.

	Day	**Normal iron**	**High iron**	**Normal iron + cadmium**	**High iron + cadmium**
Plasma iron	0	11.7 ± 2.8^{A}			
(μM)	28	11.8 ± 1.7^{Aa}	15.3 ± 2.0^{Aa}	11.8 ± 1.2^{Aa}	11.6 ± 2.5^{Aa}
TIBC	0	67.2 ± 3.2^{A}			
(μM)	28	68.1 ± 3.8^{Aab}	74.0 ± 3.6^{Abc}	79.8 ± 2.9^{Bc}	63.9 ± 3.7^{Aa}
Transferrin saturation	0	17.4 ± 3.4^{A}			
(%)	28	17.3 ± 1.9^{Aa}	20.4 ± 2.7^{Aa}	14.7 ± 2.1^{Aa}	18.2 ± 4.1^{Aa}
Cadmium in plasma	0	UD	UD		
(μM)	28	UD	UD	0.065 ± 0.018^{a}	0.048 ± 0.012^{a}
Cadmium in red blood cells	0	UD	UD		
(μM)	28	UD	UD	0.043 ± 0.004^{a}	0.042 ± 0.003^{a}

TIBC, total iron binding capacity; Transferrin saturation (%), the percentage of transferrin in the plasma bound with iron; UD, under the detection limit. Values labelled with different letters indicate statistically different (Three-way ANOVA with time, dietary iron, and dietary cadmium as independent variables, followed by a post-hoc LSD test; $p < 0.05$). However, for cadmium in plasma and cadmium in red blood cells, only a Student's *t*-test was performed. Upper case: among days in the same diet treatment (including comparison with day 0); Lower case: among treatments in the same day. Values are mean ± SEM, $n = 8$.

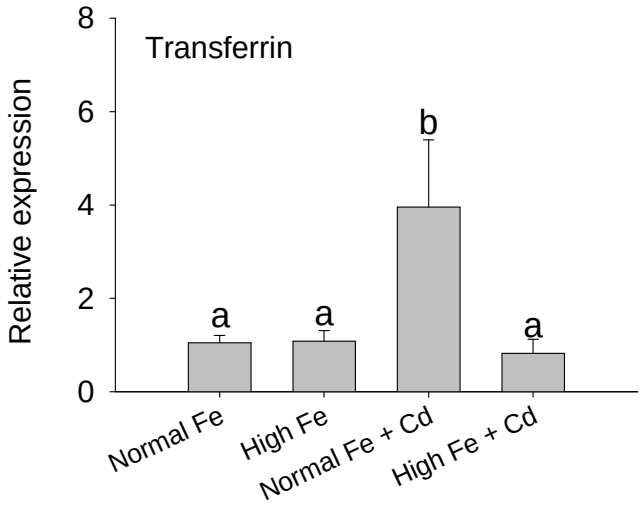

Figure 6.2: The relative mRNA expression levels of transferrin in the liver of rainbow trout after exposure to the normal iron (Fe), high Fe, normal Fe + cadmium (Cd), and high Fe + Cd diets for 28 days. The expression level of transferrin was normalized to *β-actin*. Bars labelled with different letters represent statistical difference (Two-way ANOVA with dietary Fe and Cd as independent variables; $p < 0.05$). Values are mean ± SEM ($n = 8$).

6.3.4. Tissue-specific mRNA expression of metallothioneins and heat-shock proteins

Typically, the mRNA expression level of MT-A was higher than that of MT-B in all of the tissues examined (Appendix Figure A5). No significant change occurred in either MT-A or MT-B expression of the gill among the four different dietary treatments (Figure 6.3a). In the intestine, the Cd-supplemented diet, both in the presence of normal and high Fe, produced a significant increase in the mRNA expression of MT-A and MT-B compared to the control (Figure 6.3b). In the liver, MT-A expression was significantly elevated following treatment with the high Fe diet as well as normal Fe plus Cd diet, whereas MT-B expression increased only with the latter treatment. Interestingly, both MT-A and MT-B expressions in the liver of fish fed with the high Fe plus Cd diet were similar to the control (Figure 6.3c). A two-way ANOVA revealed a significant interaction between dietary Fe and Cd treatments for MT-A and MT-B expressions in the liver ($p < 0.01$). In the kidney, high Fe in the diet suppressed the expressions of both MT-A and MT-B relative to control, whereas Cd-supplementation of the diet increased the expression of MT-B, but only with normal Fe (Figure 6.3d).

In general, the mRNA expression level of HSP-70b was higher than that of HSP-70a in all of the tissue examined (Appendix Figure A5). In the gill and liver, no significant differences were found in the mRNA expression of either HSP-70a or HSP-70b among the four different dietary treatments (Figure 6.4a and 6.4c). In the intestine, significant elevation of HSP-70a mRNA expression occurred only in the normal Fe plus Cd diet treatment, whereas no change in the HSP-70b mRNA expression was observed following treatment with the Cd-supplemented diet, either with normal or high Fe, relative to the control (Figure 6.4b). In the kidney, a significant increase of HSP-70a mRNA expression occurred only in the treatment with normal

Fe plus Cd diet, whereas the HSP-70b mRNA expression increased significantly only in the treatment with high Fe plus Cd diet relative to the control (Figure 6.4d).

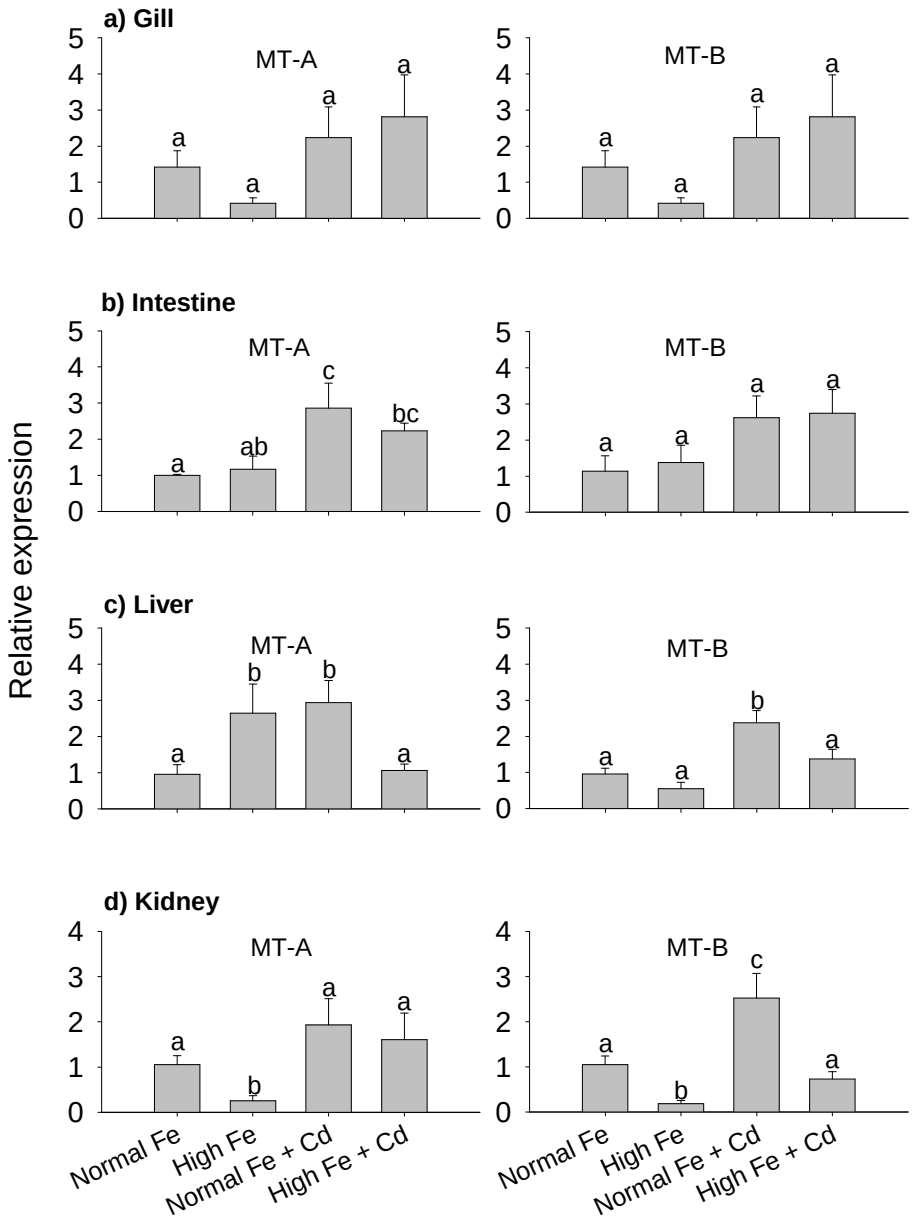

Figure 6.3: The relative mRNA expression levels of metallothionein isoform-A (MT-A) and -B (MT-B) in the **(a)** gill, **(b)** intestine, **(c)** liver, and **(d)** kidney of the rainbow trout after exposure to the normal iron (Fe), high Fe, normal Fe + cadmium (Cd), and high Fe + Cd diets for 28 days. The expression levels of MT-A and MT-B were normalized to *β-actin* from the same tissue. Bars labelled with different letters represent statistical difference within the same tissue for the same MT gene (Two-way ANOVA with dietary Fe and Cd as independent variables; $p < 0.05$). Values are mean ± SEM ($n = 8$).

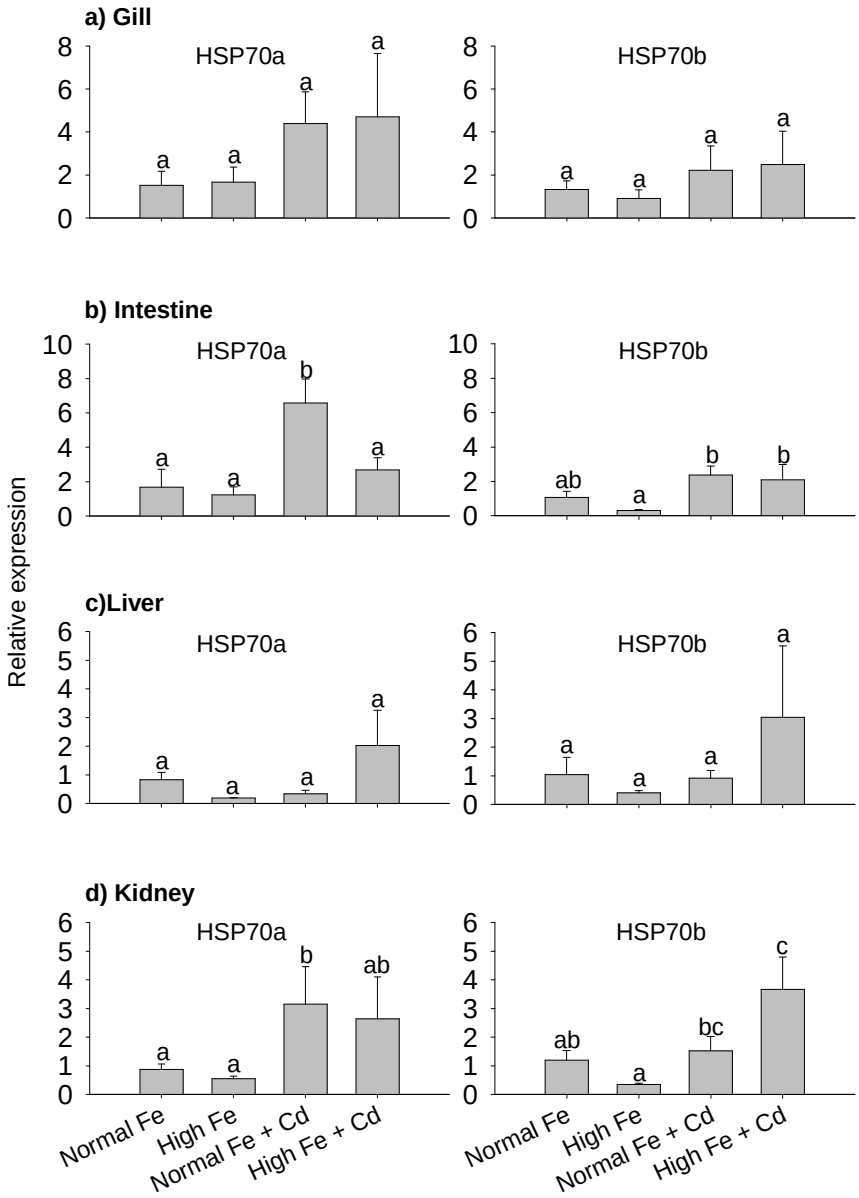

Figure 6.4: The relative mRNA expression levels of heat shock protein-70a (HSP70a) and -70b (HSP70b) in the (a) gill, (b) intestine, (c) liver, and (d) kidney of the rainbow trout following the exposure to normal iron (Fe), high Fe, normal Fe + cadmium (Cd) and high Fe + Cd diets. The expression levels of HSP70a and HSP70b were normalized to *β-actin* from the same tissue. Bars labelled with different letters represent statistical difference within the same tissue for the same HSP70 gene (Two-way ANOVA with dietary Fe and Cd as independent variables; $p < 0.05$). Values are mean ± SEM ($n = 8$).

6.4. Discussion

6.4.1. Environmental relevance of experimental diets

The present study investigated the chronic interactive effect of Cd and Fe in fish exposed to an environmentally relevant dietary regime. The Cd concentration in our *Artemia* diet was about 36 μg/g dry wt, which was comparable to the Cd level in natural prey species collected from metal-contaminated aquatic ecosystems (1–29 μg/g dry wt) (Farag *et al.*, 1999). In addition, the Fe concentration (800–1000 μg/g dry wt) in the Fe-supplemented diet was well within the range of Fe concentration (160–12,560 μg/g dry wt) found in the natural fish diet in metal-impacted environments (Winterbourn *et al.*, 2000).

6.4.2. Physiological condition, and tissue-specific and whole-body Cd burden

In the present study, no significant changes in condition factor and ISI were observed after four weeks of any dietary treatments, although there was a transient decrease in ISI of fish exposed to dietary Cd on day 14. However, we observed a significant decrease in HSI (decreased liver size) in fish exposed to dietary Cd on both day 14 and day 28, irrespective of Fe level in the diet. The decrease in HSI was possibly caused by an increase in energy allocation for the detoxification (e.g., induction of MT and HSP70 transcription) of accumulated Cd.

The present study revealed maximum Cd accumulation in the intestine followed by the kidney, stomach, liver, gill and carcass in fish exposed to dietary Cd. The tissue-specific Cd distribution pattern observed in the present study is consistent with that reported in previous studies (Szebedinszky *et al.*, 2001; Chowdhury *et al.*, 2005). A very high proportion (~80%) of

Cd accumulation in the intestine indicates that it probably acts as a barrier against Cd assimilation from diet. The Cd level in the kidney increased by more than 2-fold from day 14 to day 28 in fish exposed to Cd-supplemented diets, indicating kidney as the long-term storage site for accumulated Cd. Importantly, fish fed with the high Fe plus Cd diet exhibited a significant decrease in Cd accumulation in the stomach, intestine and the whole-body relative to fish fed with the normal Fe plus Cd diet. Furthermore, elevated dietary Fe produced a steady-state cadmium accumulation in the intestinal tissue and the whole-body by day 14, whereas fish treated with the normal Fe plus Cd diet exhibited a continuous increase in Cd accumulation with time.

Although the protective effect of dietary Fe against dietary Cd accumulation was previously reported in mammals by Włostowski *et al.* (2003), to our understanding the present study is first to demonstrate that in freshwater fish. Elevated dietary Fe is expected to decrease dietary Cd accumulation since Fe^{2+} and Cd^{2+} are known to competitively inhibit the uptake of each other in the fish intestine, likely *via* DMT1 (Kwong and Niyogi, 2009; Kwong *et al.*, 2010). The expression of DMT1 has been recorded in the stomach and intestine (Kwong *et al.*, 2010), as well as in the liver, kidney and gill of rainbow trout (Dorschner and Phillips, 1999; Cooper *et al.*, 2007). Despite of the ubiquitous mRNA expression of DMT1 in fish, a reduction in Cd accumulation by elevated dietary Fe was observed only in the gut and the whole-body. Moreover, the magnitude of reduction in Cd accumulation was about 30–50%, and the Cd levels remained significantly elevated relative to that in the control. Therefore, it is likely that additional Fe-independent pathways (e.g., Ca-dependent pathway) may exist which can mediate the transfer of dietary Cd across the gut and subsequently to other tissues (Schoenmakers *et al.*, 1992; Franklin *et al.*, 2005; Ng *et al.*, 2009).

6.4.3. Iron homeostasis and handling

We did not record any notable change in plasma Fe level as well as tissue-specific Fe concentrations in fish exposed to high Fe and/or Cd diets over 4 weeks. This suggests a strong homeostatic regulation of Fe and no apparent effect of chronic environmentally relevant dietary Cd exposure on Fe homeostasis in freshwater fish. The interactive effects of Cd exposure on Fe metabolism are well documented in mammals (Schafer and Forth, 1985; Kozlowska *et al.*, 1993), however this aspect has not been thoroughly investigated in fish. Haux and Larsson (1984) and Vincent *et al.* (1996) reported that chronic exposure to sub-lethal waterborne Cd causes anaemia in fish. They suggested the influence of Cd on Fe metabolism as one of the reasons for the development of anaemia, although they did not examine the Fe status in Cd-exposed fish. Interestingly, we observed about 4-fold increase in the hepatic mRNA expression of Tf of rainbow trout treated with the normal Fe plus Cd diet. Simultaneously, we also observed significant increase of plasma TIBC, which is indicative of plasma Tf level, in the same treatment. These findings indicate that dietary Cd exposure induces Tf synthesis in the liver resulting in an increase of plasma Tf level. Chen *et al.* (2008) previously reported increased hepatic Tf mRNA expression as well as plasma TIBC in croceine croaker (*Pseudosciaena crocea*) exposed to acute waterborne cadmium (0.03–9 mg/L) for a short period (72 h). They also recorded an increase in total plasma Fe level and Tf saturation (%) at 24 h, however both parameters decreased to the control level by 72 h. We did not observe any change in the total plasma Fe or Tf saturation (%) level in the present study probably due to the longer exposure duration which allowed fish to regulate plasma Fe status.

The mechanisms of Tf induction by Cd exposure have yet to be fully understood, however Cd has been reported to disrupt the Tf cycling in mammals (Huebers *et al.*, 1987). In mammals, the role of Tf in cadmium circulation is debatable (Zalups and Ahmad, 2003), however De Smet *et al.* (2001a) reported that a significant amount of plasma Cd binds to Tf in teleost *Cyprinus carpio*. We postulate that Cd affects the delivery of Fe into the cells possibly by disrupting the Fe-binding to Tf and/or Tf cycling in fish, and the upregulation of Tf synthesis occurs as a compensatory response to that. It is important to note that the hepatic Tf mRNA expression as well as plasma TIBC remains unaffected following treatment with the high Fe plus Cd diet, suggesting that Fe-enrichment of diet can ameliorate the effects of Cd on Fe handling in fish.

6.4.4. Transcriptional responses of metallothioneins and heat-shock proteins

In the present study, elevated dietary Fe alone influenced the mRNA expression of MT-A and MT-B in fish, however the pattern of modulation was different in different tissues. For example, elevated dietary Fe increased the hepatic mRNA expression of MT-A, but not of MT-B, whereas it suppressed the renal mRNA expression of both MT-A and MT-B. Previous studies have reported that treatment with the elevated dietary Fe increases hepatic MT level (Yasutake and Hirayama, 2004; Brown *et al.*, 2007) and decreases renal MT level in mammals (Yasutake and Hirayama, 2004). It has been proposed that high dietary Fe enhances MT turnover in the kidney (Yasutake and Hirayama, 2004), although the mechanisms of such a process are not understood at present.

More importantly, we observed that chronic dietary Cd exposure markedly increased the mRNA expression of MT genes in the intestine, liver and kidney of fish, again the induction profile of either of the two MT genes was not consistent across different tissues. In general, MT-A was more sensitive to Cd in the intestine and liver, whereas MT-B was more sensitive in the kidney. Vergani *et al.* (2007) reported greater induction of MT-A compared to MT-B in rainbow trout hepatoma cells exposed to Cd. Recently, Wu *et al.* (2008) reported greater transcriptional response of MT-A relative to MT-B in zebrafish brain during short-term (72 h) acute waterborne Cd exposure (200 μg/L). The increase in tissue-specific MT protein level in fish exposed to dietary Cd has been demonstrated by Chowdhury *et al.* (2005), however our study suggests that the increase of MT level in different tissues is probably mediated by the differential expression of two MT genes. Interestingly, we also observed that elevated dietary Fe inhibited the cadmium-induced transcriptional response of MTs in the liver and kidney of fish. The reason for this inhibition is not clear since elevated dietary Fe did not reduce hepatic or renal Cd accumulation. Nevertheless, MT synthesis occurs at the expense of energy, thus it can be suggested that elevated dietary Fe may alle*via*te the energetic cost of Cd detoxification in fish.

Although previous studies have reported induction of HSP70 protein expression in zebrafish embryo following short-term acute Cd exposure (Hallare *et al.*, 2005; Blechinger *et al.*, 2007; Matz and Krone, 2007), the present study is the first to examine the alterations in the tissue-specific expression of two HSP70 genes in fish following chronic Cd exposure. In general, dietary Cd increased the expression of HSP70 genes only in the intestine and kidney, which were also the primary sites of Cd accumulation. The mRNA expression of both HSP70a and HSP70b were induced in the intestine, but only the HSP70a was induced in the kidney. Moreover, the magnitude of induction of HSP70a mRNA expression in the intestine was more robust than that

of HSP70b. These observations indicate that HSP70a is probably more sensitive to dietary Cd exposure than HSP70b in fish. It is possible that the upregulation of HSP70 genes occurred as a response to Cd-induced oxidative damage in the intestine and kidney (Cuypers *et al.*, 2010), since oxidative stress is known to cause HSP induction (McDuffee *et al.*, 1997). Interestingly, dietary Fe was found to inhibit dietary Cd-induced increase of HSP70a expression in the intestine as well as decrease intestinal Cd accumulation, providing further evidence of the ameliorative effects of elevated dietary Fe against Cd-induced stress response in fish.

6.5. Conclusions

Overall, the present study demonstrated that chronic dietary Cd exposure induces the mRNA expressions of MT (MT-A and MT-B) and HSP70 (HSP70a and HSP70b) genes in target organs of fish. We also found that dietary Cd exposure does not produce any apparent effect on Fe homeostasis, however it induces the hepatic mRNA expression of Tf gene and increases the plasma Tf level in fish. Dietary supplementation of Fe reduces Cd burden in the gut and the whole-body, as well as ameliorates the mRNA expressions of Tf, MT and HSP70 genes in fish. These findings suggest that elevated dietary Fe can protect freshwater fish against chronic dietary Cd toxicity, at least partially. We propose that iron-enriched/contaminated natural diet may ameliorate the effects of dietary Cd exposure to fish in metal-impacted aquatic ecosystems.

CHAPTER 7: General discussion

7.1. Introduction

Dietary exposure is considered to have important ecological significance in the accumulation and toxicity of divalent metals to wild fish (Woodward *et al.*, 1994; Farag *et al.*, 1999). However, the physiological mechanisms by which the dietborne metals are absorbed across the intestinal epithelium of fish remain poorly understood. My study has shown that the apical iron transporter, divalent metal transporter-1 (DMT1), is likely involved in the uptake of several divalent metals, both essential (e.g., iron, copper, zinc and nickel) and non-essential/toxic (lead and cadmium), in the gastro-intestinal tract of fish. The dietary interactions of divalent metals may have significant physiological and toxicological implications in the homeostatic regulation of metals in wild fish, especially in populations exposed to an elevated dietary metal mixture. More importantly, my study elucidated novel pathways of dietary cadmium absorption, which will enhance our understanding of the metabolism and toxicity of dietary cadmium in fish. My study also unravelled potential molecular biomarkers (e.g., transferrin, MT and HSP70) that can be useful in assessing cadmium exposure in wild fish. In general, findings from the present research project have important implications for ecological risk assessment of metals in the aquatic environments. In this chapter, the major insights gained from my research project are discussed, including the physiology of dietary iron absorption, and the role of the iron absorptive pathway in the transport of other divalent metals, particularly cadmium, in freshwater fish. In addition, the possibility of multiple transport mechanisms for dietary cadmium as well as the influence of elevated dietary iron on cadmium metabolism in fish is also discussed. The major findings from the present research project are summarised in Figure 7.1.

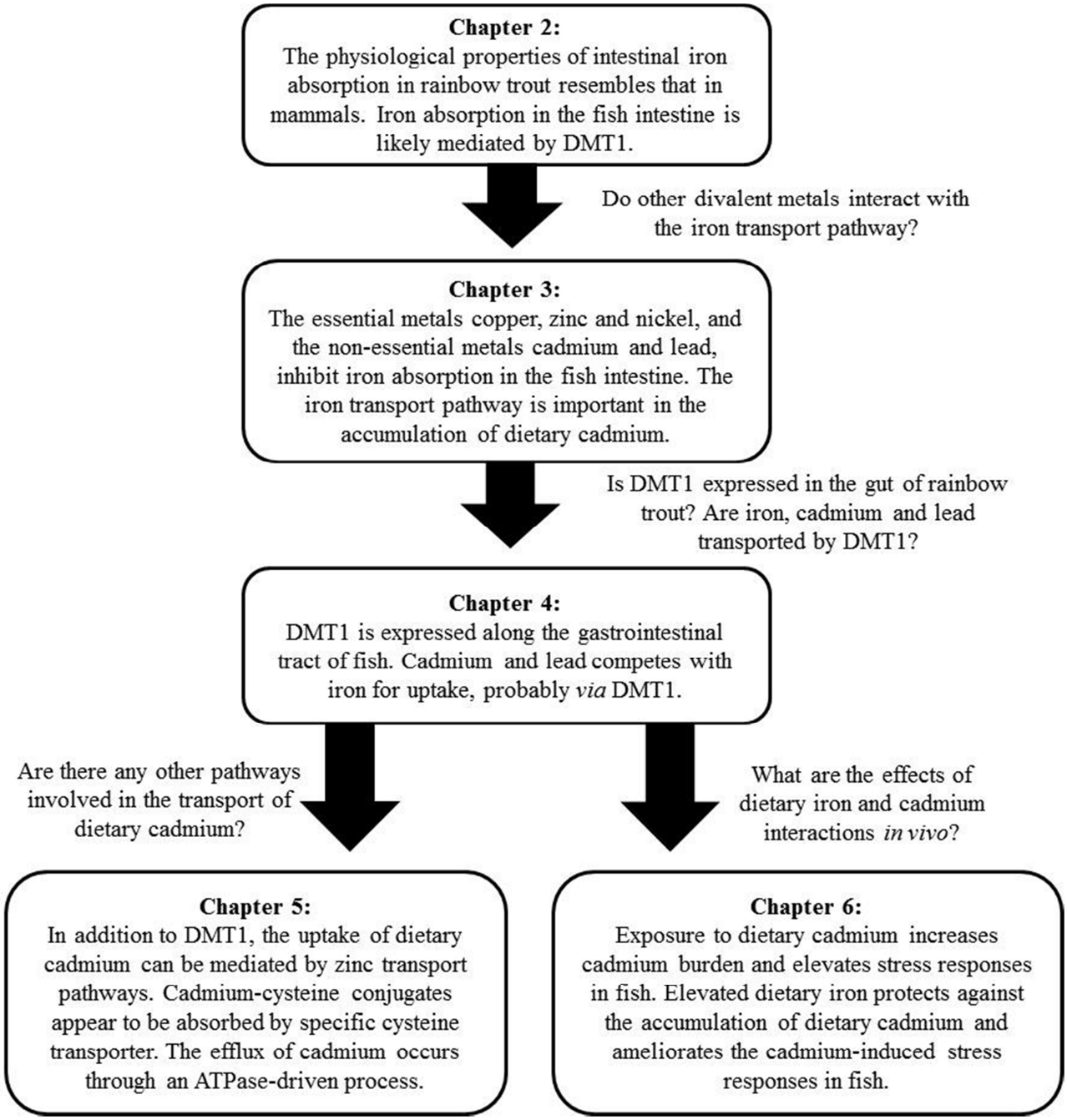

Figure 7.1: An overview of the major findings in the present research project.

7.2. Uptake and handling of dietary divalent metals in freshwater fish

7.2.1. Physiology of dietary iron absorption and homeostasis

Dietary iron exists primarily in the form of ferric iron complex, which is highly insoluble and must be reduced to the ferrous form prior to its absorption into the enterocytes *via* the ferrous iron transporter DMT1 (a Fe^{2+}/H^{+} symporter). Luminal components such as ascorbic acid (Vitamin C) can reduce ferric iron to the ferrous form and maintain it in solution, thereby enhancing its absorption by the fish intestine (Chapter 2 and 4). In mammals, the reduction of ferric iron to ferrous form occurs *via* an apical ferric reductase (McKie *et al.*, 2001). To date, no comparable homolog of mammalian ferric reductase has been identified in teleost species. Nevertheless, my study provided circumstantial evidence of extracellular conversion of ferric to ferrous iron in isolated rainbow trout enterocytes (Chapter 4), which suggested the functional role of ferric reductase in dietary iron absorption in fish.

Iron absorption occurs along the entire intestinal tract of rainbow trout, with the anterior intestine being the major site for iron absorption (Chapter 2). Although the intestinal iron absorption is found to be primarily a DMT1-mediated process (Chapter 3 and 4), it may also occur through diffusion (*via* paracellular pathways) in the anterior intestine (Chapter 2). In addition, my study has demonstrated that the DMT1-mediated apical iron uptake is highly dependent on a proton gradient and membrane potential (Chapter 4). Two different isoforms of DMT1 gene (*Nramp-β* and *–γ*) are expressed along the entire gastrointestinal tract of rainbow trout (Chapter 4). Interestingly, both DMT1 isoforms are also expressed in the stomach, indicating that the stomach is also a potential site for iron absorption in freshwater fish. Interestingly, chronic exposure to a four-fold higher level of dietary iron [high iron diet: 1100 vs.

control diet: 280 (all are in mg iron/kg of dry food weight)] did not significantly affect tissue-specific iron burden and plasma iron concentrations in rainbow trout (Chapter 6). Since there is no specific mechanism for iron excretion in vertebrates, these findings suggest that iron homeostasis is probably maintained by regulating the absorption of dietary iron in freshwater fish.

7.2.2. Role of iron transport pathway in the absorption of other divalent metals

Several different divalent metals, including both essential (copper, nickel and zinc) and non-essential (lead and cadmium), can inhibit ferrous iron absorption in the intestine of rainbow trout (Chapter 3). The interactions between iron and other divalent metals are likely due to their shared uptake through DMT1 (Chapter 3 – 5). The promiscuity of piscine DMT1 may explain the previous findings exhibiting luminal iron, copper and zinc interactions in the fish intestine (Glover and Hogstrand, 2003; Nadella *et al.*, 2007; Ojo *et al.*, 2009). However, the uptake of dietary copper and zinc may also be mediated by specific copper (copper transporter-1, Ctr1) and zinc (Zrt- and Irt-like proteins, ZIP) transporters in rainbow trout (Qiu *et al.*, 2007; Nadella *et al.*, 2011). In the stomach of rainbow trout, copper uptake is suggested to occur primarily through Ctr1 (Nadella *et al.*, 2011).

My study has indicated that nickel and lead are strong inhibitors of intestinal iron uptake in fish (Chapter 3). In addition, I demonstrated that lead inhibits iron uptake in the enterocytes through a competitive interaction, providing strong evidence that iron and lead are taken up through the same transport pathway, likely *via* DMT1 (Chapter 4). These findings are in accordance with previous evidence from mammalian systems, which indicated that DMT1 can mediate the uptake of both nickel (Tallkvist *et al.*, 2003; Davidson *et al.*, 2005; Garrick *et al.*,

2006) and lead (Bannon *et al.*, 2002; Bressler *et al.*, 2004). Overall, it is apparent that the absorption of divalent metals in the fish intestine occurs *via* multiple pathways, both iron-dependent as well as iron-independent. Nevertheless, we observed that the iron transport pathway is physiologically important in the accumulation of dietary cadmium (Chapter 3 and 6). The interactive effects of dietary iron and cadmium, and the role of DMT1 in dietary cadmium uptake, are discussed in more details in the next section (section 7.2.3).

7.2.3. Mechanisms of intestinal cadmium transport and internal handling

Cadmium appears to compete with ferrous iron for absorption *via* the apical iron transporter DMT1 in fish enterocytes (Chapter 3-5). Importantly, chronic exposure to elevated dietary iron was found to reduce the accumulation of cadmium in the stomach, intestine and the whole-body of fish (Chapter 6). It has also been reported that treatment with an iron-deficient diet increases the intestinal DMT1 expression as well as cadmium uptake in fish (Cooper *et al.*, 2006b). These observations indicate that DMT1 plays a physiologically important role in dietary cadmium accumulation in fish. Recent studies have suggested that the calcium dependent pathways (e.g., calcium channels) are an important route for cadmium absorption in the stomach of rainbow trout (Wood *et al.*, 2006; Ojo and Wood, 2008; Klinck and Wood, 2011). Klinck and Wood (2011) recently reported that the apical uptake of cadmium both in the stomach and intestine can occur *via* a mechano-sensitive L-type (voltage-gated) calcium channel. In contrast, my research has indicated that the calcium channels, either voltage-gated or voltage-insensitive, do not play a significant role in the intestinal uptake of cadmium in fish (Chapter 5). It is important to note though that Klinck and Wood (2011) used isolated gut sacs in their study as

opposed to the isolated enterocytes in my study, and the latter approach is unlikely to capture the functions of mechano-sensitive calcium channels. Thus, the potential involvement of L-type calcium channels in intestinal cadmium transport cannot be discounted. On the other hand, Ojo and Wood (2008) reported that the intestinal uptake of cadmium is inhibited by zinc and *vice versa* in fish. Similarly, my study demonstrated a competitive interaction between zinc and cadmium – providing strong evidence of a shared uptake mechanism for cadmium and zinc in the fish intestine. Interestingly, the increased extracellular bicarbonate level was found to stimulate cadmium uptake in fish enterocytes (Chapter 5). A recent molecular study in the mammalian systems has shown that the ZIP family of zinc transporters (e.g., ZIP8 – a Zn^{2+}/HCO_3^- symporter) can mediate cadmium uptake (Girijashanker *et al.*, 2008). Homologues of the mammalian ZIP transporters are known to be expressed in the gut of teleost fish, including rainbow trout (Feeney *et al.*, 2005; Qiu *et al.*, 2007). Therefore, the ZIP family of zinc transporters (e.g., ZIP8) appears to be a plausible pathway for dietary cadmium absorption in fish. Additionally, my research has indicated that organic forms of cadmium [e.g., cadmium-cysteine conjugate, $Cd(Cys)^+$], is readily bioavailable to rainbow trout enterocytes. Notably, the uptake of $Cd(Cys)^+$ was found to have a lower affinity compared to that of free inorganic cadmium ion (Chapter 5). This indicates that $Cd(Cys)^+$ gains entry into the enterocytes through a different transport system than those involved in the uptake of free cadmium ion. The uptake of $Cd(Cys)^+$ possibly occurs through the intestinal cysteine transporter due to molecular mimicry (Zalups and Ahmad, 2003).

Cadmium that enters into the enterocytes may induce the transcription of the metallothionein (MT) genes, particularly the MT isoform-A (MT-A) (Chapter 6). The increases in the mRNA level of MT may subsequently increase its protein synthesis *via* translation. The

MT protein sequesters intracellular cadmium into a metabolically unreactive form as well as increasing its retention within the enterocytes. In mammalian enterocytes, cadmium is known to bind to ferritin (an intracellular iron storage protein) as well (Granier *et al.*, 1998). Since teleost fish also have ferritin (Andersen *et al.*, 1995; Andersen, 1997), it seems reasonable that cadmium in fish enterocytes may also bind to ferritin. Interestingly, chronic waterborne lead exposure was found to induce the mRNA expression of ferritin in fish (Mager *et al.*, (2008), indicating its potential role in intracellular sequestration of lead as well.

The precise mechanism(s) of cadmium extrusion from enterocytes into the blood stream has not been fully characterized. In the mammalian intestine, the basolateral transfer of cadmium is proposed to be mediated by the iron regulated protein-1 (IREG1) (Zalups and Ahmad, 2003; Ryu *et al.*, 2004). My study has suggested that cadmium efflux from rainbow trout enterocytes occurs at least in part through an ATPase-driven process (Chapter 5), which is likely associated with the basolateral calcium-ATPase (Ca^{2+}-ATPase) and/or sodium/potassium-ATPase (Na^{+}/K^{+}-ATPase) (Schoenmakers *et al.*, 1992). Cadmium is probably transported in the body by red blood cells (Ng *et al.*, 2009) and/or bound with plasma proteins such as albumin and transferrin (De Smet *et al.*, 2001a). The induction of transferrin expression in rainbow trout exposed chronically to dietary cadmium (Chapter 6) validates the importance of plasma transferrin for systemic cadmium transport in fish. A conceptual representation of dietary cadmium transport and handling in fish is illustrated in Figure 7.2.

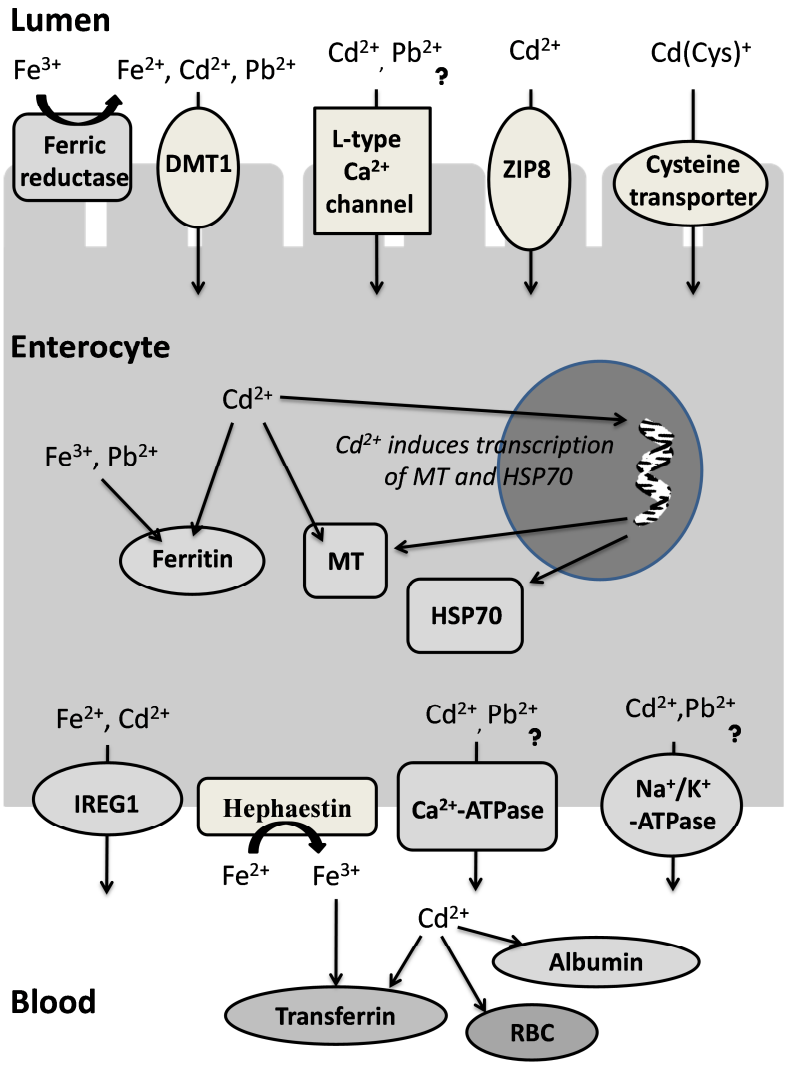

Figure 7.2: A conceptual representation of iron, cadmium and lead transport and handling in the intestinal epithelium (enterocytes) of fish. At the apical membrane, the uptake of inorganic free ferrous iron (Fe^{2+}), cadmium (Cd^{2+}) and lead (Pb^{2+}) is mediated by divalent metal transporter-1 (DMT1). Cadmium may also be taken up by Zrt- and Irt-like proteins (ZIP family of zinc transporters; ZIP8) and L-type calcium (Ca^{2+}) channel. Cadmium-cysteine conjugate $Cd(Cys)^{+}$ gains entry into enterocytes through a specific cysteine transporter. Intracellular iron, cadmium and lead may bind to iron storage protein ferritin. Cadmium may induce the transcription of metallothionein (MT), which also sequester intracellular free cadmium ion, and heat shock proteins-70 (HSP70) genes. Basolateral transfer of iron and cadmium occurs *via* iron regulated protein-1 (IREG1). Cadmium (and possibly lead) is also extruded into the blood stream by calcium-ATPase (Ca^{2+}-ATPase) and sodium/potassium ATPase (Na^{+}/K^{+}-ATPase). Following extrusion, cadmium binds to transferrin, albumin and red blood cells (RBC) in the blood. The question marks represent an uncertain process in piscine systems.

7.2.4. Physiological and molecular responses to dietary cadmium exposure

Rainbow trout chronically exposed to dietary cadmium at an environmentally-realistic level exhibited a significant increase in cadmium burden in target organs as well as the whole-body (Chapter 6). The order of cadmium accumulation in the organs followed: intestine > kidney > stomach > liver > gill > carcass. Dietary cadmium exposure did not have any apparent effects on the physiological performance of fish (e.g., no significant mortality or change in condition factors). However, we observed that fish exposed to dietary cadmium exhibited an increase in the transcription of metallothionein (MT) and heat-shock protein (HSP) genes, indicating that dietary cadmium can stimulate the stress responses in fish. I propose that these molecular endpoints may act as potential biomarkers of cadmium-induced stress in metal-contaminated wild fish populations.

The mRNA expression level of MT (MT-A and MT-B isoforms) and HSP-70 (HSP-70a and HSP-70b isoforms) increased in some target organs of fish following dietary cadmium exposure (Chapter 6). Interestingly, the tissue-specific expression of each MT and HSP-70 isoform responded differently to dietary cadmium. The increase in the transcript level of MT may subsequently increase its protein level in fish as reported by Chowdhury *et al.* (2005). The induction of MT synthesis is likely the first line of defensive mechanism against cellular cadmium toxicity. However, the up-regulation of HSP-70 genes may reflect the possible cellular damage caused by cadmium. Cadmium-induced HSP-70 expression has been associated with the formation of abnormal proteins and elevation of oxidative stress (Waisberg *et al.*, 2003; Cuypers *et al.*, 2010). The increase in the synthesis of HSP-70 may provide additional chaperone to repair denatured proteins and protect against further damage by cadmium.

Although cadmium competes with iron for intestinal absorption (Chapter 3-5), chronic exposure to dietary cadmium does not appear to cause iron deficiency in rainbow trout (Chapter 6). This observation further suggests a strong homeostatic regulation of intestinal iron absorption in freshwater fish. Interestingly however, the mRNA expression level of transferrin in the liver as well as its protein level in the plasma was significantly increased in fish exposed to dietary cadmium. It has been shown that a significant amount of plasma cadmium binds to transferrin in carp (*Cyprinus carpio)* as well as in brown trout (*Salmo trutta*) (De Smet *et al.*, 2001a). Zhu *et al.* (2006) reported that when cadmium binds to transferrin, transferrin loses its function to deliver iron into the cells. Therefore, it is likely that the up-regulation of hepatic transferrin synthesis observed in our study occurs as a compensatory response to ameliorate the effect of cadmium on systemic iron handling. I suggest that transferrin expression in the liver and/or in the plasma can be a potential biomarker of cadmium exposure in wild freshwater fish.

7.2.5. Physiological implications of dietary iron and cadmium interaction

Rainbow trout fed with an iron-supplemented diet exhibited a significant reduction in the accumulation of dietary cadmium in the gut and the whole-body (Chapter 6). The protective effect of elevated dietary iron against cadmium accumulation is probably due to the competitive interaction between cadmium and iron for intestinal absorption (Chapter 3-5). Interestingly, the elevated dietary iron also reduced the cadmium-induced transferrin expression in fish, which suggested that dietary iron can ameliorate the effect of cadmium on systemic iron handling. Moreover, my study has shown that the induction of MT and HSP70 mRNA expression by dietary cadmium was inhibited by an elevated iron diet, although the effects varied among

organs. These observations were partly due to the decrease in cadmium accumulation by elevated dietary iron. Since MT and HSP synthesis occur at the expense of energy, it is likely that elevated dietary iron alleviates the energetic cost of cadmium detoxification in fish. Overall, it is reasonable to suggest that elevated dietary iron has protective physiological implications for fish exposed to dietary cadmium.

7.3. Environmental and toxicological implications

Evidence from my research as well as from other studies has confirmed that exposure to dietary cadmium at an environmentally relevant level could lead to significant accumulation of cadmium and affect the physiology of fish. Natural diets containing elevated lead, copper, zinc or arsenic have also been shown to cause adverse effects on fish health (Mount *et al.*, 1994; Farag *et al.*, 1999; Boyle *et al.*, 2008). However, the current water quality guidelines for the protection of aquatic animals against metal toxicity are based on waterborne exposure only, and the dietary exposure is not considered in the regulatory framework in Canada as well as in other jurisdictions. Besides, the water quality criteria are typically formulated based on individual metals. My research clearly indicates that dietary interactions of divalent metals may have profound effects on the uptake and accumulation of metals, which may subsequently affect the physiological condition of fish. In the real world, exposure to metals occurs rarely in isolation, and fish are most commonly exposed to elevated concentrations of metals in mixture, both *via* water and diet. A more realistic risk assessment of metals in the aquatic ecosystems can only be achieved if dietary exposure of metals and their interactions are incorporated in the future development/refinement of regulatory frameworks. In addition, my research also highlights the usefulness of gene expression endpoints in assessing the physiological status of fish impacted by

chronic dietary metal (cadmium) exposure. The use of molecular endpoints may help in evaluating the health of metal-impacted feral fish populations, which is often difficult to assess using conventional whole organismal or sub-organismal approaches.

In freshwater fish, it is well documented that waterborne cadmium inhibits the active transport of calcium, which subsequently causes hypocalcaemia and death at acute concentrations (Wood, 2001). However, my study indicates that the absorption of dietary cadmium occurs largely through calcium-insensitive pathways. The iron (DMT1) and zinc (ZIP8) transport pathways appear to be more important for the absorption of dietary inorganic cadmium. Hence, I propose that the toxic mechanism of dietary cadmium exposure to freshwater fish is different from that of waterborne cadmium exposure. It is possible that the toxicity of dietary cadmium occurs due to the disruption of iron and zinc transport and metabolism in fish, at least in part.

Cadmium contamination in commercial fish feed is a growing concern for the aquaculture industry in many developing countries including China. Squid viscera is widely used in the preparation of fish feed as an attractant and growth stimulant (Mai et al., 2006). However, fish diet supplemented with squid viscera has been found to contain significant amount of cadmium (about 50 μg/g dry wet of feed) (Dang and Wang, 2009). Farm fish fed with this diet have been found to exhibit a significant elevation in cadmium body burden (Dang and Wang, 2009), posing serious concern for human consumption. My study indicates that supplementation of commercial fish diet with iron may reduce dietary cadmium accumulation in fish, thereby alleviating the potential risk of cadmium exposure to humans.

7.4. Future research perspectives and recommendations

My research has provided important and novel mechanistic information on the absorption of dietary iron in freshwater fish. However, the molecular mechanisms governing the systemic iron homeostasis in fish remain unresolved. Moreover, dietary exposure to metals are known to influence the uptake of waterborne metals in fish (see Niyogi and Wood, 2003 for review), and thus it will be interesting to examine the interplay between branchial and intestinal iron absorption. This is particularly important since fish could acquire a large portion of their daily iron requirement *via* the gill during periods of low dietary intake (Cooper and Bury, 2007). Examination of key iron handling proteins (e.g., ferritin, hepcidin and transferrin) as well as iron transport proteins (DMT1 and IREG1) in major transport epithelia (gill, intestine, liver and kidney) of fish in response to waterborne and dietborne iron exposure would provide important information on their homeostatic function in iron regulation. In addition, the physiological role of gastro-intestinal DMT1 in the transport of other divalent metals, such as nickel, zinc and lead, has not been fully established. Recent studies have shown that the mRNA expression of DMT1 and IREG1 can be modulated by the exposure to other divalent metals such as copper and zinc in zebrafish as well as in mammals (Yamaji *et al.*, 2001; Tennant *et al.*, 2002; Craig *et al.*, 2009); however, its toxicological implications, especially in fish exposed to metals mixture, remain to be fully elucidated.

Chronic exposure to dietary cadmium was found to induce the expression of MT and HSP genes in rainbow trout (Chapter 6), and these responses could be linked to the oxidative stress response in fish (Cuypers *et al.*, 2010). The elevated oxidative stress is typically associated with the increase in cellular reactive oxygen species (ROS) and the depletion of cellular antioxidants. Several studies have characterized the oxidative stress in fish exposed to

waterborne metals (Lange *et al.*, 2002; Manzl *et al.*, 2004; Hansen *et al.*, 2006; Craig *et al.*, 2007). However, the effects of dietary metal exposure on oxidative stress responses in fish, particularly during environmentally realistic exposure conditions, have only been studied sporadically (Farag *et al.*, 1994; Dang and Wang, 2009). Measurement of protein carbonyl content and membrane lipid peroxidation, and the tissue-specific concentrations of both enzymatic (e.g., catalase, superoxide dismutase) and non-enzymatic (e.g., the ratio of reduced to oxidized glutathione) antioxidants, may prove useful in assessing the potential oxidative damage induced by dietary cadmium exposure. In addition, the shared dietary uptake of cadmium with iron and zinc may have significant implications for their uptake, metabolism and homeostasis of these metals in fish. I hypothesize that acclimation to chronic cadmium exposure in fish involves regulation of zinc and iron uptake and metabolism. Since iron and zinc are essential for a wide variety of vital metabolic processes, new generation genomic tools (e.g., microarray) can be used to develop a comprehensive understanding of how these processes are affected by cadmium exposure.

LIST OF REFERENCES

Aegerter, S., Jalabert, B., and Bobe, J. (2005). Large scale real-time PCR analysis of mRNA abundance in rainbow trout eggs in relationship with egg quality and post-ovulatory ageing. *Mol. Reprod. Dev.* **72**, 377-385.

Alves, L. C., and Wood, C. M. (2006). The chronic effects of dietary lead in freshwater juvenile rainbow trout (*Oncorhynchus mykiss*) fed elevated calcium diets. *Aquat. Toxicol.* **78**, 217-232.

Andersen, F., Maage, A., and Julshamn, K. (1996). An estimation of dietary iron requirement of Atlantic salmon, *Salmo solar* L., parr. *Aquacult. Nutr.* **2**, 41-47.

Andersen, O. (1997). Accumulation of waterborne iron and expression of ferritin and transferrin in early developmental stages of brown trout (*Salmo trutta*). *Fish Physiol. Biochem.* **16**, 223-231.

Andersen, O., Dehli, A., Standal, H., Giskegjerde, T. A., Karstensen, R., and Rorvik, K. (1995). Two ferritin subunits of Atlantic salmon (*Salmo salar*): Cloning of the liver cDNAs and antibody preparation. *Mol. Mar. Biol. Biotech.* **4**, 164-170.

Andrews, N. C. (2000). Iron homeostasis: Insights from genetics and animal models. *Nat. Rev. Genet.* **1**, 208-217.

Arredondo, M., Munoz, P., Mura, C. V., and Nunez, M. T. (2003). DMT1 a physiologically relevant apical Cu^{1+} transporter of intestinal cells. *Am. J. Physiol.* **284**, 1525-1530.

Baldisserotto, B., Chowdhury, M. J., and Wood, C. M. (2005). Effects of dietary calcium and cadmium on cadmium accumulation, calcium and cadmium uptake from the water, and their interactions in juvenile rainbow trout. *Aquat. Toxicol.* **72**, 99-117.

Bannon, D. I., Abounader, R., Lees, P. S., and Bressler, J. P. (2003). Effect of DMT1 knockdown on iron, cadmium, and lead uptake in Caco-2 cells. *Am. J. Physiol. -Cell Physiol.* **284**, 44-50.

Bannon, D. I., Portnoy, M. E., Olivi, L., Lees, P. S. J., Culotta, V. C., and Bressler, J. P. (2002). Uptake of lead and iron by divalent metal transporter 1 in yeast and mammalian cells. *Biochem. Biophys. Res. Commun.* **295**, 978-984.

Bergman, A. N., Laurent, P., Otiang'a-Owiti, G., Bergman, H. L., Walsh, P. J., Wilson, P., and Wood, C. M. (2003). Physiological adaptations of the gut in the Lake Magadi tilapia, *Alcolapia grahami*, an alkaline- and saline-adapted teleost fish. *Comp. Biochem. Physiol. -A* **136**, 701-715.

Berntssen, M. H. G., Aspholm, O. Ø., Hylland, K., Wendelaar Bonga, S. E., and Lundebye, A. K. (2001). Tissue metallothionein, apoptosis and cell proliferation responses in Atlantic salmon (*Salmo salar L.*) parr fed elevated dietary cadmium. *Comp. Biochem. Physiol. -C* **128**, 299-310.

Bierkens, J. G. E. A. (2000). Applications and pitfalls of stress-proteins in biomonitoring. *Toxicology* **153**, 61-72.

Blechinger, S. R., Kusch, R. C., Haugo, K., Matz, C., Chivers, D. P., and Krone, P. H. (2007). Brief embryonic cadmium exposure induces a stress response and cell death in the developing olfactory system followed by long-term olfactory deficits in juvenile zebrafish. *Toxicol. Appl. Pharmacol.* **224**, 72-80.

Boyle, D., Brix, K. V., Amlund, H., Lundebye, A.-K., Hogstrand, C., and Bury, N. R. (2008). Natural arsenic contaminated diets perturb reproduction in fish. *Environ. Sci. Technol.* **42**, 5354-5360.

Bressler, J. P., Olivi, L., Cheong, J. H., Kim, Y., and Bannon, D. (2004). Divalent metal transporter 1 in lead and cadmium transport. *Ann. NY. Acad. Sci.* **1012**, 142-152.

Brodeur, J. C., Daniel, C., Ricard, A. C., and Hontela, A. (1998). In vitro response to ACTH of the interrenal tissue of rainbow trout (*Oncorhynchus mykiss*) exposed to cadmium. *Aquat. Toxicol.* **42**, 103-113.

Brown, K. E., Broadhurst, K. A., Mathahs, M. M., and Weydert, J. (2007). Differential expression of stress-inducible proteins in chronic hepatic iron overload. *Toxicol. Appl. Pharmacol.* **223**, 180-186.

Buddington, R. K., and Diamond, J. M. (1986). Aristotle revisited: The function of pyloric caeca in fish. *Proc. Nat. Acad. Sci. USA* **83**, 8012-8014.

Buddington, R. K., and Diamond, J. M. (1987). Pyloric ceca of fish: a "new" absorptive organ. *Am. J. Physiol. -Gastr. Liver Physiol.* **252**, 65-76.

Buddington, R. K., and Kuz'mina, V. (2000). Digestive system. In *The Laboratory Fish* (G. K. Ostrander, Ed.), pp. 173-180. Academic Press, San Diego.

Burge, E. J., Gauthier, D. T., and Van Veld, P. A. (2004). *In vitro* response of the striped bass natural resistance-associated macrophage protein, Nramp, to LPS and Mycobacterium marinum exposure. *Comp. Biochem. Physiol. -C* **138**, 391-400.

Burke, J., and Handy, R. D. (2005). Sodium-sensitive and -insensitive copper accumulation by isolated intestinal cells of rainbow trout *Oncorhynchus mykiss*. *J. Exp. Biol.* **208**, 391-407.

Bury, N. R., Chung, M. J., Sturm, A., Walker, P. A., and Hogstrand, C. (2008). Cortisol stimulates the zinc signaling pathway and expression of metallothioneins and ZnT1 in rainbow trout gill epithelial cells. *Am. J. Physiol. -Regul. Integr. Comp. Physiol.* **294**, 623-629.

Bury, N. R., and Grosell, M. (2003a). Iron acquisition by teleost fish. *Comp. Biochem. Physiol. -C* **135**, 97-105.

Bury, N. R., and Grosell, M. (2003b). Waterborne iron acquisition by a freshwater teleost fish, zebrafish *Danio rerio*. *J. Exp. Biol.* **206**, 3529-3535.

Bury, N. R., Grosell, M., Wood, C. M., Hogstrand, C., Wilson, R. W., Rankin, J. C., Busk, M., Lecklin, T., and Jensen, F. B. (2001). Intestinal iron uptake in the European flounder (*Platichthys flesus*). *J. Exp. Biol.* **204**, 3779-3787.

Bury, N. R., Walker, P. A., and Glover, C. N. (2003). Nutritive metal uptake in teleost fish. *J. Exp. Biol.* **206**, 11-23.

Camakaris, J., Voskoboinik, I., and Mercer, J. F. (1999). Molecular mechanisms of copper homeostasis. *Biochem. Biophys. Res. Commun.* **261**, 225-232.

Carriquiriborde, P., Handy, R. D., and Davies, S. J. (2004). Physiological modulation of iron metabolism in rainbow trout (*Oncorhynchus mykiss*) fed low and high iron diets. *J. Exp. Biol.* **207**, 75-86.

Chang, Y. C., Zouari, M., Gogorcena, Y., Lucena, J. J., and Abadia, J. (2003). Effects of cadmium and lead on ferric chelate reductase activities in sugar beet roots. *Plant Physiol. Biochem.* **41**, 999-1005.

Chen, H., Su, T., Attieh, Z. K., Fox, T. C., McKie, A. T., Anderson, G. J., and Vulpe, C. D. (2003). Systemic regulation of Hephaestin and Ireg1 revealed in studies of genetic and nutritional iron deficiency. *Blood* **102**, 1893-1899.

Chen, J., Shi, Y. H., and Li, M. Y. (2008). Changes in transferrin and hepcidin genes expression in the liver of the fish *Pseudosciaena crocea* following exposure to cadmium. *Arch. Toxicol.* **82**, 525-530.

Chen, S.-L., Wang, Z.-J., Xu, M.-Y., and Gui, J.-F. (2006). Molecular identification and expression analysis of natural resistance associated macrophage protein (Nramp) cDNA from Japanese flounder (*Paralichthys olivaceus*). *Fish Shellfish Immun.* **20**, 365-373.

Chowdhury, M. J., Baldisserotto, B., and Wood, C. M. (2005). Tissue-specific cadmium and metallothionein levels in rainbow trout chronically acclimated to waterborne or dietary cadmium. *Arch. Environ. Contam. Toxicol.* **48**, 381-390.

Chowdhury, M. J., McDonald, D. G., and Wood, C. M. (2004a). Gastrointestinal uptake and fate of cadmium in rainbow trout acclimated to sublethal dietary cadmium. *Aquat. Toxicol.* **69**, 149-163.

Chowdhury, M. J., Pane, E. F., and Wood, C. M. (2004b). Physiological effects of dietary cadmium acclimation and waterborne cadmium challenge in rainbow trout: respiratory, ionoregulatory, and stress parameters. *Comp. Biochem. Physiol. -C* **139**, 163-173.

Clearwater, S. J., Baskin, S. J., Wood, C. M., and McDonald, D. G. (2000). Gastrointestinal uptake and distribution of copper in rainbow trout. *J. Exp. Biol.* **203**, 2455-2466.

Cole, A., Furnival, C., Huang, Z. X., Ceri Jones, D., May, P. M., Smith, G. L., Whittaker, J., and Williams, D. R. (1985). Computer simulation models for the low-molecular-weight complex distribution of cadmium(II) and nickel(II) in human blood plasma. *Inorg. Chim. Acta.* **108**, 165-171.

Conrad, M. E., Umbreit, J. N., Moore, E. G., Hainsworth, L. N., Porubcin, M., and Simovich, M. J. (2000). Separate pathways for cellular uptake of ferric and ferrous iron. *Am. J. Physiol. -Gastr. Liver Physiol.* **279**, 767-774.

Cooper, C. A., and Bury, N. R. (2007). The gills as an important uptake route for the essential nutrient iron in freshwater rainbow trout *Oncorhynchus mykiss*. *J. Fish Biol.* **71**, 115-128.

Cooper, C. A., Bury, N. R., and Grosell, M. (2006a). The effects of pH and the iron redox state on iron uptake in the intestine of a marine teleost fish, gulf toadfish (*Opsanus beta*). *Comp. Biochem. Physiol. -A* **143**, 292-298.

Cooper, C. A., Handy, R. D., and Bury, N. R. (2006b). The effects of dietary iron concentration on gastrointestinal and branchial assimilation of both iron and cadmium in zebrafish (*Danio rerio*). *Aquat. Toxicol.* **79**, 167-175.

Cooper, C. A., Shayeghi, M., Techau, M. E., Capdevila, D. M., MacKenzie, S., Durrant, C., and Bury, N. R. (2007). Analysis of the rainbow trout solute carrier 11 family reveals iron import >= pH 7.4 and a functional isoform lacking transmembrane domains 11 and 12. *FEBS Lett.* **581**, 2599-2604.

Craig, P. M., Galus, M., Wood, C. M., and McClelland, G. B. (2009). Dietary iron alters waterborne copper-induced gene expression in soft water acclimated zebrafish (*Danio rerio*). *Am. J. Physiol. -Regul. Integr. Comp. Physiol.* **296**, 362-373.

Craig, P. M., Wood, C. M., and McClelland, G. B. (2007). Oxidative stress response and gene expression with acute copper exposure in zebrafish (*Danio rerio*). *Am. J. Physiol. -Regul. Integr. Comp. Physiol.* **293**, 1882-1892.

Crichton, R. R., Wilmet, S., Legssyer, R., and Ward, R. J. (2002). Molecular and cellular mechanisms of iron homeostasis and toxicity in mammalian cells. *J. Inorg. Biochem.* **91**, 9-18.

Cuypers, A., Plusquin, M., Remans, T., Jozefczak, M., Keunen, E., Gielen, H., Opdenakker, K., Nair, A. R., Munters, E., Artois, T. J., Nawrot, T., Vangronsveld, J., and Smeets, K. (2010). Cadmium stress: an oxidative challenge. *BioMetals* **23**, 927-940.

Dang, F., and Wang, W. X. (2009). Assessment of tissue-specific accumulation and effects of cadmium in a marine fish fed contaminated commercially produced diet. *Aquat. Toxicol.* **95**, 248-255.

Davidson, T., Chen, H., Garrick, M. D., D'Angelo, G., and Costa, M. (2005). Soluble nickel interferes with cellular iron homeostasis. *Mol. Cell Biochem.* **279**, 157-162.

De Smet, H., Blust, R., and Moens, L. (2001a). Cadmium-binding to transferrin in the plasma of the common carp *Cyprinus carpio*. *Comp. Biochem. Physiol. -C* **128**, 45-53.

De Smet, H., De Wachter, B., Lobinski, R., and Blust, R. (2001b). Dynamics of (Cd,Zn)-metallothioneins in gills, liver and kidney of common carp *Cyprinus carpio* during cadmium exposure. *Aquat. Toxicol.* **52**, 269-281.

Donovan, A., Brownlie, A., Dorschner, M. O., Zhou, Y., Pratt, S. J., Paw, B. H., Phillips, R. B., Thisse, C., Thisse, B., and Zon, L. I. (2002). The zebrafish mutant gene chardonnay (cdy) encodes divalent metal transporter 1 (DMT1). *Blood* **100**, 4655-4659.

Donovan, A., Brownlie, A., Zhou, Y., Shepard, J., Pratt, S. J., Moynihan, J., Paw, B. H., Drejer, A., Barut, B., Zapata, A., Law, T. C., Brugnara, C., Lux, S. E., Pinkus, G. S., Pinkus, J. L., Kingsley, P. D., Palls, J., Fleming, M. D., Andrews, N. C., and Leonard I, Z. (2000). Positional cloning of zebrafish ferroportin1 identifies a conserved vertebrate iron exporter. *Nature* **403**, 776-781.

Dorschner, M. O., and Phillips, R. B. (1999). Comparative analysis of two Nramp loci from rainbow trout. *DNA Cell Biol.* **18**, 573-583.

Elisma, F., and Jumarie, C. (2001). Evidence for cadmium uptake through Nramp2: Metal speciation studies with Caco-2 cells. *Biochem. Biophys. Res. Comm.* **285**, 662-668.

Endo, T., Kimura, O., Saitoh, H., and Sakata, M. (2000). Secretory transport of cadmium through intestinal brush border membrane via H^+-antiport. *Toxicology* **150**, 129-136.

Ezeasor, D. N., and Stokoe, W. M. (1980). Scanning electron microscopic study of the gut mucosa of the rainbow trout *Salmo gairdneri* Richardson. *J. Fish Biol.* **17**, 529-539.

Farag, A. M., Boese, C. J., Woodward, D. F., and Bergman, H. L. (1994). Physiological changes and tissue metal accumulation in rainbow trout exposed to foodborne and waterborne metals. *Environ. Toxicol. Chem.* **13**, 2021-2029.

Farag, A. M., Woodward, D. F., Brumbaugh, W., Goldstein, J. N., MacConnell, E., Hogstrand, C., and Barrows, F. T. (1999). Dietary effects of metals-contaminated invertebrates from the Coeur d'Alene River, Idaho, on cutthroat trout. *Trans. Amer. Fish. Soc.* **128**, 578-592.

Feeney, G. P., Zheng, D., Kille, P., and Hogstrand, C. (2005). The phylogeny of teleost ZIP and ZnT zinc transporters and their tissue specific expression and response to zinc in zebrafish. *Biochim. Biophys. Acta.* **1732**, 88-95.

Ford, M. J. (2001). Molecular evolution of transferring: evidence for positive selection in salmonids. *Mol. Biol. Evol.* **18**, 639-649.

Fox, M. R. S., Jacobs, R. M., Jones, A. O. L., Fry, B. E., and Stone, C. L. (1980). Effects of vitamin C and iron on cadmium metabolism. *Ann. NY. Acad. Sci.* **355**, 249-261.

Franklin, N. M., Glover, C. N., Nicol, J. A., and Wood, C. M. (2005). Calcium/cadmium interactions at uptake surfaces in rainbow trout: Waterborne versus dietary routes of exposure. *Environ. Toxicol. Chem.* **24**, 2954-2964.

Frazer, D. M., Wilkins, S. J., Becker, E. M., Murphy, T. L., Vulpe, C. D., McKie, A. T., and Anderson, G. J. (2003). A rapid decrease in the expression of DMT1 and Dcytb but not Ireg1 or hephaestin explains the mucosal block phenomenon of iron absorption. *Gut* **52**, 340-346.

Friedman, P. A., and Gesek, F. A. (1994). Cadmium uptake by kidney distal convoluted tubule cells. *Toxicol. Appl. Pharmacol.* **128**, 257-263.

Garrick, M. D., Dolan, K. G., Horbinski, C., Ghio, A. J., Higgins, D., Porubcin, M., Moore, E. G., Hainsworth, L. N., Umbreit, J. N., Conrad, M. E., Feng, L., Lis, A., Roth, J. A., Singleton, S., and Garrick, L. M. (2003). DMT1: A mammalian transporter for multiple metals. *BioMetals* **16**, 41-54.

Garrick, M. D., Singleton, S. T., Vargas, F., Kuo, H. C., Zhao, L., Knopfel, M., Davidson, T., Costa, M., Paradkar, P., Roth, J. A., and Garrick, L. M. (2006). DMT1: which metals does it transport? *Biol. Res.* **39**, 79-85.

Gatlin, D. M., and Wilson, R. P. (1986). Characterization of iron deficiency and the dietary iron requirement of fingerling channel catfish. *Aquaculture* **52**, 191-198.

Girijashanker, K., He, L., Soleimani, M., Reed, J. M., Li, H., Liu, Z., Wang, B., Dalton, T. P., and Nebert, D. W. (2008). Slc39a14 gene encodes ZIP14, a metal/bicarbonate symporter: Similarities to the ZIP8 transporter. *Mol. Pharmacol.* **73**, 1413-1423.

Glover, C. N., Bury, N. R., and Hogstrand, C. (2004). Intestinal zinc uptake in freshwater rainbow trout: evidence for apical pathways associated with potassium efflux and modified by calcium. *Biochim. Biophys. Acta. - Biomembranes* **1663**, 214-221.

Glover, C. N., and Hogstrand, C. (2002). *In vivo* characterisation of intestinal zinc uptake in freshwater rainbow trout. *J. Exp. Biol.* **205**, 141-150.

Glover, C. N., and Hogstrand, C. (2003). Effects of dissolved metals and other hydrominerals on in vivo intestinal zinc uptake in freshwater rainbow trout. *Aquat. Toxicol.* **62**, 281-293.

Goddard, W. P., Coupland, K., Smith, J. A., and Long, R. G. (1997). Iron uptake by isolated human enterocyte suspensions in vitro is dependent on body iron stores and inhibited by other metal cations. *J. Nutr.* **127**, 177-183.

Granier, T., Comberton, G., Gallois, B., Langlois D'Estaintot, B., Dautant, A., Crichton, R. R., and Précigoux, G. (1998). Evidence of new cadmium binding sites in recombinant horse L-chain ferritin by anomalous fourier difference map calculation. *Proteins* **31**, 477-485.

Grosell, M., Farrell, A. P., and Brauner, C. J. (2011). *The Multifunctional Gut of Fish*. Academic Press, San Diego.

Grosell, M., Gilmour, K. M., and Perry, S. F. (2007). Intestinal carbonic anhydrase, bicarbonate, and proton carriers play a role in the acclimation of rainbow trout to seawater. *Am. J. Physiol. -Regul. Integr. Comp. Physiol.* **293**, 2099-2111.

Grosell, M., and Jensen, F. B. (1999). NO_2^- uptake and HCO_3^- excretion in the intestine of the European flounder (*Platichthys flesus*). *J. Exp. Biol.* **202**, 2103-2110.

Groten, J. P., Sinkeldam, E. J., Muys, T., Luten, J. B., and van Bladeren, P. J. (1991). Interaction of dietary Ca, P, Mg, Mn, Cu, Fe, Zn and Se with the accumulation and oral toxicity of cadmium in rats. *Food Chem. Toxicol.* **29**, 249-258.

Gunshin, H., Mackenzie, B., Berger, U. V., Gunshin, Y., Romero, M. F., Boron, W. F., Nussberger, S., Gollan, J. L., and Hediger, M. A. (1997). Cloning and characterization of a mammalian proton-coupled metal-ion transporter. *Nature* **388**, 482-488.

Gustafsson, J. P. (2010). Visual MINTEQ. *Dep. Land Water Res. Eng., Stockholm, Sweden*.

Hallare, A. V., Schirling, M., Luckenbach, T., Köhler, H. R., and Triebskorn, R. (2005). Combined effects of temperature and cadmium on developmental parameters and biomarker responses in zebrafish (*Danio rerio*) embryos. *J. Therm. Biol.* **30**, 7-17.

Handy, R. D., Eddy, F. B., and Baines, H. (2002). Sodium-dependent copper uptake across epithelia: a review of rationale with experimental evidence from gill and intestine. *Biochim. Biophys. Acta. - Biomembranes* **1566**, 104-115.

Handy, R. D., Musonda, M. M., Phillips, C., and Falla, S. J. (2000). Mechanisms of gastrointestinal copper absorption in the african walking catfish: Copper dose-effects and a novel anion-dependent pathway in the intestine. *J. Exp. Biol.* **203**, 2365-2377.

Hansen, B. H., Rømma, S., Søfteland, L. I. R., Olsvik, P. A., and Andersen, R. A. (2006). Induction and activity of oxidative stress-related proteins during waterborne Cu-exposure in brown trout (Salmo trutta). *Chemosphere* **65**, 1707-1714.

Hansen, J. A., Lipton, J., Welsh, P. G., Cacela, D., and MacConnell, B. (2004). Reduced growth of rainbow trout (*Oncorhynchus mykiss*) fed a live invertebrate diet pre-exposed to metal-contaminated sediments. *Environ. Toxicol. Chem.* **23**, 1902-1911.

Haux, C., and Larsson, A. (1984). Long-term sublethal physiological effects on rainbow trout, *Salmo gairdneri*, during exposure to cadmium and after subsequent recovery. *Aquat. Toxicol.* **5**, 129-142.

He, L., Girijashanker, K., Dalton, T. P., Reed, J., Li, H., Soleimani, M., and Nebert, D. W. (2006). ZIP8, member of the solute-carrier-39 (SLC39) metal-transporter family: Characterization of transporter properties. *Mol. Pharmacol.* **70**, 171-180.

Hinkle, P. M., Kinsella, P. A., and Osterhoudt, K. C. (1987). Cadmium uptake and toxicity via voltage-sensitive calcium channels. *J. Biol. Chem.* **262**, 16333-16337.

Hirao, S., Yamada, J., and Kikuchi, R. (1955). Relation between chemical constituents of rainbow trout eggs and the hatching rate. *Nippon Suisan Gakkaishi* **21**, 240-243.

Hoar, W. S. (1983). *General and Comparative Physiology*. Prentice-Hall, Inc., New Jersey.

Hodson, P. V., Blunt, B. R., and Spry, D. J. (1978). Chronic toxicity of water-borne and dietary lead to rainbow trout (*Salmo Gairdneri*) in lake Ontario water. *Water Res.* **12**, 869-878.

Hogstrand, C., Wilson, R. W., Polgar, D., and Wood, C. M. (1994). Effects of zinc on the kinetics of branchial calcium uptake in freshwater rainbow trout during adaptation to waterborne zinc. *J. Exp. Biol.* **186**, 55-73.

Hollis, L., Hogstrand, C., and Wood, C. M. (2001). Tissue-specific cadmium accumulation, metallothionein induction, and tissue zinc and copper levels during chronic sublethal cadmium exposure in juvenile rainbow trout. *Arch. Environ. Contam. Toxicol.* **41**, 468-474.

Hollis, L., McGeer, J. C., McDonald, D. G., and Wood, C. M. (1999). Cadmium accumulation, gill Cd binding, acclimation, and physiological effects during long term sublethal Cd exposure in rainbow trout. *Aquat. Toxicol.* **46**, 101-119.

Hollis, L., McGeer, J. C., McDonald, D. G., and Wood, C. M. (2000). Protective effects of calcium against chronic waterborne cadmium exposure to juvenile rainbow trout. *Environ. Toxicol. Chem.* **19**, 2725-2734.

Horiguchi, H., Sato, M., Konno, N., and Fukushima, M. (1996). Long-term cadmium exposure induces anemia in rats through hypoinduction of erythropoietin in the kidneys. *Arch. Toxicol.* **71**, 11-19.

Huebers, H. A., Huebers, E., and Csiba, E. (1987). The cadmium effect on iron absorption. *Am. J. Clin. Nutr.* **45**, 1007-1012.

Iturria, S., and Nuñezb, M. T. (1998). Effect of copper, cadmium, mercury, manganese and lead on Fe^{2+} and Fe^{3+} absorption in perfused mouse intestine. *Digestion* **59**, 671-675.

Jumarie, C., Campbell, P. G. C., Berteloot, A., Houde, M., and Denizeau, F. (1997). Caco-2 cell line used as an in vitro model to study cadmium accumulation in intestinal epithelial cells. *J. Membr. Biol.* **158**, 31-48.

Jumarie, C., Fortin, C., Houde, M., Campbell, P. G. C., and Denizeau, F. (2001). Cadmium uptake by Caco-2 cells: effects of Cd complexation by chloride, glutathione, and phytochelatins. *Toxicol. Appl. Pharmacol.* **170**, 29-38.

Kawatsu, H. (1972). Studies on the anemia of fish. V. Dietary iron deficient anemia in brook trout, *Salvelinus fontinalis*. *Bull. Freshw. Fish. Res. Lab.* **22**, 59-67.

Kim, D. W., Kim, K. Y., Choi, B. S., Youn, P., Ryu, D. Y., Klaassen, C. D., and Park, J. D. (2007). Regulation of metal transporters by dietary iron, and the relationship between body iron levels and cadmium uptake. *Arch. Toxicol.* **81**, 327-334.

Kim, S.-G., Kim, J.-W., and Kang, J.-C. (2004). Effect of dietary cadmium on growth and haematological parameters of juvenile rockfish, Sebastes schlegeli (*Hilgendorf*). *Aquaculture Res.* **35**, 80-86.

Klinck, J. S., Ng, T. Y. T., and Wood, C. M. (2009). Cadmium accumulation and *in vitro* analysis of calcium and cadmium transport functions in the gastro-intestinal tract of trout following chronic dietary cadmium and calcium feeding. *Comp. Biochem. Physiol.- C* **150**, 349-360.

Klinck, J. S., and Wood, C. M. (2011). *In vitro* characterization of cadmium transport along the gastro-intestinal tract of freshwater rainbow trout (*Oncorhynchus mykiss*). *Aquat. Toxicol.* **102**, 58-72.

Knutson, M., and Wessling-Resnick, M. (2003). Iron metabolism in the reticuloendothelial system. *Crit. Rev. Biochem. Mol.* **38**, 61-88.

Kozlowska, K., Brzozowska, A., Sulkowska, J., and roszkowski, W. (1993). The effect of cadmium on iron metabolism in rats. *Nutr. Res.* **13**, 1163-1172.

Kwong, R. W. M., Andrés, J. A., and Niyogi, S. (2010). Molecular evidence and physiological characterization of iron absorption in isolated enterocytes of rainbow trout (*Oncorhynchus mykiss*): Implications for dietary cadmium and lead absorption. *Aquat. Toxicol.* **99**, 343-350.

Kwong, R. W. M., Jose, J. A., and Niyogi, S. (2011). Effects of dietary cadmium exposure on tissue-specific cadmium accumulation, iron status and expression of iron-handling and stress-inducible genes in rainbow trout: influence of elevated dietary iron. *Aquat. Toxicol.* **102**, 1-9.

Kwong, R. W. M., and Niyogi, S. (2008). An *in vitro* examination of intestinal iron absorption in a freshwater teleost, rainbow trout (*Oncorhynchus mykiss*). *J. Comp. Physiol. -B* **178**, 963-975.

Kwong, R. W. M., and Niyogi, S. (2009). The interactions of iron with other divalent metals in the intestinal tract of a freshwater teleost, rainbow trout (*Oncorhynchus mykiss*). *Comp. Biochem. Physiol. -C* **150**, 442-449.

Lacroix, A., and Hontela, A. (2004). A comparative assessment of the adrenotoxic effects of cadmium in two teleost species, rainbow trout, Oncorhynchus mykiss, and yellow perch, Perca flavescens. *Aquatic Toxicology* **67**, 13-21.

Lange, A., Ausseil, O., and Segner, H. (2002). Alterations of tissue glutathione levels and metallothionein mRNA in rainbow trout during single and combined exposure to cadmium and zinc. *Comp. Biochem. Physiol. -C* **131**, 231-243.

Larsson, D., Lundgren, T., and Sundell, K. (1998). Ca^{2+} uptake through voltage-gated L-type Ca^{2+} channels by polarized enterocytes from Atlantic cod *Gadus morhua*. *J. Membrane Biol.* **164**, 229-237.

Larsson, D., Nemere, I., Aksnes, L., and Sundell, K. (2003). Environmental salinity regulates receptor expression, cellular effects, and circulating levels of two antagonizing hormones, 1,25-dihydroxyvitamin D3 and 24,25-dihydroxyvitamin D3, in rainbow trout. *Endocrinology* **144**, 559-566.

Lee, P. L., Gelbart, T., West, C., Halloran, C., and Beutler, E. (1998). The Human Nramp2 Gene: Characterization of the Gene Structure, Alternative Splicing, Promoter Region and Polymorphisms. *Blood Cell. Mol. Dis.* **24**, 199-215.

Linder, M. C., Moriya, M., Whon, A., Kassa, A., and Gilley, C. (2006). Vesicular transport of Fe and interaction with other metal ions in polarized Caco2 Cell monolayers. *Biol. Res.* **39**, 143-156.

Liu, Z., Li, H., Soleimani, M., Girijashanker, K., Reed, J. M., He, L., Dalton, T. P., and Nebert, D. W. (2008). Cd^{2+} versus Zn^{2+} uptake by the ZIP8 HCO_3^--dependent symporter: Kinetics, electrogenicity and trafficking. *Biochem. Biophys. Res. Commun.* **365**, 814-820.

Loretz, C. A. (1995). Electrophysiology of ion transport in teleost intestinal cells. In *Cell. Mol. Appr. Fish Ionic Regul.* (C. M. Wood, and T. J. Shuttleworth, Eds.), pp. 25-56. Academic Press.

Mackenzie, B., and Garrick, M. D. (2005). Iron Imports. II. Iron uptake at the apical membrane in the intestine. *Am. J. Physiol. -Gastr. Liver Physiol.* **289**, 981-986.

Mackenzie, B., and Hediger, M. A. (2004). SLC11 family of H+-coupled metal-ion transporters NRAMP1 and DMT1. *Pflug. Arch. Eur. J. Physiol.* **447**, 571-579.

Mackenzie, B., Takanaga, H., Hubert, N., Rolfs, A., and Hediger, M. A. (2007). Functional properties of multiple isoforms of human divalent metal-ion transporter 1 (DMT1). *Biochem. J.* **403**, 59-69.

Mackenzie, B., Ujwal, M. L., Chang, M. H., Romero, M. F., and Hediger, M. A. (2006). Divalent metal-ion transporter DMT1 mediates both H^+ -coupled Fe^{2+} transport and uncoupled fluxes. *Pflug. Arch. Eur. J. Physiol.* **451**, 544-558.

Mackenzie, N. C., Brito, M., Reyes, A. E., and Allende, M. L. (2004). Cloning, expression pattern and essentiality of the high-affinity copper transporter 1 (ctr1) gene in zebrafish. *Gene* **328**, 113-120.

Mager, E. M., Wintz, H., Vulpe, C. D., Brix, K. V., and Grosell, M. (2008). Toxicogenomics of water chemistry influence on chronic lead exposure to the fathead minnow (*Pimephales promelas*). *Aquat. Toxicol.* **87**, 200-209.

Mai, K., Li, H., Ai, Q., Duan, Q., Xu, W., Zhang, C., Zhang, L., Tan, B., and Liufu, Z. (2006). Effects of dietary squid viscera meal on growth and cadmium accumulation in tissues of Japanese seabass, *Lateolabrax japonicus* (Cuvier 1828). *Aquaculture Res.* **37**, 1063-1069.

Majewski, H. S., and Giles, M. A. (1981). Cardiovascular respiratory responses of rainbow trout (*Salmo gairdneri*) during chronic exposure to sublethal concentrations of cadmium. *Water Res.* **15**, 1211-1217.

Manzl, C., Enrich, J., Ebner, H., Dallinger, R., and Krumschnabel, G. (2004). Copper-induced formation of reactive oxygen species causes cell death and disruption of calcium homeostasis in trout hepatocytes. *Toxicology* **196**, 57-64.

Martell, A. E., and Motekaitis, R. J. (1992). *Determination and Use of Stability Constants*. Wiley-VCH, New York.

Matz, C. J., and Krone, P. H. (2007). Cell death, stress-responsive transgene activation, and deficits in the olfactory system of larval zebrafish following cadmium exposure. *Environ. Sci. Technol.* **41**, 5143-5148.

McDuffee, A. T., Senisterra, G., Huntley, S., Lepock, J. R., Sekhar, K. R., Meredith, M. J., Borrelli, M. J., Morrow, J. D., and Freeman, M. L. (1997). Proteins containing non-native disulfide bonds generated by oxidative stress can act as signals for the induction of the heat shock response. *J. Cell Physiol.* **171**, 143-151.

McGeer, J. C., Szebedinszky, C., McDonald, D. G., and Wood, C. M. (2000). Effects of chronic sublethal exposure to waterborne Cu, Cd or Zn in rainbow trout. 1: Iono-regulatory disturbance and metabolic costs. *Aquat. Toxicol.* **50**, 231-243.

McKie, A. T., Barrow, D., Latunde-Dada, G. O., Rolfs, A., Sager, G., Mudaly, E., Mudaly, M., Richardson, C., Barlow, D., Bomford, A., Peters, T. J., Raja, K. B., Shirali, S., Hediger, M. A., Farzaneh, F., and Simpson, R. J. (2001). An iron-regulated ferric reductase associated with the absorption of dietary iron. *Science* **291**, 1755-1759.

McKie, A. T., Marciani, P., Rolfs, A., Brennan, K., Wehr, K., Barrow, D., Miret, S., Bomford, A., Peters, T. J., Farzaneh, F., Hediger, M. A., Hentze, M. W., and Simpson, R. J. (2000). A novel duodenal iron-regulated transporter, IREG1, implicated in the basolateral transfer of iron to the circulation. *Mol. Cell* **5**, 299-309.

Meyer, J. S., Adams, W. J., Brix, K. V., Luoma, S. N., Mount, D. R., Stubblefield, W. A., and Wood, C. M. (2005). *Toxicity of Dietborne Metals to Aquatic Organisms*. SETAC Press, Pensacola.

Moulis, J.-M. (2010). Cellular mechanisms of cadmium toxicity related to the homeostasis of essential metals. *BioMetals* **23**, 877-896.

Mount, D. R., Barth, A. K., Garrison, T. D., Barten, K. A., and Hockett, J. R. (1994). Dietary and waterborne exposure of rainbow trout (*Oncorhynchus mykiss*) to copper, cadmium, lead and zinc using a live diet. *Environ. Toxicol. Chem.* **13**, 2031-2041.

Nadella, S. R., Grosell, M., and Wood, C. M. (2006). Physical characterization of high-affinity gastrointestinal Cu transport in vitro in freshwater rainbow trout *Oncorhynchus mykiss*. *J. Comp. Physiol. -B* **176**, 793-806.

Nadella, S. R., Grosell, M., and Wood, C. M. (2007). Mechanisms of dietary Cu uptake in freshwater rainbow trout: evidence for Na-assisted Cu transport and a specific metal carrier in the intestine. *J. Comp. Physiol. -B* **177**, 433-446.

Nadella, S. R., Hung, C., and Wood, C. M. (2011). Mechanistic characterization of gastric copper transport in rainbow trout. *J. Comp. Physiol. -B* **181**, 27-41.

Nemeth, E., Tuttle, M. S., Powelson, J., Vaughn, M. D., Donovan, A., Ward, D. M., Ganz, T., and Kaplan, J. (2004). Hepcidin regulates cellular iron efflux by binding to ferroportin and inducing its internalization. *Science* **306**, 2090-2093.

Ng, T. Y. T., Klinck, J. S., and Wood, C. M. (2009). Does dietary Ca protect against toxicity of a low dietborne Cd exposure to the rainbow trout? *Aquat. Toxicol.* **91**, 75-86.

Ng, T. Y. T., and Wood, C. M. (2008). Trophic transfer and dietary toxicity of Cd from the oligochaete to the rainbow trout. *Aquat. Toxicol.* **87**, 47-59.

Niyogi, S., Kent, R., and Wood, C. M. (2008). Effects of water chemistry variables on gill binding and acute toxicity of cadmium in rainbow trout (*Oncorhynchus mykiss*): A biotic ligand model (BLM) approach. *Comp. Biochem. Physiol. -C* **148**, 305-314.

Niyogi, S., Pyle, G. G., and Wood, C. M. (2007). Branchial versus intestinal zinc uptake in wild yellow perch (*Perca flavescens*) from reference and metal-contaminated aquatic ecosystems. *Can. J. Fish. Aqua. Sci.* **64**, 1605-1613.

Niyogi, S., and Wood, C. M. (2003). Effects of chronic waterborne and dietary metal exposures on gill metal-binding: Implications for the biotic ligand model. *Hum. Ecol. Risk Assess.* **9**, 813-846.

Niyogi, S., and Wood, C. M. (2004). Kinetic analyses of waterborne Ca and Cd transport and their interactions in the gills of rainbow trout (*Oncorhynchus mykiss*) and yellow perch (*Perca flavescens*), two species differing greatly in acute waterborne Cd sensitivity. *J. Comp. Physiol. -B* **174**, 243-253.

Ojima, N., Yamashita, M., and Watabe, S. (2005). Quantitative mRNA expression profiling of heat-shock protein families in rainbow trout cells. *Biochem. Biophys. Res. Commun.* **329**, 51-57.

Ojo, A. A., Nadella, S. R., and Wood, C. M. (2009). In vitro examination of interactions between copper and zinc uptake via the gastrointestinal tract of the rainbow trout (*Oncorhynchus mykiss*). *Arch. Environ. Contam. Toxicol.* **56**, 244-252.

Ojo, A. A., and Wood, C. M. (2007). *In vitro* analysis of the bioavailability of six metals via the gastro-intestinal tract of the rainbow trout (*Oncorhynchus mykiss*). *Aquat. Toxicol.* **83**, 10-23.

Ojo, A. A., and Wood, C. M. (2008). In vitro characterization of cadmium and zinc uptake via the gastro-intestinal tract of the rainbow trout (*Oncorhynchus mykiss*): Interactive effects and the influence of calcium. *Aquat. Toxicol.* **89**, 55-64.

Okubo, M., Yamada, K., Hosoyamada, M., Shibasaki, T., and Endou, H. (2003). Cadmium transport by human Nramp 2 expressed in *Xenopus laevis* oocytes. *Toxicol. Appl. Pharmacol.* **187**, 162-167.

Olivi, L., Sisk, J., and Bressler, J. (2001). Involvement of DMT1 in uptake of Cd in MDCK cells: Role of protein kinase C. *Am. J. Physiol.* **281**, 50-53.

Park, J. D., Cherrington, N. J., and Klaassen, C. D. (2002). Intestinal absorption of cadmium is associated with divalent metal transporter 1 in rats. *Toxicol. Sci.* **68**, 288-294.

Pfaffl, M. W. (2001). A new mathematical model for relative quantification in real-time RT-PCR. *Nucl. Acids Res.* **29**, 2002-2007.

Picard, V., Govoni, G., Jabado, N., and Gross, P. (2000). Nramp 2 (DCT1/DMT1) expressed at the plasma membrane transports iron and other divalent cations into a calcein-accessible cytoplasmic pool. *J. Biol. Chem.* **275**, 35738-35745.

Pick, U. (1982). The interaction of vanadate ions with the Ca-ATPase from sarcoplasmic reticulum. *J. Biol. Chem.* **257**, 6111-6119.

Pigman, E. A., Blanchard, J., and Laird, H. E. (1997). A study of cadmium transport pathways using the Caco-2 cell model. *Toxicol. Appl. Pharmacol.* **142**, 243-247.

Powell, J. J., Jugdaohsingh, R., and Thompson, R. P. H. (1999). The regulation of mineral absorption in the gastrointestinal tract. *Proc. Nutr. Soc.* **58**, 147-153.

Pratap, H. B., and Bonga, S. E. W. (1993). Effect of ambient and dietary cadmium on pavement cells, chloride cells, and Na^+/K^+-ATPase activity in the gills of the freshwater teleost Oreochromis mossambicus at normal and high calcium levels in the ambient water. *Aquat. Toxicol.* **26**, 133-150.

Pratap, H. B., Fu, H., Lock, R. A. C., and Wendelaar Bonga, S. E. (1989). Effect of waterborne and dietary cadmium on plasma ions of the teleost *Oreochromis mossambicus* in relation to water calcium levels. *Arch. Environ. Contam. Toxicol.* **18**, 568-575.

Qiu, A., Glover, C. N., and Hogstrand, C. (2007). Regulation of branchial zinc uptake by 1[alpha],25-(OH)2D3 in rainbow trout and associated changes in expression of ZIP1 and ECaC. *Aquat. Toxicol.* **84**, 142-152.

Qiu, A., Shayeghi, M., and Hogstrand, C. (2005). Molecular cloning and functional characterization of a high-affinity zinc importer (DrZIP1) from zebrafish (*Danio rerio*). *Biochem. J.* **388**, 745-754.

Raffin, S. B., Woo, C. H., and Roost, K. T. (1974). Intestinal absorption of hemoglobin iron heme cleavage by mucosal heme oxygenase. *J. Clin. Invest.* **54**, 1344-1352.

Raja, K. B., Simpson, R. J., and Peters, T. J. (1992). Investigation of a role for reduction in ferric iron uptake by mouse duodenum. *Biochim. Biophys. Acta.* **1135**, 141-146.

Robinson, J. D., and Mercer, R. W. (1981). Vanadate binding to the (Na^+/ K^+)-ATPase. *J. Bioenerg. Biomembr.* **13**, 205-218.

Rogers, J. T., and Wood, C. M. (2004). Characterization of branchial lead-calcium interaction in the freshwater rainbow trout *Oncorhynchus mykiss*. *J. Exp. Biol.* **207**, 813-825.

Rolfs, A., and Hediger, M. A. (1999). Metal ion transporters in mammals: Structure, function and pathological implications. *J. Physiol.* **518**, 1-12.

Ryu, D. Y., Lee, S. J., Park, D. W., Choi, B. S., Klaassen, C. D., and Park, J. D. (2004). Dietary iron regulates intestinal cadmium absorption through iron transporters in rats. *Toxicol. Lett.* **152**, 19-25.

Sacher, A., Cohen, A., and Nelson, N. (2001). Properties of the mammalian and yeast metal-ion transporters DCT1 and Smf1p expressed in *Xenopus laevis* oocytes. *J. Exp. Biol.* **204**, 1053-1061.

Saeij, J. P. J., Wiegertjes, G. F., and Stet, R. J. M. (1999). Identification and characterization of a fish natural resistance-associated macrophage protein (NRAMP) cDNA. *Immunogenetics* **50**, 60-66.

Saghari Fard, M. R., Weisheit, C., and Poynton, S. L. (2007). Intestinal pH profile in rainbow trout *Oncorhynchus mykiss* and microhabitat preference of the flagellate *Spironucleus salmonis* (Diplomonadida). *Dis. Aquat. Organ.* **76**, 241-249.

Said, H. M., and Ma, T. Y. (1994). Mechanism of riboflavine uptake by Caco-2 human intestinal epithelial cells. *Am. J. Physiol.* **266**, 15-21.

Savigni, D. L., and Morgan, E. H. (1998). Transport mechanisms for iron and other transition metals in rat and rabbit erythroid cells. *J. Physiol.* **508**, 837-850.

Schafer, S. G., and Forth, W. (1985). The interaction between cadmium and iron: A review of the literature. *Trace Elem. Med.* **2**, 158-162.

Schoenmakers, T. J. M., Klaren, P. H. M., Flik, G., Lock, R. A. C., Pang, P. K. T., and Wendelaar Bonga, S. E. (1992). Actions of cadmium on basolateral plasma membrane proteins involved in calcium uptake by fish intestine. *J. Membrane Biol.* **127**, 161-172.

Scudiero, R., Temussi, P. A., and Parisi, E. (2005). Fish and mammalian metallothioneins: A comparative study. *Gene* **345**, 21-26.

Shahsavarani, A., McNeill, B., Galvez, F., Wood, C. M., Goss, G. G., Hwang, P. P., and Perry, S. F. (2006). Characterization of a branchial epithelial calcium channel (ECaC) in freshwater rainbow trout (*Oncorhynchus mykiss*). *J. Exp. Biol.* **209**, 1928-1943.

Sharp, P. A. (2003). Ctr1 and its role in body copper homeostasis. *Int. J. Biochem. Cell Biol.* **35**, 288-291.

Shayeghi, M., Latunde-Dada, G. O., Oakhill, J. S., Laftah, A. H., Takeuchi, K., Halliday, N., Khan, Y., Warley, A., McCann, F. E., Hider, R. C., Frazer, D. M., Anderson, G. J., Vulpe, C. D., Simpson, R. J., and McKie, A. T. (2005). Identification of an intestinal heme transporter. *Cell* **122**, 789-801.

Shears, M. A., and Fletcher, G. L. (1983). Regulation of Zn^{2+} uptake from the gastrointestinal tract of a marine teleost, the winter flounder (*Pseudopleuronectes americanus*). *Can. J. Fish. Aqua. Sci.* **40**, 197-205.

Sibthorpe, D., Baker, A.-M., Gilmartin, B. J., Blackwell, J. M., and White, J. K. (2004). Comparative analysis of Two slc11 (Nramp) Loci in *Takifugu rubripes*. *DNA Cell Biol.* **23**, 45-58.

Simons, T. J. B., and Pocock, G. (1987). Lead enters bovine adrenal medullary cells through calcium channels. *J. Neurochem.* **48**, 383-389.

Souza, V., Bucio, L., and Gutiérrez-Ruiz, M. C. (1997). Cadmium uptake by a human hepatic cell line (WRL-68 cells). *Toxicology* **120**, 215-220.

Stubblefield, W. A., Steadman, B. L., Point, T. W. L. A., and Bergman, H. L. (1999). Acclimation-induced changes in the toxicity of zinc and cadmium to rainbow trout. *Environ. Toxicol. Chem.* **18**, 2875-2881.

Stumm, W., and Morgan, J. J. (1996). *Aquatic Chemistry*. John Wiley & Sons, New York.

Sugawara, N., Chen, B.-Q., Sugawara, C., and Miyake, H. (1988). Effect of Cadmium on Fe^{3+}-transferrin formation in the rat intestinal mucosa. *Bull. Environ. Contam. Toxicol.* **41**, 50-55.

Szebedinszky, C. S., McGeer, J. C., McDonald, D. G., and Wood, C. M. (2001). Effects of chronic Cd exposure via the diet or water on internal organ-specific distribution and subsequent gill Cd uptake kinetics in juvenile rainbow trout (*Oncorhynchus mykiss*). *Environ. Toxicol. Chem.* **20**, 597-607.

Tacnet, F., Watkins, D. W., and Ripoche, P. (1990). Studies of zinc transport into brush-border membrane vesicles isolated from pig small intestine. *Biochim. Biophys. Acta. - Biomembranes* **1024**, 323-330.

Talbot, A. T., Pottinger, T. G., Smith, T. J., and Cairns, M. T. (2009). Acute phase gene expression in rainbow trout (*Oncorhynchus mykiss*) after exposure to a confinement stressor: A comparison of pooled and individual data. *Fish Shellfish Immun.* **27**, 309-317.

Tallkvist, J., Bowlus, C. L., and Lönnerdal, B. (2001). DMT1 gene expression and cadmium absorption in human absorptive enterocytes. *Toxicol. Lett.* **122**, 171-177.

Tallkvist, J., Bowlus, C. L., and Lönnerdal, B. (2003). Effect of iron treatment on nickel absorption and gene expression of the divalent metal transporter (DMT1) by human intestinal Caco-2 cells. *Pharmacol. Toxicol.* **92**, 121-124.

Tandy, S., Williams, M., Leggett, A., Lopez, J. M., Dedes, M., Ramesh, B., and al., e. (2000). Nramp2 expression is associated with pH-dependent iron uptake across the apical membrane of human intestinal Caco-2 cells. *J. Biol. Chem.* **275**, 1023-1029.

Teichmann, R., and Stremmel, W. (1990). Iron uptake by human upper small intestine microvillous membrane vesicles. Indication for a facilitated transport mechanism mediated by a membrane iron-binding protein. *J. Clin. Invest.* **86**, 2145-2153.

Tennant, J., Stansfield, M., Yamaji, S., Srai, S. K., and Sharp, P. (2002). Effects of copper on the expression of metal transporters in human intestinal Caco-2 cells. *FEBS Lett.* **527**, 239-244.

Teucher, B., Olivares, M., and Cori, H. (2004). Enhancers of iron absorption: Ascorbic acid and other organic acids. *Int. J. Vitam. Nutr. Res.* **74**, 403-419.

Thévenod, F. (2010). Catch me if you can! Novel aspects of cadmium transport in mammalian cells. *BioMetals* **23**, 857-875.

Thomas, C., and Oates, P. S. (2004). Differences in the uptake of iron from Fe(II) ascorbate and Fe(III) citrate by IEC-6 cells and the involvement of ferroportin/IREG-1/MTP-1/SLC40A1. *Pflug. Arch. Eur. J. Physiol.* **448**, 431-437.

Trinder, D., Oates, P. S., Thomas, C., Sadleir, J., and Morgan, E. H. (1999). Localisation of divalent metal transporter I (DMT1) to the microvillus membrane of rat duodenal enterocytes in iron deficiency, but to hepatocytes in iron overload. *Gut* **46**, 270-276.

Tsien, R. W., Hess, P., McCleskey, E. W., and Rosenberg, R. L. (1987). Calcium channels: mechanisms of selectivity, permeation, and block. *Ann. Rev. Biophys. Chem.* **16**, 265-290.

US-EPA (2001). Update of ambient quality criteria for cadmium. *EPA-822-R-01–001*, Office of Water, Washington, DC.

Verbost, P. M., Flik, G., Lock, R. A., and Wendelaar Bonga, S. E. (1987). Cadmium inhibition of Ca^{2+} uptake in rainbow trout gills. *Am. J. Physiol.* **253**.

Verbost, P. M., Van Rooij, J., Flik, G., Lock, R. A. C., and Wendelaar Bonga, S. E. (1989). The movement of cadmium through freshwater trout branchial epithelium and its interference with calcium transport. *J. Exp. Biol.* **145**, 185-197.

Vergani, L., Lanza, C., Borghi, C., Scarabelli, L., Panfoli, I., Burlando, B., Dondero, F., Viarengo, A., and Gallo, G. (2007). Efects of growth hormone and cadmium on the transcription regulation of two metallothionein isoforms. *Mol. Cell Endocrinol.* **263**, 29-37.

Vielma, J., and Lall, S. P. (1997). Dietary formic acid enhances apparent digestibility of minerals in rainbow trout, *Oncorhynchus mykiss*. *Aquacult. Nutr.* **3**, 265-268.

Vincent, S., Ambrose, T., Cyril Arun Kumar, L., and Selvanayagam, M. (1996). Heavy metal cadmium influenced anaemia in the riverine major carp, *Catla catla* (Ham.). *J. Environ. Biol.* **17**, 81-84.

Vulpe, C. D., Kuo, Y. M., Murphy, T. L., Cowley, L., Askwith, C., Libina, N., Gitschier, J., and Anderson, G. J. (1999). Hephaestin, a ceruloplasmin homologue implicated in intestinal iron transport, is defective in the sla mouse. *Nature Genet.* **21**, 195-199.

Waisberg, M., Joseph, P., Hale, B., and Beyersmann, D. (2003). Molecular and cellular mechanisms of cadmium carcinogenesis. *Toxicology* **192**, 95-117.

Watanabe, T., Kiron, V., and Satoh, S. (1997). Trace minerals in fish nutrition. *Aquaculture* **151**, 185-207.

Weiser, M. M. (1973). Intestinal epithelial-cell surface membrane glycoprotein synthesis. 1. Indicator of cellular differentiation. *J. Biol. Chem.* **248**, 2536-2541.

Wicklund Glynn, A. (2001). The influence of zinc on apical uptake of cadmium in the gills and cadmium influx to the circulatory system in zebrafish (*Danio rerio*). *Comp. Biochem. Physiol.- C* **128**, 165-172.

Wilson, R. W. (1999). A novel role for the gut of seawater teleosts in acid-base balance. In *Regulation of Tissue pH in Plants and Animals* (S. Egginton, E. W. Taylor, and J. A. Raven, Eds.), pp. 257-274. Cambridge University Press, Cambridge.

Wilson, R. W., Wilson, J. M., and Grosell, M. (2002). Intestinal bicarbonate secretion by marine teleost fish-why and how? *Biochim. Biophys. Acta. - Biomembranes* **1566**, 182-193.

Winterbourn, M. J., McDiffett, W. F., and Eppley, S. J. (2000). Aluminium and iron burdens of aquatic biota in New Zealand streams contaminated by acid mine drainage: Effects of trophic level. *Sci. Total Environ.* **254**, 45-54.

Włostowski, T., Krasowska, A., and Bonda, E. (2003). An iron-rich diet protects the liver and kidneys against cadmium-induced injury in the bank vole (*Clethrionomys glareolus*). *Ecotox. Environ. Safe.* **54**, 194-198.

Wolf, K. (1963). Physiological salines for freshwater teleosts. *Prog. Fish Cultur.* **25**, 135-140.

Wood, C. M. (2001). Toxic responses of the gill. In *Target Organ Toxicity in Marine and Freshwater Teleosts, vol. 1: Organs* (D. W. Schlenk, and W. H. Benson, Eds.), pp. 1-89. Taylor and Francis, Washington, DC, USA.

Wood, C. M., Franklin, N. M., and Niyogi, S. (2006). The protective role of dietary calcium against cadmium uptake and toxicity in freshwater fish: an important role for the stomach. *Environ. Chem.* **3**, 389-394.

Woodward, D. F., Brumbaugh, W. G., Delonay, A. J., Little, E. E., and Smith, C. E. (1994). Effects on rainbow trout fry of a metals-contaminated diet of benthic invertebrates from the clark fork river, Montana. *Trans. Amer. Fish. Soc.* **123**, 51-62.

Worthington, M. T., Browne, L., Battle, E. H., and Luo, R. Q. (2000). Functional properties of transfected human DMT1 iron transporter. *Am. J. Physiol. -Gastr. Liver Physiol.* **279**.

Wu, S. M., Zheng, Y. D., and Kuo, C. H. (2008). Expression of mt2 and smt-B upon cadmium exposure and cold shock in zebrafish (*Danio rerio*). *Comp. Biochem. Physiol. -C* **148**, 184-193.

Yamaji, S., Tennant, J., Tandy, S., Williams, M., Singh Srai, S. K., and Sharp, P. (2001). Zinc regulates the function and expression of the iron transporters DMT1 and IREG1 in human intestinal Caco-2 cells. *FEBS Lett.* **507**, 137-141.

Yang, L., Zhou, L., and Gui, J. F. (2004). Molecular basis of transferrin polymorphism in goldfish (*Carassius auratus)*. *Genetica* **121**, 303-313.

Yasutake, A., and Hirayama, K. (2004). Effects of iron overload on hepatic and renal metallothionein levels in rats. *J. Health Sci.* **50**, 372-378.

Yeung, C. K., Glahn, R. P., and Miller, D. D. (2005). Inhibition of iron uptake from iron salts and chelates by divalent metal cations in intestinal epithelial cells. *J. Agric. Food Chem.* **53**, 132-136.

Zalups, R. K., and Ahmad, S. (2003). Molecular handling of cadmium in transporting epithelia. *Toxicol. Appl. Pharmacol.* **186**, 163-188.

Zhang, L., and Wang, W. X. (2007). Gastrointestinal uptake of cadmium and zinc by a marine teleost *Acanthopagrus schlegeli*. *Aquat. Toxicol.* **85**, 143-153.

Zhu, J. Y., Huang, H. Q., Bao, X. D., Lin, Q. M., and Cai, Z. (2006). Acute toxicity profile of cadmium revealed by proteomics in brain tissue of *Paralichthys olivaceus*: Potential role of transferrin in cadmium toxicity. *Aquat. Toxicol.* **78**, 127-135.

Zoller, H., Koch, R. O., Theurl, I., Obrist, P., Pietrangelo, A., Montosi, G., Haile, D. J., Vogel, W., and Weiss, G. (2001). Expression of the duodenal iron transporters divalent-metal transporter 1 and ferroportin 1 in iron deficiency and iron overload. *Gastroenterology* **120**, 1412-1419.

APPENDIX

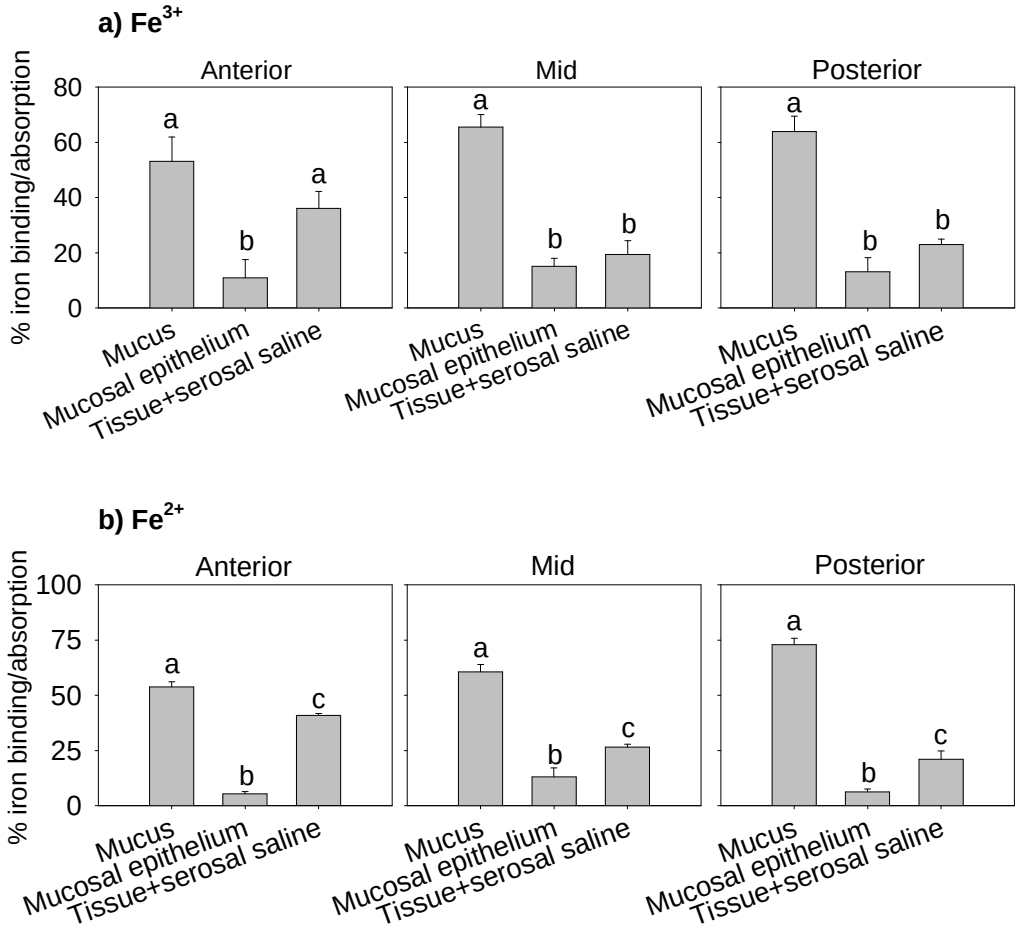

Figure A1: The relative distribution (%) of **(a)** ferric (Fe^{3+}) or **(b)** ferrous (Fe^{2+}) iron in the mucus, mucosal epithelium and tissue plus serosal saline in the isolated anterior, mid and posterior intestine of rainbow trout, exposed to 2 μM iron at 15°C for 2 h. Bars labelled with different letters are significantly different within the same intestinal segment (One-way ANOVA followed by a post-hoc LSD test; $p \leq 0.05$). Values are mean ± SEM ($n = 5$).

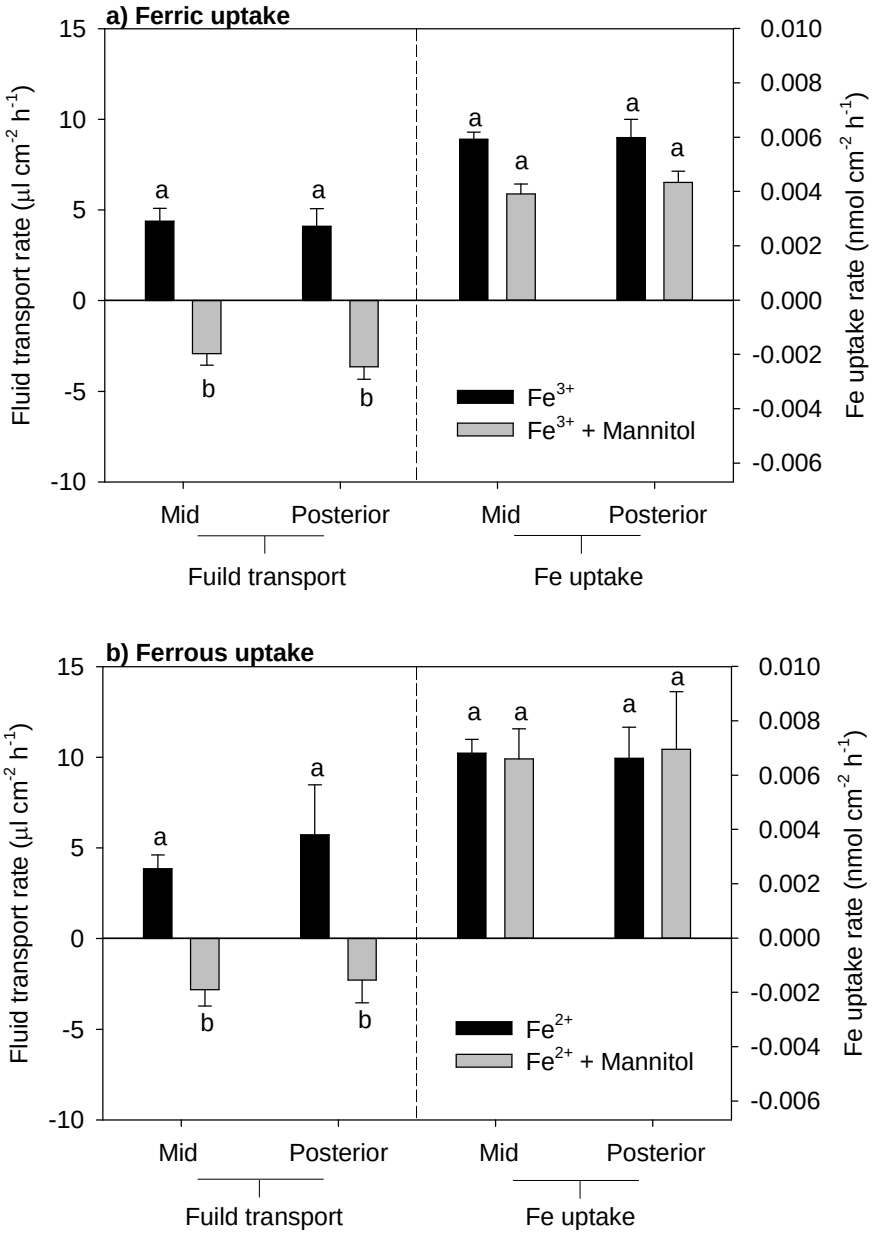

Figure A2: The effects of mannitol (350 mM) in the mucosal saline on the fluid transport rate (positive values represent the net fluid transport from the mucosal to the serosal side, and vice versa for the negative values), ferric (Fe^{3+}) and ferrous (Fe^{2+}) iron uptake rates in the mid and posterior intestine exposed to 2 µM iron at 15°C for 2 h. Bars labelled with different letters are significantly different (One-way ANOVA followed by a post-hoc LSD test; $p \leq 0.05$). Values are mean ± SEM ($n = 5$).

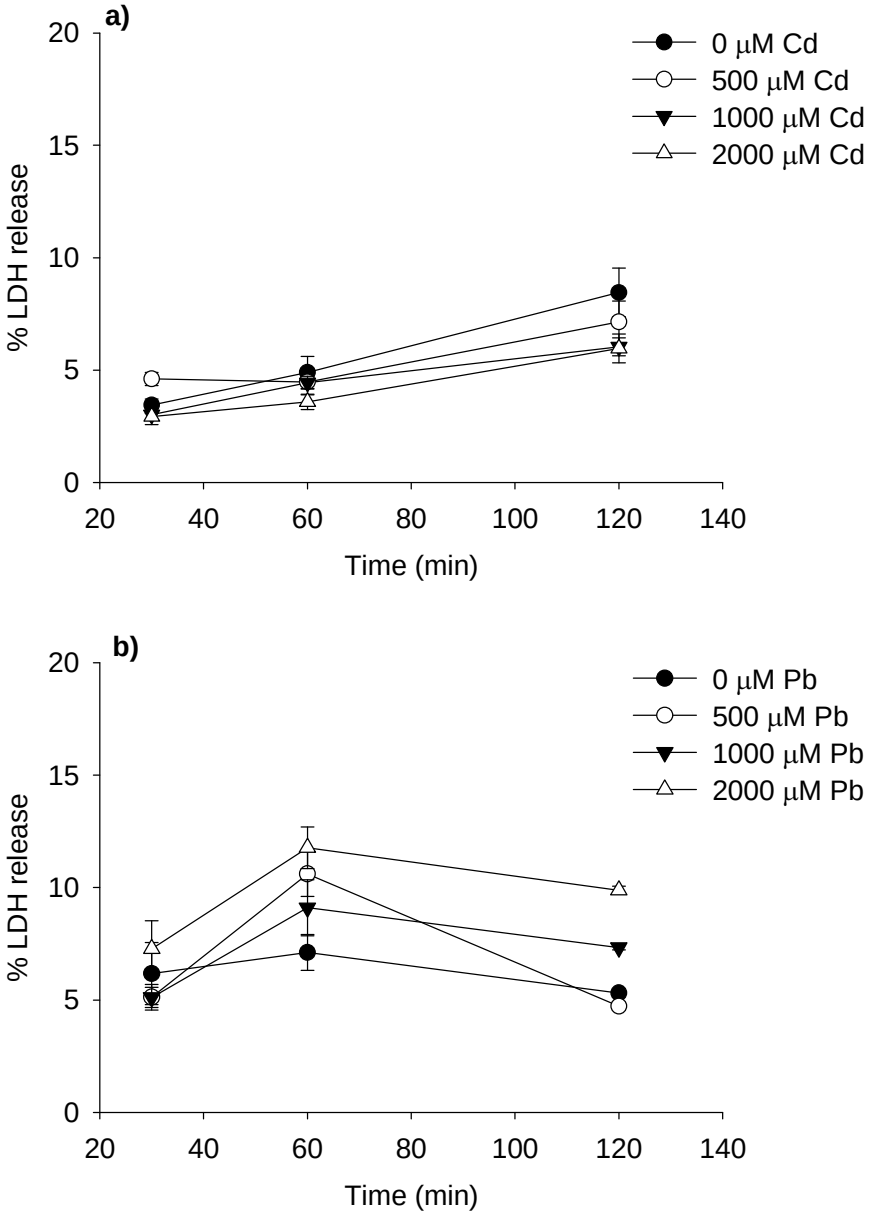

Figure A3: The effects of different concentrations of extracellular **(a)** cadmium (Cd) or **(b)** lead (Pb) on the release of lactate dehydrogenase (LDH) (data are presented as % relative to intracellular LDH) from isolated rainbow trout enterocytes to the exposure media over time. No statistical difference was recorded across times and among treatments. Values are mean ± SEM (n = 5-6).

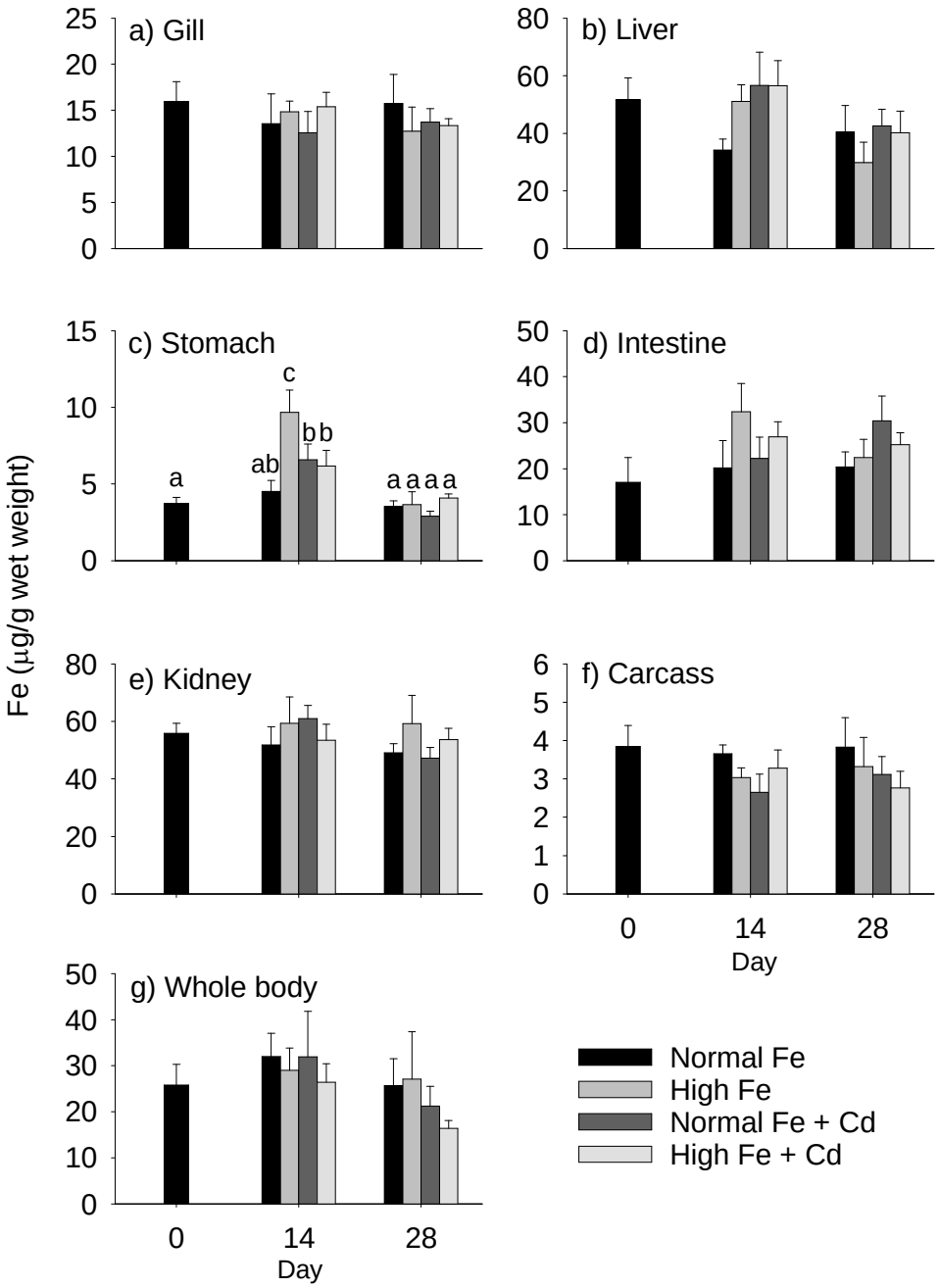

Figure A4: Concentrations of iron (Fe) (µg/g wet weight) in the **(a)** gill, **(b)** liver, **(c)** stomach, **(d)** intestine, **(e)** kidney, **(f)** carcass and **(g)** whole-body of rainbow trout exposed to the normal iron, high Fe, normal Fe + cadmium (Cd), and high Fe + Cd diets. In the stomach, bars labelled with different letters represent statistical difference. No statistical difference was recorded in other organs (Three-way ANOVA with time, dietary Fe, and dietary Cd as independent variables, followed by a post-hoc LSD test; $p < 0.05$). Values are mean ± SEM ($n = 8$).

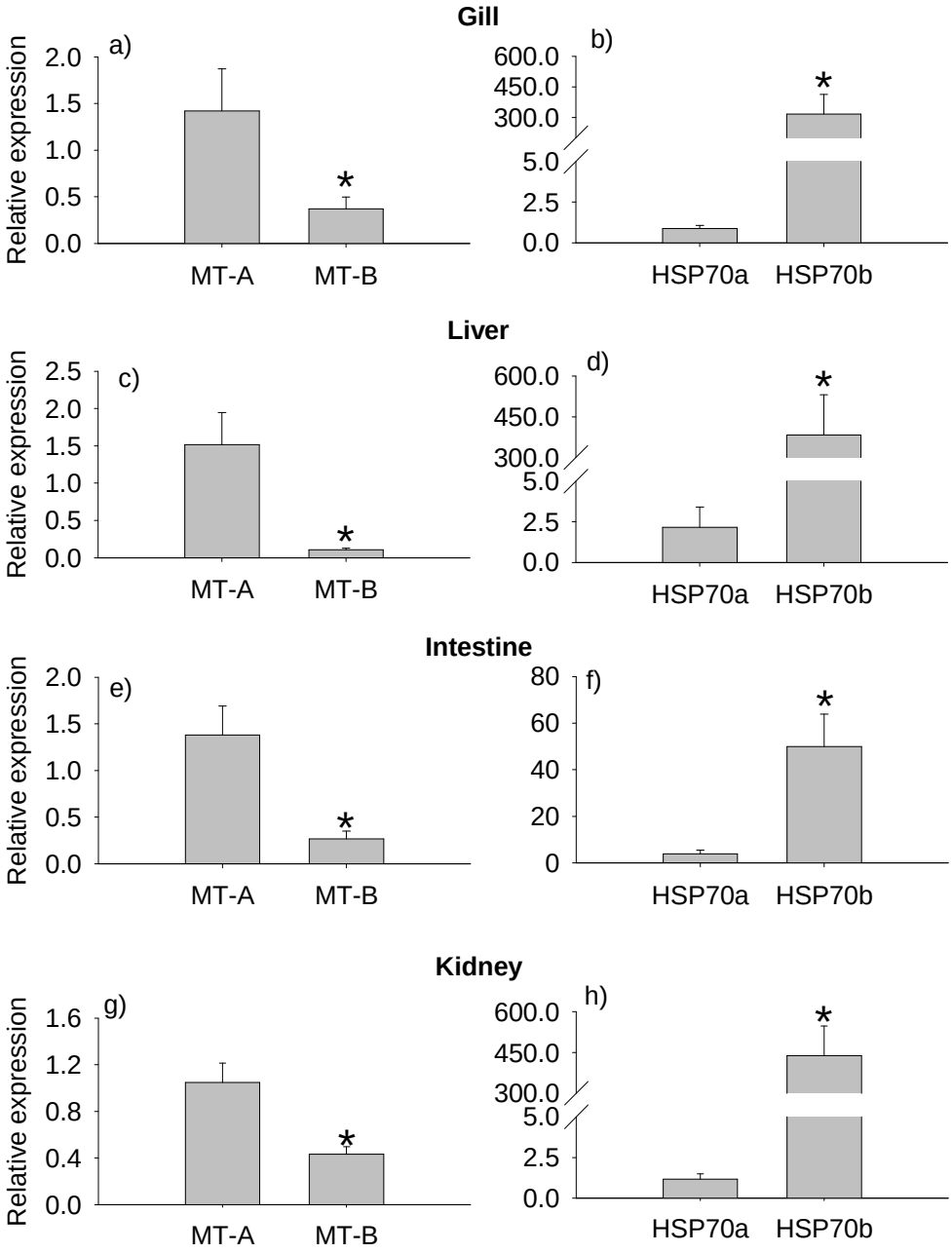

Figure A5: The mRNA expression profile of metallothionein-A (MT-A) and -B (MT-B), and heat shock protein-70a (HSP70a) and -70b (HSP70b) in the **(a, b)** gill, **(c, d)** intestine, **(e, f)** liver, and **(g, h)** kidney of rainbow trout. The expression levels of all genes were normalized to *β-actin* from the same tissue, and were expressed relative to either MT-A or HSP70a for the respective gene. Bar labelled with an asterisk represents statistical difference (Student's *t*-test; $p < 0.05$). Values are mean ± SEM ($n = 8$).